UNIVERSITY OF ALBERTA

A PRELIMINARY STUDY OF THE HYDRAULICS OF LOUVER ARRAYS

by

DARREN M. SHEPHERD ©

A THESIS
SUBMITTED TO THE FACULTY OF GRADUATE STUDIES AND RESEARCH
IN PARTIAL FULFILLMENT OF THE REQUIREMENTS FOR THE DEGREE OF
MASTER OF SCIENCE

IN

WATER RESOURCES ENGINEERING

DEPARTMENT OF CIVIL & ENVIRONMENTAL ENGINEERING

EDMONTON, ALBERTA
FALL 1998

0-612-34415-0

UNIVERSITY OF ALBERTA

Faculty of Graduate Studies and Research

The undersigned certify that they have read, and recommended to the Faculty of Graduate Studies and Research for acceptance, a thesis entitled **A Preliminary Study of the Hydraulics of Louver Arrays** by **Darren M. Shepherd** in partial fulfillment of the requirements for the degree of **Master of Science** in **Water Resources Engineering.**

Mr. C. Katopodis

Dr. N. Rajaratnam

Dr. D. Zhu

Dr. J. Feddes

Date: 26 Aug 98

ABSTRACT

The purpose of this preliminary study was to advance the understanding of the hydraulics of louver arrays used to guide downstream migrating fish away from water intakes. This investigation was conducted in two phases: Phase One involved the field testing of a prototype louver array and Phase Two was a laboratory-based continuation of the first phase, except that it was conducted using a different louver design. Water surface profiles, velocity measurements, qualitative flow observations, and photographs were obtained for a total of 28 physical arrangements and discharges. Velocity measurements taken within the bypass section confirmed that the velocity was uniform and increased in the downstream direction. Proportional bypass discharge and bypass acceleration were both found to be functions of louver array angle, louver attack angle, slat spacing, and proportional bypass width. Being a preliminary investigation of louver array hydraulics, several recommendations have been presented for consideration in further studies.

DEDICATED TO MY LOVING PARENTS,

SANDRA AND AINSLEY SHEPHERD,

FOR THEIR CONTINUAL SUPPORT AND ENCOURAGEMENT

THROUGHOUT MANY YEARS OF ACADEMICS

ACKNOWLEDGMENTS

The author gratefully acknowledges the guidance and encouragement provided by his supervisors, Mr. C. Katopodis and Dr. N. Rajaratnam. Their ongoing enthusiasm towards this study was both inspirational and contagious.

Special appreciation goes to Mr. S. Lovell for his invaluable assistance with practical aspects of the study. On a personal level, Mr. Lovell's encouragement and support was unparalleled. In addition, he designed and constructed both the flume used in Phase One and the louver arrays of Phase Two.

The author sincerely thanks Dr. G. Anderson for his cooperation and assistance throughout Phase One of the study. It was his expertise that greatly expanded the understanding of the biological aspect of louvers.

Dr. S. Wu is duly noted for his assistance with the hydraulic analysis and testing procedures of Phase One, providing the computer software for recording velocity data in Phase Two, and giving academic support whenever called upon.

Special thanks to Mr. K. Chandler for the time and effort he spent designing and constructing the louver array of Phase One. In addition, his assistance throughout the field testing was much appreciated.

ACKNOWLEDGMENTS (continued)

The first phase of the study would not have been possible without the assistance and cooperation of the staff at the Sam Livingston fish hatchery in Calgary. In particular, Mr. D. DePape and Mr. W. Schenk are gratefully acknowledged for their generosity.

The author sincerely thanks Mr. P. Fedun and Ms. J. Eaket for their assistance throughout Phase Two of the study. In addition, the generosity and support provided by the staff at Northwest Hydraulic Consultants Limited (NHCL) throughout the writing of this thesis is duly noted. Recognition also goes to those fellow graduate students who have assisted on numerous occasions.

This thesis was financially supported by a research grant through the Natural Sciences and Engineering Research Council of Canada (NSERC). This support is gratefully acknowledged.

TABLE OF CONTENTS

LIST OF EQUATIONS

LIST OF TABLES

LIST OF FIGURES

LIST OF FIGURES (continued)

LIST OF PHOTOGRAPHIC PLATES

LIST OF PHOTOGRAPHIC PLATES (continued)

Plate **Description** **Page**

APPENDICES

A Water Surface Profiles (Phase Two)

B Velocity Profiles

LIST OF SYMBOLS

B	flume width [m]
f	frequency reading of *StreamFlo* probe [Hz]
F	Froude number of any section 'X' [unitless]
FGE	fish guiding efficiency [%]
g	acceleration due to gravity [m/s^2]
h	louver slat height [m]
ht	tailgate height [m]
L	louver array length [m]
Q	total flume discharge [m^3/s]
Q^*	magnetic flowmeter reading of the pump discharge [converted from volts to m^3/s]
Q_b	discharge of the bypass exit section [m^3/s]
$\frac{Q_b}{Q}$	proportional bypass discharge [unitless]
R^2	squared correlation coefficient [unitless]
s	louver slat spacing [m]
t	louver slat thickness [m]
u	velocity of any depth 'y' [m/s]
Δu	incremental area of discharge of velocity 'u' [m/s]
U	width-averaged velocity of any section 'X' [m/s]
U_o	depth-averaged (center plane) velocity of the approach section [m/s]

LIST OF SYMBOLS (continued)

$\frac{U}{U_o}$ bypass acceleration [unitless]

w louver slat width [m]

X distance in the horizontal direction from the entrance of the louver array [m]

y distance in the vertical direction from the flume bed [m]

Y flow depth of any section 'X' [m]

Y_o flow depth of the approach section [m]

$\frac{y}{Y}$ normalized flow depth [unitless]

$\frac{Y_b}{Y_o}$ normalized flow depth of the bypass section [unitless]

$\frac{Y_c}{Y_o}$ normalized flow depth of the canal section [unitless]

$\left(\frac{Y_b}{Y_o}\right)'$ normalized mean flow depth of the bypass section [unitless]

$\left(\frac{Y_c}{Y_o}\right)'$ normalized mean flow depth of the canal section [unitless]

Z distance in the transverse direction from the left wall of the flume [m]

Z_b bypass width of any section 'X' [m]

$\frac{Z_b}{B}$ proportional bypass width [unitless]

ΔY_b reduction in flow depth of the bypass section (from entrance to exit) [m]

ΔY_c reduction in flow depth of the canal section (from entrance to exit) [m]

LIST OF SYMBOLS (continued)

θ	louver array angle [degrees]
Ψ	louver attack angle [degrees]
Ψ_1	upstream louver attack angle (within the bypass section) [degrees]
Ψ_2	downstream louver attack angle (within the canal section) [degrees]
ω	engine speed of the I-H Flume [rev/min]

1.0 INTRODUCTION

1.1 General

The prevention of fish loss at water intakes has been a challenging task to both engineers and biologists since the early years of this century. Intakes for domestic water supply systems are common near population centres and, for irrigation purposes in rural areas. In addition, the growth of new industries in the past few decades has lead to the need for water intakes at hydroelectric generating facilities. A continual increase in the number of water intake systems found along the paths of downstream migrating fish leads to the possibility of an increase in fish mortality in areas where fish diversion devices are not employed.

Alternatives to be considered at water intakes include fish screens and fish guidance systems. Fish screens are used extensively around the world and particularly in western North America. Although they usually offer a high level of fish protection with fish guiding efficiency values (FGE's) approaching 100%, they are commonly accompanied by higher costs than other alternatives. Fish guidance systems, such as the louver array, are typically used in both the eastern United States and Canada at hydroelectric installations. They tend to offer a slightly lower and more variable level of fish protection at a lower overall cost.

The implementation of the louver array as a means of fish protection dates back to the 1950's. Its use was necessary in diverting fish from pump intakes (Bates and Vinsonhaler, 1957) and hydroelectric power intakes (Ruggles and Ryan, 1964). Since the mid-1960's, there has been little research performed on louvers. In addition, much of the work that has been done is either highly qualitative or biological in content. Based on such findings, it seems that there is still a lot to be learned about the hydraulics of the louver array.

Fish diversion devices, such as the louver array, have been defined by ASCE (1982) as physical structures designed to alter flow conditions at the device in such a way that fish will be guided away from the main intake flow and diverted into a bypass.... The fish are then returned to safety through a fish return system.

Louvers have been defined by Ruggles and Ryan (1964) as a series of vertical slats placed in a diagonal line across the migratory path of downstream migrating fish.... Each slat is set at right angles to the direction of flow.... The migrants, upon approaching the slats, tend to avoid them while continuing downstream and thus are guided to a bypass at the downstream end of the louver line.

1.2 Development of an Effective Louver Array

In selecting a fish diversion device, it is necessary to determine the effectiveness of the structure in protecting the species and life stages of both local and downstream migrating fish that come in contact with the water intake system. Secondly, the placement and construction of the structure must be considered so that ice, large debris, and plugging from fine debris are manageable. Thirdly, the device should be designed so that its effect on the amount of discharge drawn in by the intake system is minimized.

Lastly, the costs of construction and maintenance must be reasonable for the overall scope of the project.

The design of effective structural measures for assisting downstream passage of juvenile outmigrants and riverine species is dependent upon behavioural criteria, and the knowledge of physical, hydraulic, and biological information which are critical to success (O.T.A., 1995). Selecting the proper arrangement of the louver array, how to position the louver array for the site, and meeting the bypass criteria involves a series of major decisions. Ott (1994) describes how factors such as project location, site geology, [louver array] material, type of stream debris and sedimentation, power considerations at the site, icing conditions, and the species of fish to be [diverted] all must be considered in the final design. Although, gathering, understanding, and analyzing information on all of these factors is essential to the success of a fish diversion device, good communication and cooperation between the engineers and biologists is of primary importance. If these guidelines are not established, what may appear to be well developed from an engineering perspective, may not necessarily meet the specific physical and biological criteria for the given site, and vice versa.

Research and development over the years, both hydraulic and biological, lead Mussalli *et al.* (1988) to conclude that louvers were effective. Results on their success were not always consistent so prototype and/or model testing of a louver array is recommended prior to its installation. Since each facility is site- and species-specific, thorough hydraulic and biological analysis is required in order to determine the optimum design criteria for the diversion device.

1.3 Thesis Objective

The objective of this investigation on using louver arrays as an effective means of guiding downstream migratory fish is to advance the understanding of the hydraulics of flow. Even though the research is being conducted at a preliminary stage, contributions from this study in regards to the flow characteristics within the louver array, as well as the determination of which physical parameters are significant to louver performance, will be beneficial to the science of louver array hydraulics.

This study of the hydraulics of louver arrays has basically been conducted in two phases. The first phase involved the field testing of a louver array for the purpose of reducing entrainment levels of juvenile rainbow trout (*O. mykiss*) within the Carseland irrigation canal, located approximately 50-km southeast of Calgary on the Bow River. Both the hydraulic and biological testing of the prototype louver array was conducted in a mobile experimental flume at the Sam Livingston fish hatchery in Calgary and in a similar rectangular flume at the T. Blench Hydraulics Laboratory at the University of Alberta. Information gathered from the first phase was then used to continue research into the second phase of the study. Phase Two involved the recording of water surface profiles, velocity profiles, qualitative flow observations, and photographs for a total of 22 different louver array arrangements and discharges.

2.0 LITERATURE REVIEW

The following literature review is intended to give the reader a basic understanding of louvers. The first section will focus on the history of louvers and shall be followed by a discussion on the flow characteristics associated with a louver array. Upon reviewing this fundamental information, an appreciation will be developed as to the criteria required in designing an effective louver array. The final section will address some of the other important factors required for successful downstream passage of fish.

2.1 History of Louvers

Late in 1951, original research into louvers as an effective means of safely guiding downstream migrating fish was conducted at Tracy, California by the U.S. Fish and Wildlife Service and the U.S. Bureau of Reclamation. The louver array was to be considered as an alternative method for fish diversion after testing revealed that the several types of fish screens initially installed were not performing adequately. From their studies of louvers in a test flume at the Coleman fish hatchery of the U.S. Fish and Wildlife Service and in the pilot structure at the Delta-Mendota Canal intake, Bates and Vinsonhaler (1957) discovered that striped bass, salmon, shad, catfish, and other species could be successfully diverted and collected by this system.

The awareness of high mortality rates of anadromous fish species, due to the presence of intake facilities, stressed the need for testing of the louver array within the coastal rivers of Canada. Ruggles *et al.* (1993) explained how mortality occurring at the smolt stage adversely affects the rate of adult recruitment and hence the yield from any specific fish stock originating from spawning areas upstream of the intake facility.

In 1957, 1958, and 1959, tests were conducted on an experimental louver installation on the Puntledge River [Vancouver Island, British Columbia] in an attempt to provide a satisfactory solution to the problem of screening downstream migrating chinook salmon fry (*Oncorhynchus tschawytscha*) from the water intake canal of the Puntledge River powerhouse.... Research was continued at Robertson Creek in 1960, 1961, and 1962 to evaluate the louver principle for guiding sockeye salmon (*O. nerka*) and coho salmon (*O. kisutch*) smolts from the water intake canal of a proposed hydroelectric project on the Stamp River System (Ruggles and Ryan, 1964). Due to intake canal velocities of 4.0 ft/s (Ruggles and Ryan, 1964), the use of a screen type of diversion structure was neither hydraulically nor economically feasible. In order to accommodate a fish screen system, it was estimated that the intake canal velocity would have to be about 0.4 ft/s (Ruggles and Ryan, 1964), thus drastically reducing the operating potential of the facility.

Having to screen the entire flow depth can become expensive if the canal in which the louver array is to be installed is relatively deep. Ruggles *et al.* (1993) sought out to resolve this economic problem by developing and testing a new concept based on the original louver array of Bates and Vinsonhaler (1957). Their research focused on testing the use of a floating louver array for downstream migrating fish guidance in a power canal of the Holyoke Dam located about 140-km upstream of the mouth of the

Connecticut River (Ruggles *et al.*, 1993). With the power canal having a depth of 6.0-m, it was decided that the louver array be designed for submergence depths of 2.4, 1.8 and 1.2-m. The concept of screening only the surface flow was based on observations made by Ruggles *et al.* (1993) that salmon smolts and downstream migrating anadromous clupeids tend to migrate near the water surface. With the results from the preliminary tests by Ruggles *et al.* (1993) showing that floating louvers are an effective alternative for downstream fish diversion, their use can now be considered in areas where they were once thought to be uneconomical and impractical.

Unlike extensive studies on upstream fish passage (*i.e.* fishway systems), laboratory research on louvers is very limited. Bates and Vinsonhaler (1957) should be partially accredited for their study, as there is seldom a first paper written on a pilot experiment which provides the research community with such a concise understanding of the principles of louvers. However, new ideas and/or applications are highly likely to occur with continued research on this topic. To study the hydraulics of louvers with the same intensity as it was done with fishways (Rajaratnam *et al.*, 1987, Katopodis, 1982; Sikora, 1997), could lead to new discoveries and further applications.

2.2 Flow Characteristics of a Louver Array

It is crucial that the hydraulic engineers involved in the evaluation of the louver array are able to thoroughly gather, analyze, and understand the necessary hydraulic data. Flow conditions created by the louver array must be suitable for the fish species expected to use it. As pointed out by O.T.A. (1995), outmigrating juveniles depend a great deal on hydrology and hydraulics to guide their movement.

The presence of a louver array within an intake facility creates an obstruction to flow. Bates and Vinsonhaler (1957) were the first to state that as water flows downstream and along the louver sections, small portions are progressively sliced off by each projecting louver slat.... Besides causing head loss, the louvers divert the flow into a channel at right angles to the main channel when the louver slats are placed at right angles to the direction of flow. As illustrated in Figure 1, this sudden change in flow direction creates an eddy between each louver slat with some of the flow being discharged to the downstream side of the array. To eliminate any problems that the circulating flow region could create, Bates and Vinsonhaler (1957) had flow straightening vanes developed to redirect the flow so it again paralleled the approach flow. The consequence of using a louver array without flow straightening vanes is best described by Bates and Vinsonhaler (1957): *When a system of louvers without flow straightening vanes is placed at an angle across a channel, a backwater build-up increases progressively upstream until at the upper end of the system very little water flows through.... This build-up is reflected by a water velocity increase of nearly 2.5 times from the upstream end of the louvers to the downstream end.* By keeping undesired backwater conditions to a minimum, ensures that a relatively equal distribution of flow is being discharged at each section between the flow straightening vanes.

In addition to making hydraulic observations on flow conditions within a louver array, it is necessary to simultaneously observe the behaviour of the fish as they pass through the system. It has been recommended by Ruggles and Ryan (1964) that changes in velocity in the flow upstream of a guiding apparatus should be gradual and that the flow into the fish bypass should accelerate gradually. In relation to this statement, Bates and Vinsonhaler (1957) observed that if a reduction in velocity occurs just ahead of or within the bypass, the fish usually stall in their movement and swim back upstream.... The confusion thus created may cause them to move between the louver slats rather than through the bypass.

Since the louver array acts under the influence of a local width contraction and subcritical flow conditions, one would expect the depth to gradually decrease and the velocity to gradually increase as the flow within the bypass section continues downstream towards the exit. Henderson (1966) states that as long as the contraction is not a severe one and the flow can be passed through it without requiring more specific energy than the upstream flow possesses, the contraction does not act as a "choke" [*a condition under which the available specific energy is no longer sufficient to pass the flow through the contraction*]... The flow within the contraction is therefore subcritical, as is the uniform flow for a great distance upstream and downstream. Being able to determine whether or not critical flow conditions are reached within the louver array is important to understanding how the contraction affects the flow. For this reason, it may be beneficial to calculate the Froude number (F) at various sections along the length of the louver array.

Bates and Vinsonhaler (1957) were able to form a correlation between the approach velocity and the required swimming speed of the target fish. Using vector analysis, they were able to determine the two components of the approach velocity as:

$$V_a = \sqrt{V^2 + V_s^2} \quad [1]$$

where V_a is the approach velocity component perpendicular to the individual louver slats, V is the velocity component parallel to the line of louvers, and V_s is the velocity component representative of the speed at which a fish must swim to overcome the force of component V_a and remain at a constant distance from the line of louvers while moving along component V.

Using basic trigonometry, Bates and Vinsonhaler (1957) also calculated the formula for the swimming speed in relation to the approach velocity as:

$$V_s = V_a \sin\theta \quad [2]$$

where θ is the louver array angle in degrees.

Figure 2 illustrates how varying the louver array angle alters the velocity component representative of the swimming speed of the fish. This principle aids in understanding why fish capable of swimming up to 1.0 ft/s, for example, are not swept through the system when approach velocities are well in excess of this value. It also provides an understanding as to why Bates and Vinsonhaler (1957) drew the conclusion that angles to flow greater than 40 degrees provided little or no guidance and the fish had difficulty finding the bypass. By applying vector analysis to louver projects prior to testing, it is possible to make an estimate as to what angle to set the louver array at and then be able to defend such a suggestion.

2.3 Design Criteria of a Louver Array

2.3.1 Location

Determining the location of the louver array within the canal intake is crucial to the success of the diversion device. To be effective, flow conditions occurring at the entrance to the louver array should be attractive to the approaching fish. ASCE (1982) states that fish will not enter the diversion device if they sense turbulence. To achieve acceptable flow conditions, it is necessary to place the array in a section of the canal where the approaching velocity has a relatively uniform profile. For example, employing the array immediately downstream of the canal entrance where flow is non-uniform and often turbulent would not be desirable. It is also required that trashracks be implemented a short distance upstream of the louver array to prevent damage from large debris. Along with protecting the louver array, Weitkamp and Elder (1993) point out that both the streamlining and the angle of these trashracks are important in eliminating eddies [thus creating a more uniform flow condition].

An important decision that could affect the guiding efficiency is in determining which canal intake along the river system (assuming more than one exists) the louver array should be employed at. In most cases, louver arrays are implemented at existing facilities where entrainment by the intake system is already known to cause excessive fish mortality rates. Before the louver array is installed, a biological study should be done so that an estimate of the occurrence and distribution of fish within the reach can be determined. This preliminary study would be useful in the future when comparisons are to be made on the fish entrainment levels of the water intake system prior to and following the installation of the louver array.

2.3.2 Construction Materials

An important factor in developing a feasible fish diversion device involves selecting materials that are easy to construct and maintain. From a biological perspective, the louver system must be "fish-friendly". Therefore, materials that have a tendency to corrode in water should be avoided as the metal particles that are shed into the channel may cause harm to the fish. Past studies have been conducted with the louver slats supported by wooden frames (Bates and Vinsonhaler, 1957; Ruggles and Ryan, 1964) and tubular steel frames (Ducharme, 1972), while in a recent study, the use of lexan was investigated (Anderson *et al.*, 1998). Louver slats have been made from such materials as steel (Bates and Vinsonhaler, 1957; Ruggles and Ryan, 1964) and polypropylene (Anderson *et al.*, 1998; Ruggles *et al.*, 1993). Regardless of the material chosen, the louver slats should have smooth edges to prevent injury to those fish that happen to come in physical contact with them. In practice, the louver slats should be rigidly housed within the top and bottom panels. If movement is permitted, the flow characteristics known to occur between each slat may cause them to oscillate. These oscillatory effects are undesired as they may lead to a decrease in both the structural integrity and the performance of the louver array.

2.3.3 Dependent Variables of a Louver Array

Along with influencing the hydraulic aspects of flow, the design criteria of each of the following 4 dependent variables of a louver array can have consequential effects on fish guiding efficiency:

1) *Louver array angle* (θ) - the acute angle which the line of louver slats makes with the channel wall. All of the fish diversion projects involving louvers in the U.S. and Canada have be conducted with a louver array angle ranging from 11 to 20 degrees (Bates and Vinsonhaler, 1957; Bates and Jewett, 1961; Ruggles and Ryan, 1964; Ruggles *et al.*, 1993, Stira and Robinson, 1997).

2) *Louver attack angle* (Ψ) - the angle which the broad face of the louver slats makes with the approaching flow. Most researchers have adopted a louver attack angle of 90 degrees as being standard. Although many have tried angles other than 90 degrees, the smallest attack angles used for preliminary testing of a louver array was conducted by Anderson *et al.* (1998) at angles of 41.2 and 31.4 degrees.

3) *Louver slat spacing* (s) - the maximum clear distance between two adjacent louver slats. Bates and Vinsonhaler (1957) state that spacing of slats appears to be related to the fish size and the amount and kind of debris present.

4) *Bypass width* (Z_b) - the width of the bypass exit. The bypass width will affect the amount of flow going to bypass and hence, lost for operational purposes. From a biological perspective, the bypass width will be dependent upon whether the target fish travel down the louver array in schools or individually.

2.3.4 The Fish Return System

After the fish are safely guided by the louver array, they must then be carried through a fish return system and reintroduced to the river. It is crucial that this process is undertaken without undue fatigue, injury or delay to the bypassed fish. ASCE (1982) states that a transportation system for the diverted fish is required between the diversion structure and the source water. They also define it in the following terms: *A return system consists of a bypass and a transition section, a pipeline, and an adequate [amount of flow] to discharge the fish back to their natural water.* Furthermore, Ruggles and Hutt (1984) state that the bypass design and the methods of collecting and returning salvaged fish to their natural environment should be based on the size, behaviour and physiology of the fish species to be protected.

The design of the fish return system is of utmost importance for successful fish passage. The following design criteria of a conveyance structure were described in a conference paper published in 1977 by Mussalli and Taft (ASCE, 1982):

1) All surfaces of conveyance structures must be smooth to prevent abrasion to fish.
2) The system size must be based on the size and number of fish.
3) Transport velocities must be larger than the sustained cruising speed of the fish.
4) Materials used for the structures must minimize biofouling.
5) Long radius ($r/d > 2.5$) bends must be provided so that fish do not abrade on the sides at the bend.
6) Pipe joints must be constructed carefully so that all edges match and there are no jagged protuberances.

7) Valves, meters, etc., must provide clear passage for the fish and create as little obstruction as possible.

8) All transitions must be gradual to prevent flow separation and rapid changes in velocity.

9) Smooth transitions must be provided where flow from several pipes or channels combine.

10) In Northern latitudes, above ground sluiceways or pipes must be protected from freezing. Buried pipes must be located below the frost depth.

11) A recovery pool may be necessary where shock or disorientation of fish can occur.

12) The outlet must be located well away from the intake to prevent re-entrainment.

13) The outlet must be located in an area where predation will be minimum and where water quality is adequate.

In relation to the last two statements, O.T.A. (1995) points out that the outfall pipes typically release fish above the water's surface to avoid the creation of a hydraulic jump [and to prevent re-entrainment by outmigrating fish].... Releasing fish above the water surface may also alleviate disorientation and help to prevent schooling [which is an attractive sight to predators].

2.4 Other Key Factors for Successful Downstream Fish Passage

2.4.1 Fish Physiology and Behaviour

Each facility must be designed with consideration of both the behavioural and physiological traits of the fish species known to be present. Although a louver array may prove to be successful at a specific site, the design criteria cannot simply be applied to another location where a similar type of fish protection system is desired.

Providing for effective downstream fish passage begins with acquiring knowledge of the life stages and species present within the study. This information can be used to determine the size (*i.e.*, width, depth and length) and swimming capabilities of the fish; these two factors influence both the structural and the hydraulic design of the diversion system. In addition, the average size of the fish species can also be used to determine the required spacing of the louver slats and the dimensions of the fish return system. In common with most fish populations, length within a single age cohort follows an approximately normal distribution (Turnpenny, 1981).

Swimming capabilities of the fish allow the hydraulic engineer to determine the maximum allowable approach velocity entering the louver array. Brett (1963) states that the idea is to maintain approach velocities within fish cruising speeds. Although this guideline may be important for alternative methods of fish diversion, it has already been shown from Figure 2 of subsection 1.4.2 that the maximum allowable approach velocity can be calculated by dividing the fish swimming speed by the sine of the louver array angle. As a generalization, Blaxter (1969) states that most species can maintain cruising speeds of 2 to 3 body lengths per second, but salmonids and clupeids can probably maintain speeds of about 4 body lengths per second or more. With consideration of the above statistics, it is possible to maintain channel velocities within a range where the fish are able to maneuver their way towards the bypass and escape being drawn into the louver array. If the velocities are too high, the fish will be out of control and not be able to respond to the obstruction when moving along the array. In addition, the fish may overexert themselves by attempting to remain within the bypass section and away from the louver slats. A louver array can not be considered successful if, as a result of being bypassed, the fish have experienced excessive stress levels and end up in a state of shock.

Knowledge of the life stages and fish species that will be using the louver array may aid in the understanding and prediction of natural behaviours. Although O.T.A. (1995) points out that it becomes impossible to predict how a fish might alter its behaviour when it encounters a hydropower facility or water bypass, general trends could be developed and used if research into behavioural mechanisms continues. Contrary to and despite the above statement, O.T.A. (1995) are also of the opinion that downstream protection devices must take advantage of natural fish behaviour.

The presence and behaviour of fish species at a diversion device may occur for various reasons. Climatic conditions caused considerable daily variations within the general seasonal patterns.... Different species show markedly different seasonal patterns (Langford *et al.*, 1977). Since fish are unpredictable, even within a species, biological testing becomes quite a repetitious task. In evaluating an alternative fish diversion system, Winchell *et al.* (1992) made certain that each test combination of the required velocities was replicated several times in daytime and at night. In their study, Ruggles and Ryan (1964) found that significant differences in fish guiding efficiency occurred between daytime and nighttime migration. They suggested that it may have been caused by either, a) a visual response of test fish to louvers at various light intensities, or b) a basic change in behaviour of the relatively small numbers of fish [for this specific study] that migrate during the day. Through constant monitoring, Winchell and Sullivan (1991) were able to ensure that the target fish were in peak migratory (smolted) condition at the time of testing. The reason for their precise timing is due to the smolts being most susceptible to scale loss injury during this stage in their lives.

Vital information about behavioural traits can be gathered through qualitative observations on the position of a fish moving downstream along a louver system. Anderson *et al.* (1998) obtained such information from the field testing of a louver array for the guidance of juvenile rainbow trout (*O. mykiss*). The first behaviour pattern observed was that the test fish would typically orient themselves parallel to the flow and actively swim against the current. They were also observed migrating to the base and sides of the experimental flume where flow was significantly lower than that found at its center-plane. Their movements throughout the length of the louver array would be similar to those shown in Figure 3. Further observations revealed that the fish continued to face upstream and showed little to no lateral movement as they were carried with the flow towards the bypass at the downstream end of the louvers. A second behaviour pattern, shown in Figure 4 involved the display of lateral movement away from the louvers with the fish placing their lateral side against the approaching flow. When this occurred, an increase in downstream movement occurred and these fish tended to move towards the bypass at a faster rate than those that demonstrated the behavioural pattern described by Figure 3. A third behaviour pattern was typical of fish which, upon entering the louver array facing upstream, would turn and make darting flashes towards the louver array in an attempt to get through. As illustrated by Figure 5, this attempt would generally be unsuccessful and the fish would orient themselves facing downstream while swimming along the louver array for a brief moment before turning around to face the approaching flow. These fish tended to move through the length of the louver array faster than both those behavioural patterns described by Figures 3 and 4. Similar observations on the position of a fish moving downstream along a louver system were also described by Bates and Vinsonhaler (1957), along with the two following observations: *When velocities exceeded swimming speed, it was observed that fish orient themselves to the line of louvers at angles from it ranging up to 90 degrees.... The magnitude of the change in orientation is a function of the velocity of flow and the angle of the line of louvers.*

2.4.2 Control of Debris Accumulation

The accumulation of large amounts of debris along the face of a louver array may create a significant reduction in both the fish guiding efficiency and the operation efficiency of the facility. Although Clay (1961) stresses the importance of keeping screens clean to reduce approach velocities and head loss, the same hydraulic guideline can be applied to louvers. From a biological perspective, changes in flow conditions as a result of the louver slats being partially clogged with debris could possibly lead to an increase in the injury rates of fish.

Knowledge of the size, type, and concentration of debris that is found within the river upstream of the louver array would be beneficial in the prediction and prevention of future accumulation problems. An investigation of debris flow conducted by Smith (1982) required collecting river samples from a transect across the river near the water intake of the facility.... A total of nine samples collected on each run were taken from near-surface, mid-depth and near-bottom for the stations near each bank and at mid-channel. Due to the annual variability of debris concentration within a river reach, testing of clogging rates should be repeated several times throughout the year. Smith (1982) observed that the clogging rate for a screen is a function of water chemistry, hydraulic conditions, sediment and detritus load, screen material, orientation to flow and size of opening. Disregarding the two variables of screen material and size of opening, the remaining variables would also apply to a louver array. Other variables that could be considered for the clogging rate of a louver array are louver slat spacing and bypass width.

2.4.3 Diversion Time

It is important to bypass downstream migrating fish through a diversion system in a safe and efficient manner. Unnecessary periods of delay within the system can lead to undue stress, fatigue or injury of the fish. The occurrence of such physical and emotional abuse has the possibility of creating immediate or latent mortality. Such factors can be avoided as long as all aspects of the biological and hydraulic design criteria are fully addressed. Ideally, the diversion time of fish moving through a louver array system, from entrance to exit, should be comparable to the time it would take the fish to travel the bypassed length of the river under unaffected, natural conditions.

3.0 EXPERIMENTAL INVESTIGATIONS

3.1 General

Since this study involved testing of the louver arrays under both field and laboratory conditions, the experimental investigations conducted for each were not identical. Therefore, to avoid confusion as to which phase of the study is being addressed, the sections of this chapter have been subdivided by their respective phases.

3.2 Experimental Apparatus

3.2.1 Phase One

The field testing of a prototype louver array was conducted in the Ichthyo-Hydraulics Mobile Experimental Flume, referred to from here on as the *I-H Flume*. This experimental flume was built for the purpose of studying fish responses to hydraulic structures under near-prototype conditions. Since it was mobile, the I-H flume allowed for testing near rivers and streams, as well as indoors. The flume was designed and constructed through the collaboration of the Freshwater Institute, Department of Fisheries and Oceans, Government of Canada, and the T. Blench Hydraulics Laboratory, Department of Civil and Environmental Engineering, University of Alberta.

The I-H Flume, which was illustrated in the plan view of Figure 6, consisted of five detachable components for ease of transportation. Two identical components, each 9.75-m in length (X), made up the rectangular testing channel. The headtank, the tailtank, and the pump skid were the remaining three components. The testing section of the flume, located between the headtank and tailtank, was 19.5-m in length, 1.0-m in width (B), and capable of handling a maximum flow depth (Y) of 1.2-m. The headtank and tailtank were both 2.4-m^2 in plan and each contained a fish holding compartment. This allowed the fish to be introduced and tested whether they were moving upstream or downstream. A variable speed diesel-powered pump capable of circulating up to 640-L/s (22.6-ft^3/s) of water between the two tanks controlled the flume discharge (Q). The flow was pumped from the tailtank to the headtank through a 16 inch diameter return pipe located parallel to the flume. One wall of the test flume section was constructed from clear lexan to allow for visual observations.

Due to winter weather conditions, the remaining two louver series were completed indoors in the T. Blench Hydraulics Laboratory at the University of Alberta. These test series were performed in a 36.9-m long, 0.90-m wide, and 0.90-m deep horizontal flume. The flow was pumped from the floor sump and piped into the flume headtank. A gate valve located immediately downstream of the pump controlled the amount of discharge entering the flume. A magnetic flow meter located just downstream of the valve allowed for accurate values to be read from a voltmeter and converted to discharge. Flow conditions within the flume section were controlled by a tailgate located at the downstream end of the flume. Due to the varying widths of the two flumes used in this study, the bypass width of the louver array had to be slightly narrower in order to incorporate 23% of the total flume width. This percentage is identical to all of the series done in the I-H Flume, except for one series at a louver array angle of 17.0 degrees that took up 26% of the flume width.

The prototype louver array was constructed and designed by Applied Biometrics Inc. (ABI) at the University of Waterloo. It was composed of sections of top and bottom lexan panels, each between 1.0 and 1.2-m in length. At louver array angles of 7.2 and 17.0 degrees, for tests performed in the I-H Flume, the array was 2.3 and 5.6-m in length (L), respectively. Due to contrasting flume dimensions, the two 17.0 degree series that were carried out in the laboratory flume consisted of a total array length of 2.1-m. The 0.90-m high vertical slats (h) were evenly spaced 60-mm apart. Each louver slat was constructed of black polypropylene having a width (w) and thickness (t) of 64.0 and 3.4-mm, respectively. A useful design feature for the testing of various louver attack angles was the ability for the louver slats to pivot in unison while set in place.

A unique characteristic of the louver slat was the use of a convex shape instead of the usual flat face. Due to the convex shape of the louver slat, as seen in Figure 7, the flow became re-directed as it passed through the array and into the canal section. For such a design, each louver performed in a manner similar to the flow straightening vanes used by Bates and Vinsonhaler (1957). The flow struck the louvers at an upstream attack angle (Ψ_1) of 55.3 degrees and then exited the array at a downstream attack angle (Ψ_2) of 20.0 degrees. Instead of using an average of these two angles, the louver attack angle was taken as the angle of the straight line formed from tip-to-tip of a slat. As a result, the louver attack angle for the 7.2 and 17.0 degree arrays was 41.2 and 31.4 degrees, respectively. This louver attack angle was taken with respect to the direction of flow.

3.2.2 Phase Two

The laboratory testing of a prototype louver array, illustrated in Figures 8a and 8b, was conducted in the same flume as the two additional series of Phase One. However, this particular array was designed and constructed at the T. Blench Hydraulics Laboratory of the University of Alberta. Being of a preliminary nature, the design of the louver array employed in this phase of the study was purposely kept simple. Tests were performed at louver array angles of 10 and 15 degrees to flow. The attack angle of the louver slats for both cases was set at 90 degrees (perpendicular) to flow. The louver slats were made from galvanized sheet metal and, unlike those curved slats of the first phase, had a flat profile. Each slat was 0.81-m in height, 50-mm in width, and 3.2-mm in thickness. The panels of the wooden support structure were designed so that the louver slats could be slid in through the top panel and fitted into the bottom panel. With a 50-mm spacing between each of the slot openings, the louver slat spacing could be set at any multiple of this value. In order to study the hydraulic effects of the opening between the louver slats, it was decided that a spacing of 50 and 100-mm be used. The proportional bypass width at the exit section of the louver array (Z_b/B) was set at 5, 10, and 15% of the total flume width. At these respective values, the lengths of the louver array were 4.875, 4.675, and 4.375-m, respectively, for the 10 degree array, and 3.215, 3.065, and 2.915-m, respectively, for the 15 degree array. To ensure that the louver array was located at a section where the flow had stabilized, it was employed approximately 20-m downstream of the headtank.

3.3 Experimental Nomenclature

3.3.1 Phase One

In a technical report submitted to the Alberta Department of Environmental Protection by the author and several others (Anderson *et al.*, 1998), the six series of Phase One were coded with respect to the louver array angle and engine speed of the I-H Flume pump (ω). For example, L7.2_775 was one of the six abbreviations and, when deciphered, explained that the test was being performed on a 7.2 degree louver array at an engine speed of 775-rev/min. Using a flume calibration chart, it was possible to determine the approach depth-averaged velocity (U_o) from the engine speed value. Although the system of code addressed here was used in the technical report, for the sake of simplicity, it has been made to adopt the nomenclature of Phase Two.

3.3.2 Phase Two

An abbreviated system of code was devised for Phase Two of the study in order to prevent confusion as to which test series was being referenced. This system was used to fully describe the four physical variables of louver array angle, proportional bypass width, approach-depth averaged velocity, and louver slat spacing for any given series. For example, Series *10/0.05/0.30/B* was one of many such abbreviations and so happens to be the initial test of the investigation. Proceeding from left to right, the first designation refers to the louver array angle of either 10 or 15 degrees to flow. The second designation indicates that the proportional bypass width as a fraction will be 0.05, 0.10, or 0.15. The third designation corresponds to the approach depth-averaged velocity and it can vary between 0.30 and 0.60-m/s. The capital letter of the last designation defines the louver slat spacing and will be either 'A' or 'B' depending on whether the spacing is 50 or 100-mm, respectively. When an asterisk (*) is used in place of any of the four designations, it means that all of the values within that designation are included.

When its abbreviation is deciphered, the example of Series *10/0.05/0.30/A* describes the arrangement as a louver array set at 10 degrees to flow with a proportional bypass width of 5%, an approach depth-averaged velocity of 0.30-m/s, and a louver slat spacing of 50-mm. If the second designation of the above example were to be replaced by an asterisk so that it was coded as Series *10/*/0.30/A*, this would indicate the inclusion of Series *10/0.05/0.30/A*, *10/0.10/0.30/A*, and *10/0.15/0.30/A*.

Including the six series of Phase One into the nomenclature determined for this phase of the study does not affect the designations of the abbreviated system of code. However, the letter 'C' had to be added to the fourth designation in order to describe a louver slat spacing of 60-mm, common to all of the Phase One series.

3.4 Experimental Procedure

3.4.1 Phase One

3.4.1.1 General

The aim of this phase of the study was to examine the suitability and effectiveness of a louver system for the guidance of hatchery-reared juvenile rainbow trout (*O. mykiss*). From a hydraulics perspective, this meant developing an understanding of the flow characteristics of the louver array that occurred for various physical arrangements and discharges. Consequently, the three variables of discharge, louver array angle, and louver attack angle were altered to produce the six test series. The alteration of the latter variable was done indirectly as a result of the changes made to the louver array angle. By keeping the louver slats in a fixed position on the support structure, any change in the louver array angle directly influenced the angle at which the slats impinged the flow.

Four of the six test series were conducted outdoors in the I-H Flume at the Sam Livingston fish hatchery in Calgary. Shortly after the hydraulic data had been gathered and analyzed, it was decided that two more series were still necessary for the 17 degree louver array. As already mentioned in subsection 3.2.1, winter weather conditions forced the remaining tests to be completed indoors at the T. Blench Hydraulics Laboratory of the University of Alberta. Including the data from these two tests aided in making the overall findings for the 17 degree louver array more conclusive.

3.4.1.2 Flume Calibration

Since this was the first time the I-H Flume had ever been used, it was necessary to examine its operating performance and also conduct a flow calibration. Upon entering the headtank, a significant portion of the flow energy was dissipated by a perforated baffle wall. Immediately after being calmed by the baffle, the flow had to then be turned 180 degrees by two turning vanes spaced equidistant to one another and the adjacent flume wall. By injecting red dye at various locations within the flume section (while operating at a moderate discharge), it was observed that the flow was relatively stable by the time it had traveled about 3 to 4-m downstream of the headtank exit. Knowledge of this flow characteristic concluded that uniform flow conditions would most likely be achieved if the louver array were located with its entrance just downstream of the midway section of the flume. Velocity profiles taken at three equidistant locations across the flume at this section further indicated that the flow was, in fact, relatively uniform and one-dimensional.

Since the I-H Flume was calibrated against the output of its pump, all of the approach depth-averaged velocities had to be determined with respect to the rpm gauge reading of the diesel engine. A calibration curve was determined by taking a center-plane velocity profile at the midway section of the flume with a *StreamFlo* velocity meter. From this curve, it was determined that at readings of 775, 1200, and 1800-rev/min, the equivalent approach depth-averaged velocities were 0.20, 0.35, and 0.50-m/s, respectively.

Since the two series performed at the T. Blench Hydraulics Laboratory were to be used in conjunction with the other four series tested in the I-H Flume, it was desired to have similar flow parameters. At a flow depth of approximately 0.60-m, it was found that the laboratory flume was able to achieve the same approach depth-averaged velocities as those used in the I-H Flume. To ensure that the louver array was located at a section where the flow had stabilized, it was employed approximately 20-m downstream of the headtank.

3.4.1.3 Velocity Measurements

Velocity measurements were recorded using a *StreamFlo* velocity meter. Frequency values (f) were read directly from the current meter box using a 10 second average and then converted from hertz to velocity using calibration charts. To ensure that the measurements being recorded were accurate, the average of 5 frequency values was obtained at each velocity meter depth (y) within the section. If the current meter gave low and inaccurate readings it was usually an indication that fine debris was caught up in and impeding the propeller.

Velocity profiles were obtained at specified locations along the length of the louver array. After using six profile sections for Series *7.2/0.23/0.30/C*, it was determined that four sections would be adequate for the remaining two tests of the 7.2 degree louver array. Since the array length was significantly shorter at a 17 degree angle to flow, only three profile sections were employed for these three test series. Velocity measurements for each profile were taken vertically from the flume bed to within at least 10% of the water surface. Velocity distributions taken at various points throughout the length of the bypass section were located equidistant from the louver array and the flume wall. Depending on the series being tested, the depth-averaged approach velocity was located between 0.10 and 0.34-m upstream of the louver array entrance in the center-plane of the flume.

3.4.2 Phase Two

3.4.2.1 General

This phase of the study was a laboratory-based continuation of the preliminary testing of a prototype louver array for the guidance of downstream migrating fish. Having more time budgeted for this phase allowed for a greater number of physical parameters and discharges to be tested. In contrast to the field testing, it was possible to study this louver array using equipment that could measure velocity and flow depth with higher levels of accuracy. To contribute to the understanding of the hydraulics of louvers, water surface profiles, velocity measurements, qualitative flow observations, and photographs were obtained for the 22 test series that were conducted.

3.4.2.2 Water Surface Profiles

A total of 84 different water surface profiles were measured, recorded, and analyzed for both the bypass and canal sections of the louver array. Using these profiles, it was possible to visualize how the water surface varied for the different arrangements and discharges. In addition, differences between the water surface profiles of the bypass and canal sections of any given series could also be observed. From a quantitative perspective, the values obtained from the water surface profiles made it possible to determine the elevation losses that occurred throughout the length of the louver array.

The setup of the measuring device allowed for complete mapping of the water surface profile at any point within the louver array. To determine the water surface level for each point along the louver array involved using a point gauge fitted with a vernier of one-tenth of a millimetre accuracy. The point gauge was secured to, and capable of. sliding along an aluminum support that spanned the width of the flume. The support was placed along the top of the flume walls and secured on one side by a clamp.

The flow depth at any point within a cross-section was obtained by calculating the difference between the point gauge reading of the flume bed and the water surface. For any given test series, the flow depth at the approach section was taken in the center-plane of the flume at a location 2.0-m upstream of the louver array entrance. Numerous flow depths were measured at sections throughout the louver array up to and including the exit of the bypass and canal. For the accuracy of the gauging instrument to be beneficial, it was necessary to determine when its tip had just come into contact with the water surface. The easiest way to determine the point of initial contact was by slowly lowering the gauge towards the water surface and observing when a surface wake instantaneously began forming downstream of the gauge's tip. In those sections of the louver array where the water surface level was not constant, personal judgment had to be used in order to determine an approximate value.

3.4.2.3 Velocity Measurements

In order to achieve a more thorough understanding of the flow characteristics of the louver array, it was necessary to conduct measurements on velocity for the various geometrical arrangements and discharges. By altering the 4 physical variables of discharge, proportional bypass width, louver slat spacing, and louver array angle, a total of 22 series of velocity profiles were obtained. Had it not been for a generalization that was discovered from an analysis of the first 12 velocity profiles of Series *10/*/*/B*, the testing of 20 more series would have been required. This important realization also made it possible to conduct the same experimental work on the 15 degree louver array without exceeding the time limits of the study. From this point onward, it was determined that only one-third of the previously expected tests would need to be conducted. To maintain the context of this subsection, specific details of this generalization will not be addressed until Section 4.

Velocity measurements were recorded using a Prandtl-type pitot-static tube and a transducer. Re-calibration of the transducer was done on a daily basis if it was used for an 8 hour period, otherwise, every 3 to 4 days was found to be adequate. The static and total head lines coming from the Prandtl tube were connected to the transducer, capable of measuring velocities up to 1.58-m/s. The differential pressure reading of the transducer was converted into inches by the carrier demodulator and then recorded into the computer. The time required to analyze the differential pressure readings was drastically reduced through the application of an in-house software package developed by Dr. S. Wu at the T. Blench Hydraulics Laboratory. For each velocity measurement, this user-friendly program was set up to record a total of 400 samples at a rate of 40 samples per second. To ensure that the test data was accurate, any velocity measurement that produced a standard deviation greater than 0.025 was rejected and tested again.

By injecting red dye into areas of the bypass section where velocity profiles were to be taken, it was determined that the flow, if not parallel, was angled less than 5 degrees to the flume walls for the entire length of the louver array. Based on this observation, the Prandtl tube was aligned so that it paralleled the flume walls for all measurements. Confidence in this decision was provided by Rajaratnam and Muralidhar (1967) in their statement that the magnitude of the velocity could still be satisfactorily measured using the Prandtl tube if the angle of the velocity vector with the tube was less than about 15 to 20 degrees. Obtaining velocity data for the canal section would have required the use of an instrument capable of measuring three-dimensional flow. Therefore, to keep within the scope and time frame of the study, velocity measurements within the canal were left for future research.

Determination of the velocity profile locations was based upon visual observations of flow within the bypass section of the louver array and from the experience gained in recording velocity measurements in Phase One of the study. Locations of the velocity profiles were done at various sections along the louver array length. Velocity points were recorded in the vertical direction from the flume bed to within about 10% of the water surface. Regarding both phases of the louver study, the uppermost point in any profile was given a false value equal to the data point previously measured below it. This procedure was performed so that a mean velocity for the profile could be calculated for the entire flow depth and also to indicate the elevation of the water surface. For all series of Phase Two, the velocity profile of the approach section was measured 2.0-m upstream of the louver array entrance in the center-plane of the flume. For about the upper two-thirds of the 10 degree louver array, 3 equidistant velocity profiles were recorded at each cross-section. Since a reduction in the width of the bypass occurred as the flow progressed downstream along the array, there was continually less space for profiles to be recorded without becoming overly discrete. Therefore, in the second last cross-section of the same arrangement, only 2 equidistant profiles were necessary. For the 15 degree louver array, all of the cross-sections located between the entrance and exit contained only 2 equally spaced velocity profiles. Regardless of the louver arrangement, the bypass exit had only one velocity profile at the center point between the last louver slat and the adjacent flume wall.

3.4.2.4 Photography

The main purpose of this part of the study was to capture several of the flow characteristics within the louver array, which are best described pictorially. In addition, having actual photographs of the experimental apparatus is believed to be beneficial to the viewer in developing a clear picture as to what was being studied. All of the photographs were shot using a Pentax K-1000 manual focus camera. Comparisons and contrasts could be made as similar photographs were taken for both louver array angles at an approach depth-averaged velocity of about 0.50-m/s. The only difference between the two arrays may be in the scale of the picture, as the 10 degree louver array was shot with a wide-angle 28-mm lens and the 15 degree louver array was shot with a standard 50-mm lens.

A 640 by 420-mm thread grid, which consisted of an aluminum frame and 25-mm square wire grids, contributed a great deal to the preliminary understanding of the flow patterns within the canal section of louver arrays. A tuft of woolen black thread approximately 25-mm long was secured at each intersection of the wires. Using high-speed film, it was possible to capture an overall image of the grid as a representation of the flow pattern occurring for that particular canal section and flow depth. With the grid located horizontal to and just below the water surface, worthwhile images of the flow pattern were produced. Since the water surface was disturbed and air bubbles were present, photographs of the thread grid when it was submerged by more than about 25% of the flow depth were unclear and, therefore, had to be excluded.

4.0 EXPERIMENTAL RESULTS AND ANALYSIS

4.1 Experimental Results

4.1.1 General

This section will address both the qualitative and quantitative aspects of the louver array for the various physical parameters and discharges. Although this study on louver array hydraulics was conducted in two phases, a vast majority of the data was obtained from the louver arrays tested in the second phase. The experimental data of all 28 test series was summarized and then illustrated accordingly in Tables 1 and 2. In regards to Phase One of the study, contributions of quantitative data consisted of the six velocity profiles measured for the 7.2 and 17 degree louver array arrangements. As a result, the following three subsections that pertain to qualitative flow observations, water surface profiles, and velocity profiles will be with respect to the experimental results of Phase Two, unless stated otherwise.

4.1.2 Qualitative Flow Observations

Throughout the second phase of this study, hydraulic characteristics of the louver array were observed for all of the test series, as it was believed that a visual appreciation of the flow would be beneficial. In addition to studying the flow with the naked eye, photographs for Series *10/0.10/0.50/A*, *15/0.05/0.50/A*, and *15/0.05/0.50/B* were taken using a 35-mm camera with high-speed film. By capturing still-shot images for these 3 series, additional flow characteristics that would not have been visible during the normal operation of the louver array could now be observed.

A general conclusion that was drawn from Phase Two of the study was how remarkably similar the flow conditions were for all of the test series conducted. Although the range of discharges present may have caused a slight change in their magnitude, the overall characteristics of the flow remained unchanged. As a result, those qualitative observations stated in this subsection that lack reference to any one specific test series should be considered to address the entire phase of the study.

The flow depth within the bypass section of the louver array was the first factor considered in the qualitative portion of this study. At a location immediately upstream of the louver array entrance, the flow depth was noted as being constant. By injecting red dye at various points within the cross-section, it was then established that the flow was relatively uniform. Viewing the flume test section in profile, as illustrated in Plate 3, it became apparent that the reduction in flow depth was non-linear as the flow progressed downstream towards the exit section of the bypass. Within approximately the upper two-thirds of the louver array, the flow depth decreased gradually in the longitudinal direction. Beyond this point, the water surface level shown in Plate 11 began to decrease at a much faster rate as the flow proceeded towards the bypass exit. Although it was clearly visible that the bypassed flow had significantly increased in velocity over a short distance, there was no indication that either supercritical flow conditions had been reached or a hydraulic jump had formed downstream of the louver array. The presence of surface waves caused the water surface to become non-uniform, making it difficult to accurately determine whether or not the flow depth in the transverse direction could be considered constant.

Surface waves were visible throughout the entire length of the bypass section and their presence increased as they continued downstream. These surface waves, visible in Plate 10, were thought to be created by the minute portion of flow that was deflected by each individual louver slat and could be seen traveling across the bypass section at angles much greater than what the louver array was angled at. Once the waves reached the adjacent flume wall, they were reflected back towards the array. Based solely on observations of surface waves, it seemed as if the flow was constantly being deflected as it moved along the louver array. However, further analysis indicated that the surface waves were by not characteristic of the overall direction of flow. Using red dye, it was determined that the flow below the water surface remained relatively parallel to the flume walls as it traveled downstream.

Since velocity measurements within the canal section were not attainable for this study, it was necessary to obtain as much information as possible from qualitative flow observations. Series *10/0.10/0.50/A* and *15/0.05/0.50/A* of Plates 1 and 10, respectively, were used to illustrate the contrast in flow conditions between the two main sections of each louver array. Compared to the bypass section, there seems to be significantly more turbulence occurring in the canal section. This visual observation was verified as slugs of red dye, injected at various points within the canal section, were immediately broken up by the erratic flow. It was also visible to the naked eye that the flow depth throughout the canal section fluctuated over time. Making reference to a mark on the flume wall, the water level varied by about $\pm$20-mm in the vertical direction. The flow of the canal section could be described by a progressive depth increase in the upstream direction, downstream flushing of the built-up water, and then repetition of the procedure. Based on this observation, it was prematurely concluded that flow depth measurements within the canal section would have to be recorded at an average flow depth between the two extremes. Viewing Plate 4 of Series *10/0.10/0.50/A*, it was determined that the upstream half of the louver array structure did not substantially contribute to the passing of water into the canal section. Especially for the first few louver slats, the flow was being re-directed in the direction of the flume wall and, consequently, the built-up flow progressed upstream to create a backwater effect. The same phenomenon was also apparent for Plates 12 and 13 of Series *15/0.05/0.50/A*; however, a smaller portion of louver slats contributed to the backwater effect and the flow was being effectively passed through the downstream two-thirds of the louver array. As mentioned by Bates and Vinsonhaler (1957) in their study, it was possible to eliminate the effects of backwater by employing flow-straightening vanes within the system of louvers.

To demonstrate how the non-uniform flow conditions of the canal section affected the overall performance of the louver array, a 2-inch square block of ¾-inch thick plywood was placed approximately halfway downstream of, and up against, the louver array structure. While floating at the water surface, the wooden block remained within one louver slat width of the array and in a stationary position. When placed next to the louver array at about 0.25-m upstream of the exit section, the block slowly began to progress upstream as it flowed atop the eddying water. Once it reached approximately the halfway point where it was previously placed, the block again remained stationary. The final tests involved placing the block of wood at the same horizontal distances along the louver array as the two tests previously conducted, but closer to the flume wall. In both cases, the wooden block progressed downstream and almost parallel to the flume wall without any noticeable delays. Only in regards to what occurs at the water surface, it was illustrated that the flow was non-uniform immediately after it passed through the louver slats. However, the flow did re-align with the flume wall to some extent, as distance from the louver array increased.

A more precise understanding of the flow directions within the canal section was obtained by inserting a thread grid in the horizontal plane, just below the water surface. With the grid wires aligned so that they ran parallel to the flume walls, the tufts of thread gave a good indication as to the flow direction within each 25-mm square area. Illustrated in Plate 8 of Series *10/0.10/0.50/A*, the flow patterns within the upper third of the louver array structure contained a substantial amount of circulating flow. Further downstream near the exit section of the louvers, Plate 9 of Series *10/0.10/0.50/A* revealed that a majority of the flow had become re-aligned with the flume walls. Nonetheless, the eddying flow that was characteristically found at a location proximal to the louver array was still present to some extent. Instead of capturing flow patterns in two different locations, Plates 14 through 17 were photographed in order to illustrate the differences between Series *15/0.05/0.50/A* and *15/0.05/0.50/B*. The narrower louver slat spacing of Series *15/0.05/0.50/A* seemed to produce eddies of slightly less intensity, and also had more thread tufts either angled to or perpendicular to the flume walls. In spite of this observation, it was difficult to determine any largely distinguishing features.

Although observations had been made on the two main sections of the louver array, it was equally necessary to obtain an understanding of the flow conditions that occurred between the louver slats. Upon turning the approaching flow by an angle of 90 degrees, an intense eddy was created between each louver slat with the magnitude of the intensity increasing in the downstream direction. At the water surface, the flow that was impinged between the louver slats initially rode up against the protruding face of the downstream slat before plunging into the canal section. To determine whether or not a similar behaviour was occurring throughout the entire flow depth, red dye was injected at various vertical points between two adjacent louver slats. The flow was found to be non-uniform in the vertical direction, as the dye boiled up towards the water surface. In fact, the flow could definitely be described as being three-dimensional within close proximity of the louver array structure. The observation of the flow boiling up towards the water surface indicated that a higher discharge into the canal section was occurring through the lower portion of the louver slats. In addition to the occurrence of eddying flow conditions, it was determined that the flow depth between neighboring louver slats was characteristically less than the adjacent flow depth of the bypass section. The difference between the two flow depths was observed to increase the further downstream along the louver array measurements were taken. Furthermore, it was quite obvious that a majority of the discharge into the canal was being contributed from the bypass section within the vicinity of the exit.

4.1.3 Water Surface Profiles

In Phase Two of the louver study, a total of 84 water surface profiles were measured for the various physical arrangements and discharges. The water surface profiles, graphically illustrated in Appendix A, were recorded in both the horizontal and transverse direction. The transverse profiles of Graphs A-1.1 to A-1.4 illustrated that the water surface level throughout the length of the louver array remained relatively parallel with respect to the flume bed. If there was any apparent deviation from a zero slope, it was observed to be in the direction towards the louver array structure. With nearly a constant flow depth across the bypass section, the transverse water surface levels of a particular section were width-averaged in order to obtain a single flow depth measurement. The same procedure was also performed on the data points of the canal section, as similar characteristics of the water surface were observed there. Having only one data point to contend with at each transverse section prevented the profile graphs from becoming cluttered with unnecessary data. Graphs A-2.1 to A-2.4 of Appendix A, which illustrated the water surface profile along the horizontal axis, were indicative of the width-averaged profiles of the bypass section and the canal section. By observing these graphs, it was apparent that the water surface profile for all of the series was slightly higher in the bypass section than in the canal section. In spite of this generalization, the graphs showed that the difference between each corresponding elevation was practically negligible.

The quantitative measurements of the water surface profiles along the horizontal axis were found to be similar to the qualitative observations mentioned on this topic.

Previously addressed in subsection 4.1.2, the water surface profile was observed to gradually decrease within approximately the upper two-thirds of the louver array and then decrease at a much faster rate as the flow proceeded towards the exit section. Although this statement was made only in regards to the bypass section of the louver array, it was also found to be applicable to the canal section now that it had been quantitatively proven to bear similar profile characteristics.

Since velocity measurements were not attainable within the canal section of the louver array, it was necessary to obtain as much information as possible from the water surface profiles alone. In order to compare related test series, the water surface profiles along the horizontal axis were observed in a non-dimensional form. These normalized water surface profiles of the 10 and 15 degree louver arrangements were graphically illustrated by Figures 9 through 16. Using Figures 9, 11, 13, and 15, it was possible to study the test series of differing proportional bypass widths for the 10 and 15 degree louver arrays. A similar analysis was also conducted using Figures 10, 12, 14, and 16 for the various louver arrangements tested at different approach depth-averaged velocities. A correlation between the approach depth-averaged velocity and the normalized flow depth at each cross section was found to occur in Figures 9, 11, 13, and 15. On a consistent basis, the series within each figure that contained the highest approach depth-averaged velocity tested, produced the lowest values of normalized flow depth. In regards to Figures 10, 12, 14, and 16, the general consensus was that testing the proportional bypass width at 5, 10, or 15% of the total flume width had no significant effect on the width-averaged water surface profile within either section. In addition to these experimental results, the water surface profile data could have also been used to determine the elevation loss occurring throughout the length of the louver array. However, details of this important factor will be later mentioned in the section that pertains to the analysis of the data.

4.1.4 Velocity Profiles

Velocity measurements within the bypass section were taken for both phases of the study on louver array hydraulics. A total of six test series was equally divided between the 7.2 and 17 degree louver array arrangements employed in Phase One. Due to time constraints and the inaccessibility of highly accurate instrumentation in this field study, it was decided that only center-plane velocity profiles within the bypass section be measured. This decision was later justified by measuring sample velocity profiles with the current meter at various sections along the array, which revealed that velocity in the transverse direction varied insignificantly. In reference to all six of the test series, Figures 17 and 18 indicated that the center-plane velocity profiles of the bypass section were relatively uniform. In Phase Two of the study, it was believed that using the Prandtl tube could possibly determine even the slightest change in transverse velocity. As a result, all of the cross-sections of the 22 series, excluding the approach and exit, had 2 to 3 profiles recorded (depending on the available width at the particular section). Observations of the 10 degree louver array velocity profiles of Figures 19 through 22 illustrated that a decrease in velocity occurred in the direction of the louver array structure. As for Figures 23 and 24 of the 15 degree velocity profiles, such variance among any particular section could be described as being either scattered or absent. In addition to these general observations, there was a common phenomenon occurring exclusively at the bypass exit section of all louver arrangement and discharges of Phase Two. Although the uppermost point of each profile was already mentioned as being a false value (*i.e.*, equal to the measured data point below it), Figures 19 through 22 illustrated a significant reduction in velocity occurring within about the upper 30% of the bypass section. This localized decrease could have been a result of flow disturbances occurring within this region, which caused the Prandtl tube to read incorrectly. Another possibility may have been due to the significant amount of flow that was qualitatively observed to enter the canal section through the last few slats of the array. Such a flow loss, especially if it was occurring exclusively within the upper region of the bypass section, would create a reduction in velocity.

4.2 Analysis

4.2.1 General

Using the experimental data, it was possible to further analyze the flow conditions occurring within the louver array. From a practical perspective, the velocity profiles of Phases One and Two were used to determine the percentage of flow that was being discharged throughout the bypass section of the louver array. Furthermore, these profiles were necessary in order to determine the hydraulic performance of the louver arrays with respect to the increase in velocity occurring between the approach and exit sections. The water surface profiles measured during Phase Two of the study allowed for the reduction in flow depth that occurred along the horizontal axis to be analyzed.

The hydraulic factors that were analyzed in this louver study will be presented in the following subsections under three categories, namely: proportional bypass discharge, bypass acceleration, and overall reduction in flow depth.

4.2.2 Proportional Bypass Discharge

The proportional bypass discharge is expressed as *the ratio of discharge at any section along the bypass to the total flume discharge of the approach section.* The value of the proportional bypass discharge at the approach section, which was assumed to be equal to the discharge at the louver array entrance, was unity. Therefore, any section located downstream of the entrance was found to be less than unity, as a portion of the flow was continually being discharged into the canal section. Values of discharge were determined from the velocity profile(s) recorded within the bypass sections of the louver array for each test series. In order for these discharge values to be represented in terms of proportional bypass discharge, they were normalized with respect to the discharge of the approach section. The series of data collected were then graphed in the non-dimensional form of proportional bypass discharge versus proportional bypass width, with the latter variable being defined as a percentage of the total flume width. The relationship between the proportional bypass discharge and the proportional bypass width for both phases of the study was graphically illustrated by Figure 25. Using normalized graphs made it possible to observe the various series with respect to one another, since all of the data was now expressed in the same form.

Determination of the proportional bypass discharge was found to be crucial for studies on the hydraulic performance of the louver array, as it provided an indication of the amount of flow occurring throughout the bypass section of the louver array. Most importantly, the proportional bypass discharge at the exit section indicated how much flow was being lost for operational purposes to the bypass / fish return system. In conjunction with maintaining optimum flow conditions within the bypass section, it was equally necessary to attempt to minimize the proportional bypass discharge at the exit of the louver array. In addition, there must be consideration given towards the minimum allowable flow rates required for the safe passage of the target fish back to their natural environment.

Analysis of the initially tested velocity profiles of the 10 degree louver array, previously shown in Figures 19 through 22, revealed an interesting generalization with respect to the proportional bypass discharge. This discovery was made as a result of superimposing the data points of Series *10/0.05/*/B*, *10/0.10/*/B*, and *10/0.15/*/B*. Regardless of the proportional bypass width being evaluated, the data points of each series plotted on top of one another and formed curves that were practically identical in shape. The generalization of these 3 series concluded that it was unnecessary to perform tests on the louver arrays by varying the proportional bypass width. This provides an explanation as to why all 3 of the proportional bypass widths of the 10 degree louver array with a louver slat spacing of 100-mm were conducted, whereas only one proportional bypass width was tested for the remaining series of Phase Two. Through the elimination of unnecessary testing, this generalization provided enough time for the study to include the 15 degree louver array. Due to time constraints, it was previously determined that there was only enough time to thoroughly test the 10 degree louver array in Phase Two. In spite of these timesaving benefits, the discovery of the generalization was not recognized as being a groundbreaking one. In regards to proportional bypass discharge, the similarity of the flow conditions observed from the 12 tests of Series *10/*/*/B* made practical sense. For example, if the proportional bypass width of a certain louver array was originally tested at a value of 0.05 and then increased to 0.15, the amount of discharge at the location where the proportional bypass width was 0.15 would not be expected to differ between either case. Therefore, assuming flow throughout the bypass section of the louver array was subcritical, the experimental data that was determined for any particular setting of the proportional bypass width could be expected to represent all others.

To enhance the pattern formed by the data points, a best-fit line was determined for each of the six data series of Figure 25. The best-fit lines were determined using the following second-order polynomial equation, which was known to satisfy the hydraulic conditions of the louver array:

$$\frac{Q_b}{Q} = m\left(\frac{Z_b}{B}\right) + (1-m)\left(\frac{Z_b}{B}\right)^2 \qquad [3]$$

where Q_b/Q is the proportional bypass discharge, Z_b/B is the proportional bypass width, and 'm' is a constant.

The values of the constant 'm' determined for the six sets of series, given within Table 3 and illustrated by the best-fit lines within Figure 25, provided a good approximation to the proportional bypass discharge occurring at any bypass section of the various louver arrangements and discharges of this study. By substituting a value of proportional bypass width into any of the six equations, it was possible to obtain a good estimate as to the amount of flow exiting the bypass section of the desired louver array.

Although several other equations were considered, the polynomial form of Equation 3 was chosen since it accurately fit the data and was known to satisfy the hydraulic conditions of the louver array. In the approach section, where the proportional bypass width was a value of unity, the equation also produced a value of unity. If the louver array were to extend all the way across the flume, in which case the proportional bypass width would achieve a value of zero, the equation also went to zero.

4.2.3 Bypass Acceleration

Bypass acceleration was a term coined by Ruggles and Ryan (1964) to describe the *ratio of the depth-averaged velocity [at the bypass exit section] to the approach depth-averaged velocity*. From this definition, it is both evident and important to realize that bypass acceleration is not true acceleration in terms of velocity over time.

The concept of bypass acceleration was observed in Phase One as being an important biological factor in the assessment of a particular louver arrangement, due to its relation to the swimming abilities of the target fish. Previous louver studies conducted on the guidance of downstream migrating fish (Bates and Vinsonhaler, 1957; Ruggles and Ryan, 1964; Anderson *et al.*, 1998) were found to be most effective when a gradual increase in velocity occurred throughout the louver array length. By computing, within each test series, the ratio of the width-averaged velocities throughout the bypass section to the approach depth-averaged velocity, it was possible to show the bypass acceleration occurring throughout the horizontal length of the bypass section. Presented in a non-dimensional form, Figure 26 illustrated this gradual increase in velocity and allowed for comparisons to be made between the plotted series. The graphs of bypass acceleration versus proportional bypass width were found to be subject to the same generalization that was discovered for the proportional bypass discharge. At the sake of being redundant, the data points of the initial 12 tests of Series *10/*/*/B* plotted on top of one another and formed curves that were practically identical in shape, regardless of the proportional bypass width being tested. Following the same procedure, testing was only required with a single proportional bypass width for the remaining series of Phase Two.

As done in the previous section and illustrated in Figure 26, a best-fit line was determined for the three data series of each testing phase in order to emphasize the experimental results. The two best-fit lines for the graph of bypass acceleration versus proportional bypass width were best described by a decaying exponential function of the following form:

$$\frac{U}{U_o} = c\,e^{-d\left(\frac{Z_b}{B}\right)} \qquad [4]$$

where U/U_o is the bypass acceleration, Z_b/B is the proportional bypass width, and the letters 'c' and 'd' are constants.

The form of the equation was automatically determined by the built-in *Trendline* function of Microsoft Excel (Version 7.0). Using this application, an equation and a squared correlation coefficient (R^2) was obtained for each data series of the 6 graphs. From an observation of Figure 26, it was apparent that the chosen form of the bypass acceleration equation provided a good approximation to the experimental data.

By using Equation 4, substituting in the constant values for 'c' and 'd' given in Table 4, and selecting a value of proportional bypass width, it was possible to obtain a good estimate of the magnitude of velocity occurring at any transverse section of the desired louver array.

4.2.4 Overall Reduction in Flow Depth

Using the experimental data of the water surface profiles for the various louver arrangements and discharges, it was possible to analyze the overall reduction in flow depth occurring within both the bypass and canal section (ΔY_b and ΔY_c, respectively). Since the required data was not gathered for the six series of the 7.2 and 17 degree louver array, this subsection will only be applicable to Phase Two of the study. Figures 27 and

28 illustrated the overall reduction in flow depths with respect to the various width-averaged velocities tested. In all 12 graphs, the canal section of the louver array was observed as having higher reduction values than the bypass section. The reduction in flow depth of the bypass section was considered to occur mainly as a result of the increase in velocity, which was apparent throughout the array length. Within the canal section, the same reasoning was concluded; however, it was also expected that the presence of the additional depth decrease was due to a certain amount of head loss occurring as the flow was passed through the louver slats. Those series that were conducted with a louver slat spacing of 100-mm were able to discharge the flow through the system without incurring as much of a reduction in flow depth. This observation might reinforce the idea that the wider louver slat spacing created less of a head loss for the louver array system. Similar to those observations made in subsections 4.2.2 and 4.2.3, varying the proportional bypass width by 5, 10, and 15% of the total flume width resulted in a relatively insignificant change in the overall reduction in flow depth for common louver arrangements (*i.e.*, arrays which had the same louver array angle and louver slat spacing). A further analysis of Figures 27 and 28 also illustrated that the relationship between the reduction in flow depth and the approach depth-averaged velocity could be considered almost linear.

5.0 CONCLUSIONS AND RECOMMENDATIONS

5.1 Conclusions

The louver array is a hydraulic structure used to safely guide downstream migrating fish away from water intakes located within a river system. The effectiveness of this fish diversion device, both hydraulically and biologically, is dependent upon the parameters of discharge, louver array angle, louver attack angle, slat spacing, and bypass width. With the wide range of flow conditions that can be created by the altering any of these parameters, it is necessary to conduct prototype and/or model testing of the louver array prior to its installation. Due to the unpredictable behaviour of fish upon being introduced to the structure, an in-depth biological study is also required in order to determine the optimum design criteria for the fish diversion device. Above all, good communication and cooperation between the hydraulic engineers and the biologists is of utmost importance in order for the physical, hydraulic, and biological criteria for the given site to be established from the perspectives of both parties.

The aim of this preliminary study on using a louver array as an effective means of guiding downstream migrating fish was primarily to achieve an understanding of the hydraulics of flow. In addition, it was expected that the determination of which physical parameters were significant to its overall performance would be beneficial in advancing the science of this particular fish diversion device.

To fulfill the objectives of the study, the louver arrays were tested under both field and laboratory conditions of Phases One and Two, respectively. Although six series of velocity profiles was the extent of the qualitative data obtained in Phase One, many qualitative observations were made from both a hydraulic and a biological perspective. With first-hand knowledge and an appreciation of the flow characteristics of a louver array, the second phase of the study was assembled with much confidence and consideration of the variables involved. In Phase Two, water surface profiles, velocity profiles, qualitative flow observations, and photographs were obtained for a total of 22 different physical arrangements and discharges.

Observations of flow recorded during the experimental study provided insight into the hydraulic conditions that occurred throughout the louver array. Many of the comments made on various aspects of the flow were later verified by similar results obtained from the quantitative data. Since velocity measurements in the canal section where unattainable due to the presence of a three-dimensional flow structure, qualitative flow observations were made using the naked eye, a red dye solution, and/or a thread grid. Information within this study that pertained to the canal section of the louver array, was expected to be beneficial for continuing studies in deciding what and how quantitative data should be gathered.

The water surface profiles measured in Phase Two of the study were found to bear characteristics similar to the qualitative flow observations mentioned in regards to the same topic. The water surface profile of both the bypass and canal sections were observed to gradually decrease within about the upper two-thirds of the louver array and then decrease at a much faster rate as the flow proceeded towards the exit section.

Increasing the magnitude of the approach depth-averaged velocity was found to cause a decrease in the normalized flow depth values of both flow sections. Testing the structure at a proportional bypass width of 5, 10, or 15% of the total flume width had no significant effect on the width-averaged water surface profiles of either section. In the transverse direction, the water surface level remained relatively parallel with the flume bed throughout the array length. If there was any apparent deviation from a zero slope, it was observed to be in the direction of the louver array. Further analysis of the water surface profile data provided information on the overall reduction in flow depth occurring in both the bypass and canal section. By plotting ΔY_b and ΔY_c versus U_o, a close to linear relationship was produced for each series of Phase Two. For those arrangements having the same louver array angle and slat spacing, variation of the proportional bypass width had an insignificant effect on the flow depth at any section of a given test series.

The velocity profiles measured in both phases of the study were used to determine the flow structure of the bypass section for various physical arrangements and discharges. The data for each series indicated that the flow remained relatively uniform throughout the bypass section of the louver array. In addition, profiles taken across the bypass width at each section illustrated that the reduction in velocity occurring transversely towards the louver structure was either minor or insignificant.

Determining the hydraulic performance of the louver array involved the use of the velocity profile data in order to form the non-dimensional terms of proportional bypass discharge and bypass acceleration. Results of the normalized graphs of Q_b/Q versus Z_b/B

and a versus Z_b/B revealed that the percentage of discharge occurring within the bypass section, which occurred for a particular physical arrangement of the louver system, was independent of the approach depth-averaged velocity. From an analysis of the same sets of graphs, it was determined that the proportional bypass discharge and the bypass acceleration were both functions of louver array angle, louver slat spacing, and proportional bypass width. Based on Figures 25 and 26, which respectfully addressed the relationship of proportional bypass discharge and bypass acceleration to proportional bypass width, it would be possible to determine which of the various louver arrangements would satisfy both the hydraulic and biological design criteria for a given site.

5.2 Recommendations

In addition to providing a substantial contribution to the understanding and advancement of louver array hydraulics, this detailed investigation also lead to the creation of several new ideas that needed to be addressed. With a basic understanding of louver arrays now developed, the following recommendations could be considered in further studies:

I. A quantitative study of the flow structure occurring throughout the canal section of the louver array.

II. Determination of the benefits of using flow straightening vanes, as described by Bates and Vinsonhaler (1957). If the vanes prove to be successful in maintaining flow uniformity throughout the louver array, it may also be possible to obtain velocity measurements within the canal section.

III. Testing of a simple louver array with separate channels immediately downstream of the louver array for both the bypass and canal sections. In addition, the flow distribution may be controlled if each channel is governed by individual tailgates.

IV. A detailed study of a louver array designed with various louver array angles for the purpose of creating an equal distribution of flow through the entire length of the louver slats. This particular study would not be necessary if recommendation **II** were to conclude that flow straightening vanes were able to achieve this goal.

V. A detailed laboratory investigation involving the convex-shaped louver slats of Phase One. Comparisons could be drawn between it, the present study, and the study proposed in recommendation II.

VI. Determination of the amount of hydraulic head loss and the backwater effects created by the presence of the louver array.

Table 1: Hydraulic Summary of Phase One Data

Series Name	@ exit section	
	Q_b/Q	U/U_o
7.2/0.23/0.20/C	0.385	1.67
7.2/0.23/0.34/C	0.354	1.54
7.2/0.23/0.50/C	0.364	1.58
17/0.23/0.20/C	0.343	1.46
17/0.23/0.35/C	0.339	1.46
17/0.26/0.52/C	0.343	1.32

Table 2: Hydraulic Summary of Phase Two Data

Series Name	@ exit section		
	Q_b/Q	U/U_o	Y/Y_o
10/0.15/0.30/A	0.347	2.37	0.942
10/0.15/0.40/A	0.346	2.47	0.903
10/0.15/0.50/A	0.338	2.52	0.863
10/0.15/0.60/A	0.321	2.64	0.781
10/0.05/0.30/B	0.135	2.58	0.944
10/0.05/0.40/B	0.129	2.52	0.920
10/0.05/0.50/B	0.122	2.52	0.870
10/0.05/0.60/B	0.117	2.58	0.820
10/0.10/0.30/B	0.229	2.41	0.951
10/0.10/0.40/B	0.214	2.29	0.929
10/0.10/0.50/B	0.202	2.28	0.889
10/0.10/0.60/B	0.200	2.42	0.829
10/0.15/0.30/B	0.340	2.29	0.955
10/0.15/0.40/B	0.330	2.28	0.929
10/0.15/0.50/B	0.310	2.23	0.894
10/0.15/0.60/B	0.306	2.34	0.841

Table 3: Constant Value for the Proportional Bypass Discharge Equation

$$\frac{Q_b}{Q} = m\left(\frac{Z_b}{B}\right) + (1-m)\left(\frac{Z_b}{B}\right)^2$$

Series Name	'm' value	R^2
7.2 / * / * / C	1.789	0.991
17 / * / * / C	1.529	0.999
10 / * / * / A	2.195	0.997
10 / * / * / B	2.138	0.993
15 / * / * / A	2.217	0.998
15 / * / * / B	2.006	0.999

Table 4: Constant Values for the Bypass Acceleration Equation

$$\frac{U}{U_o} = c\, e^{-d\left(\frac{Z_b}{B}\right)}$$

Series Name	'c' value	'd' value	R^2
7.2 / * / * / C	1.89	0.625	0.960
17 / * / * / C	1.57	0.453	0.974
10 / * / * / A	2.90	1.080	0.994
10 / * / * / B	2.63	0.984	0.993
15 / * / * / A	2.87	1.080	0.986
15 / * / * / B	2.38	0.879	0.986

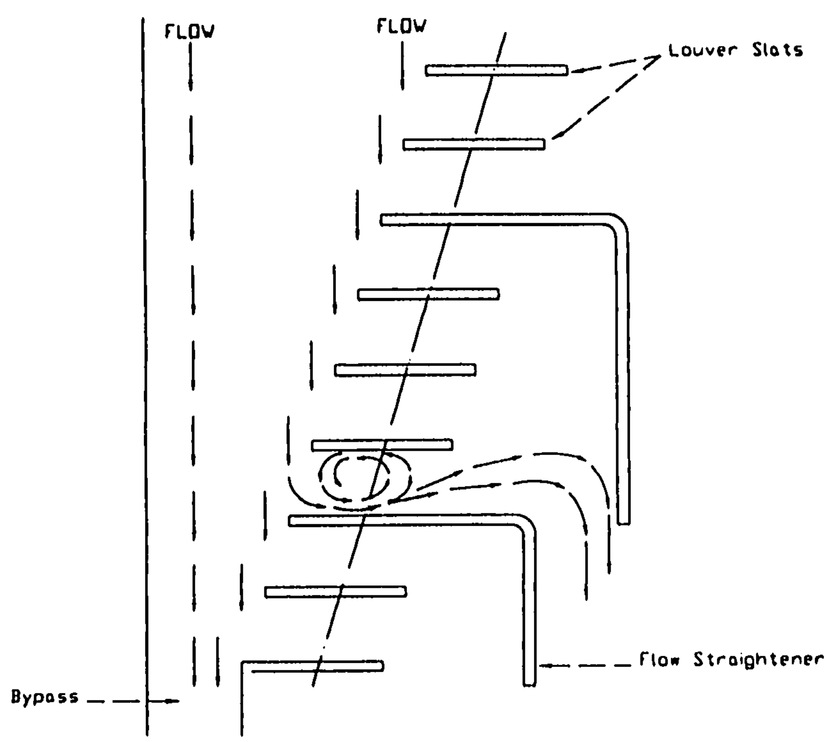

Figure 1: Definition sketch of flow through the louver slats (Bates and Vinsonhaler, 1957).

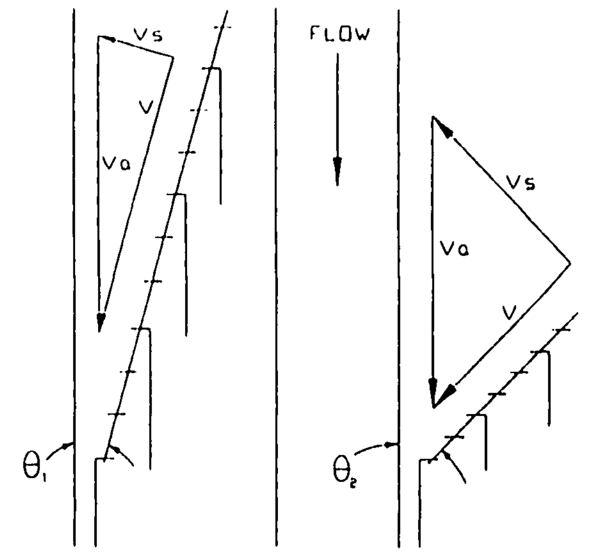

Fig. 2a **Fig. 2b**

Va = Approach velocity of flow (ft/s)
Vs = Swimming speed of fish (ft/s)
V = Resultant movement of fish (ft/s)
θ = Angle of the line of louvers (degrees)

Va	θ_1	Vs	θ_2	Vs
5.0	11.5°	1.00	45°	3.5
4.0		0.80		2.8
3.0		0.60		2.1
2.0		0.40		1.4
1.0		0.20		0.7

Figure 2: Vector diagrams illustrating magnitude of swimming effort which must be expended by fish to move parallel parallel to the louver line (Bates and Vinsonhaler, 1957).

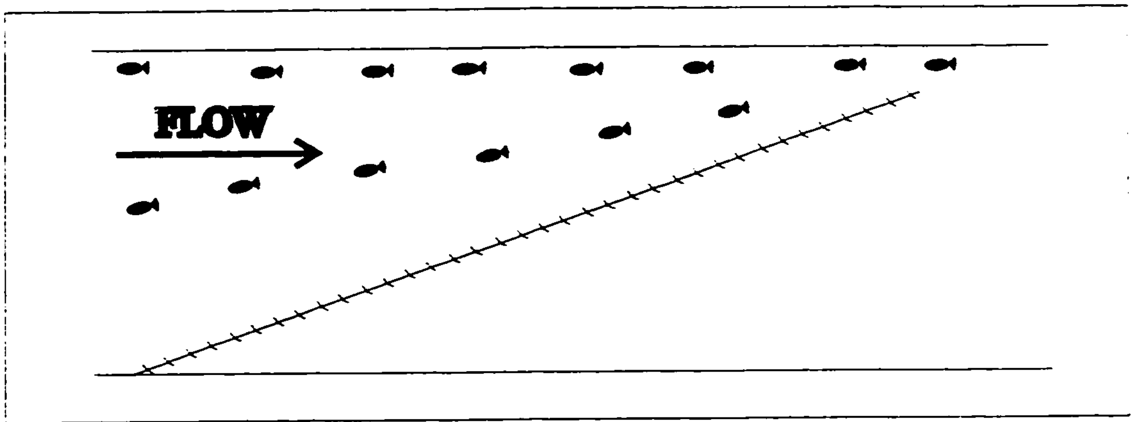

Figure 3: Representation of a typical fish movement along the louver array.

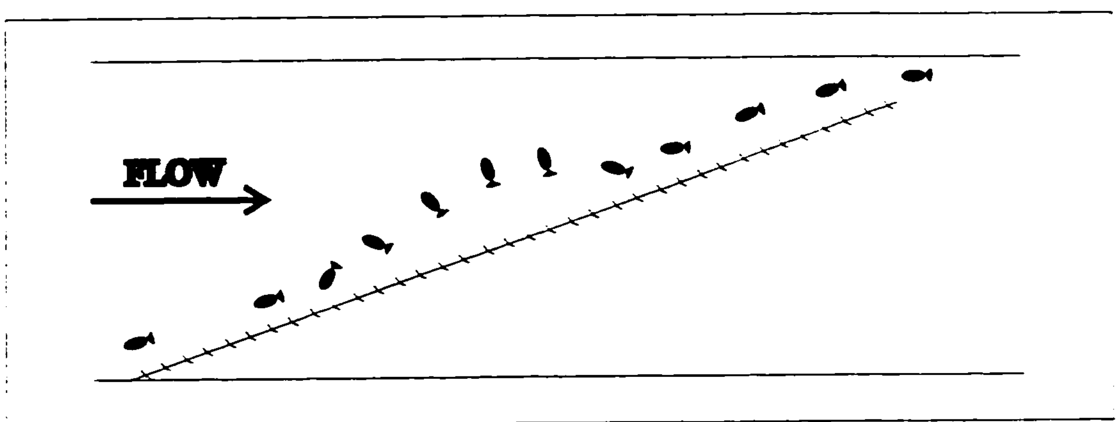

Figure 4: Representation of a typical fish movement along the louver array.

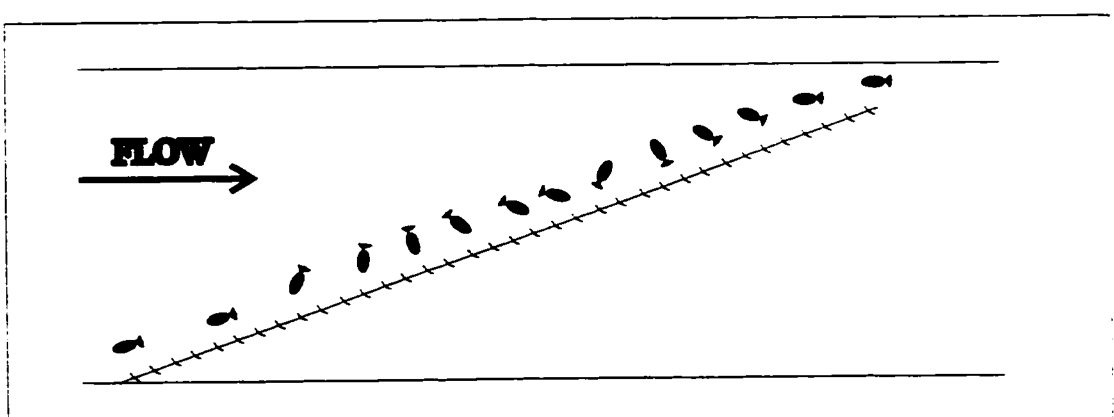

Figure 5: Representation of a typical fish movement along the louver array.

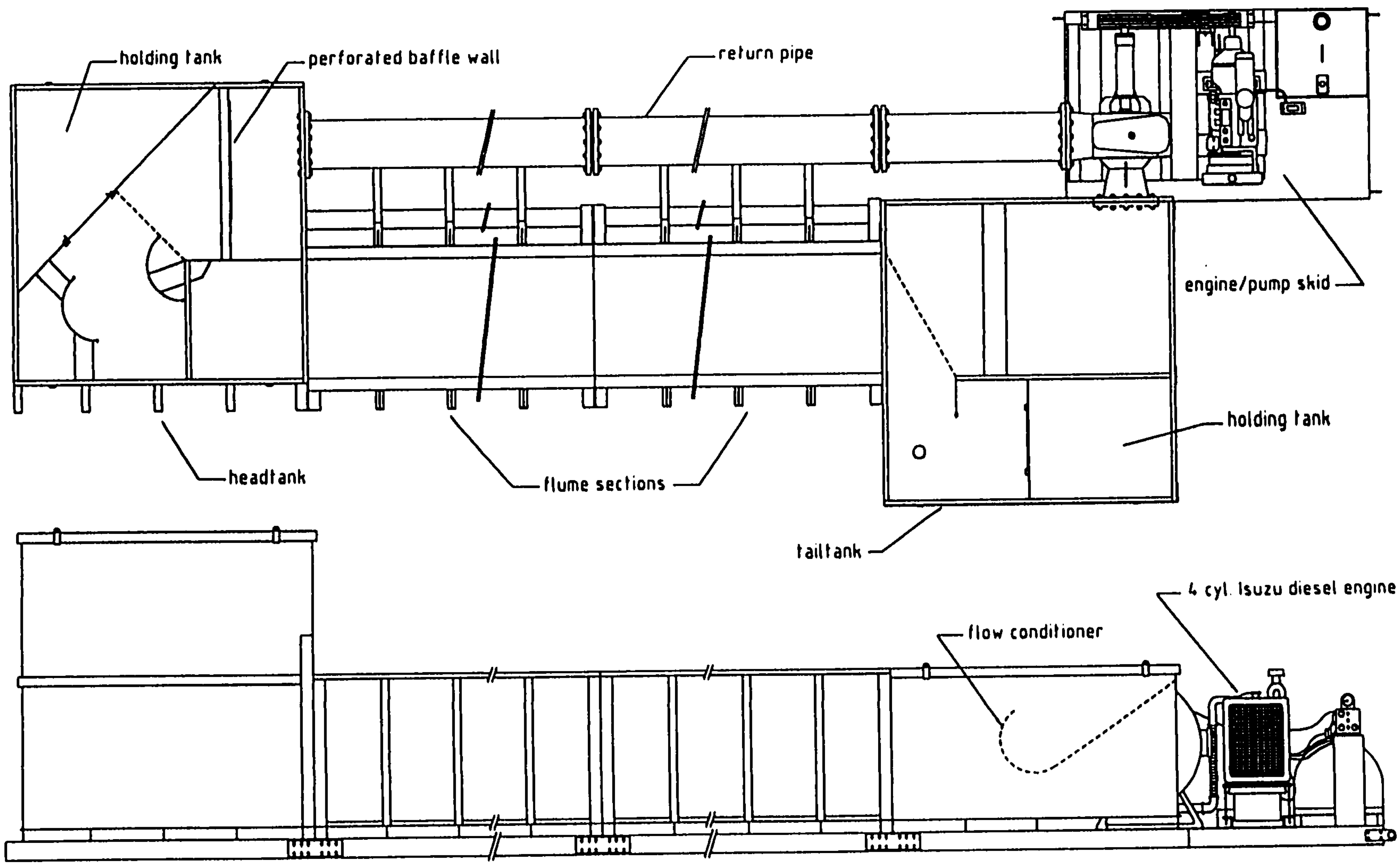

Figure 6: Plan view and profile view of the I-H Flume.

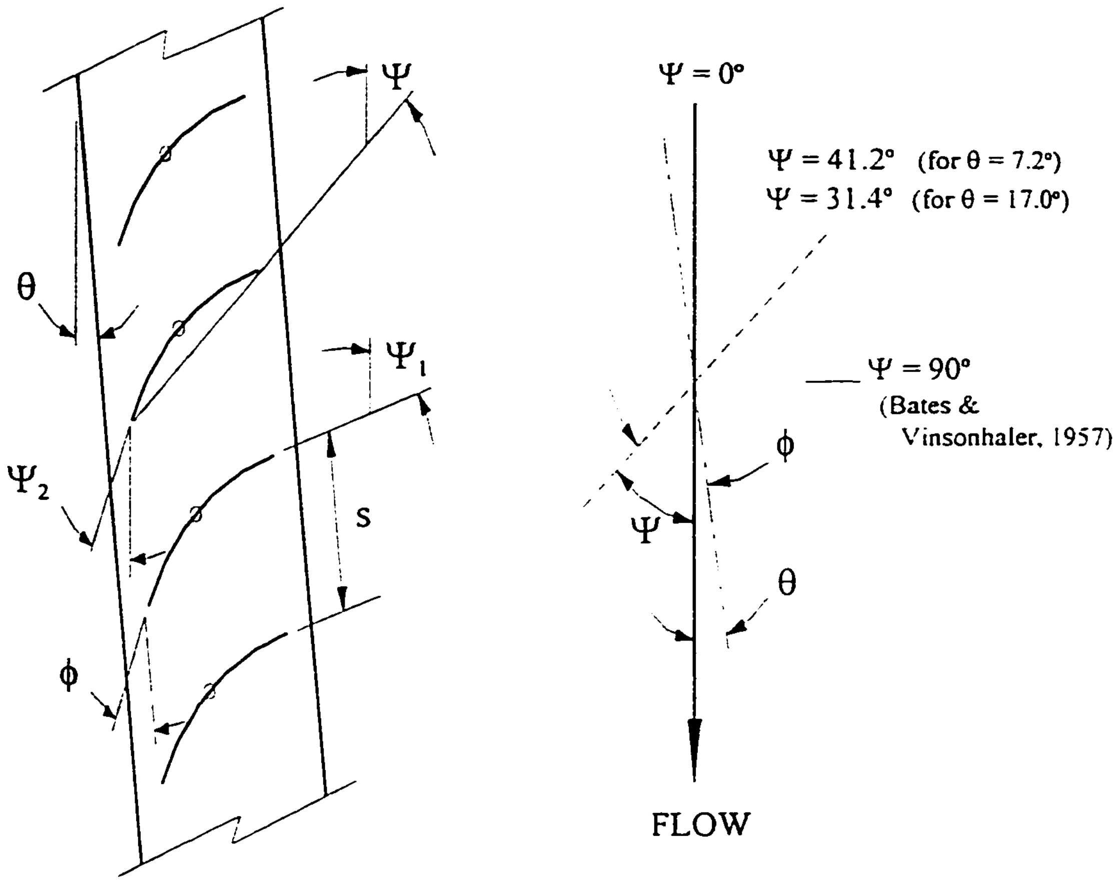

Louver pitch, $\phi = 48.4°$

Louver attack angle (for $\theta = 7.2°$): $\Psi = \phi - \theta = 48.4° - 7.2°$
$= \mathbf{41.2°}$

Louver attack angle (for $\theta = 17.0°$): $\Psi = \phi - \theta = 48.4° - 17.0°$
$= \mathbf{31.4°}$

Figure 7: Plan view of the louver slats used in Phase One and calculations of the louver attack angle (Ψ).

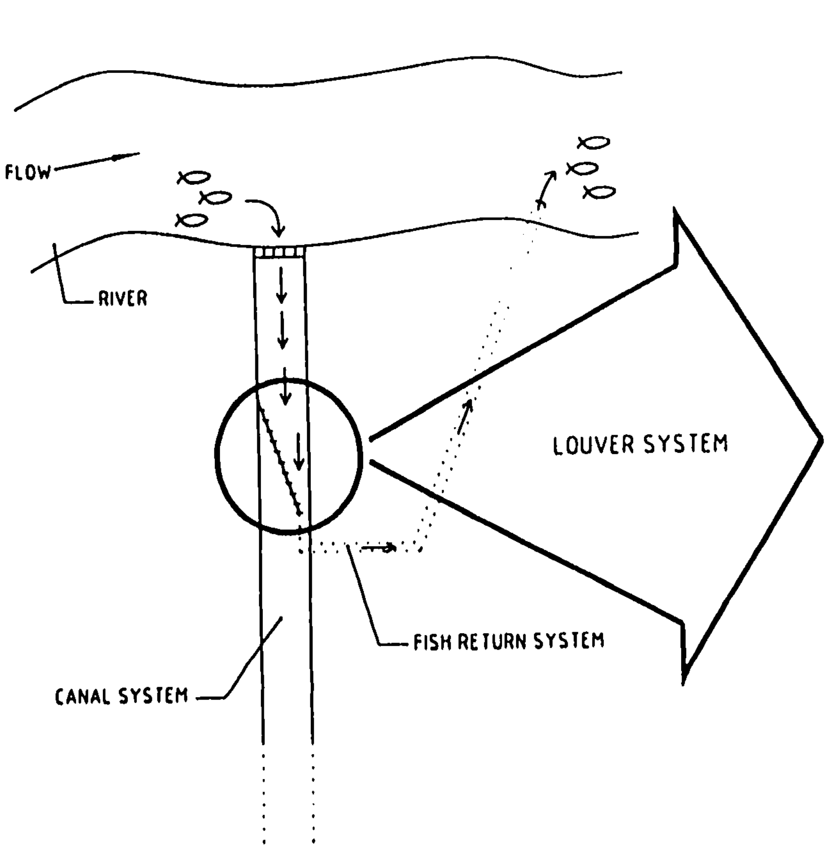

Figure 8a: Definition sketch of a louver array within a river system (not to scale).

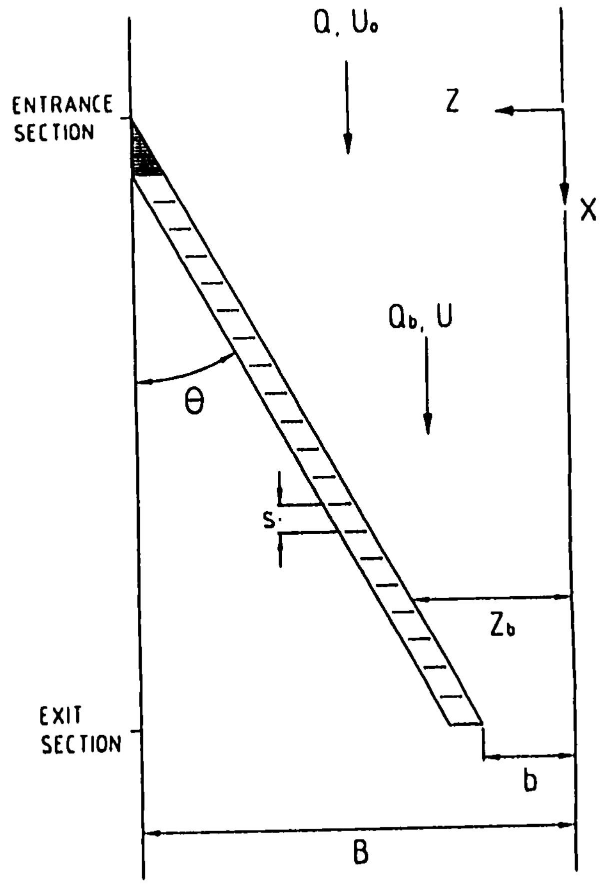

Figure 8b: Definition sketch of the louver setup of Phase Two (not to scale).

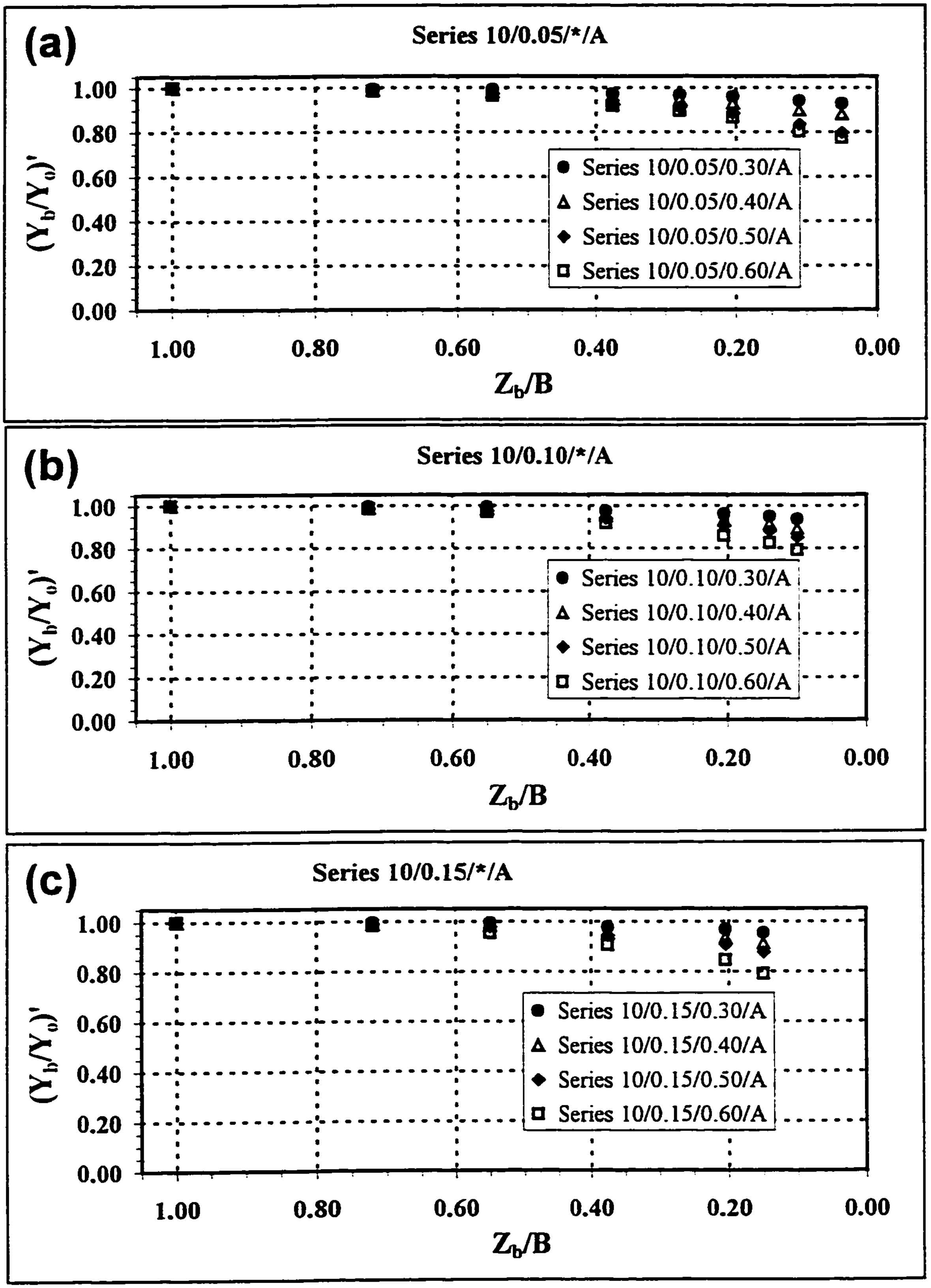

Figures 9(a-c): Averaged Normalized Flow Depth versus Proportional Bypass Width.

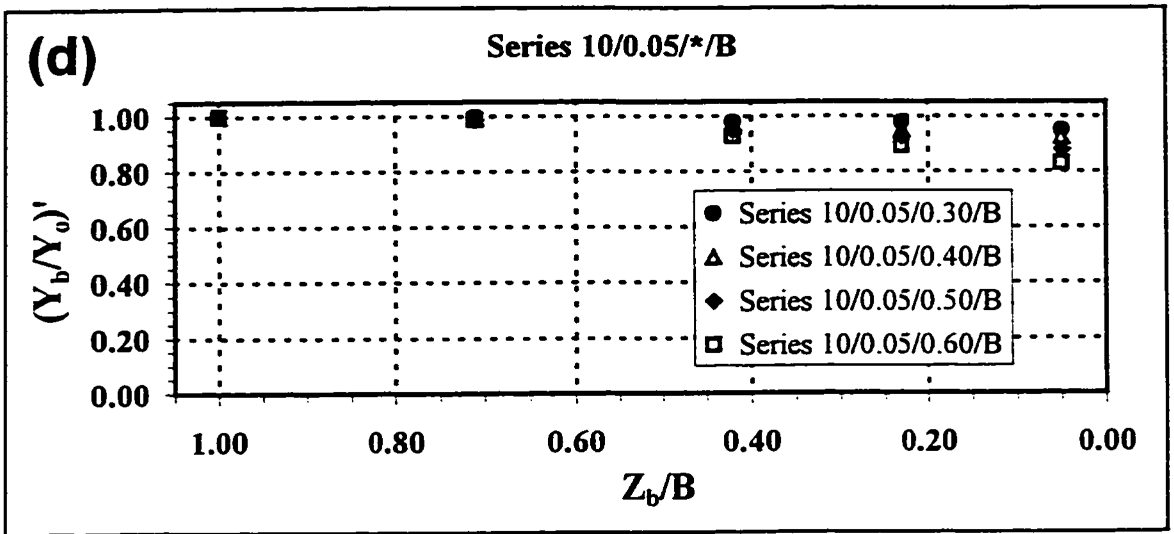

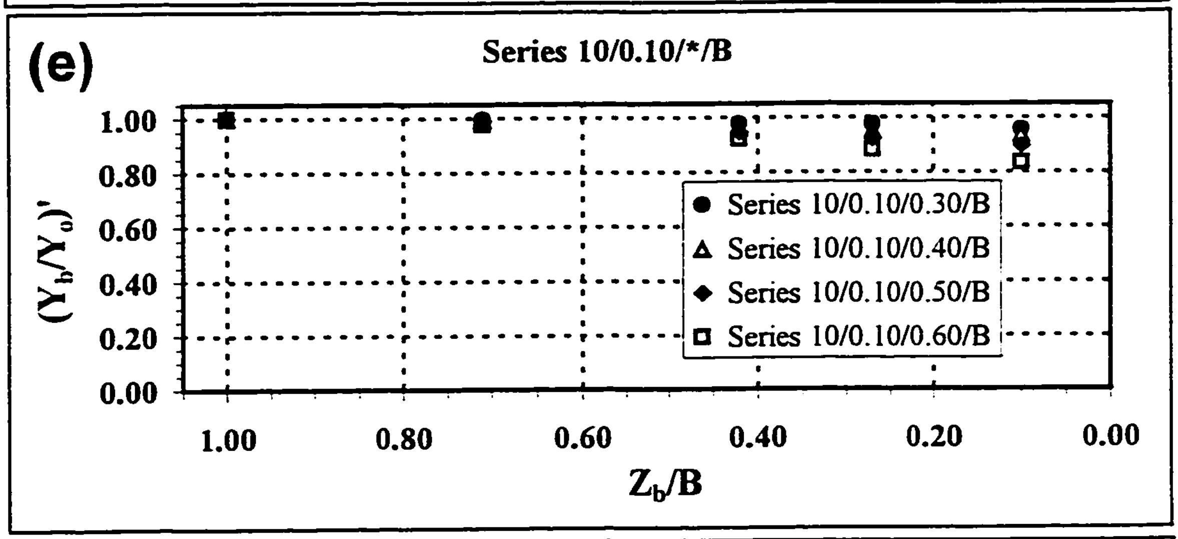

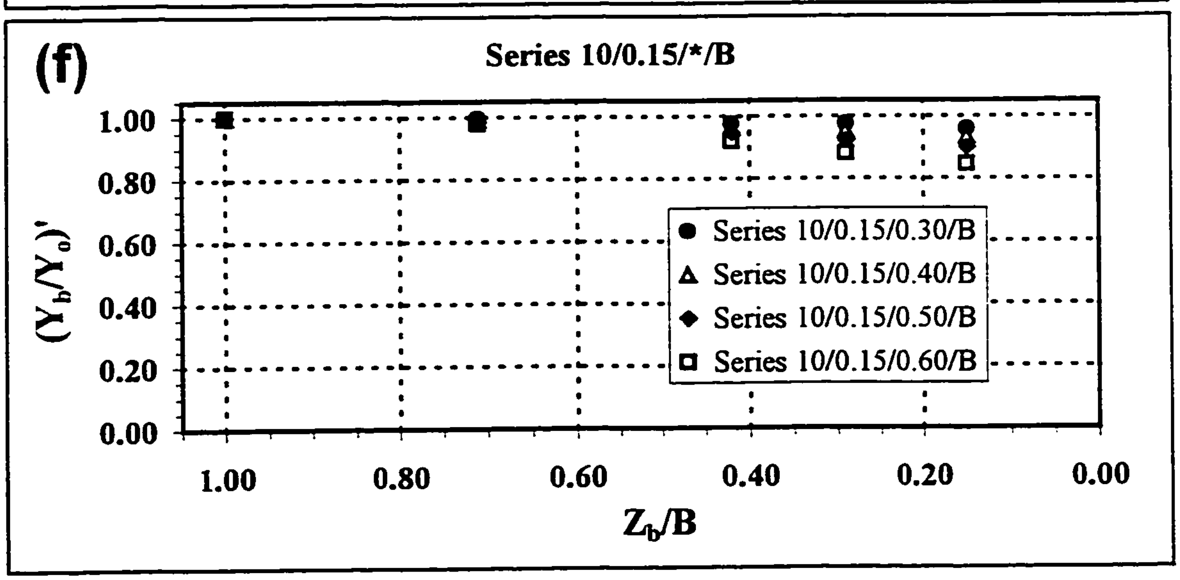

Figures 9(d-f): Averaged Normalized Flow Depth versus Proportional Bypass Width.

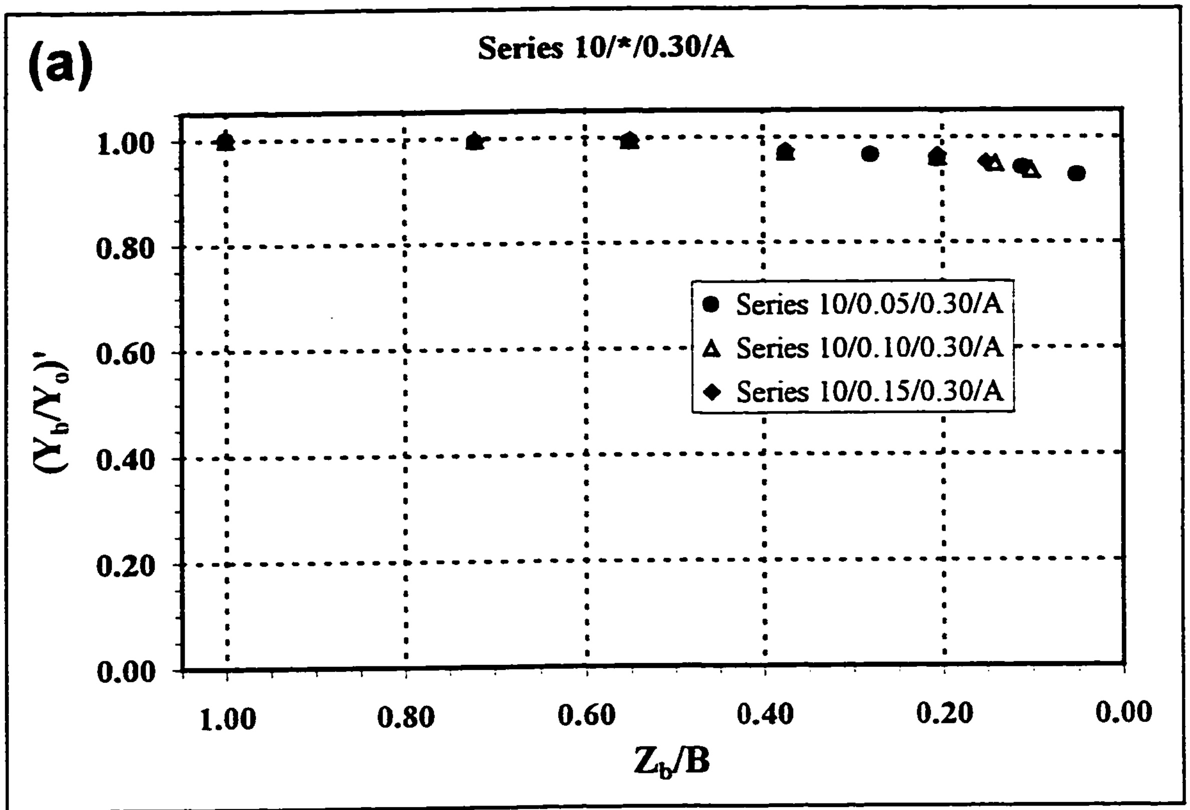

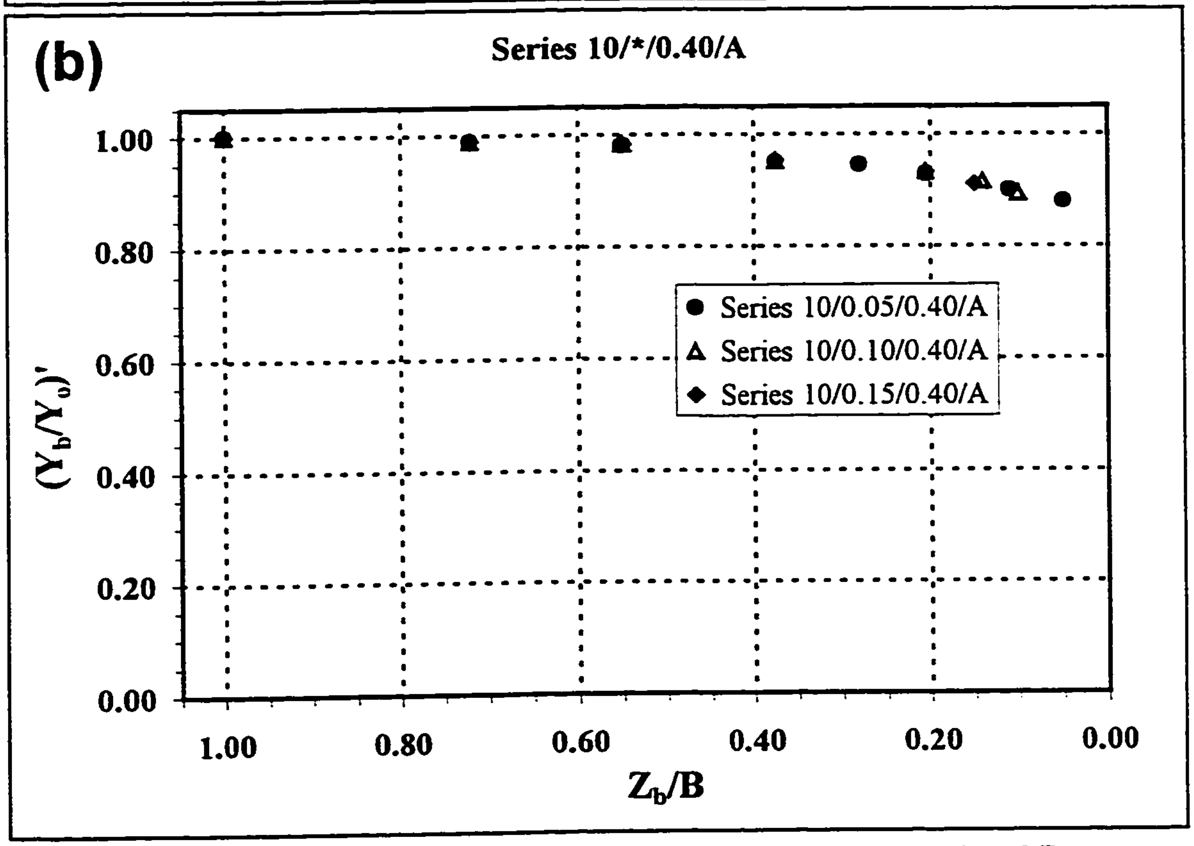

Figures 10(a-b): Averaged Normalized Flow Depth versus Proportional Bypass Width.

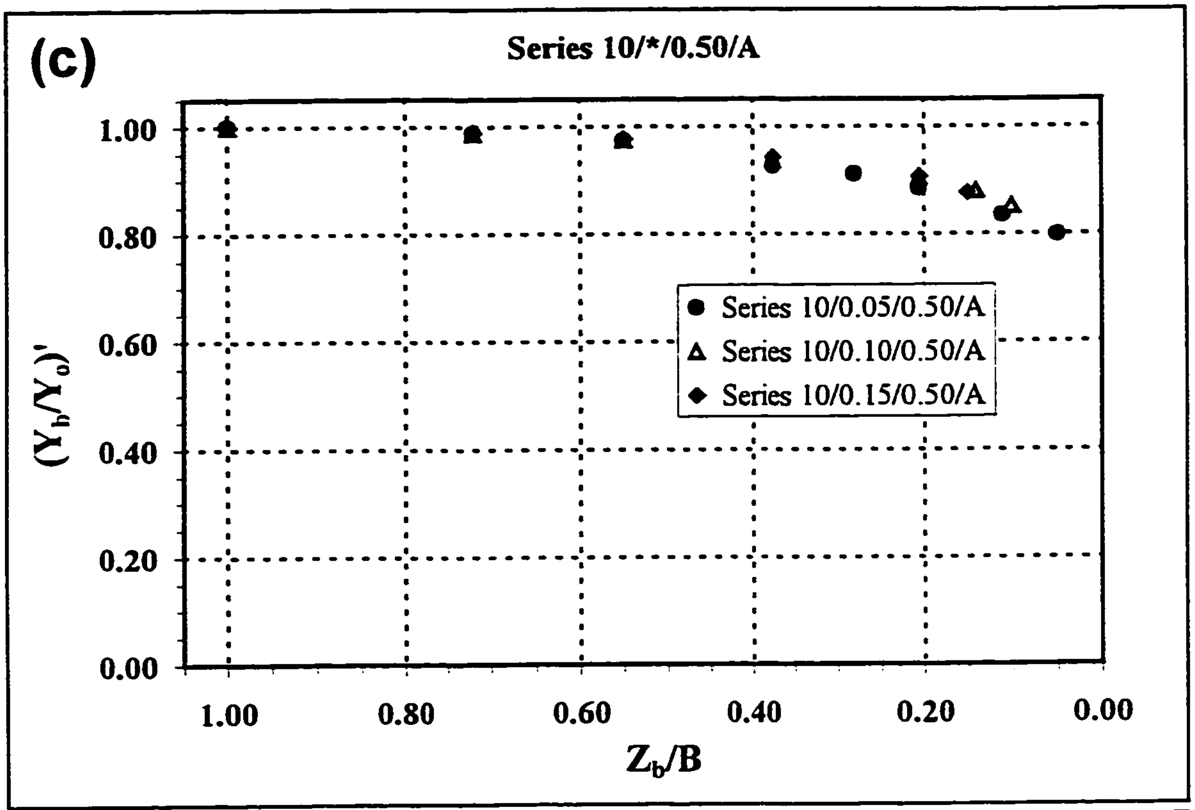

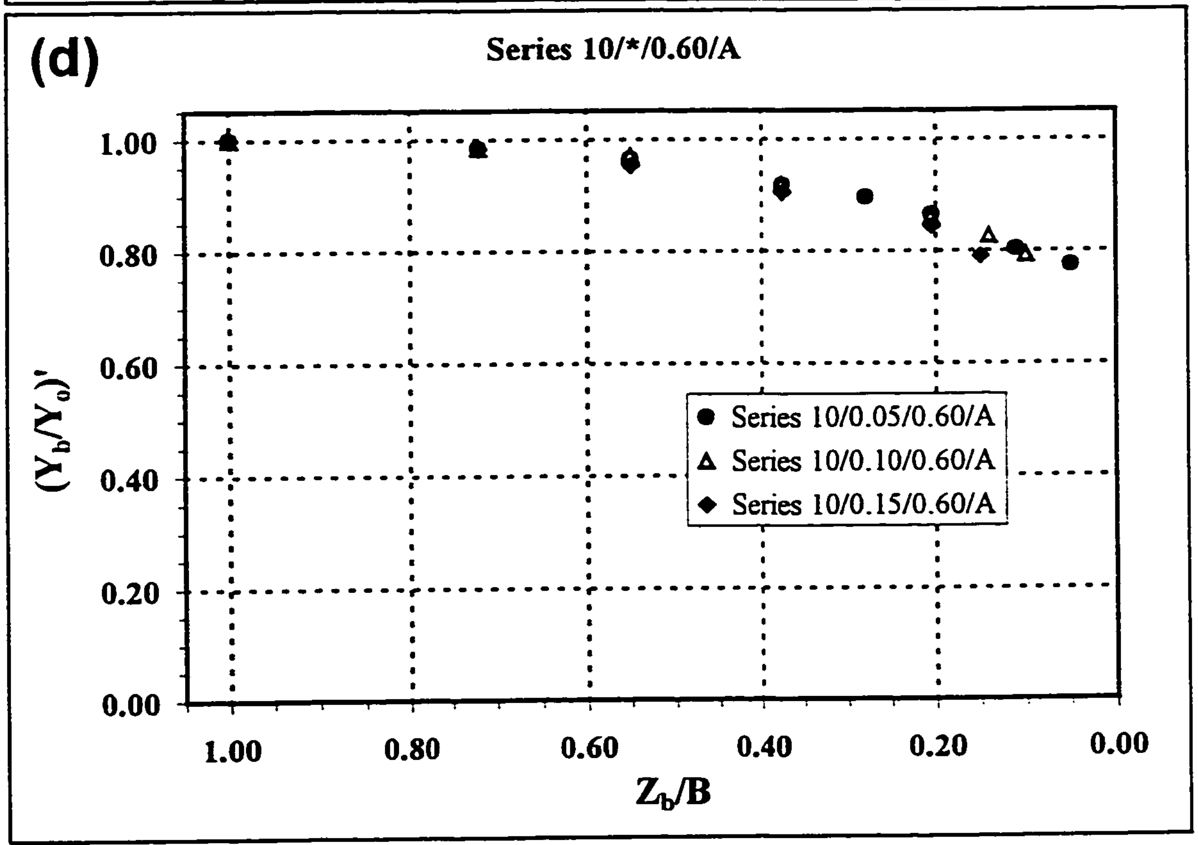

Figures 10(c-d): Averaged Normalized Flow Depth versus Proportional Bypass Width.

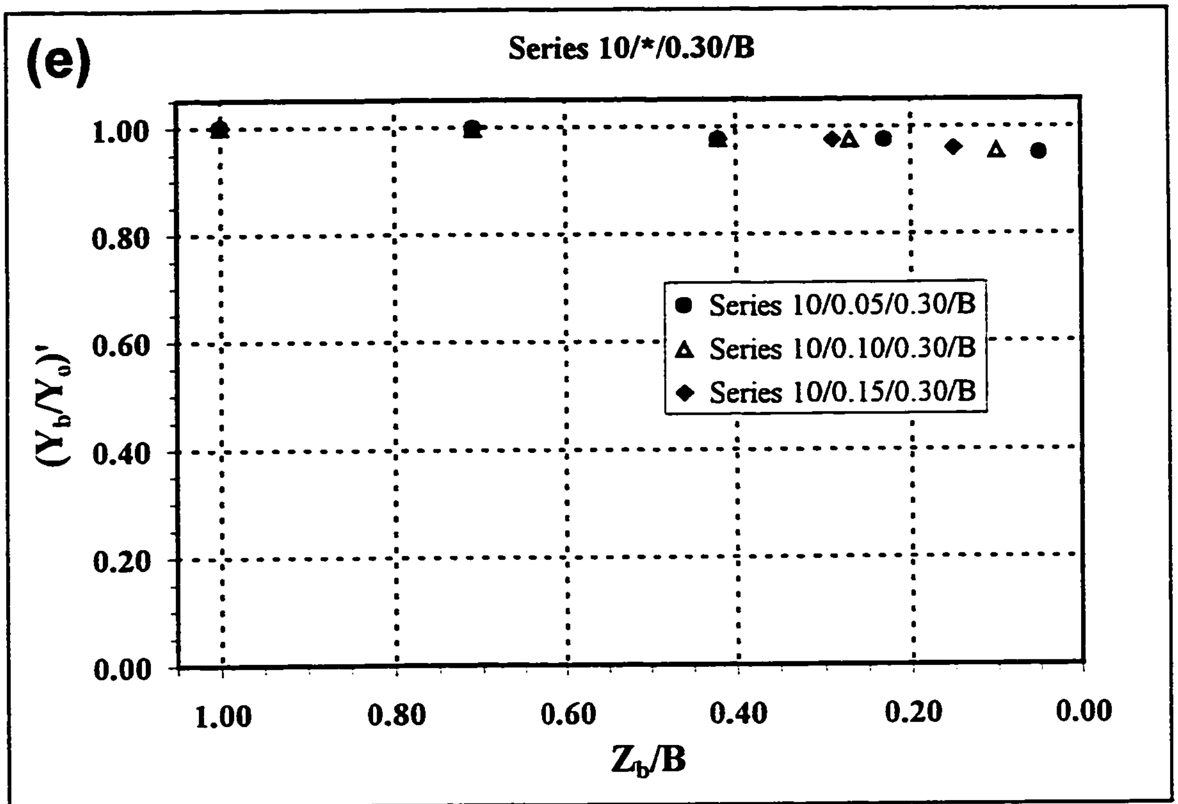

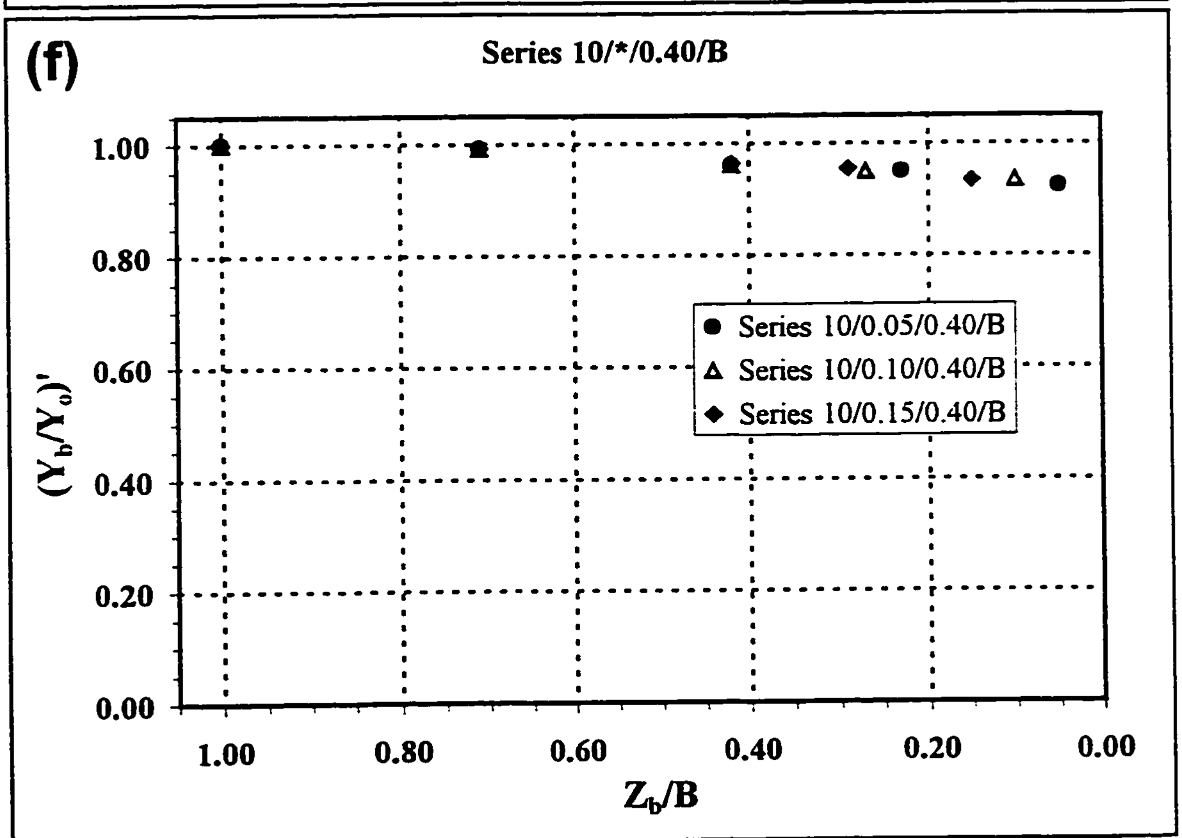

Figures 10(e-f): Averaged Normalized Flow Depth versus Proportional Bypass Width.

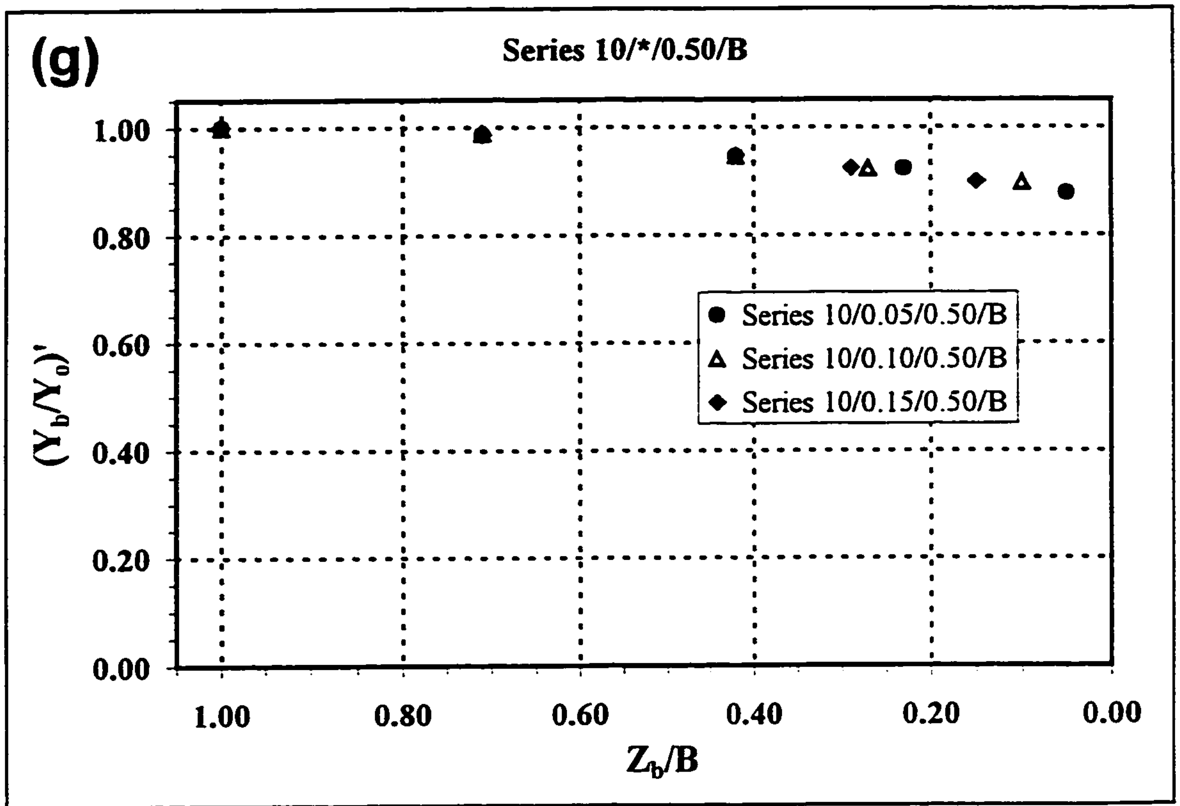

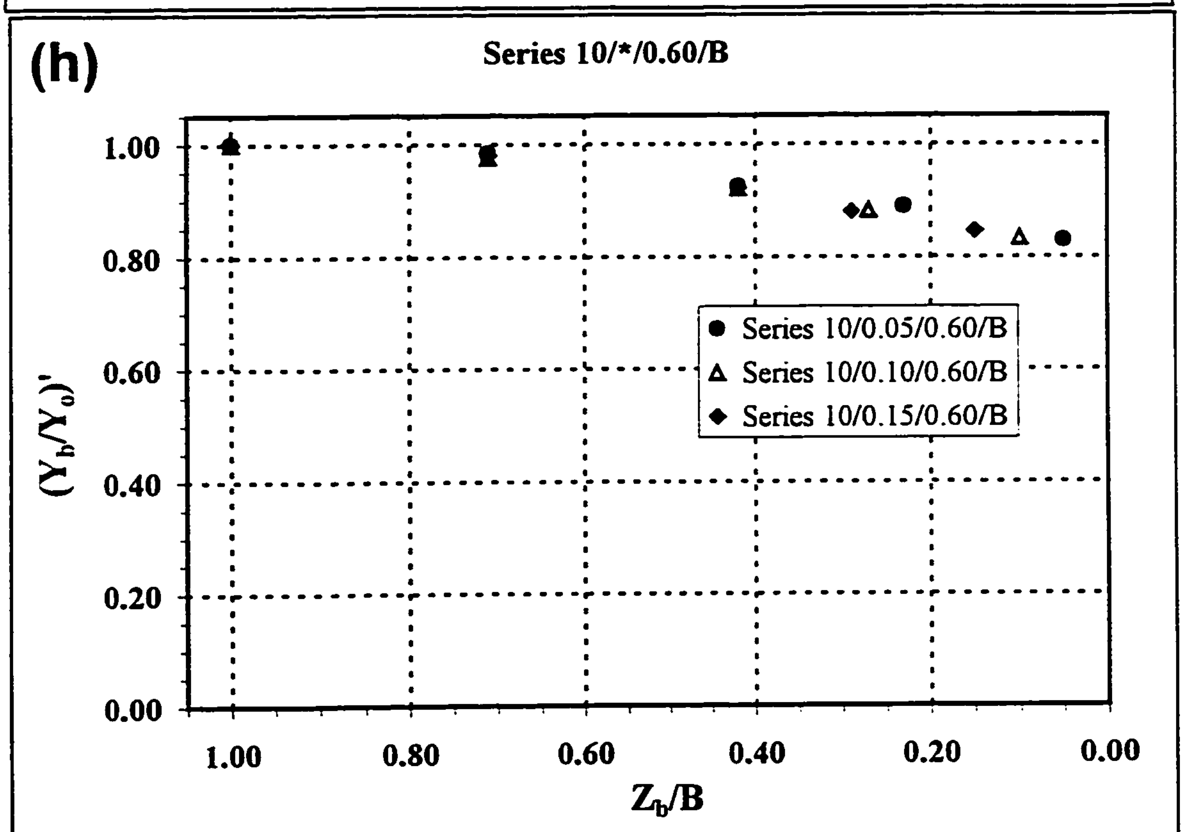

Figures 10(g-h): Averaged Normalized Flow Depth versus Proportional Bypass Width.

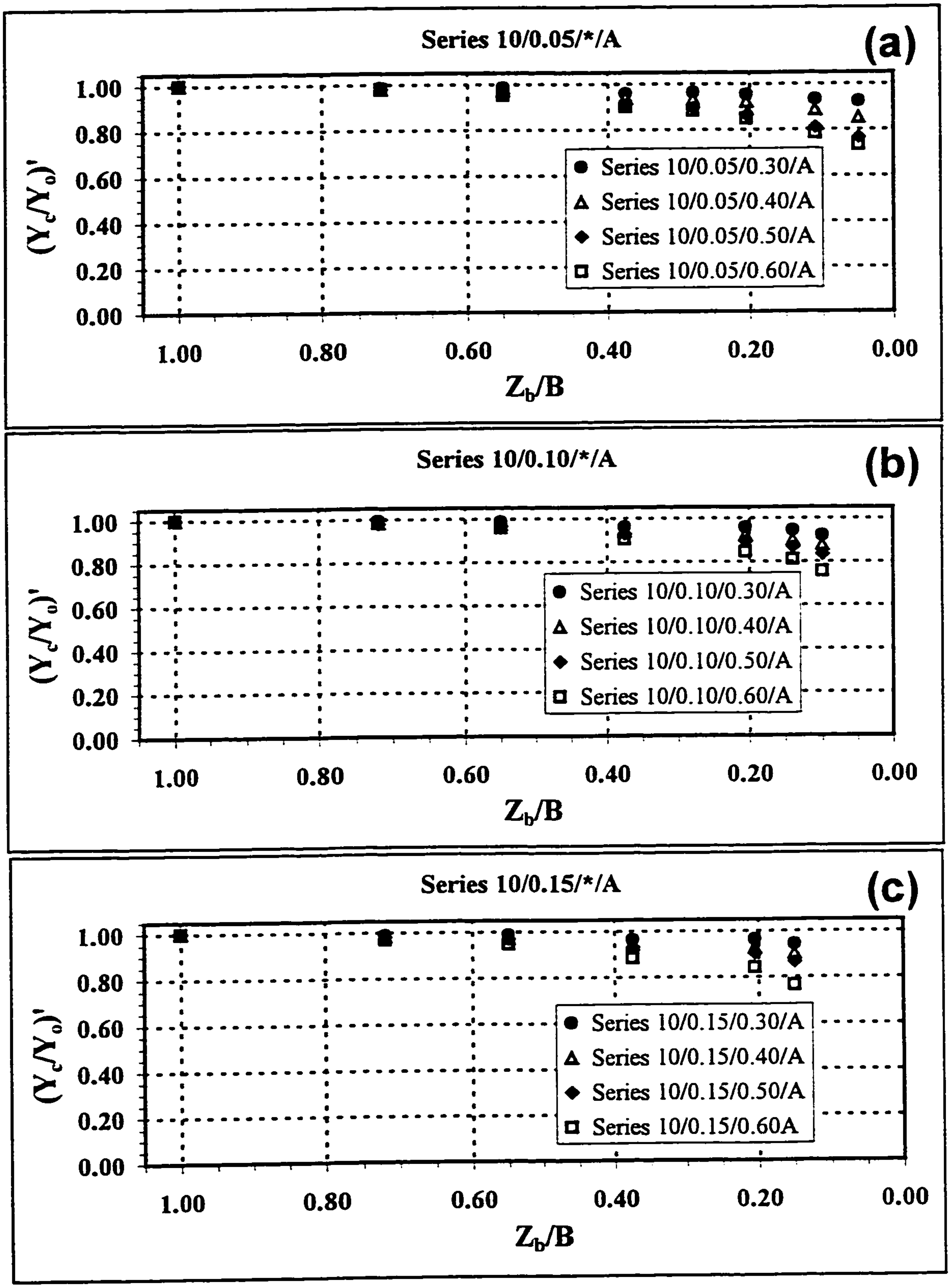

Figures 11(a-c): Averaged Normalized Flow Depth versus Proportional Bypass Width.

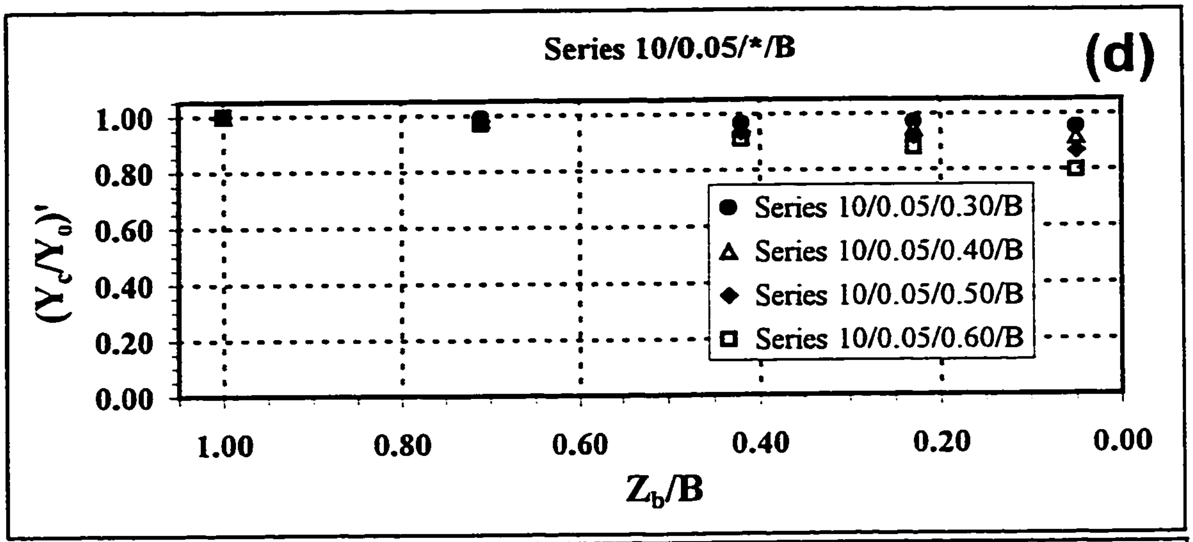

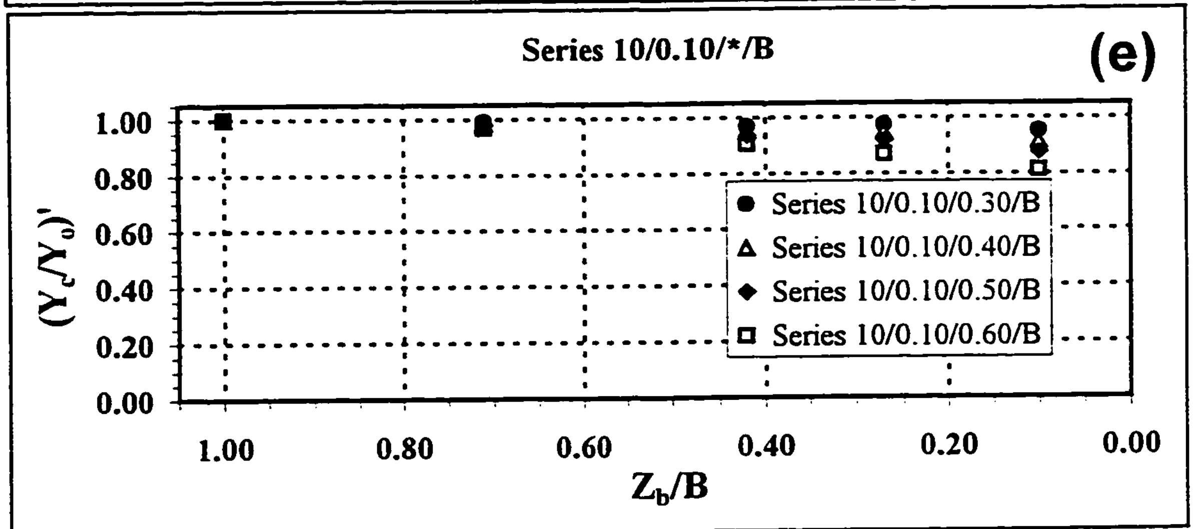

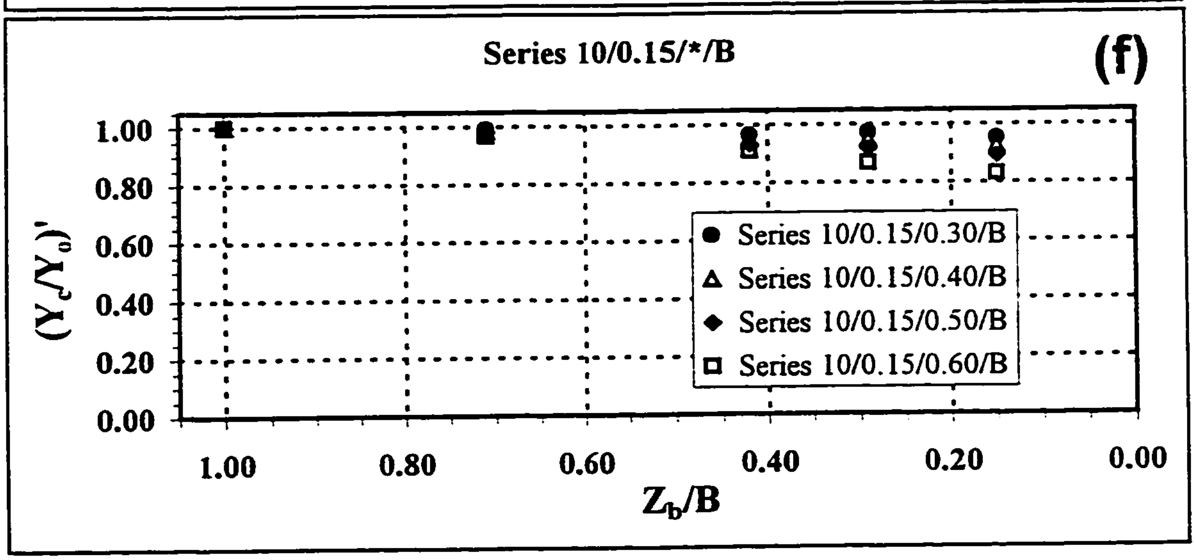

Figures 11(d-f): Averaged Normalized Flow Depth versus Proportional Bypass Width.

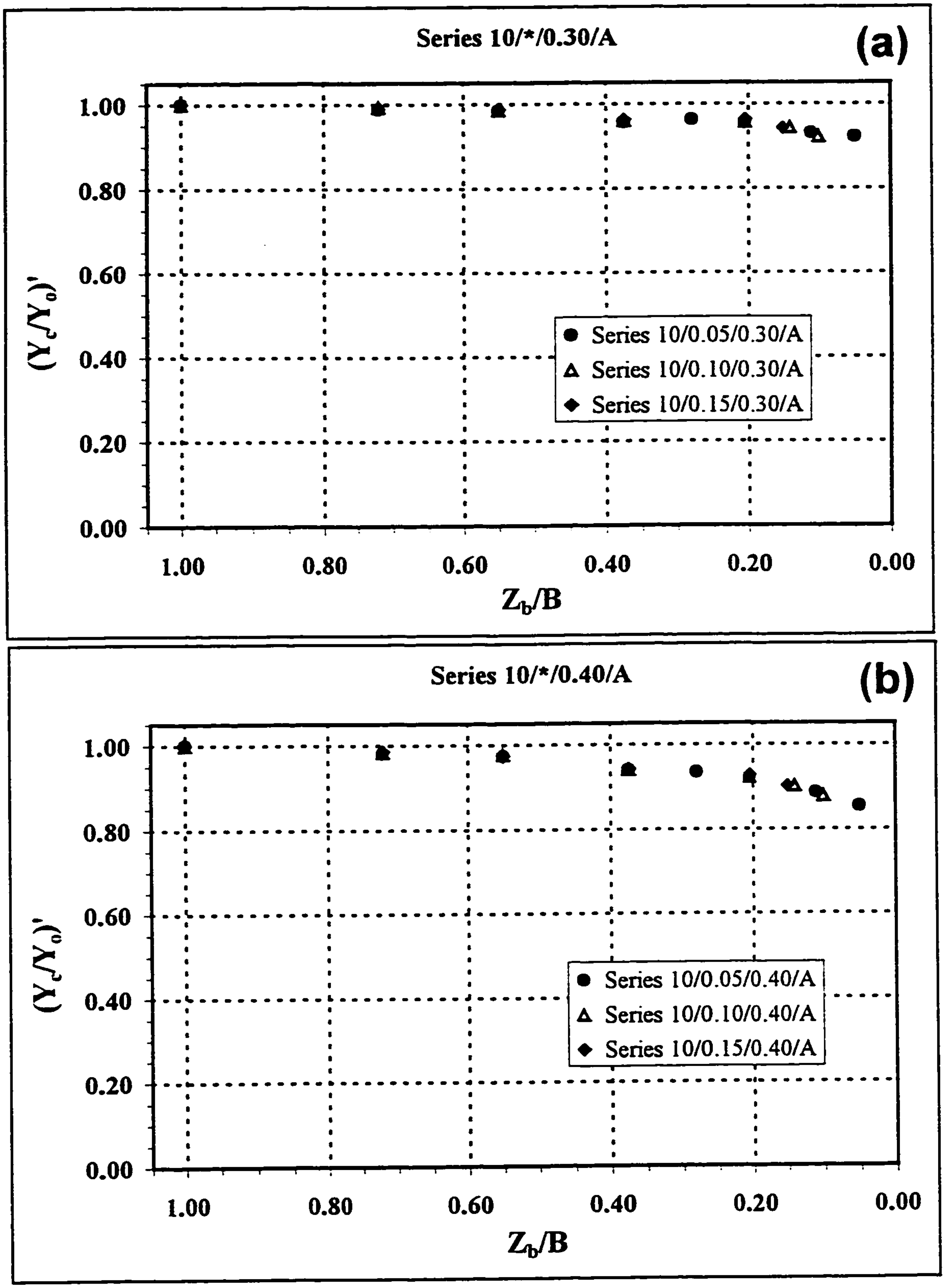

Figures 12(a-b): Averaged Normalized Flow Depth versus Proportional Bypass Width.

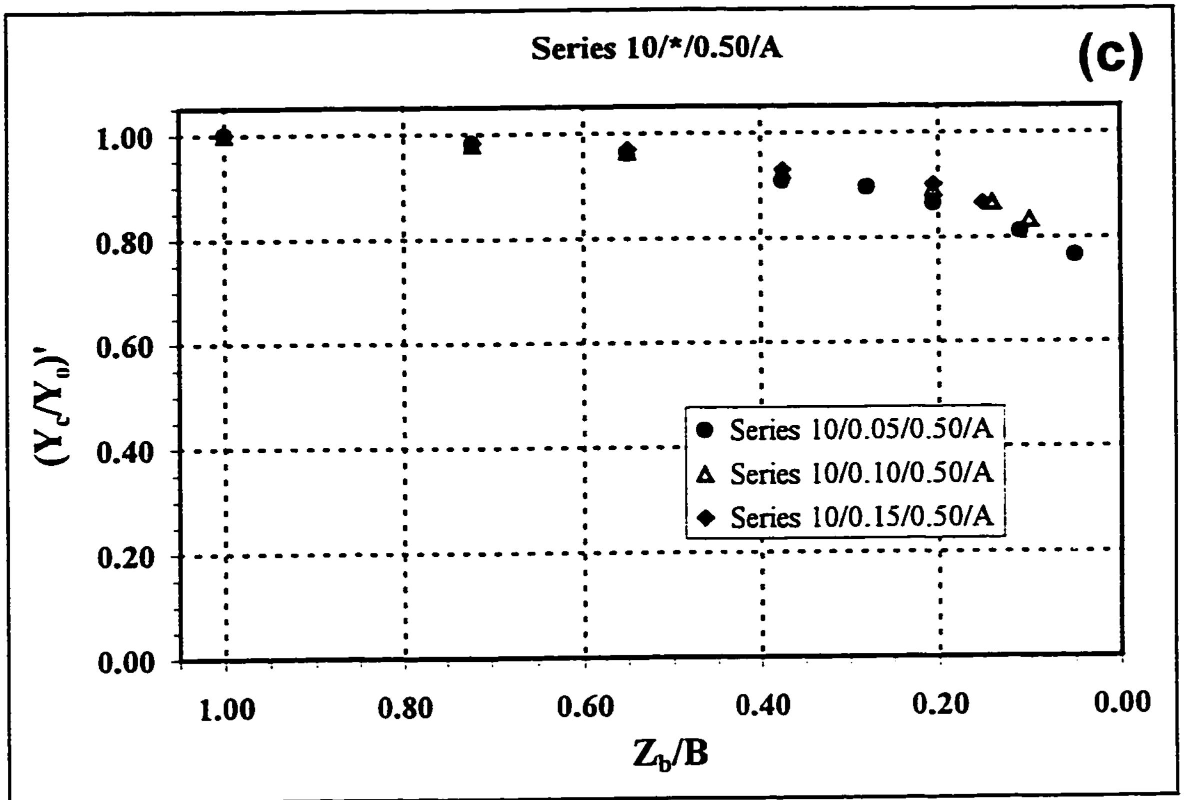

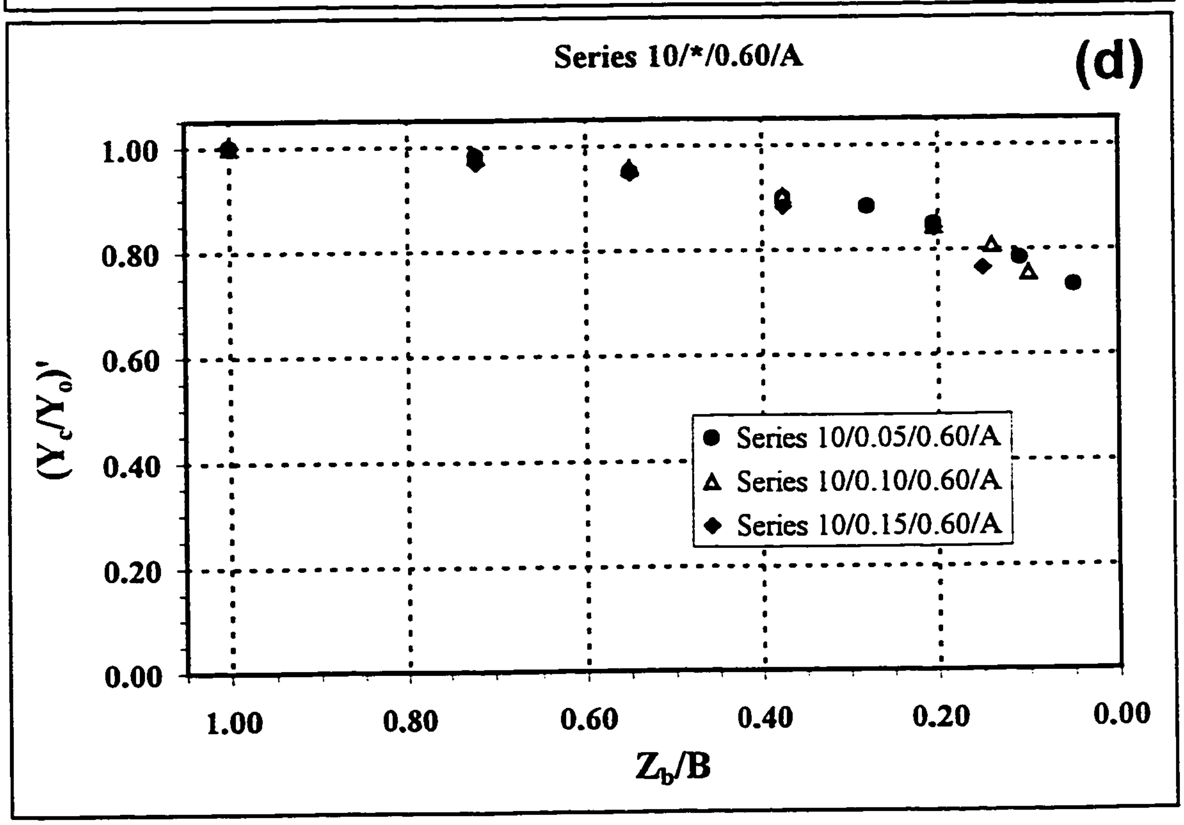

Figures 12(c-d): Averaged Normalized Flow Depth versus Proportional Bypass Width.

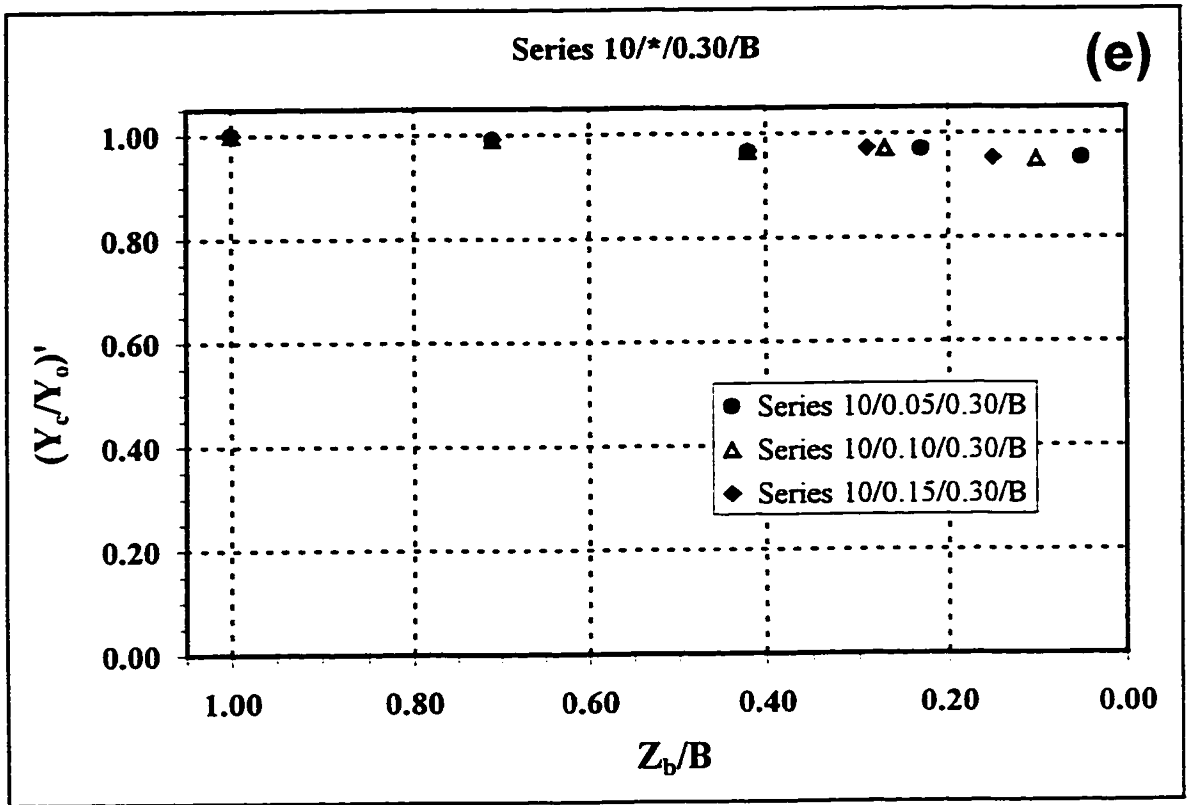

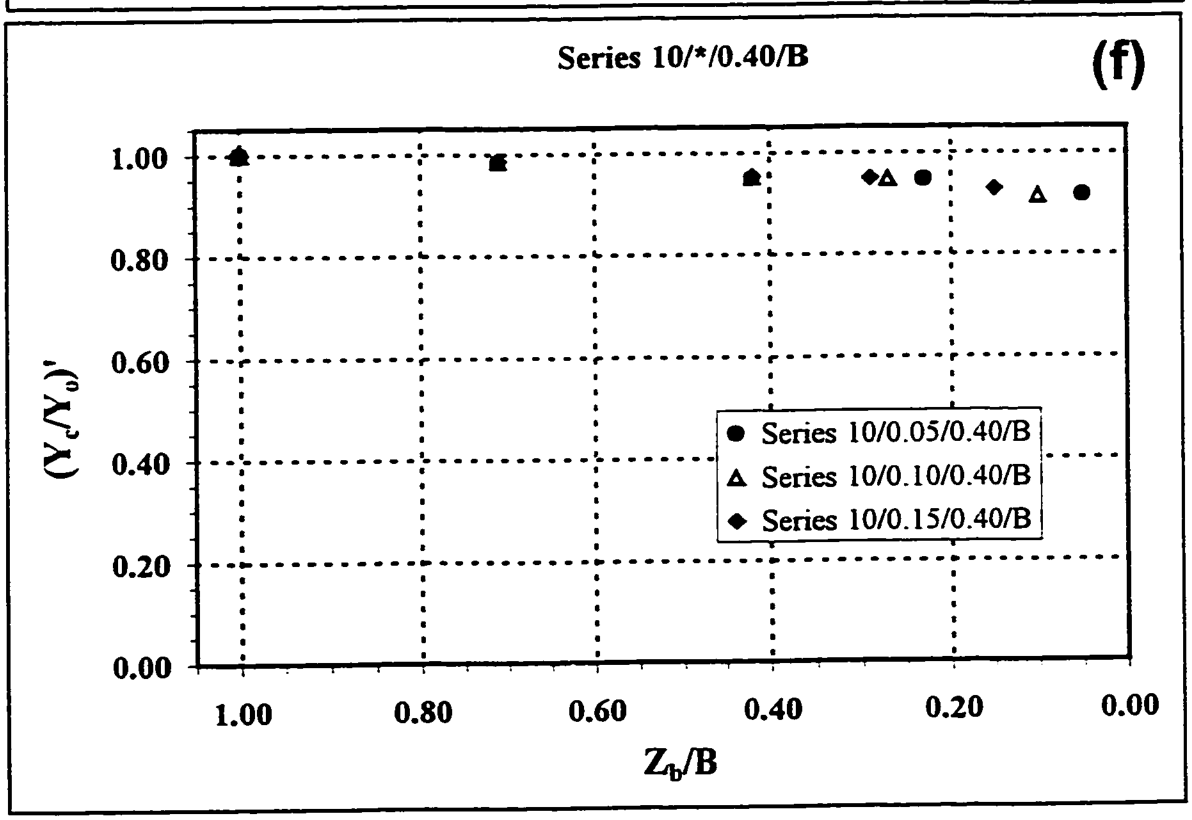

Figures 12(e-f): Averaged Normalized Flow Depth versus Proportional Bypass Width.

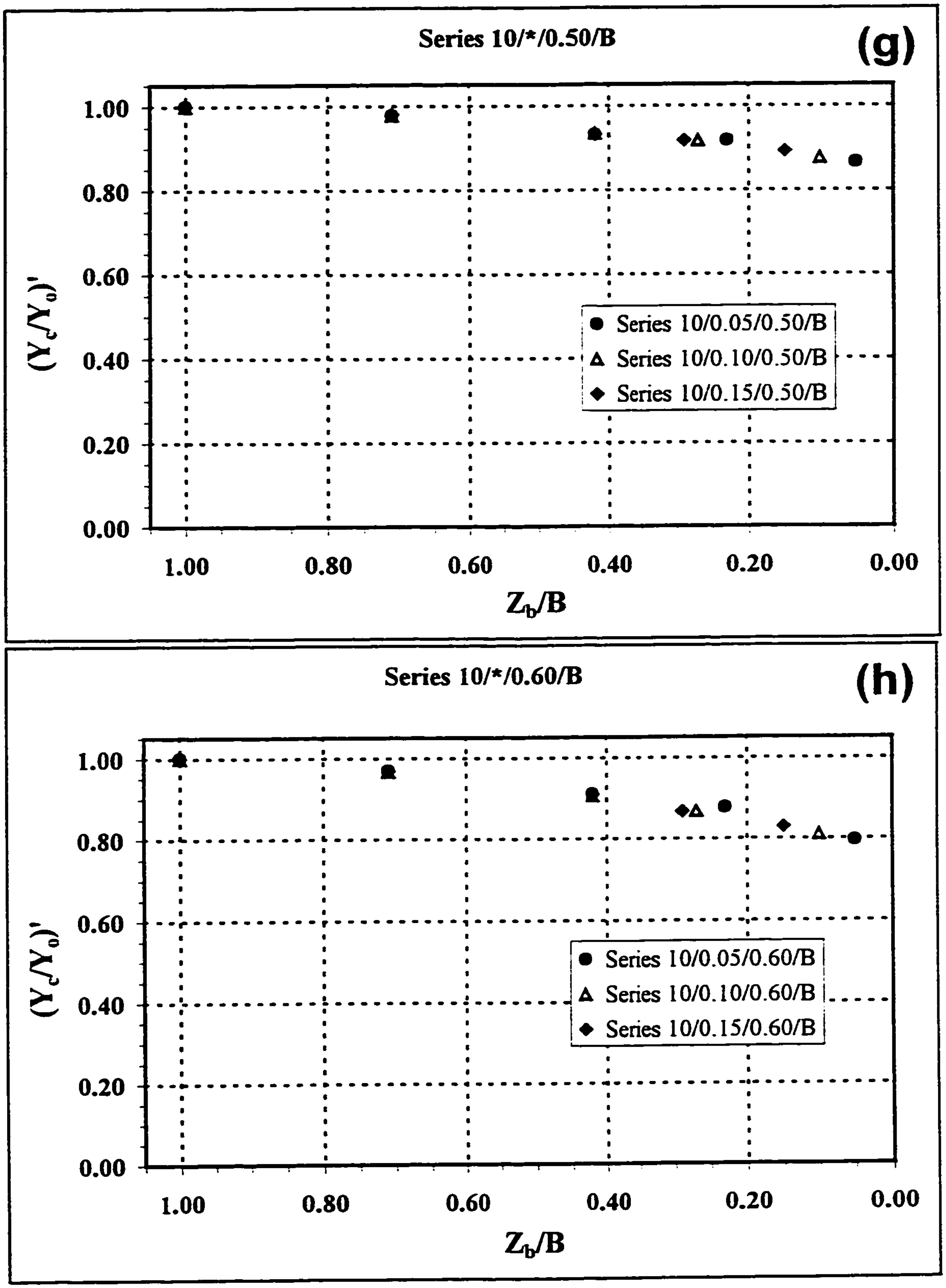

Figures 12(g-h): Averaged Normalized Flow Depth versus Proportional Bypass Width.

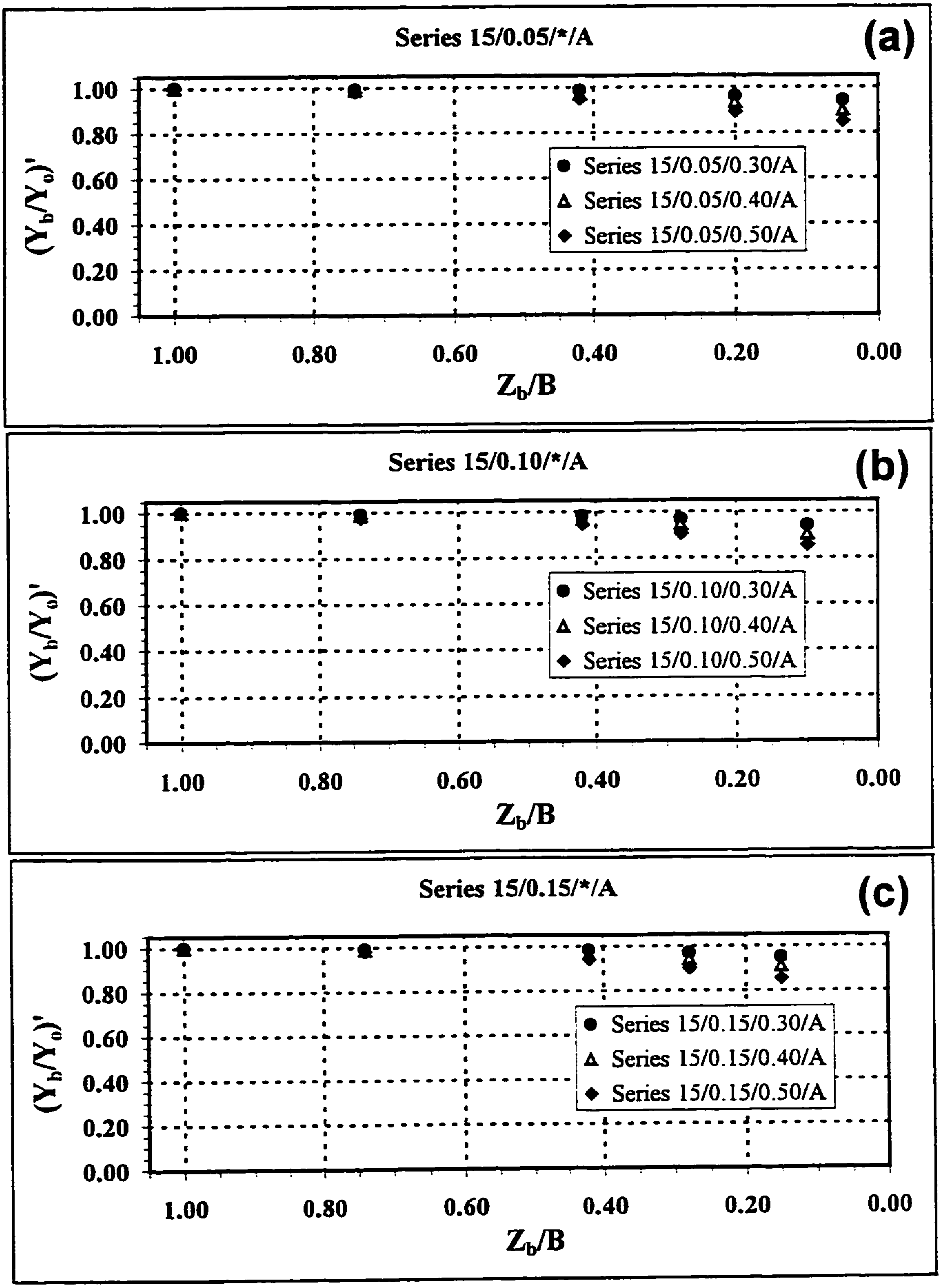

Figures 13(a-c): Averaged Normalized Flow Depth versus Proportional Bypass Width.

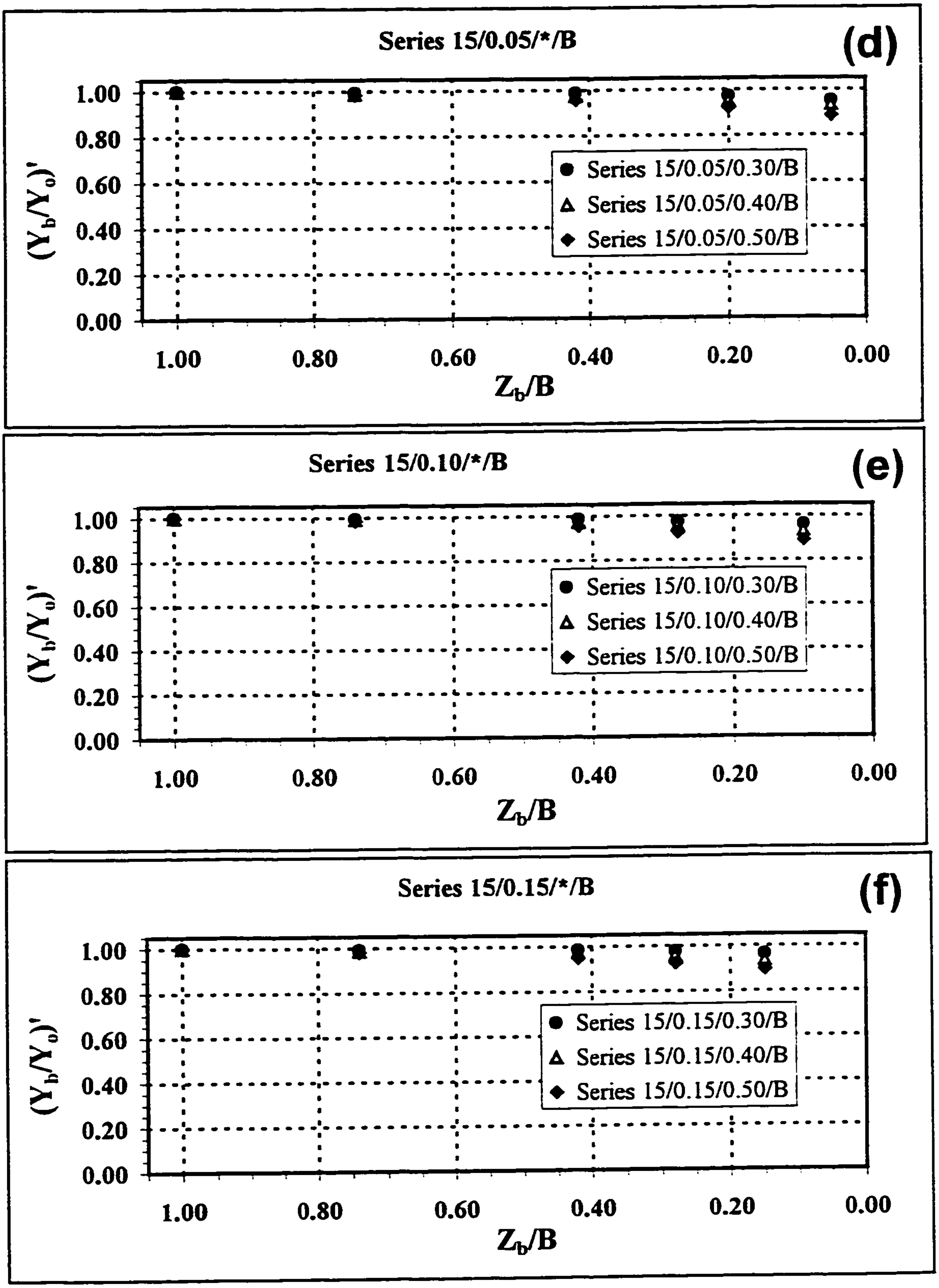

Figures 13(d-f): Averaged Normalized Flow Depth versus Proportional Bypass Width.

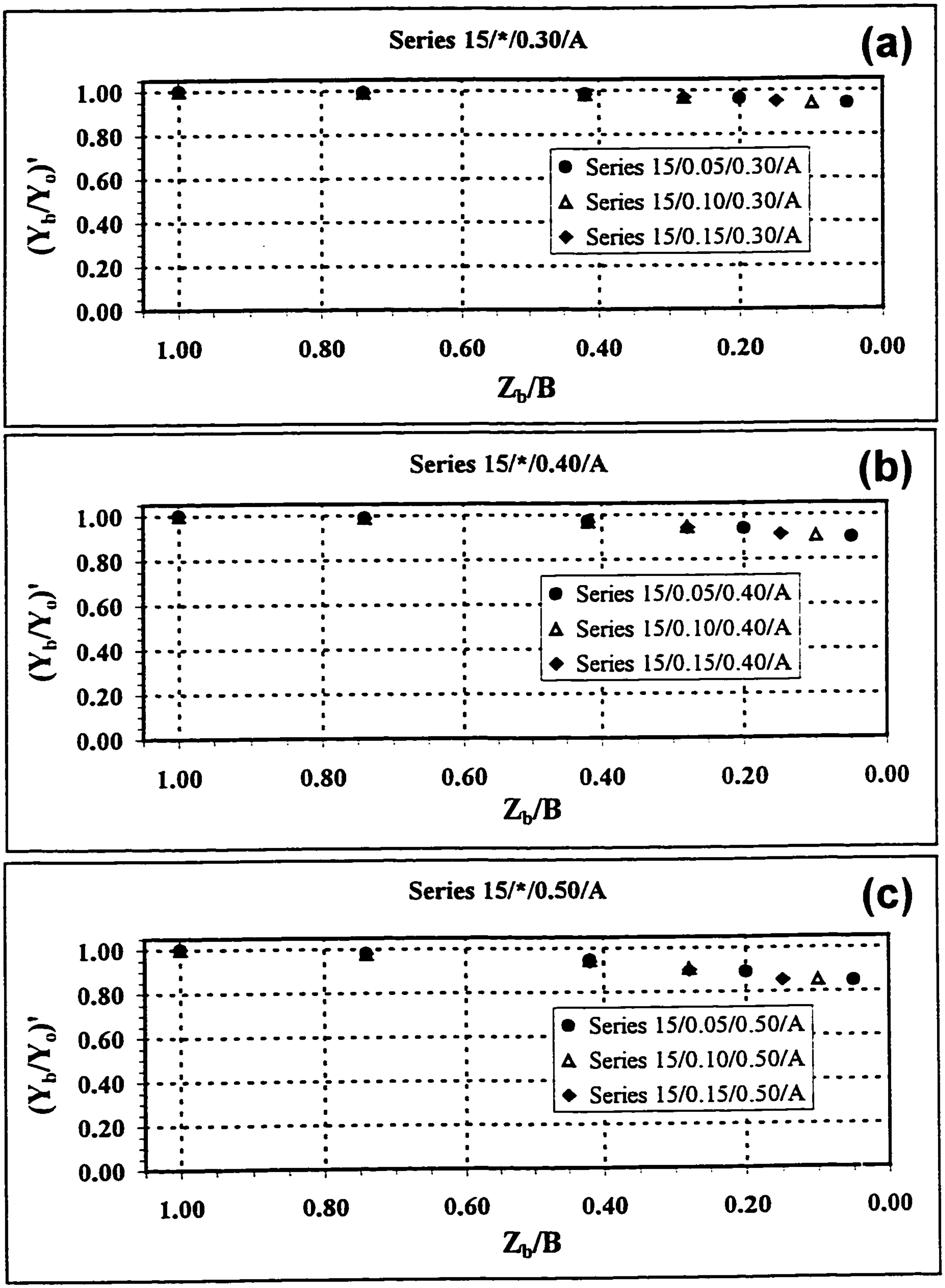

Figures 14(a-c): Averaged Normalized Flow Depth versus Proportional Bypass Width.

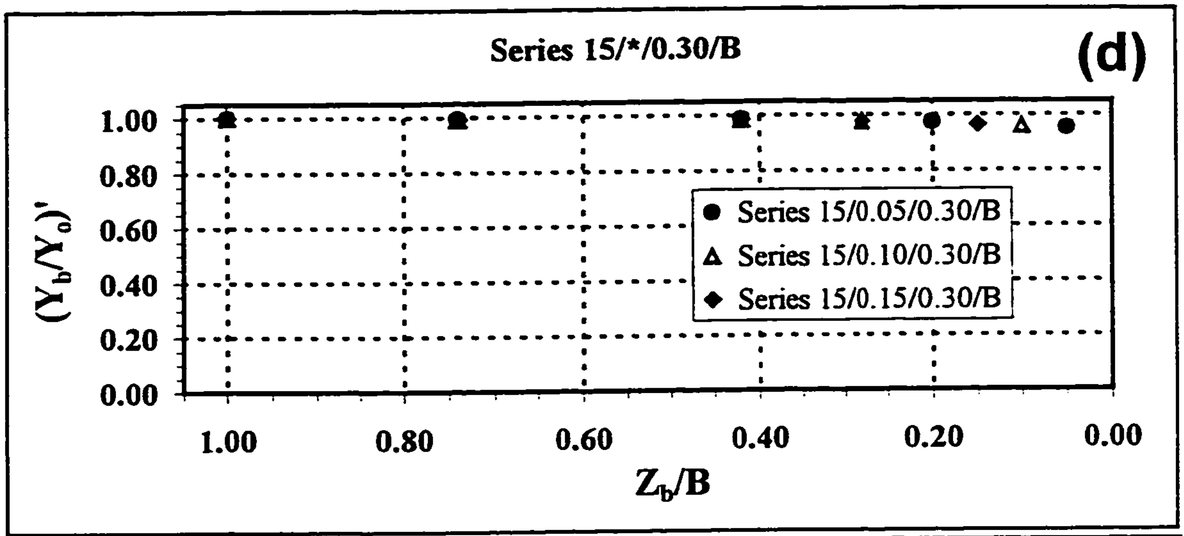

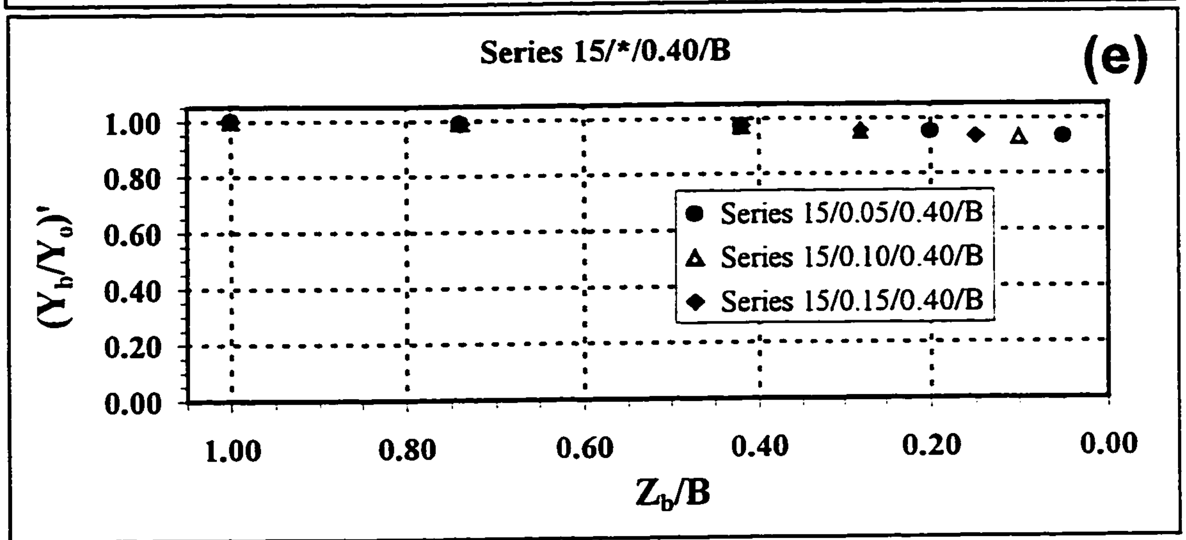

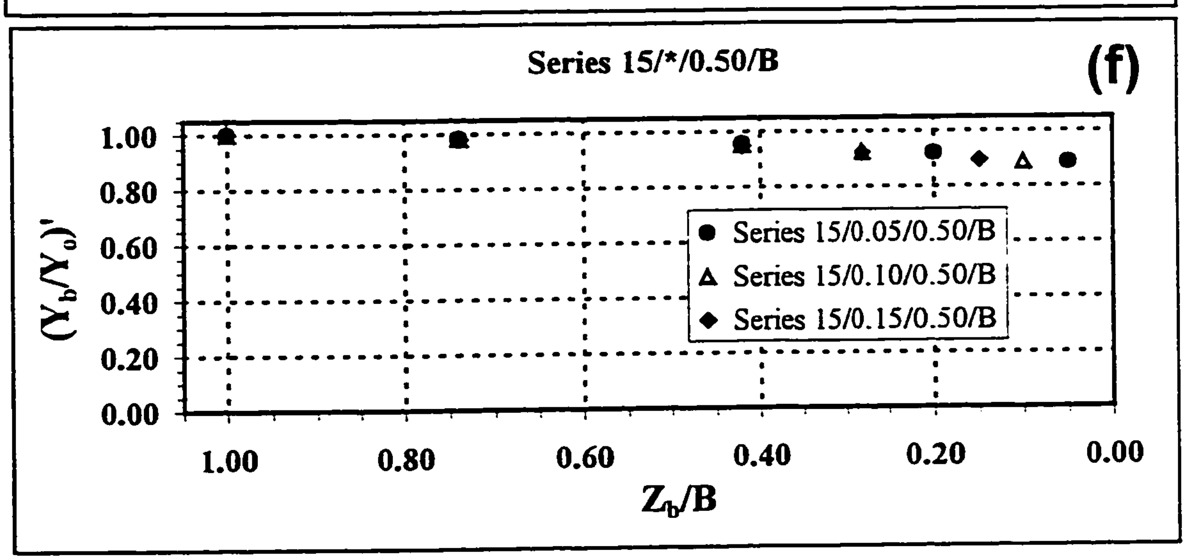

Figures 14(d-f): Averaged Normalized Flow Depth versus Proportional Bypass Width.

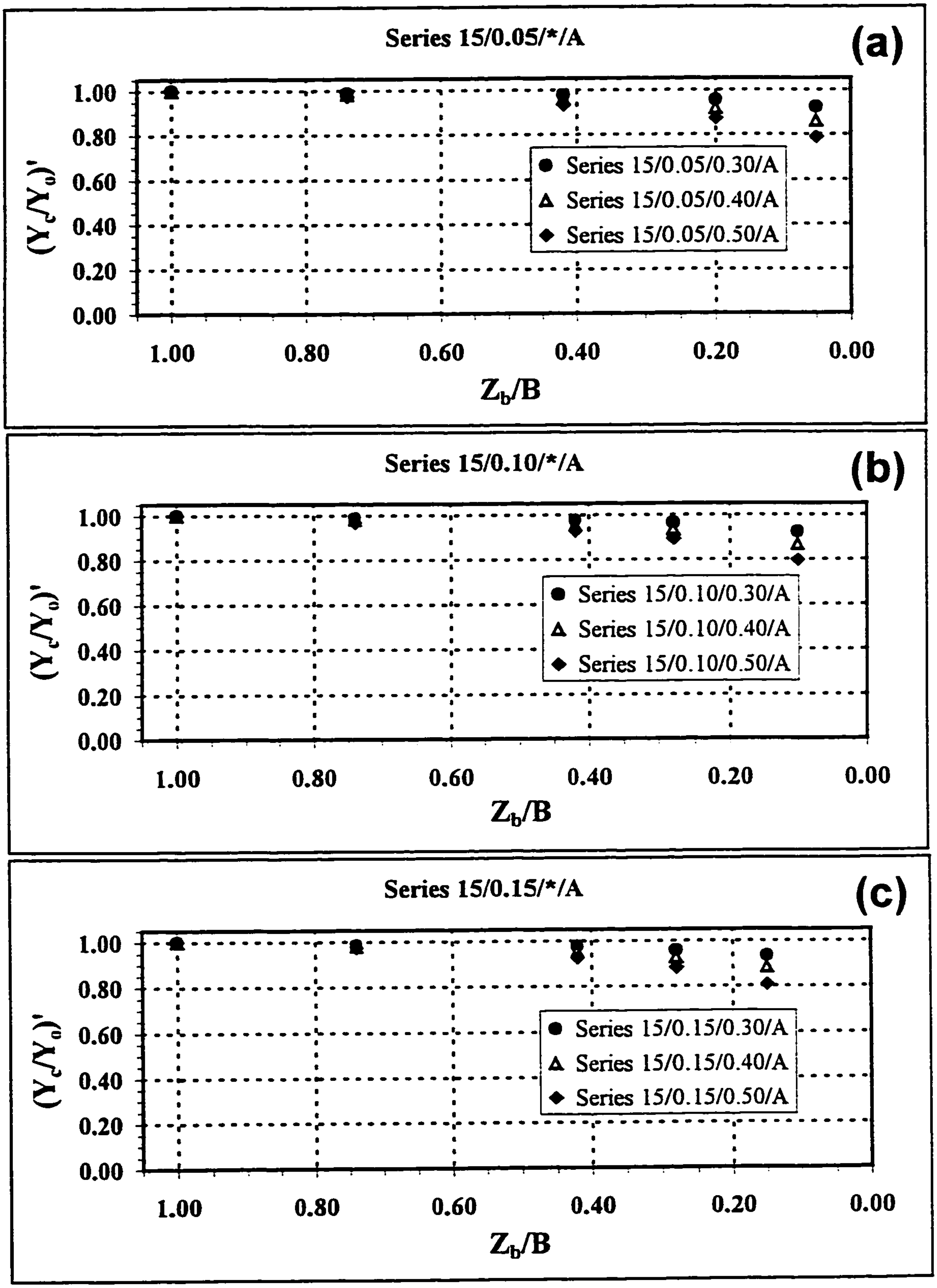

Figures 15(a-c): Averaged Normalized Flow Depth versus Proportional Bypass Width.

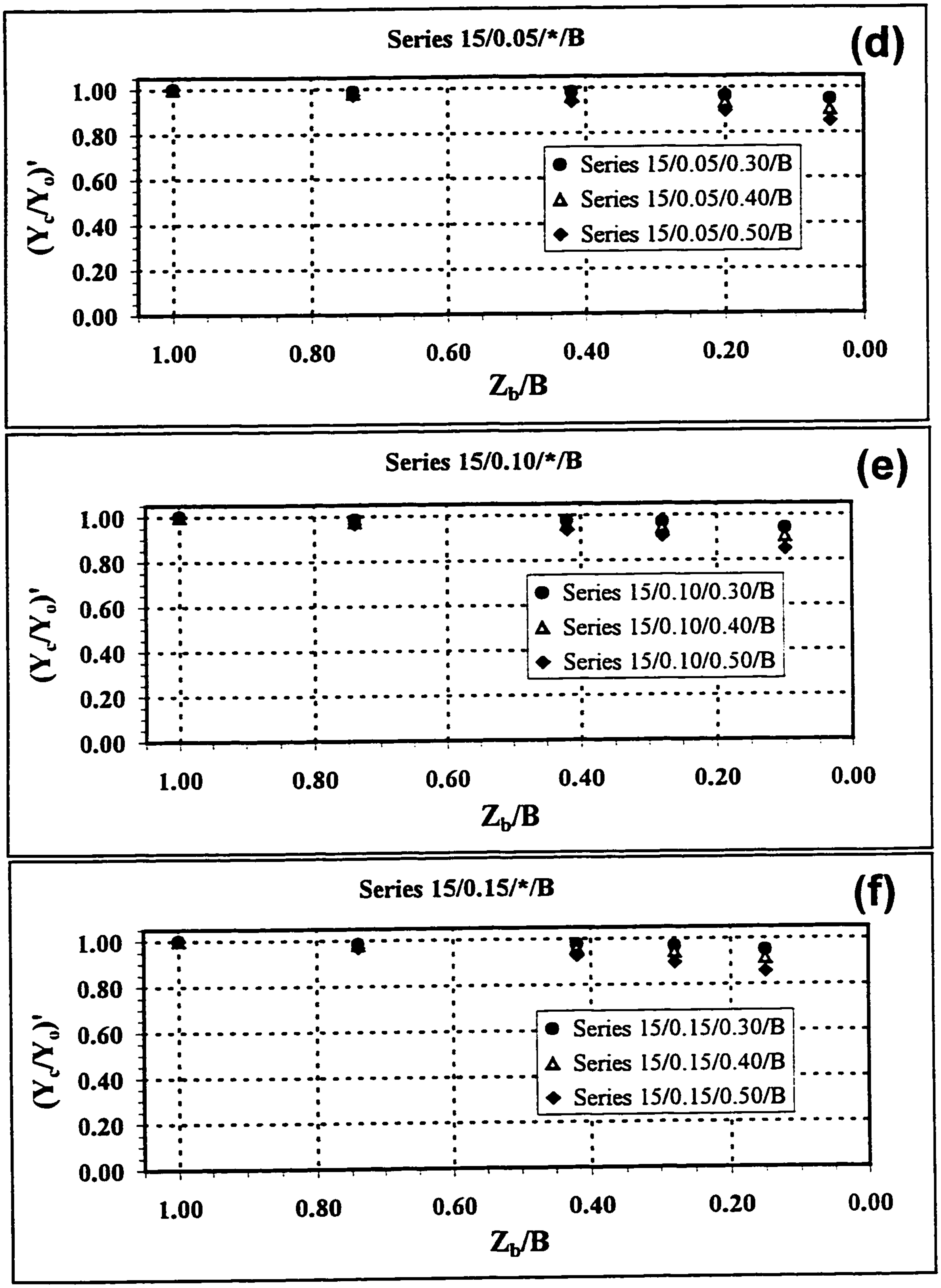

Figures 15(d-f): Averaged Normalized Flow Depth versus Proportional Bypass Width.

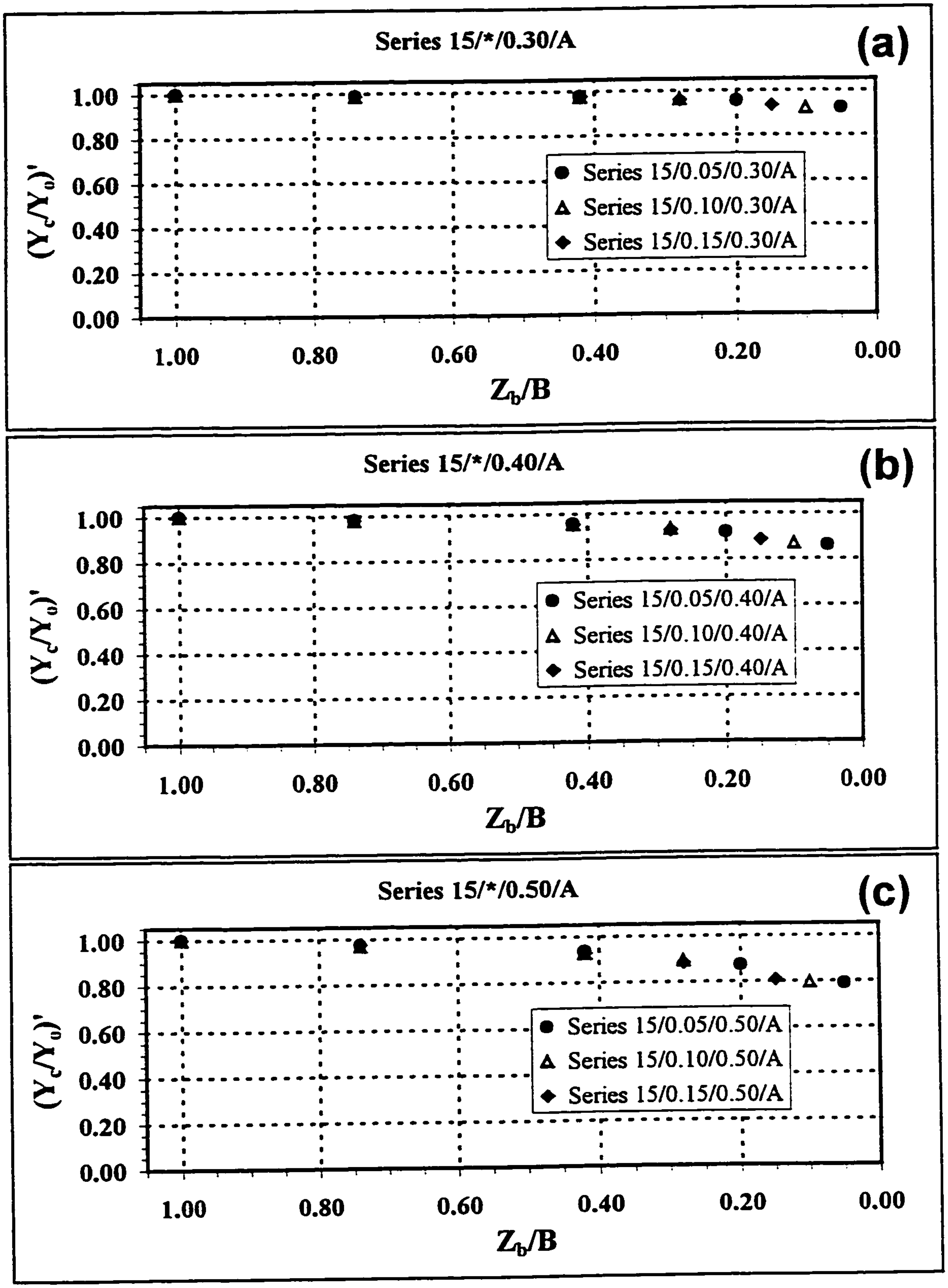

Figures 16(a-c): Averaged Normalized Flow Depth versus Proportional Bypass Width.

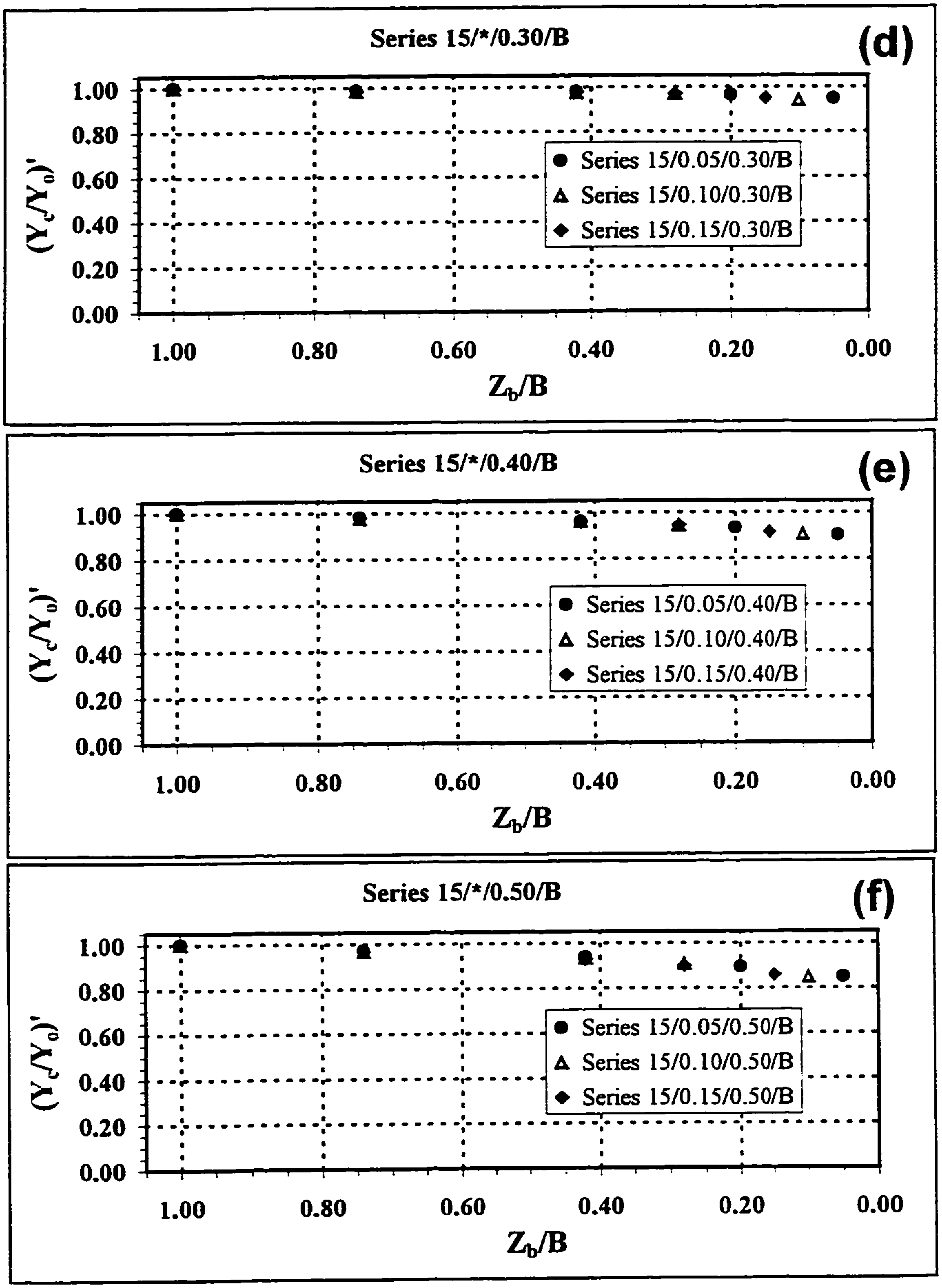

Figures 16(d-f): Averaged Normalized Flow Depth versus Proportional Bypass Width.

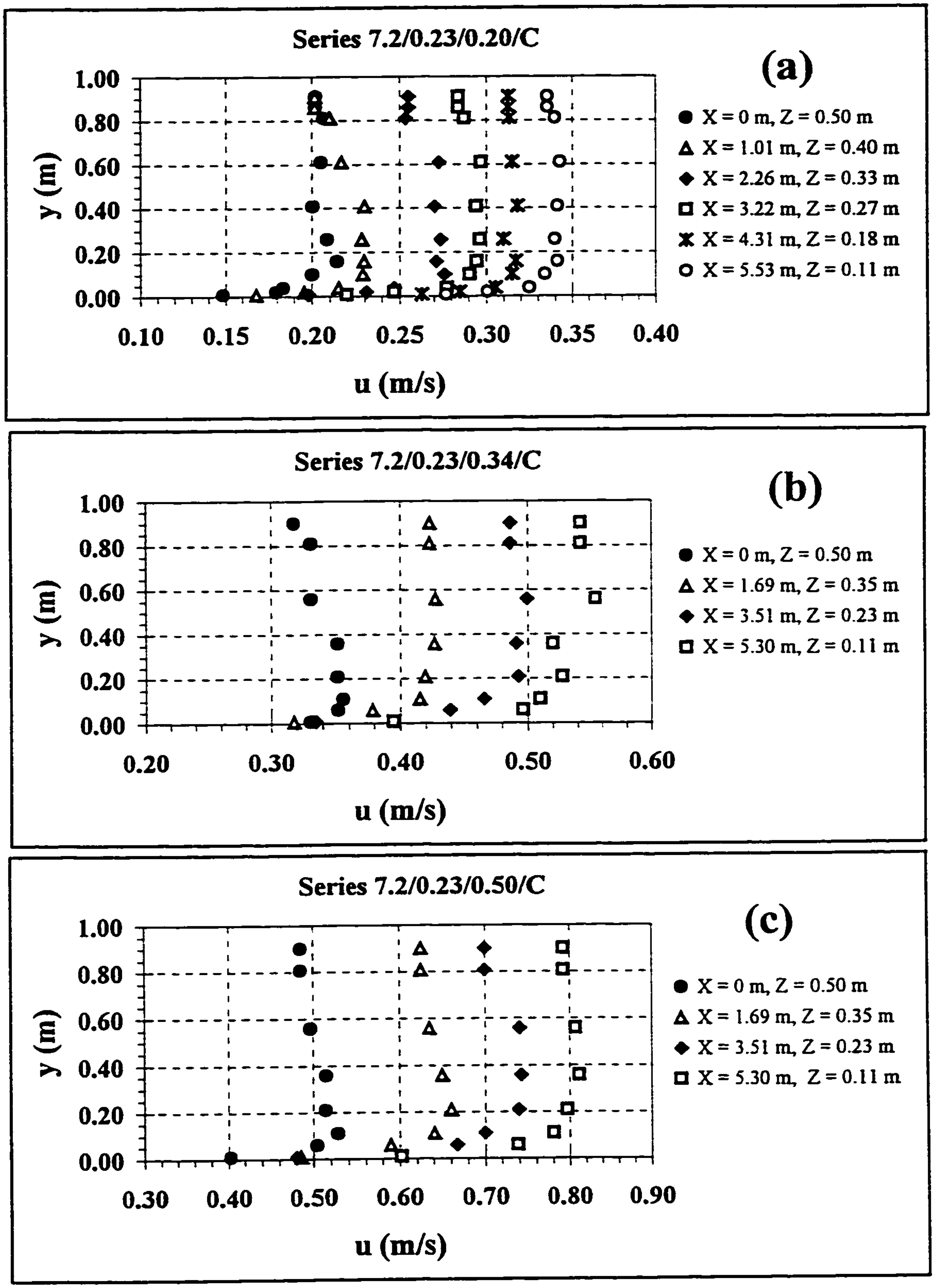

Figures 17(a-c): Center-Plane Velocity Profiles Within the Fish Bypass Section.

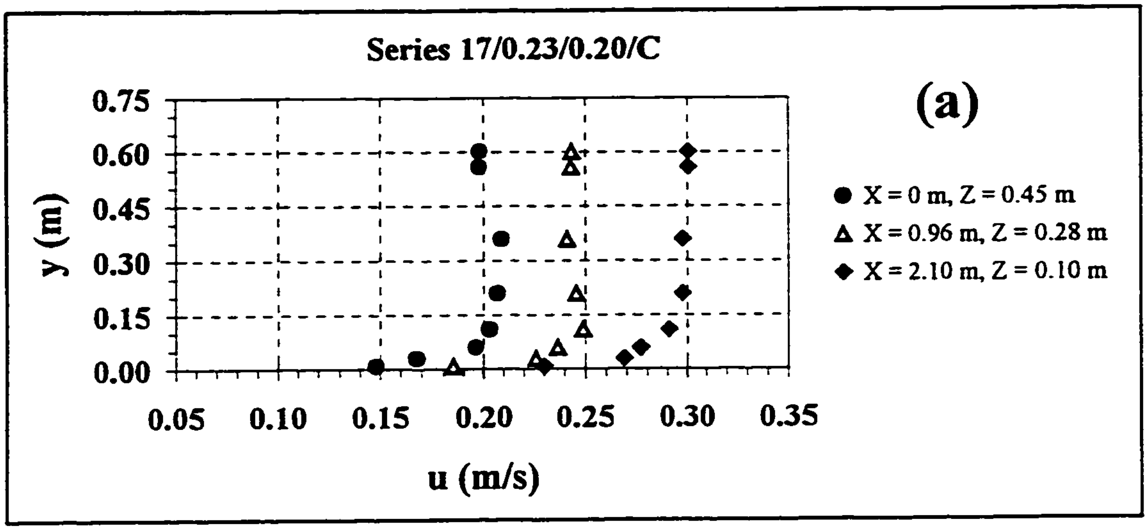

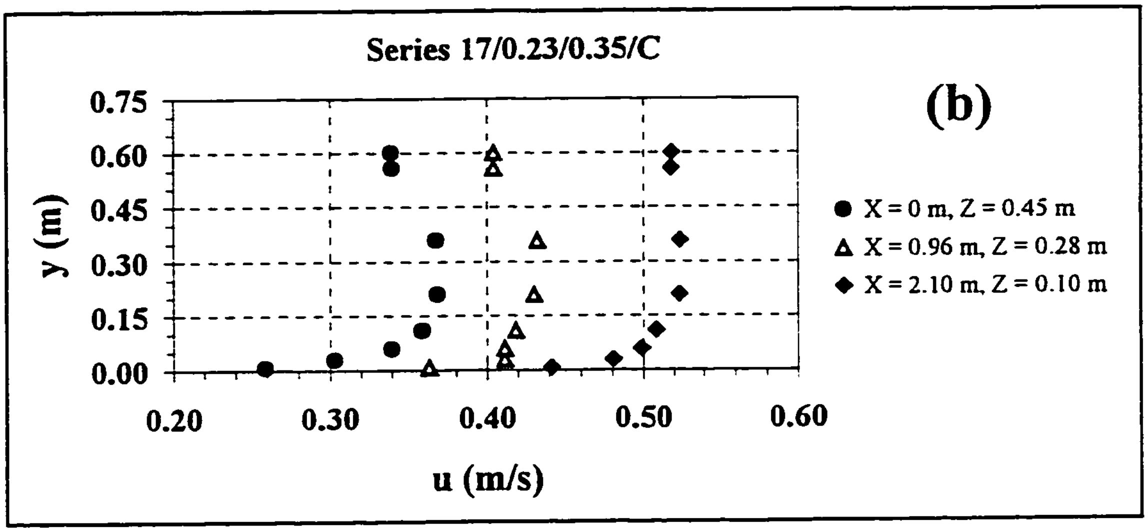

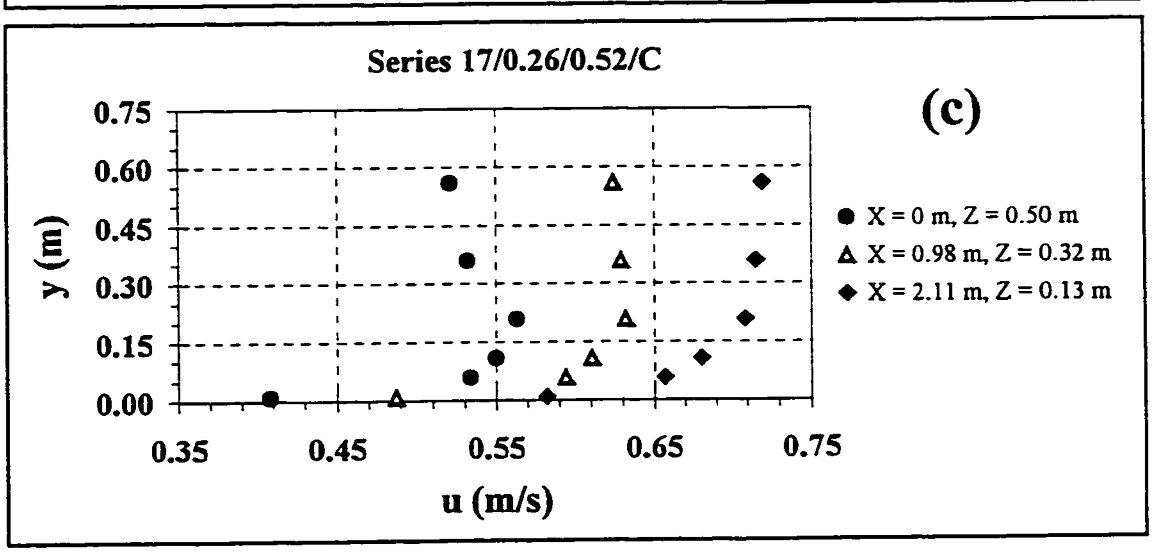

Figures 18(a-c): Center-Plane Velocity Profiles Within the Fish Bypass Section.

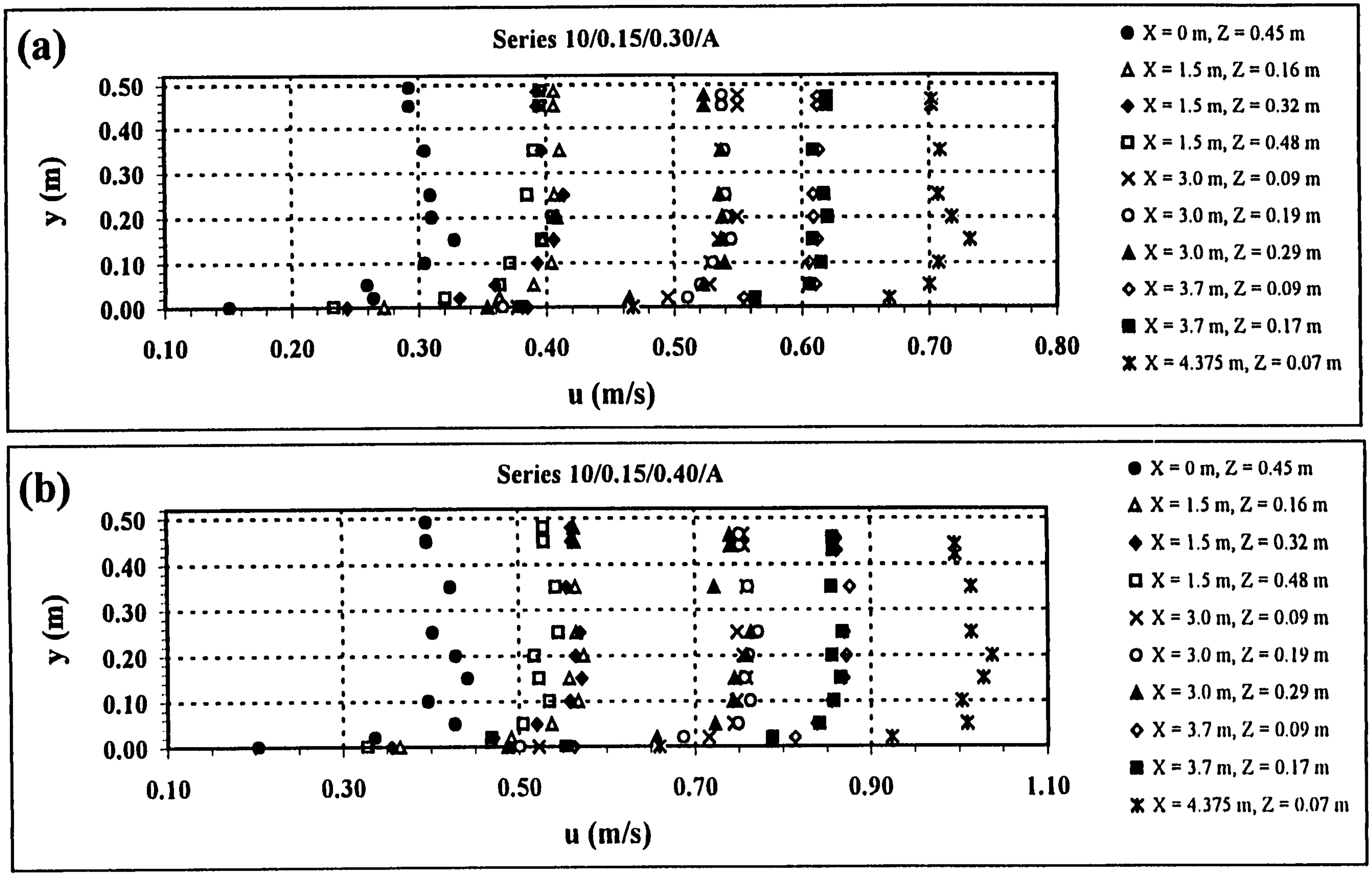

Figures 19(a-b): Velocity Profiles Within the Fish Bypass Section.

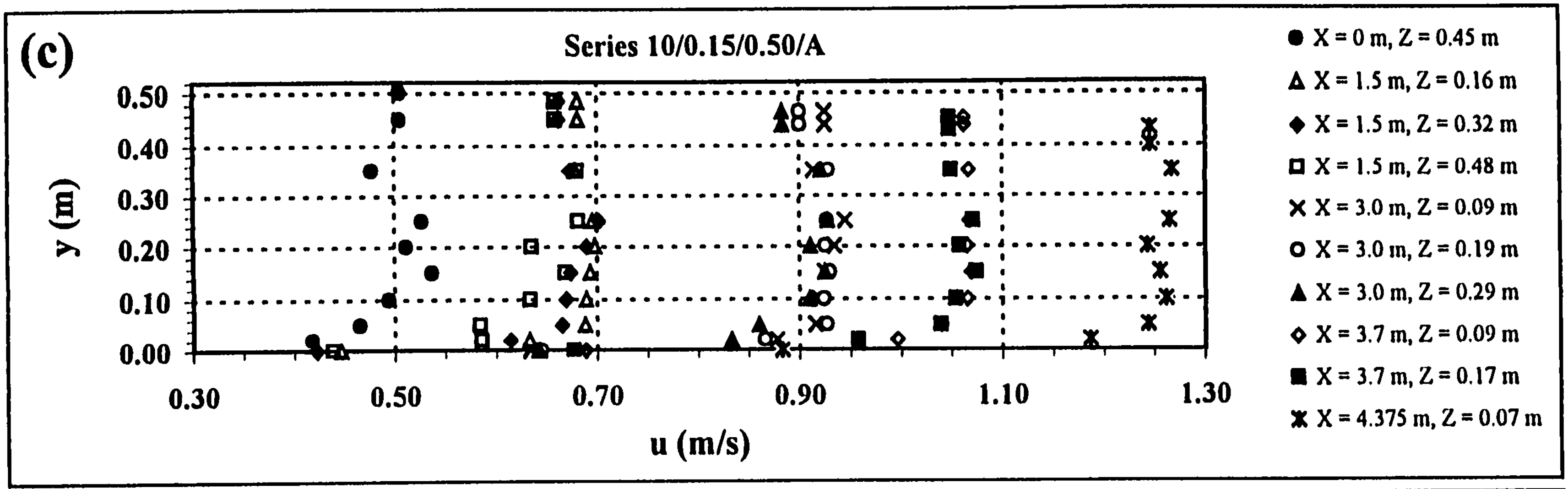

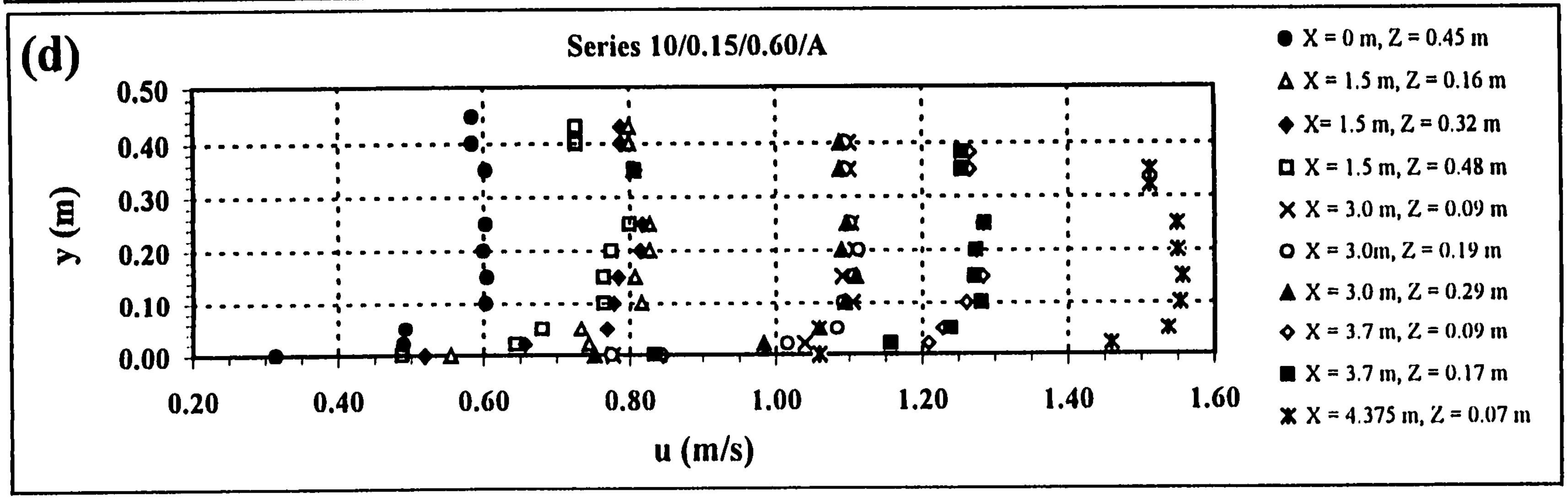

Figures 19(c-d): Velocity Profiles Within the Fish Bypass Section.

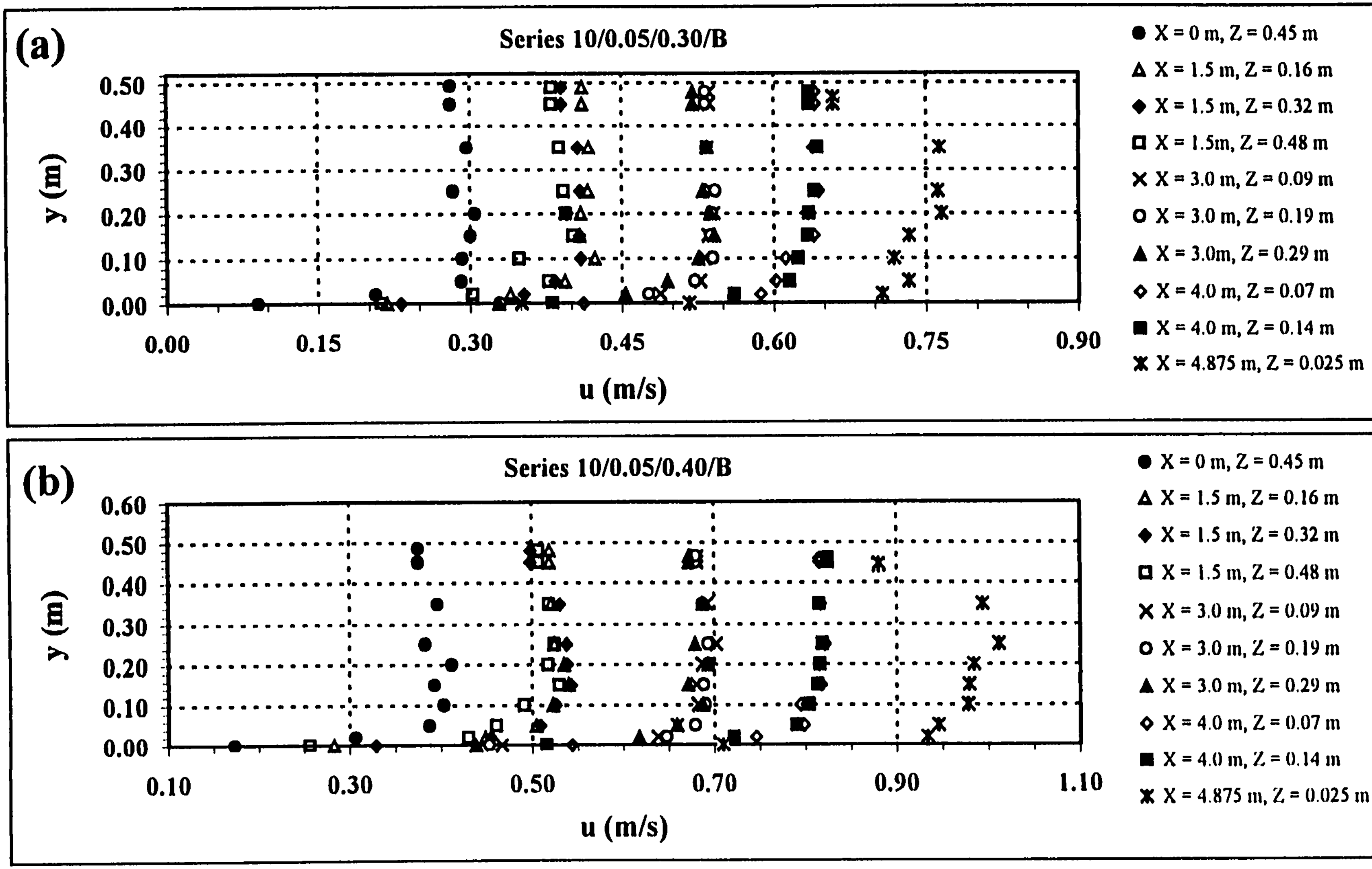

Figures 20(a-b): Velocity Profiles Within the Fish Bypass Section.

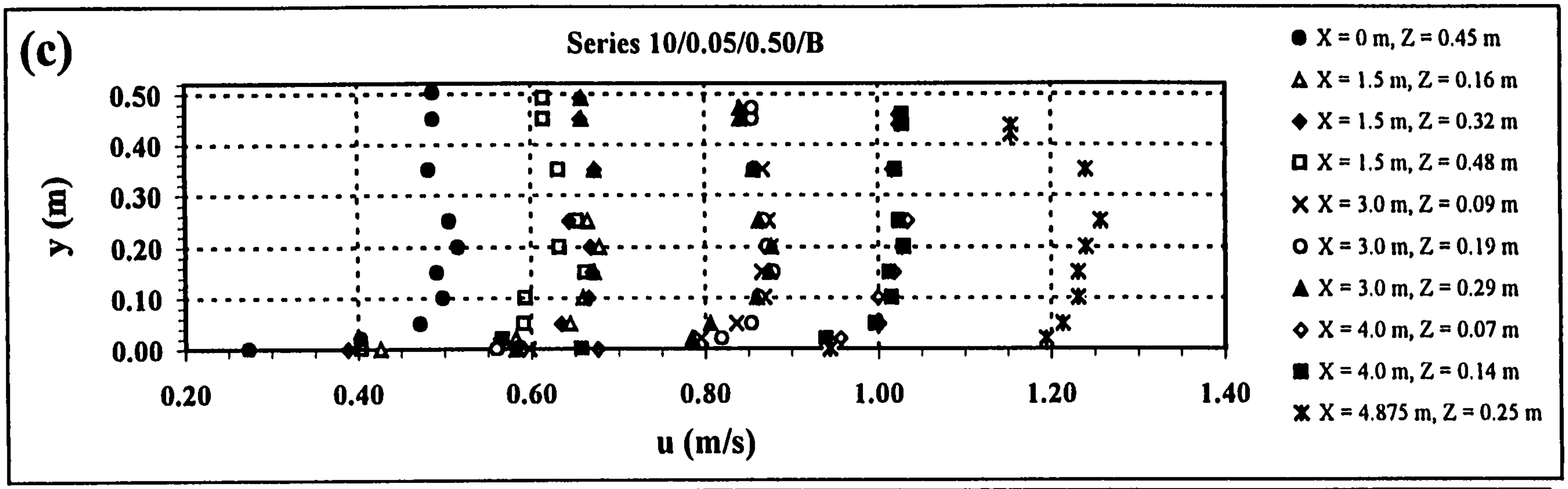

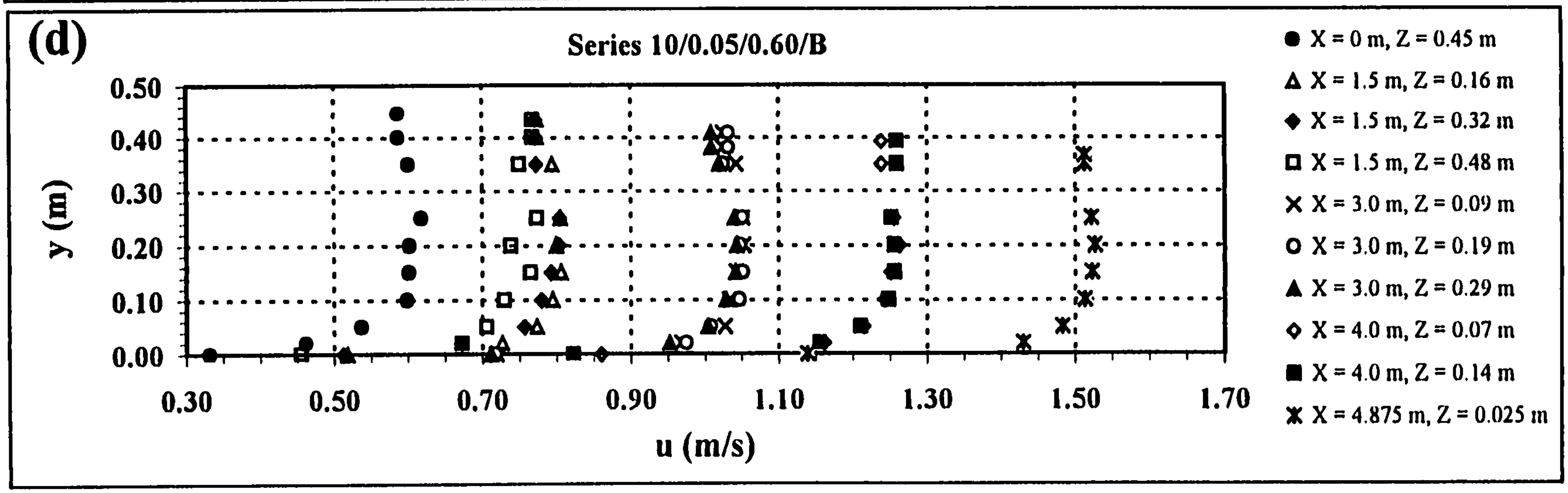

Figures 20(c-d): Velocity Profiles Within the Fish Bypass Section.

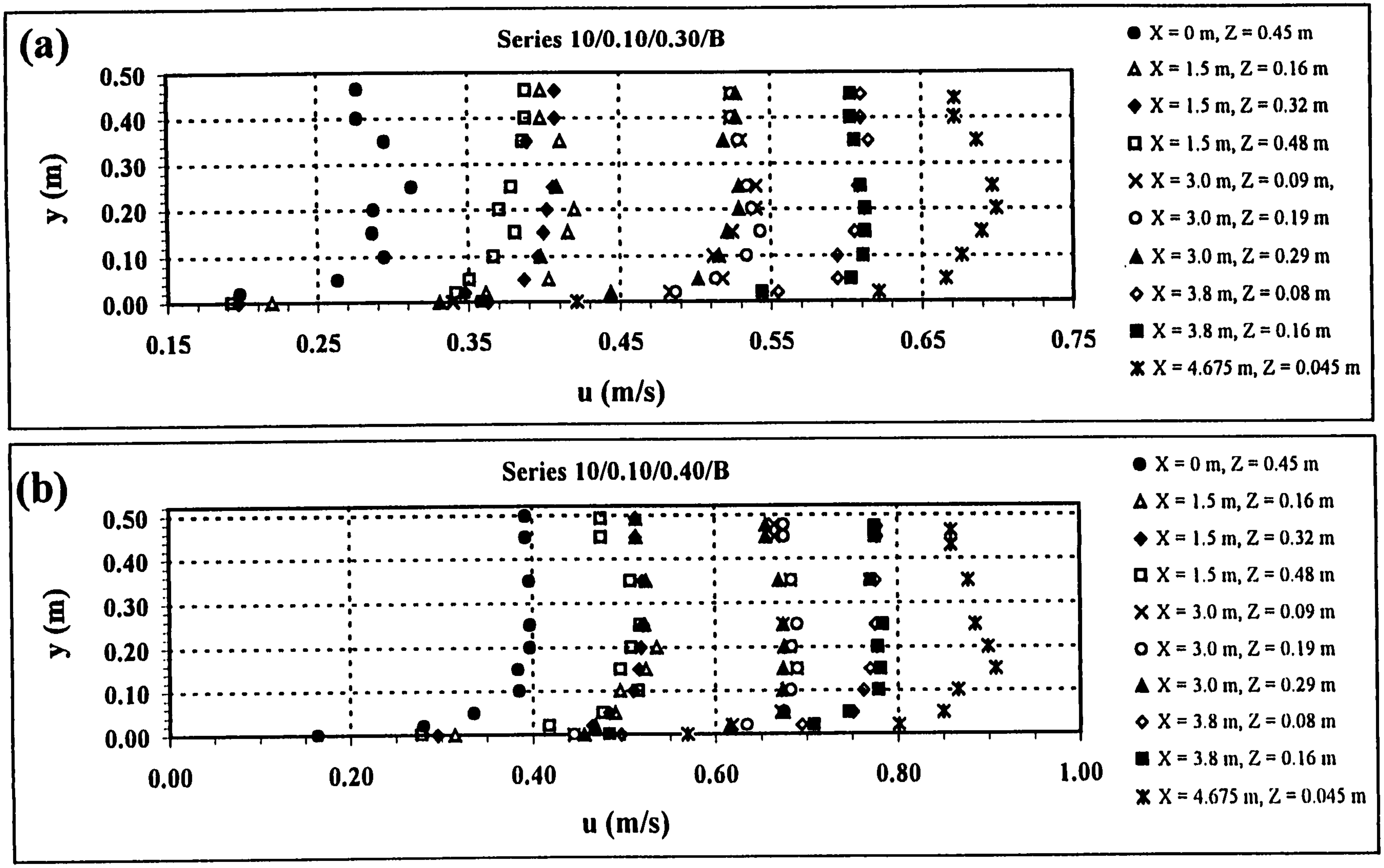

Figures 21(a-b): Velocity Profiles Within the Fish Bypass Section.

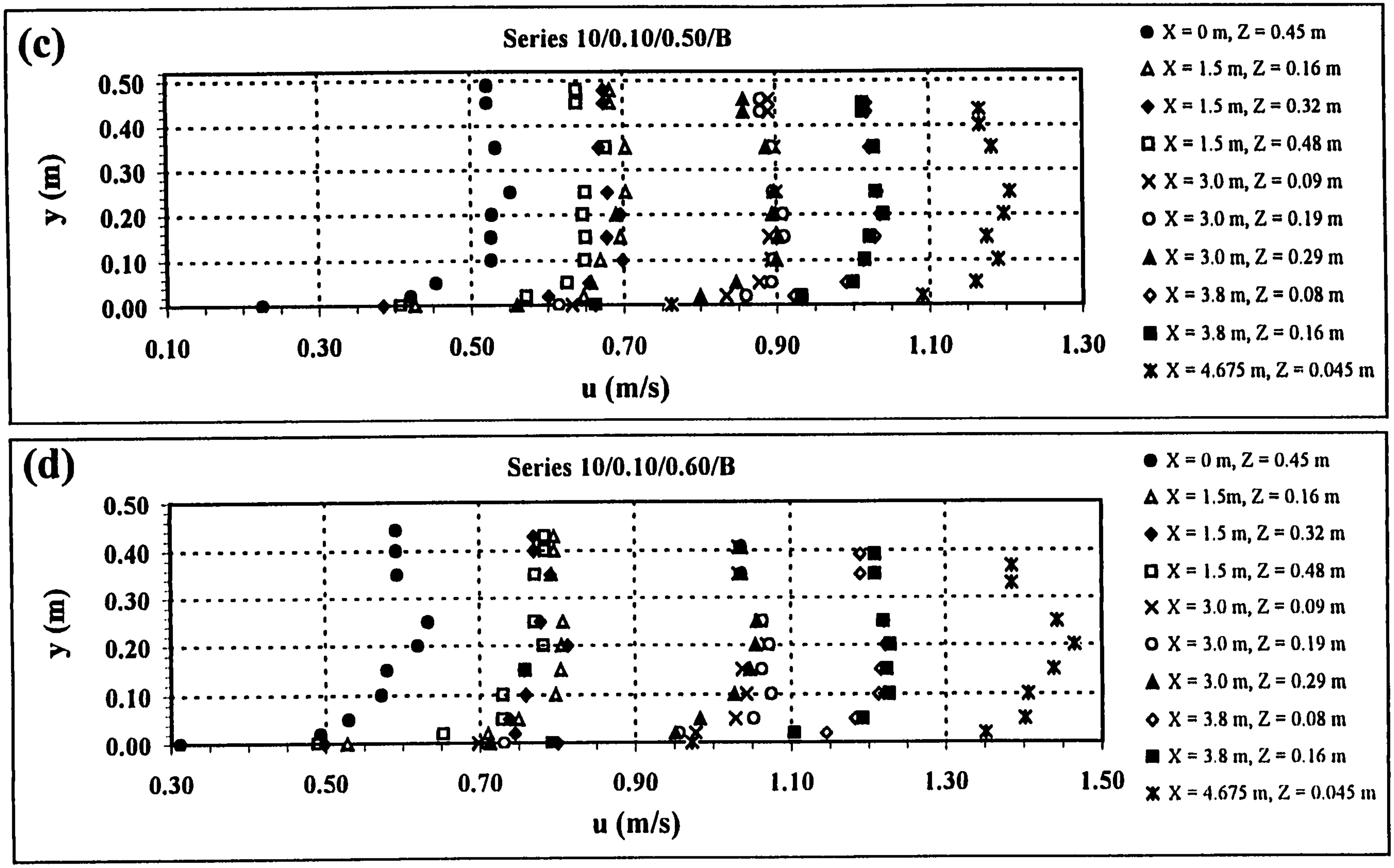

Figures 21(c-d): Velocity Profiles Within the Fish Bypass Section.

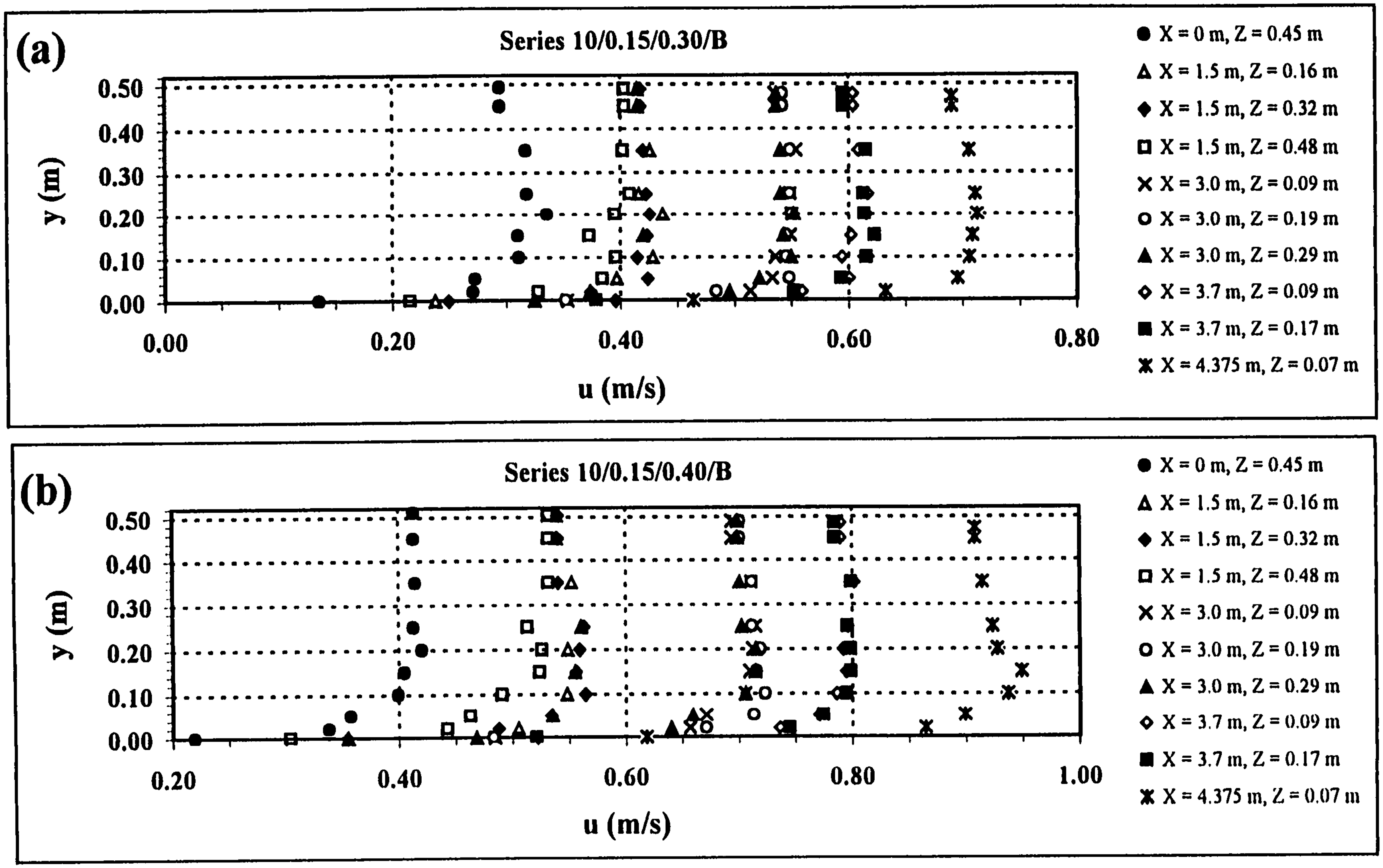

Figures 22(a-b): Velocity Profiles Within the Fish Bypass Section.

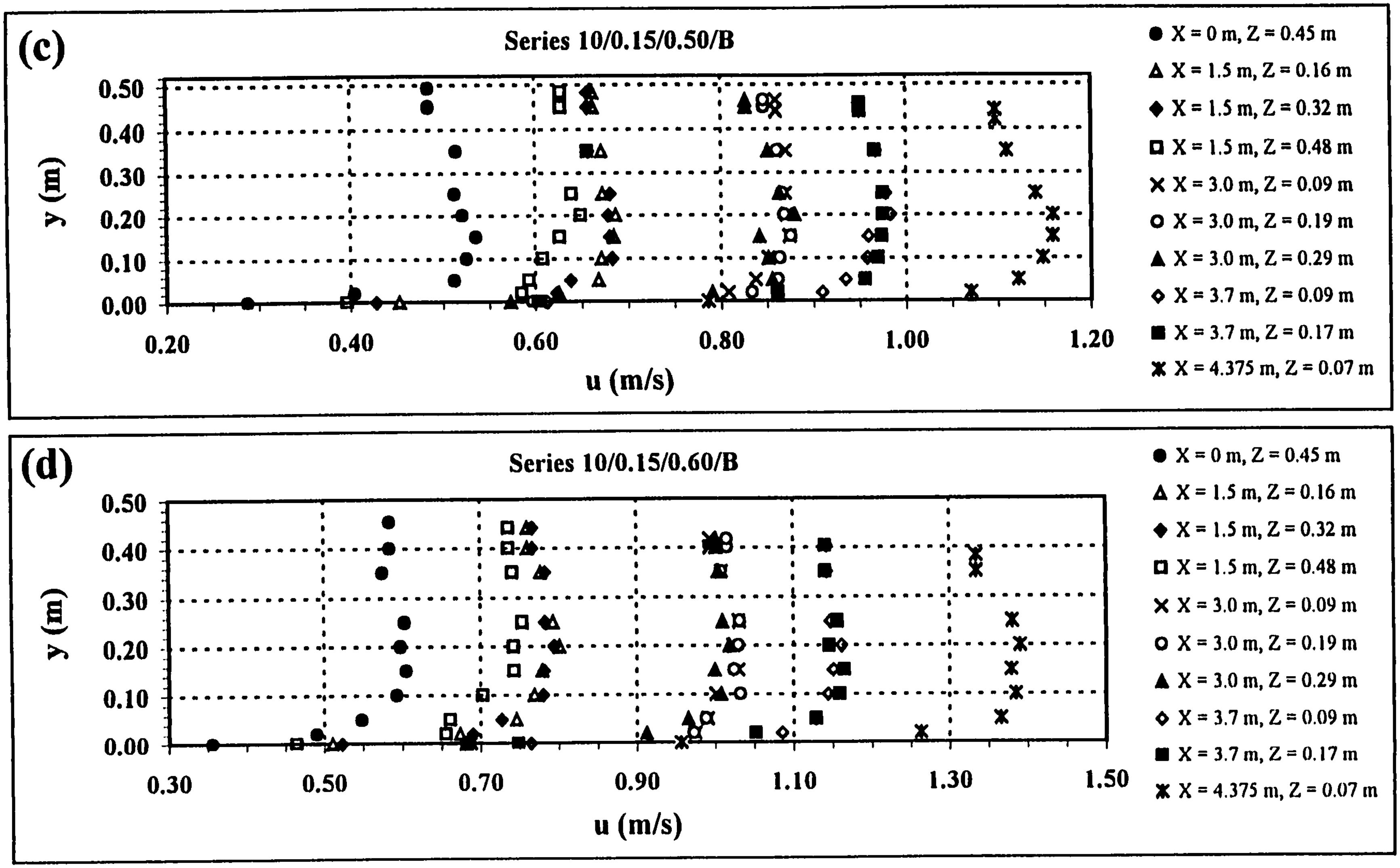

Figures 22(c-d): Velocity Profiles Within the Fish Bypass Section.

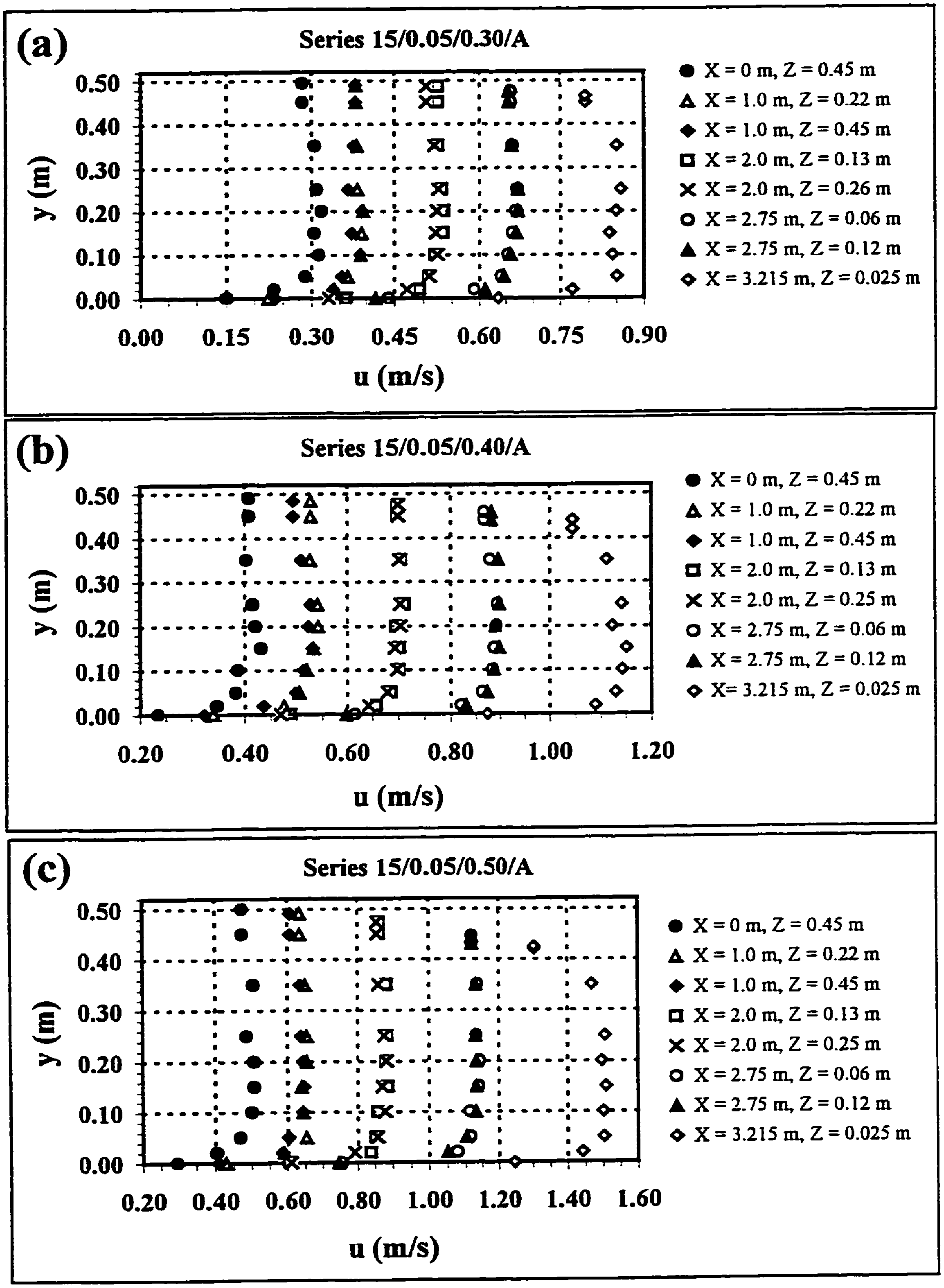

Figures 23(a-c): Velocity Profiles Within the Fish Bypass Section.

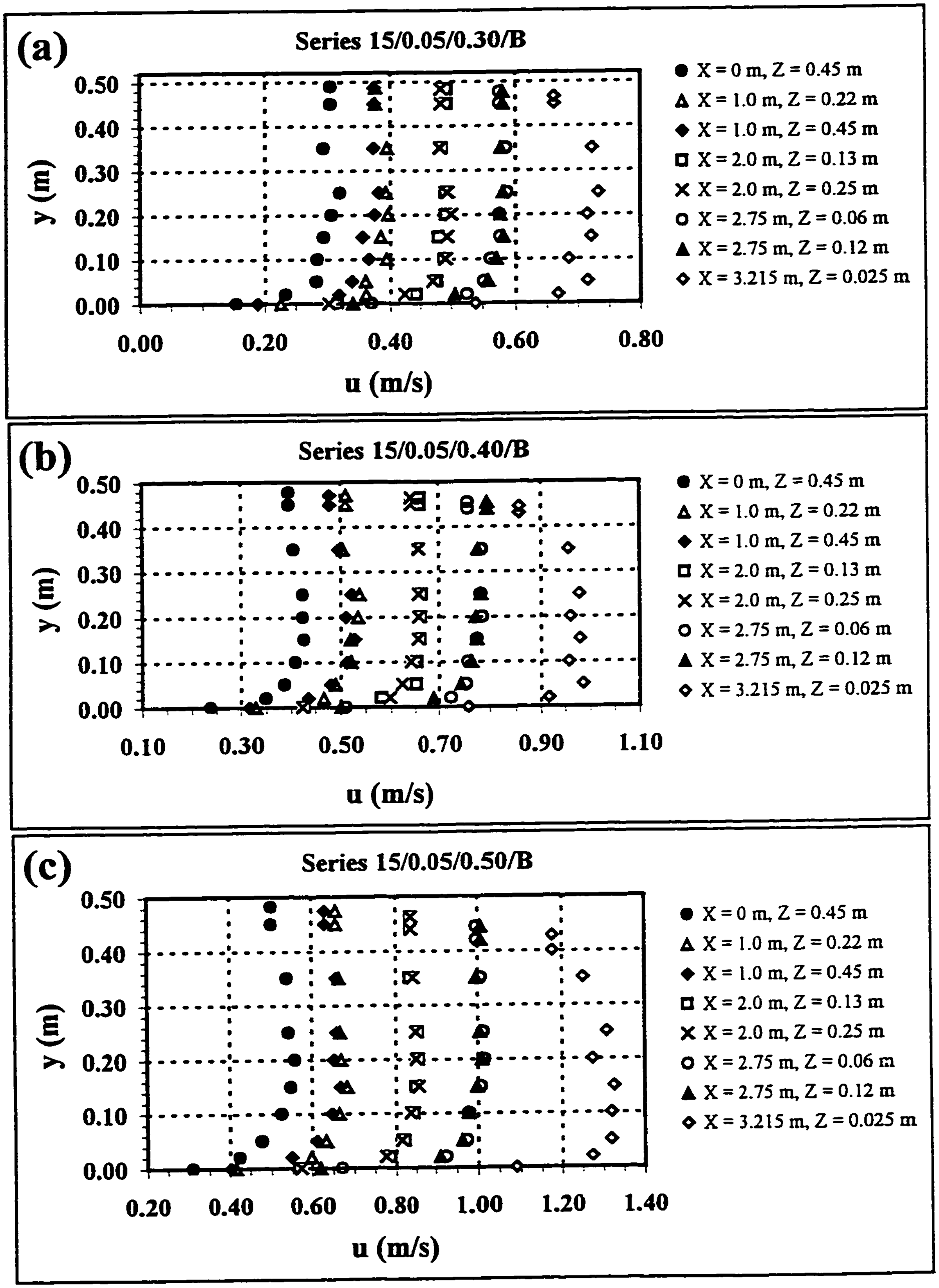

Figures 24(a-c): Velocity Profiles Within the Fish Bypass Section.

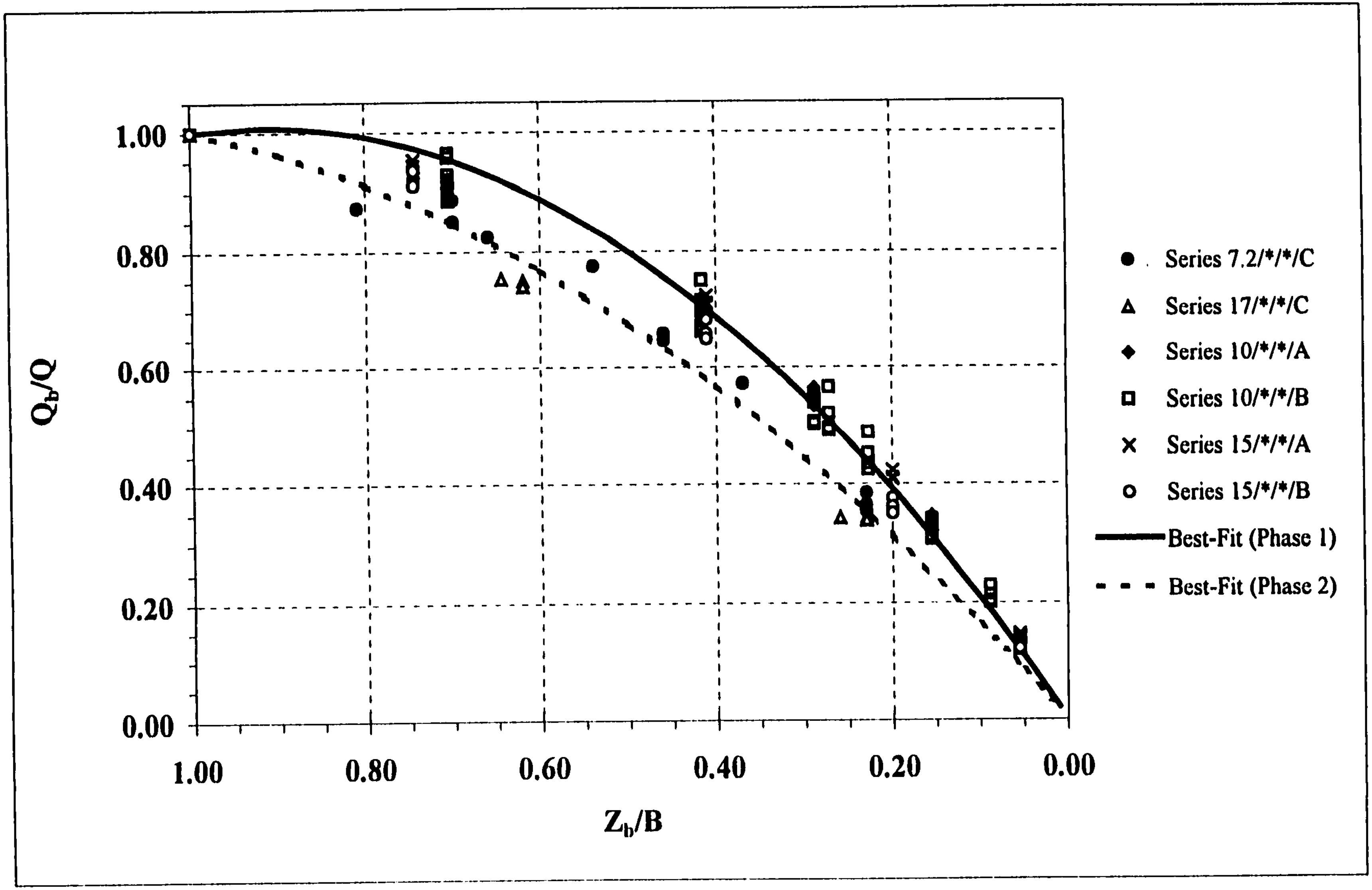

Figure 25: Proportional bypass discharge versus Proportional bypass width.

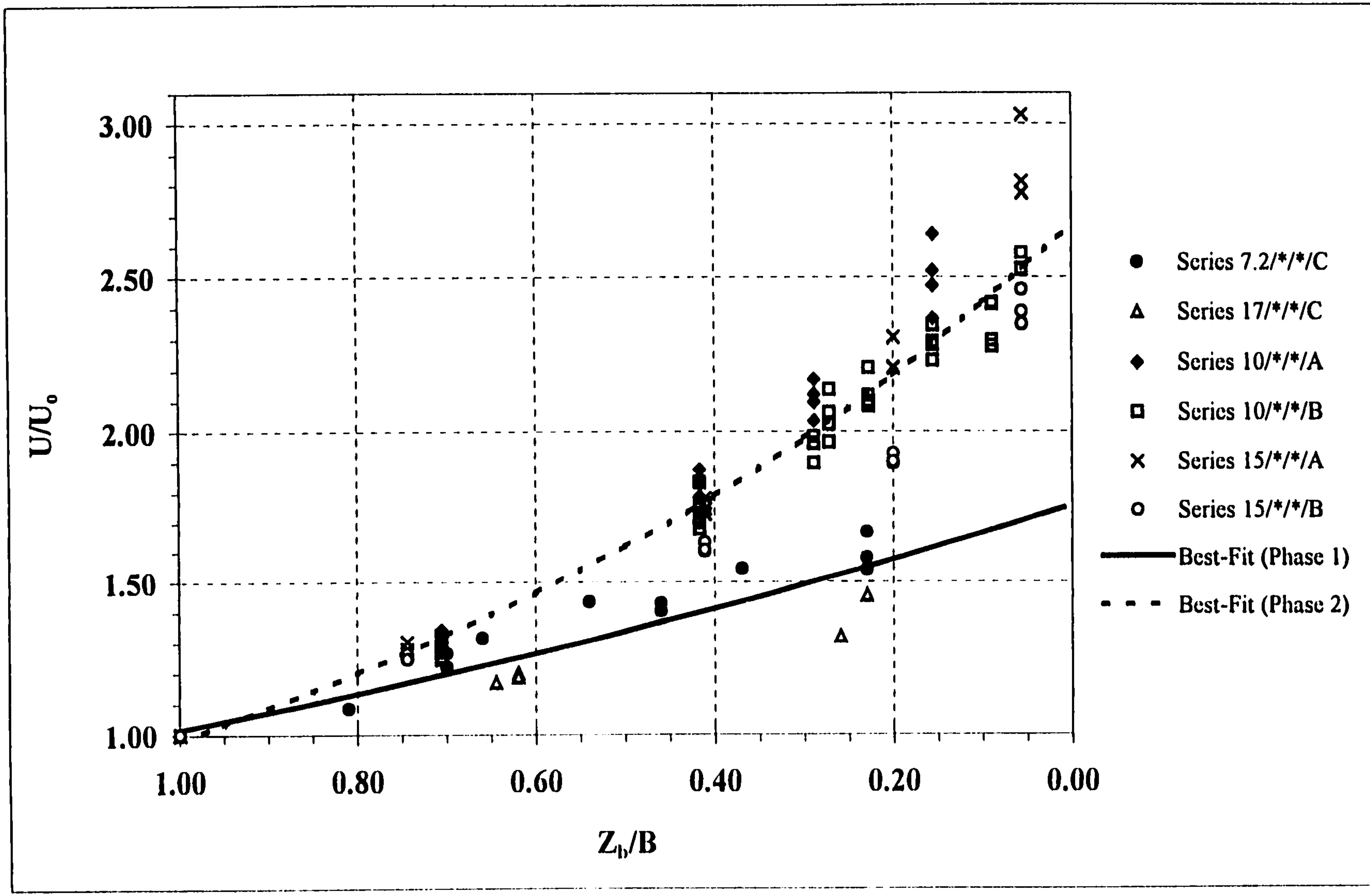

Figure 26: Bypass acceleration versus Proportional bypass width.

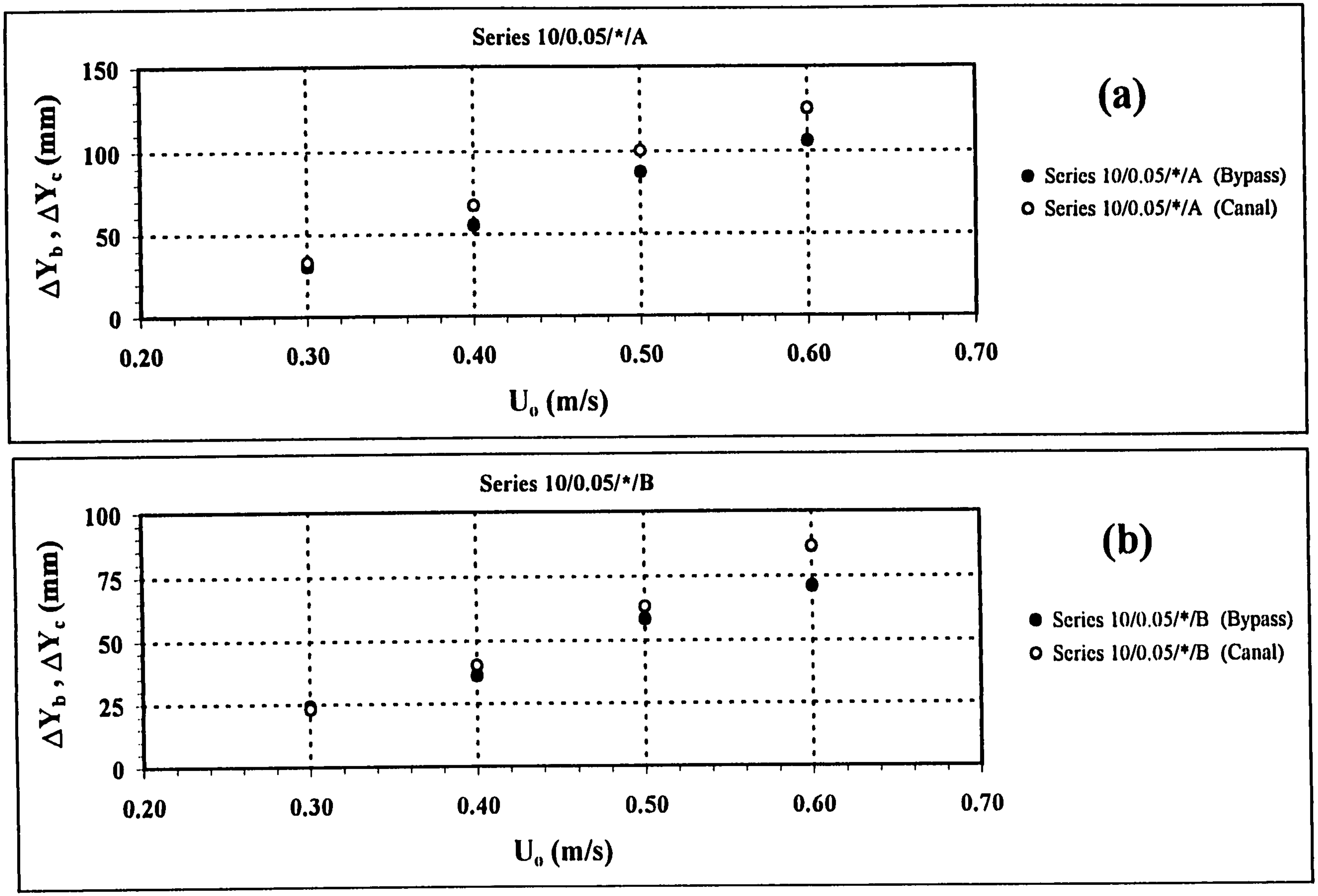

Figures 27(a-b): Reduction in flow depths versus Approach depth-averaged velocity.

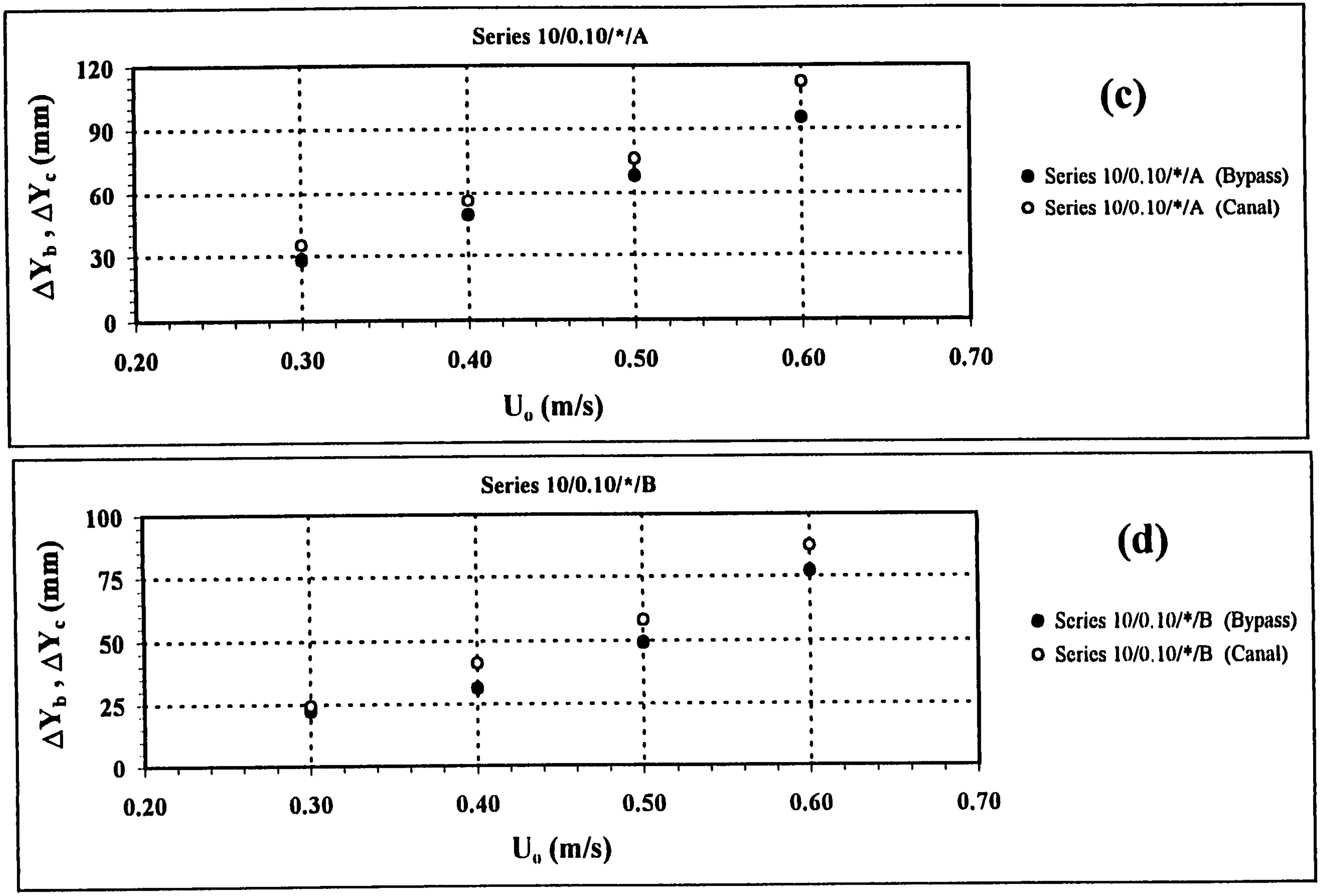

Figures 27(c-d): Reduction in flow depths versus Approach depth-averaged velocity.

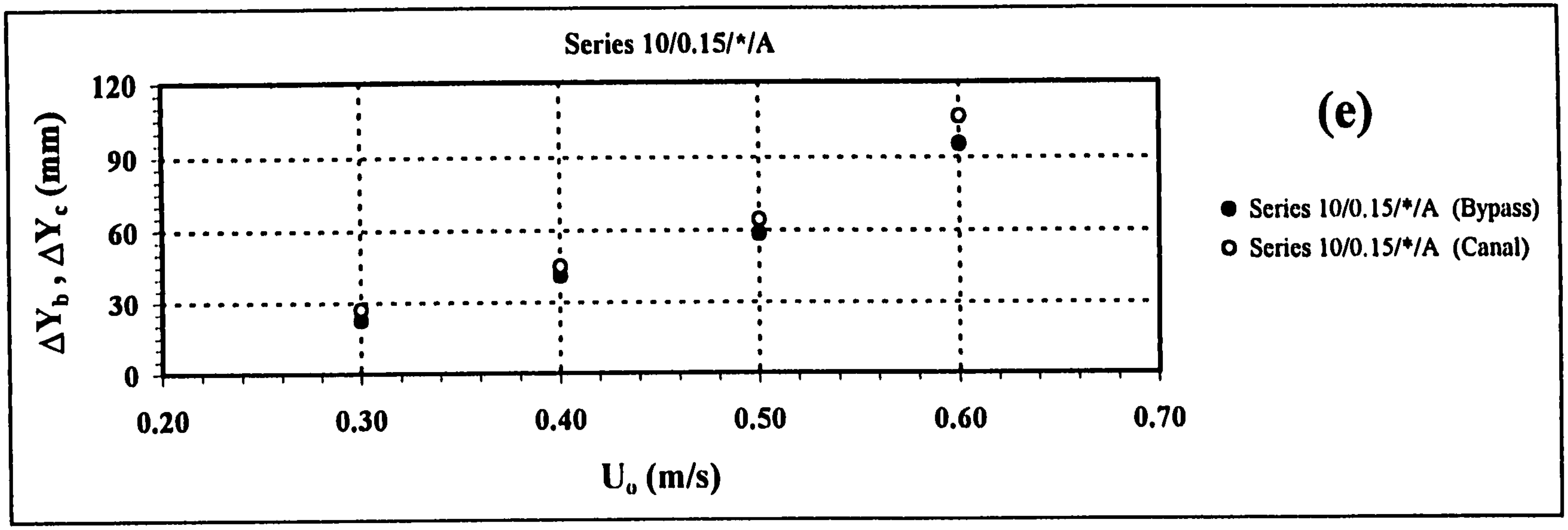

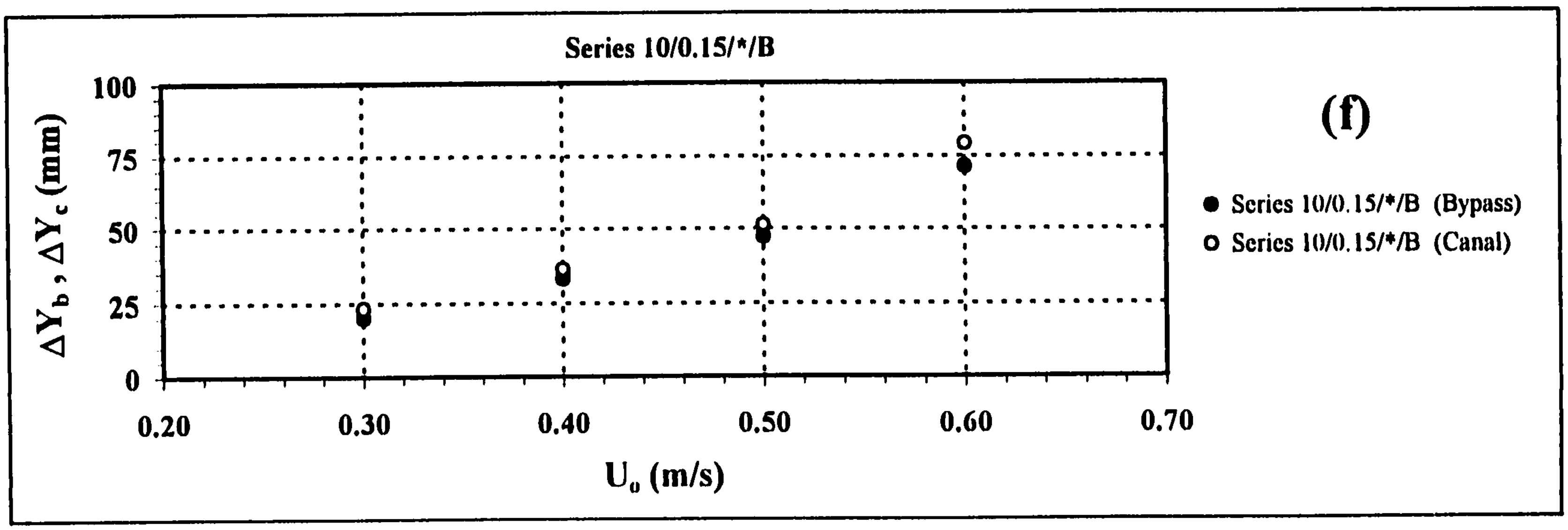

Figures 27(e-f): Reduction in flow depths versus Approach depth-averaged velocity.

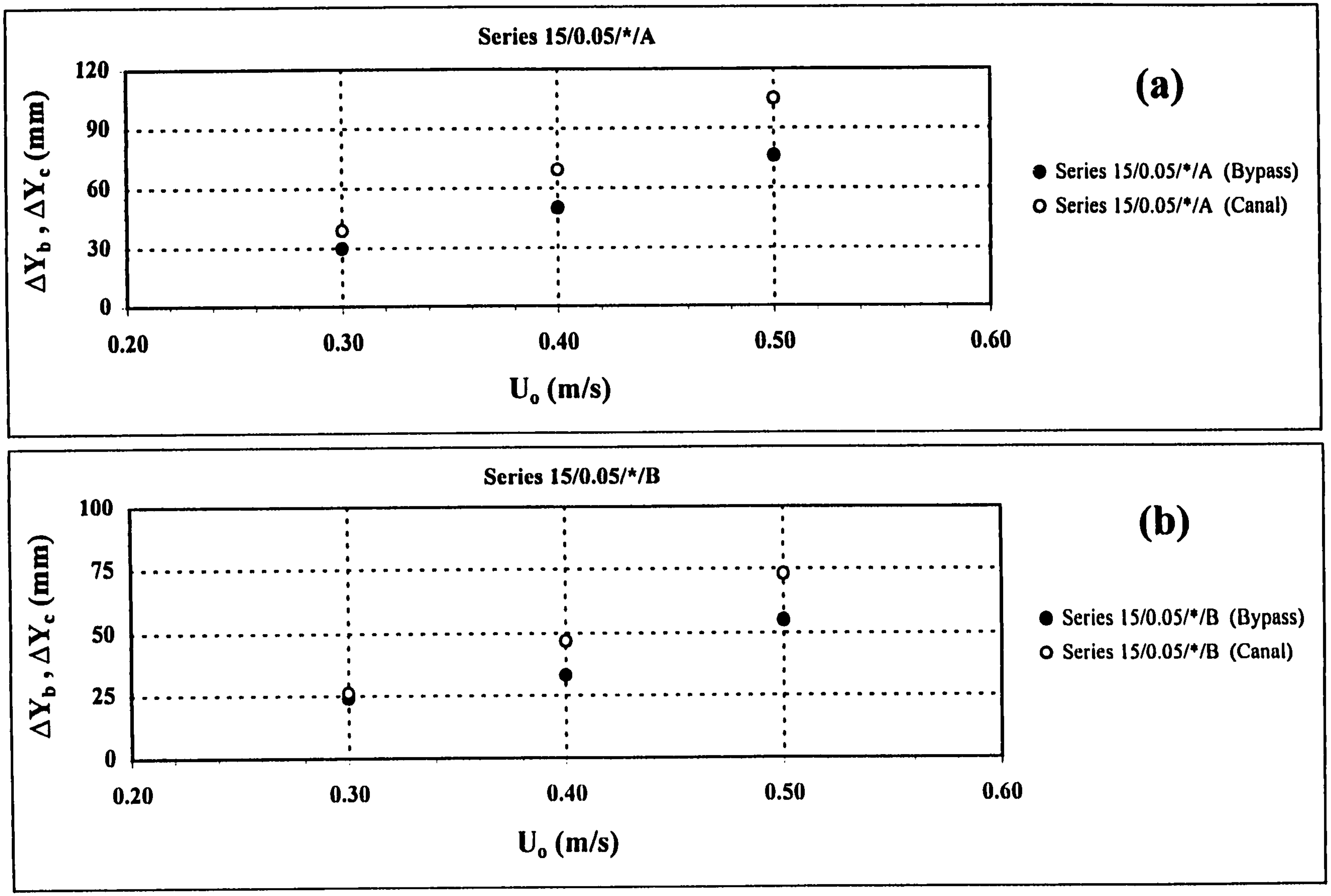

Figures 28(a-b): Reduction in flow depths versus Approach depth-averaged velocity.

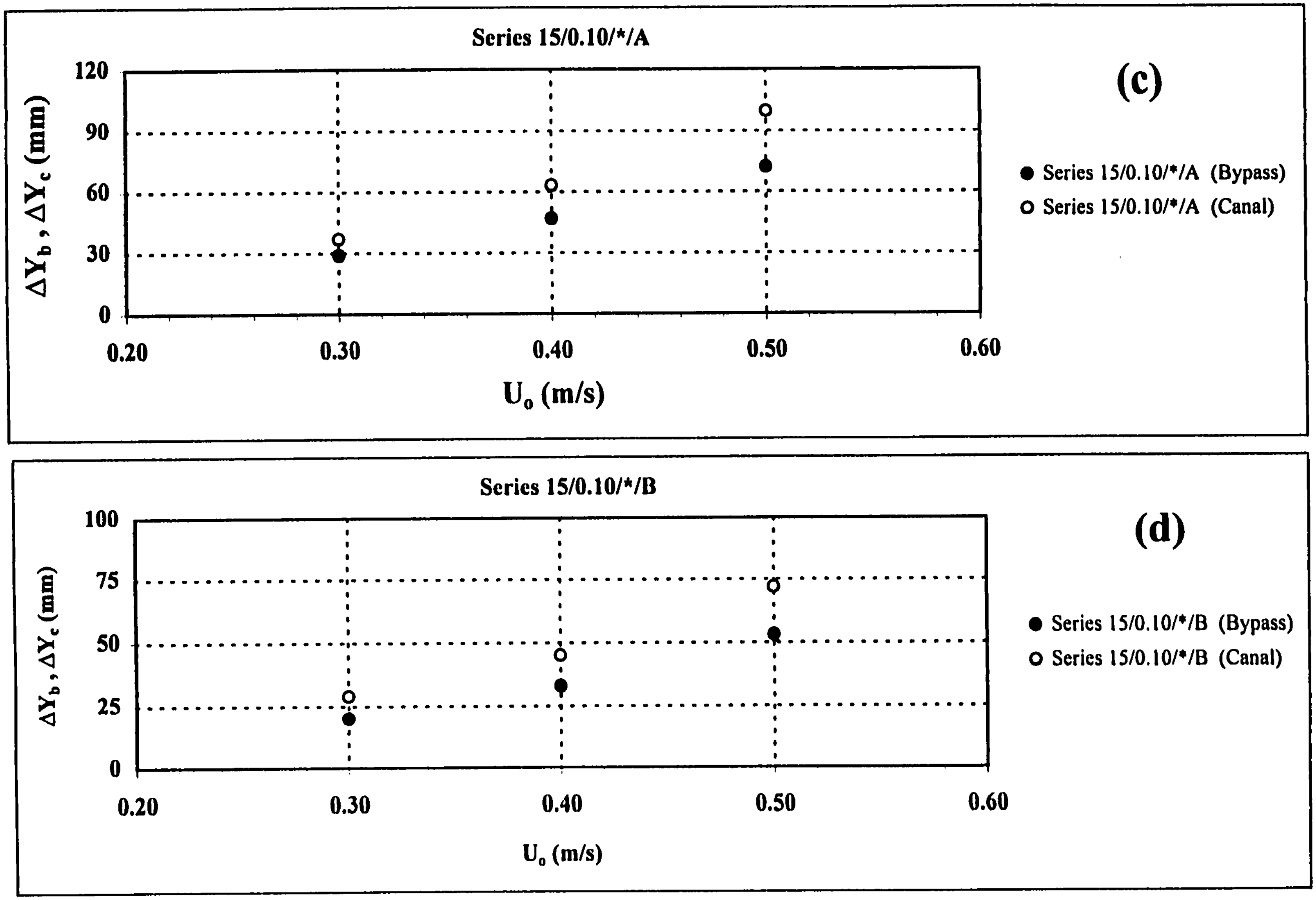

Figures 28(c-d): Reduction in flow depths versus Approach depth-averaged velocity.

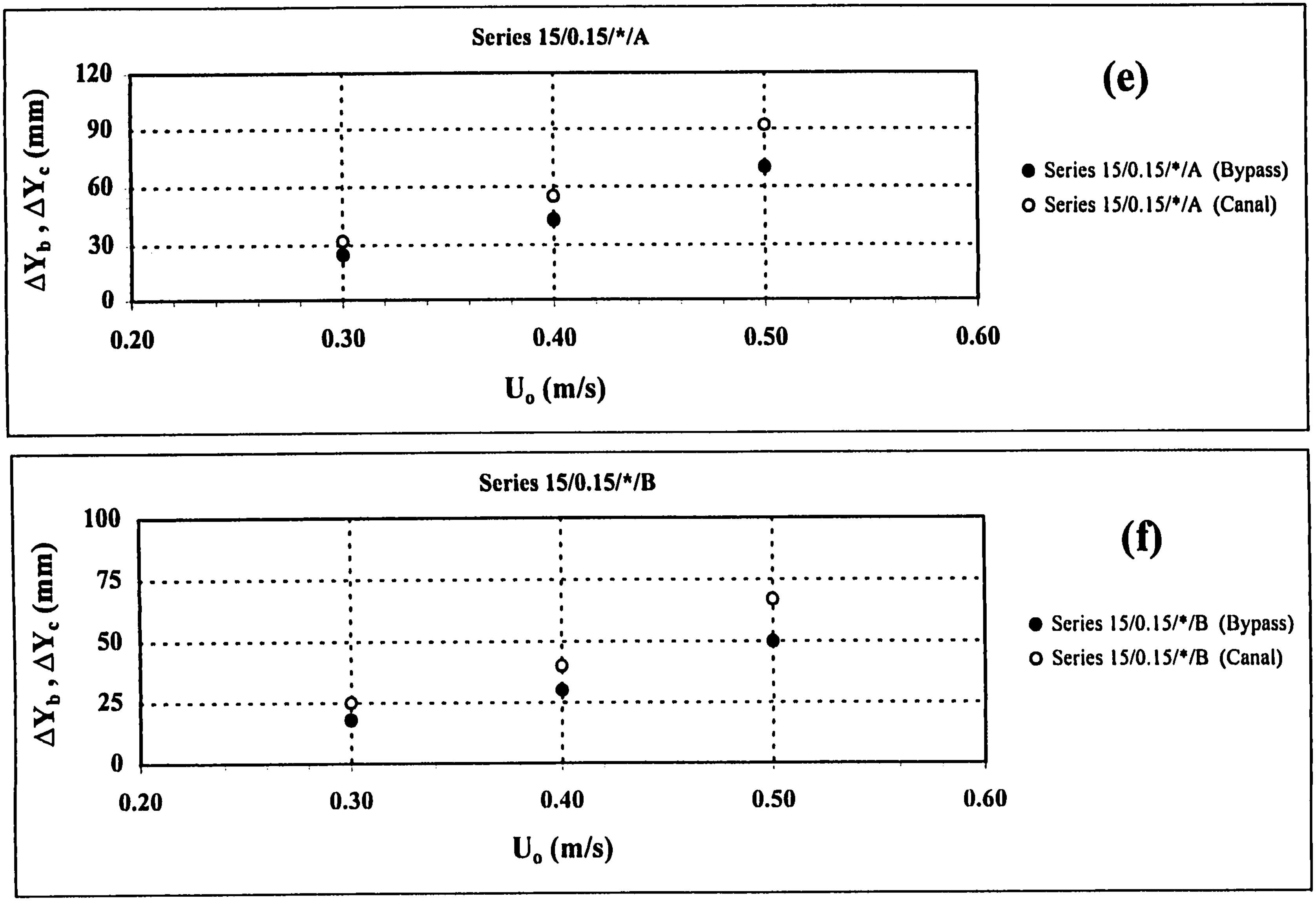

Figures 28(e-f): Reduction in flow depths versus Approach depth-averaged velocity.

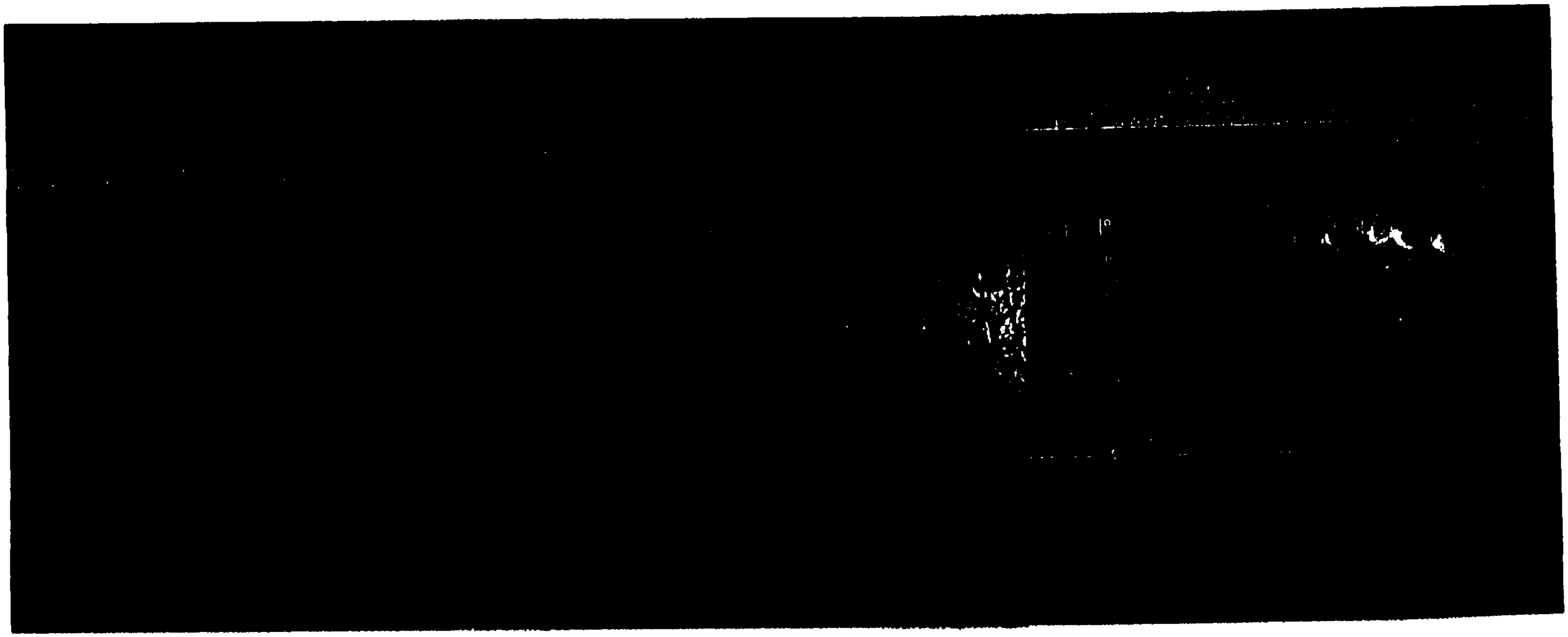

Plate 1: Plan view of the 10 degree louver array of Phase Two (Series *10/0.10/0.50/A*).

Plate 2: Plan view of the flow entering the canal section through the louver slats just upstream of the exit section (Series *10/0.10/0.50/A*).

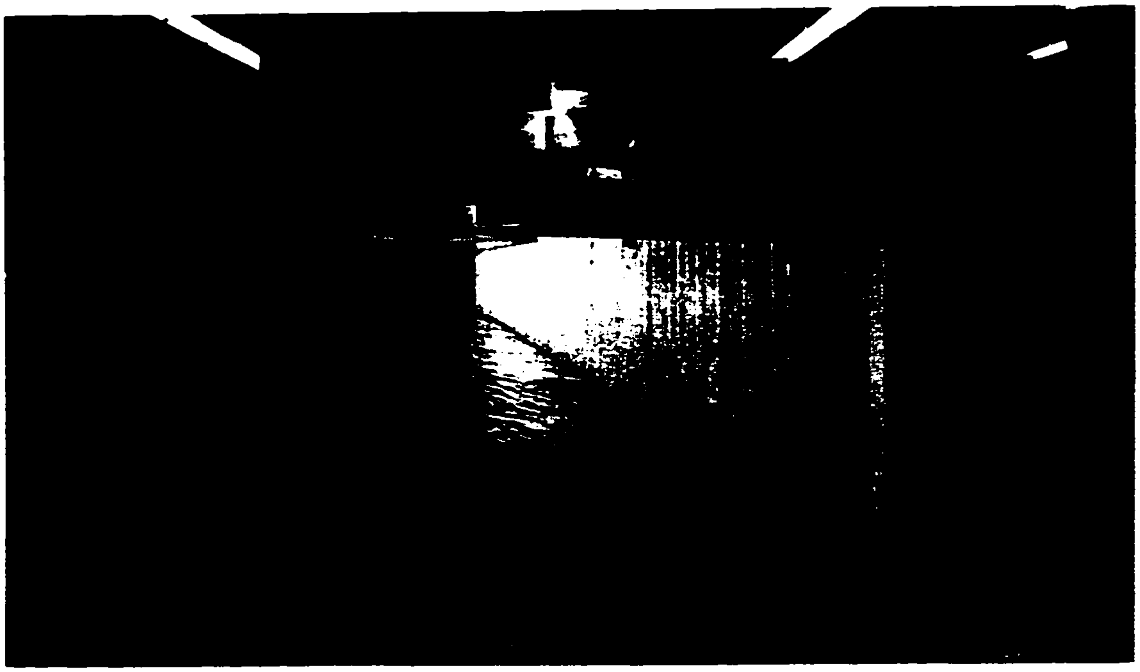

Plate 3: Water surface profile of Series *10/0.10/0.50/A* .

Plate 4: Looking upstream at the exit sections of the bypass and canal (Series *10/0.10/0.50/A*).

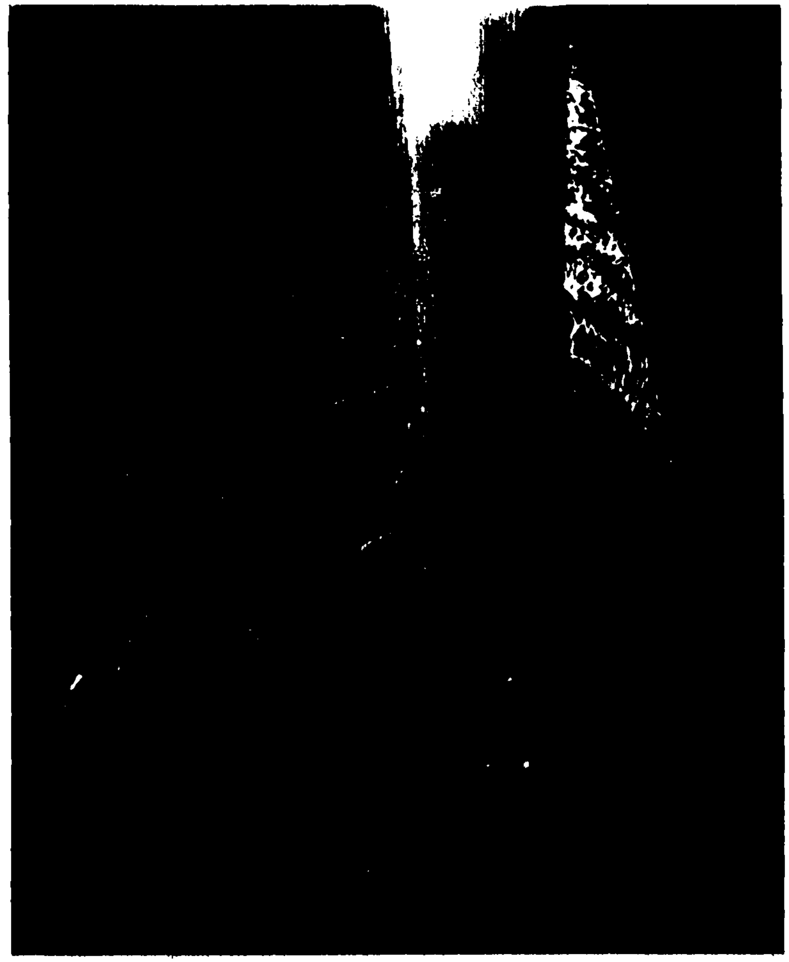

Plate 5: Close-up view of the exit section (Series *10/0.10/0.50/A*).

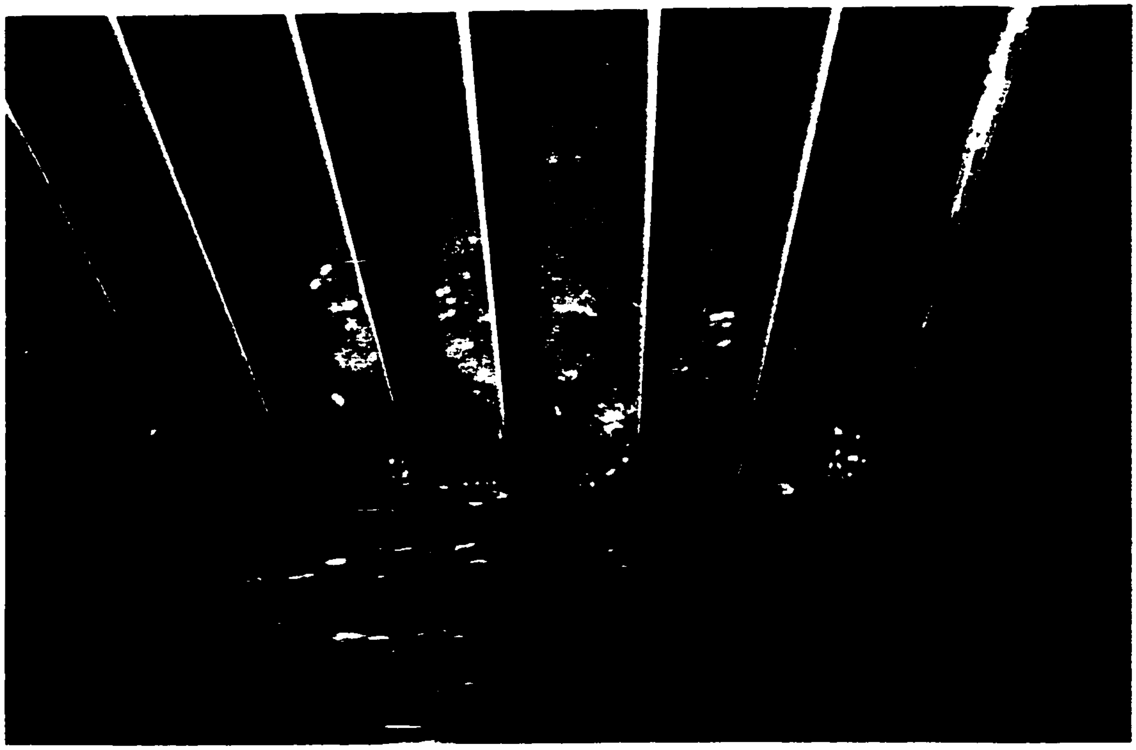

Plate 6: Close-up view of the flow within the bypass section and between the louver slats near the exit section (Series *10/0.10/0.50/A*).

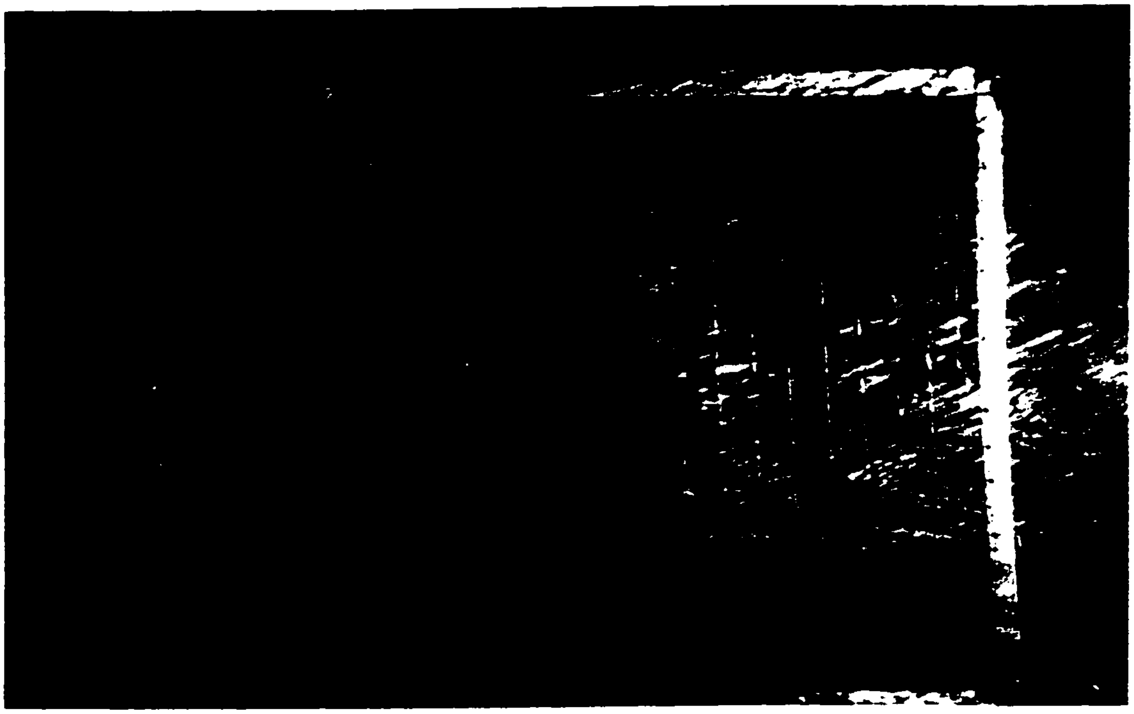

Plate 7: Thread grid used to illustrate the flow pattern within the fish bypass section (Series *10/0.10/0.50/A*).

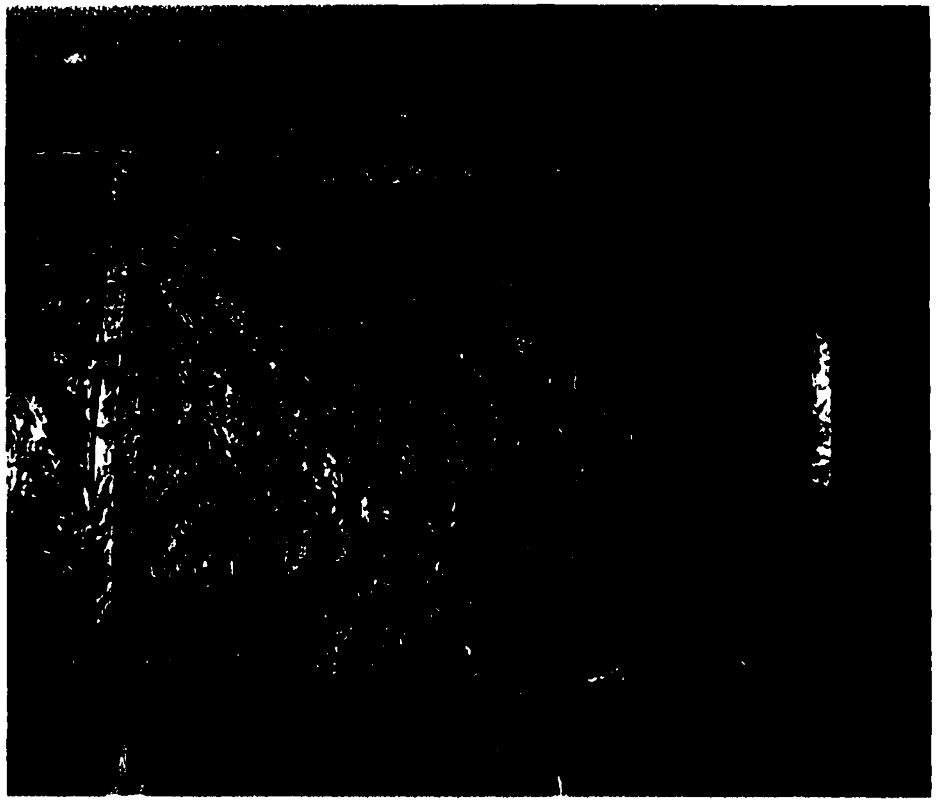

Plate 8: Close-up view of flow pattern within the canal section. The thread grid is located within the upper third of the louver array (Series *10/0.10/0.50/A*).

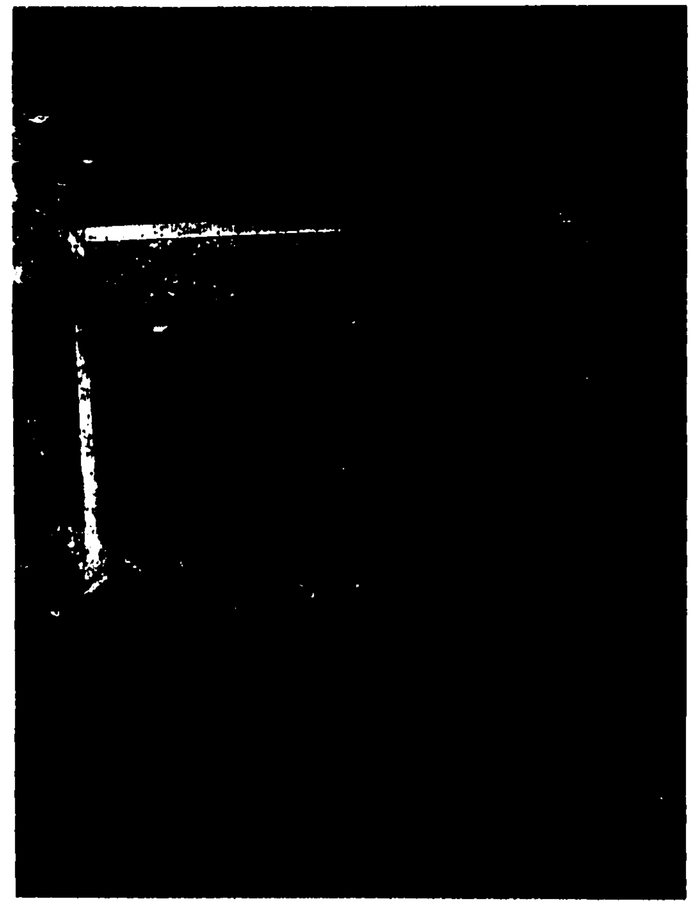

Plate 9: Thread grid used to illustrate the flow pattern within the canal section. The downstream end of the grid is just upstream of the exit section (Series *10/0.10/0.50/A*).

Plate 10: Plan view of the 15 degree louver array of Phase Two (Series *15/0.05/0.50/A*).

Plate 11: Looking downstream at the water surface profile of Series *15 0.05 0.50 A*.

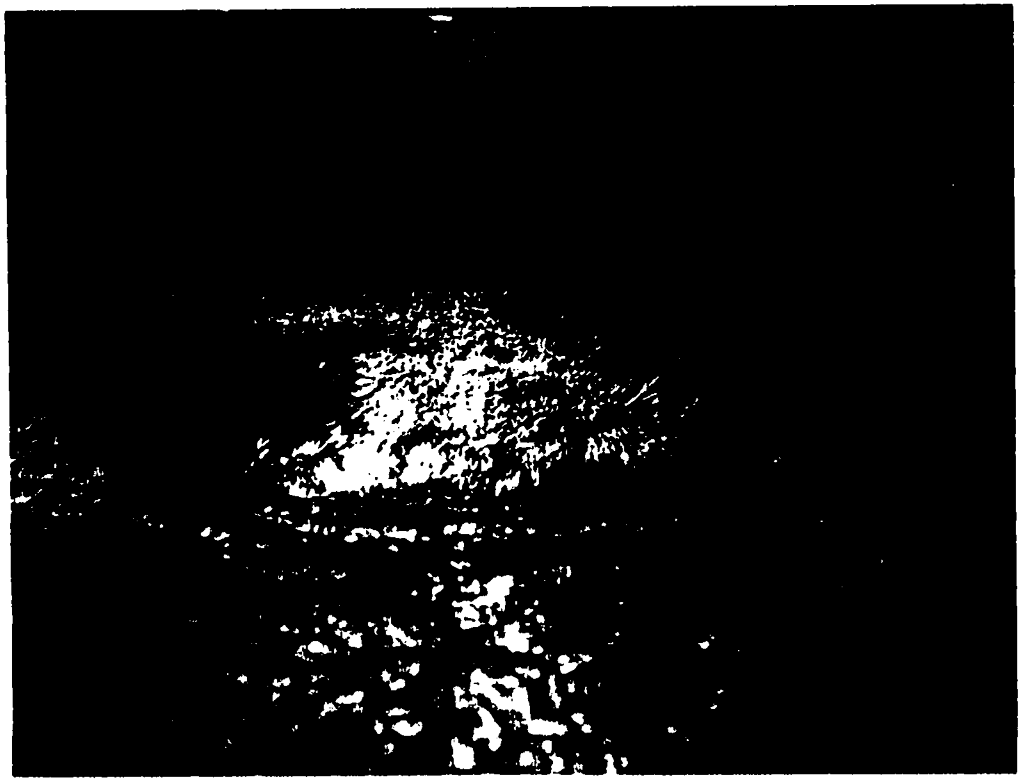

Plate 12: Looking upstream along the louver array. Bypass and canal exit sections in the foreground (Series *15/0.05/0.50/A*).

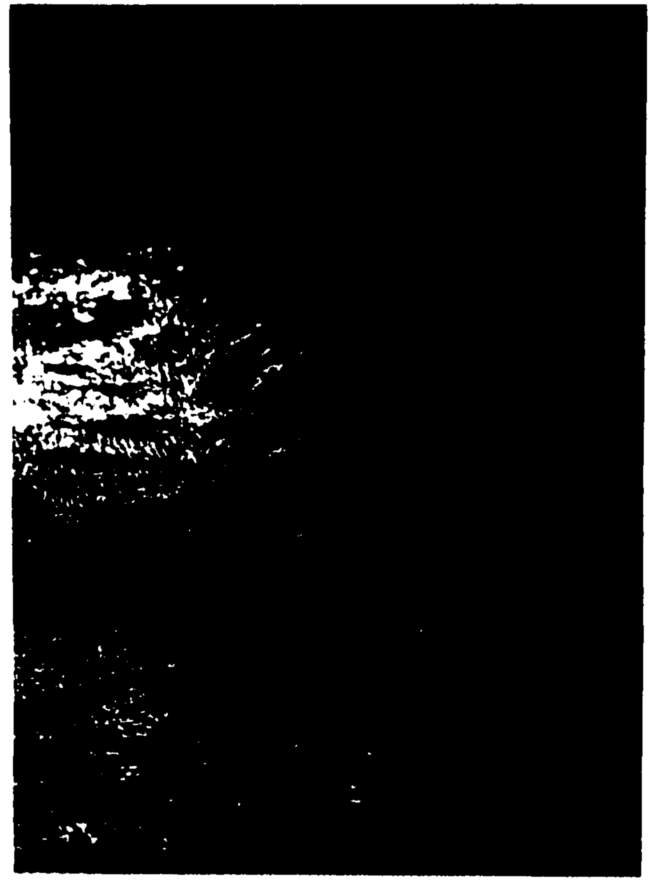

Plate 13: Close-up view of the exit section (Series *15/0.05/0.50/A*).

Plate 14: Close-up view of the bypass section and flow between the louver slats just downstream of halfway (Series *10/0.10/0.50/A*).

Plate 15: Close-up view of the bypass section and flow between the louver slats just downstream of halfway (Series *10/0.10/0.50/B*).

Plate 16: Close-up view of the flow entering the canal section through the louver slats just upstream of the exit location (Series *15/0.05/0.50/A*).

Plate 17: Close-up view of the flow entering the canal section through the louver slats just upstream of the exit location (Series *15/0.05/0.50/B*).

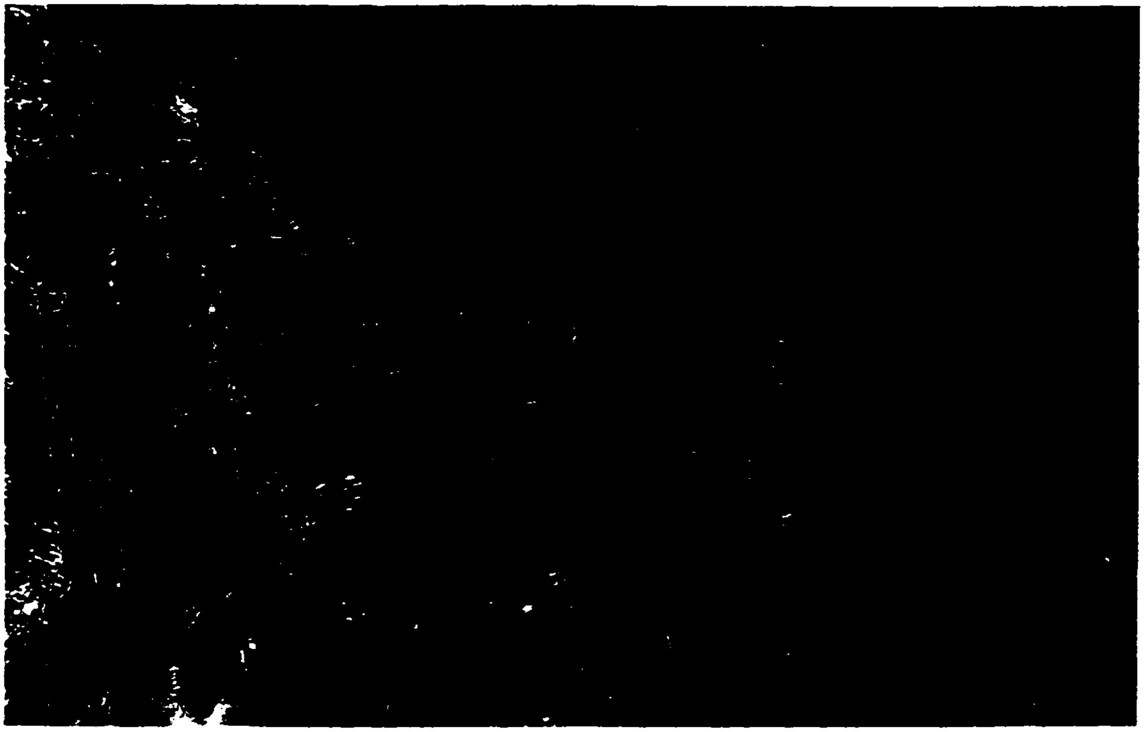

Plate 18: Thread grid placed just below the water surface with the downstream end of the grid traversing the exit location (Series *15/0.05/0.50/A*).

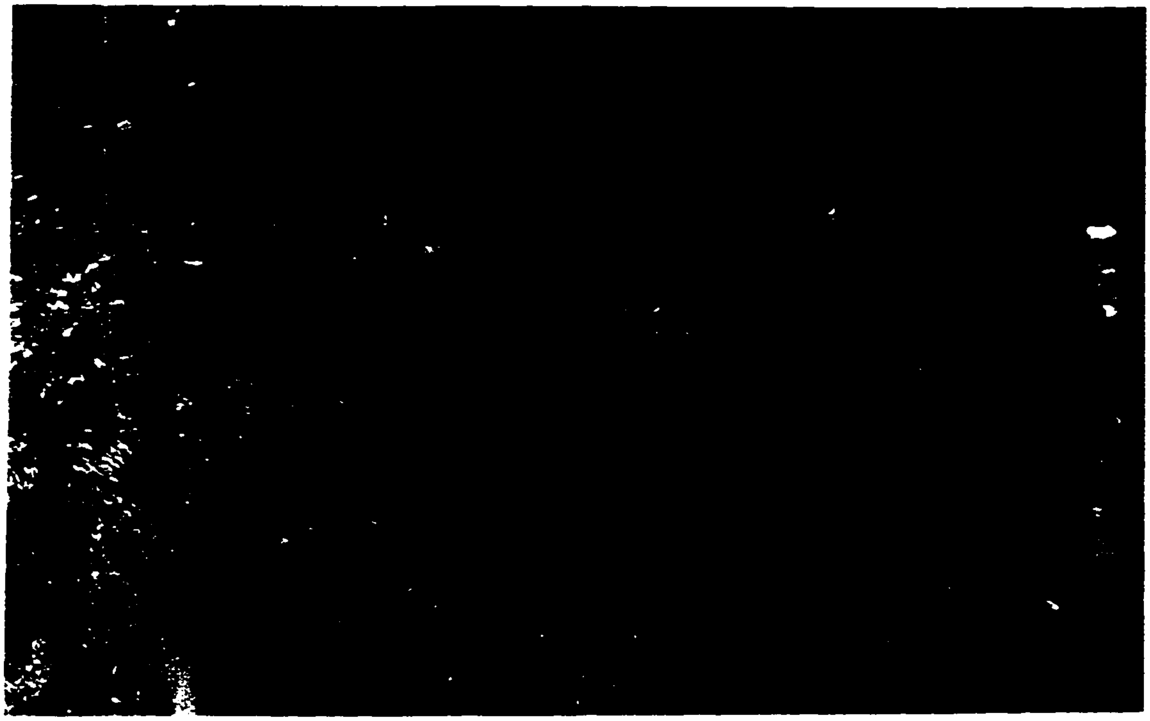

Plate 19: Thread grid placed just below the water surface with the downstream end of the grid traversing the exit location (Series *15/0.05/0.50/B*).

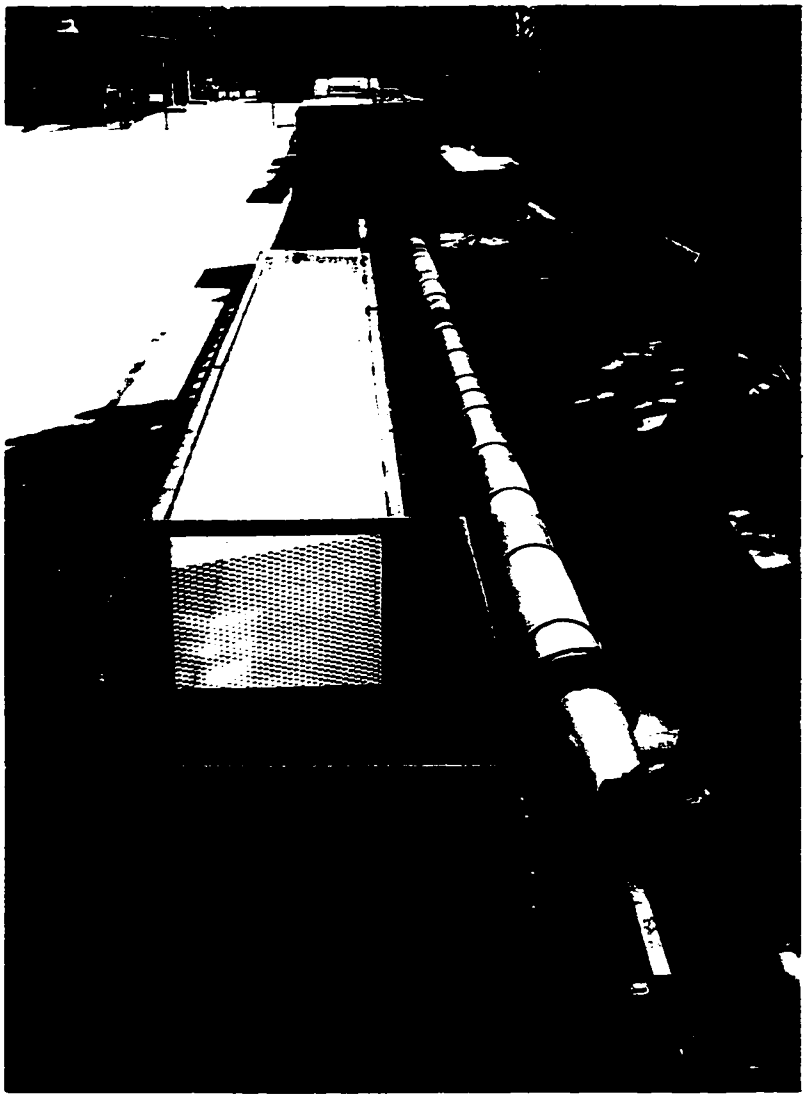

Plate 20: View of the I-H Flume looking upstream towards the headtank.

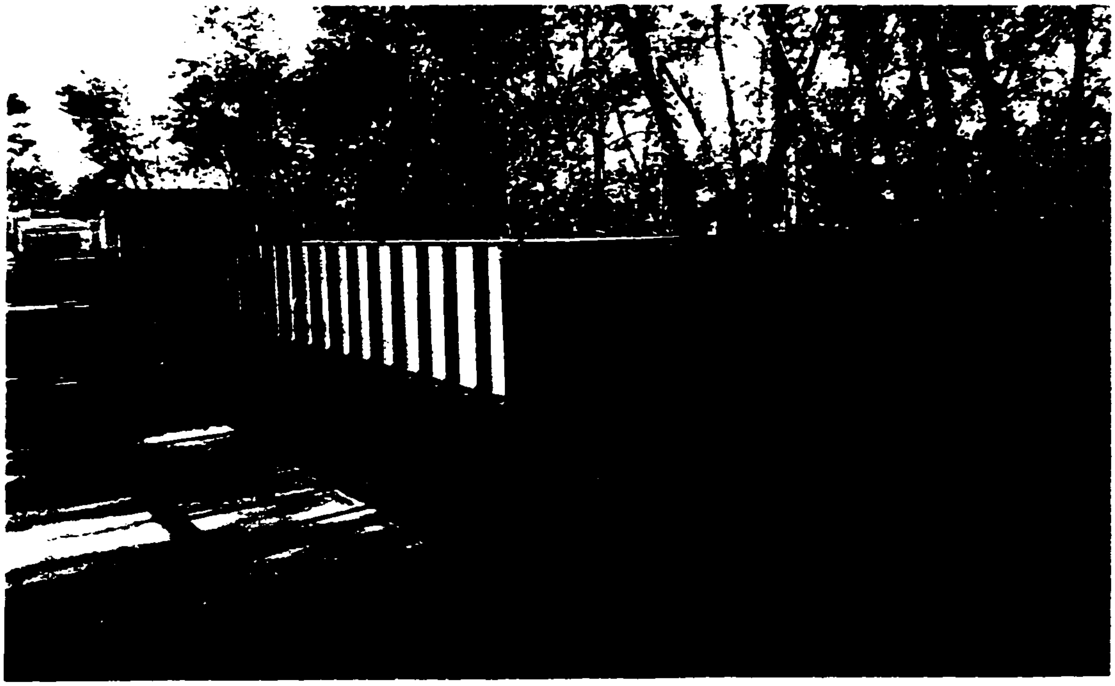

Plate 21: General view of the I-H Flume showing the test flume section (tailtank in foreground).

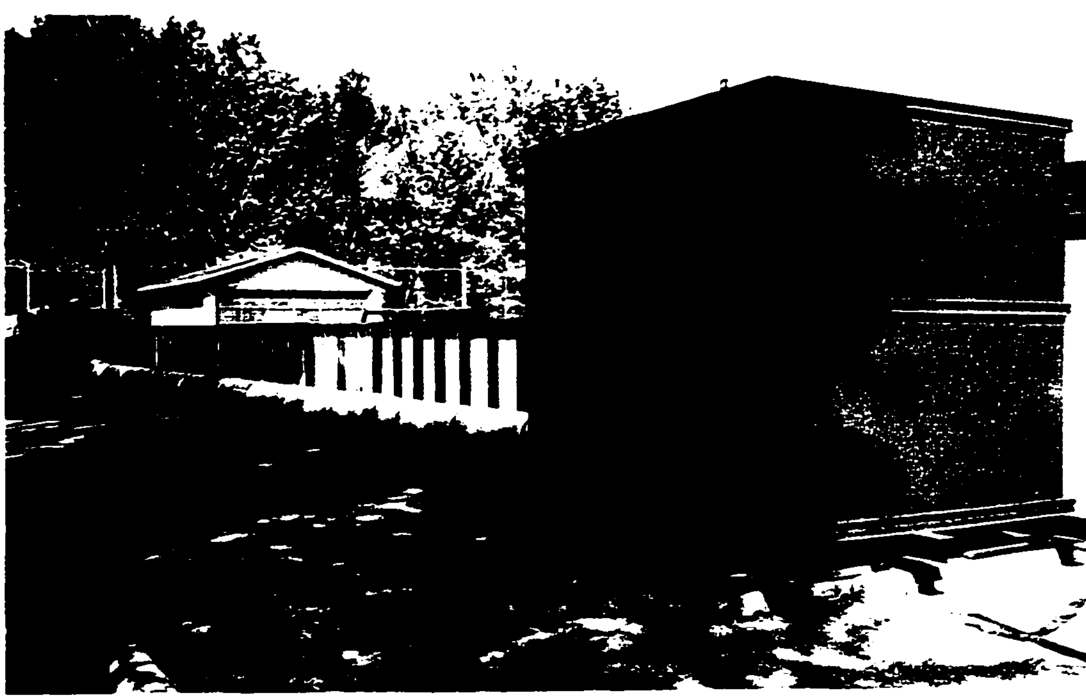

Plate 22: General view of the I-H Flume showing the return pipe (headtank in foreground).

Plate 23: Looking downstream at the 7.2 degree louver array of Phase One.

Plate 24: Looking upstream at the 7.2 degree louver array of Phase One.

Plate 25: Profile view of the 7.2 degree louver array of Phase One.

Plate 26: Set-up of the point gauge used to measure the water surface profiles of Phase Two.

Plate 27: Set-up of the Prandtl tube used to measure the velocity profiles of Phase Two.

REFERENCES

Anderson, W.G., Shepherd, D., Katopodis, C., McKinley, R.S., and Rajaratnam, N., (1998). "***Laboratory and Field Testing of a Louver Array for the Guidance of Juvenile Rainbow Trout***", Technical Report prepared by Applied Biometrics Inc. (ABI), Waterloo, Ontario and Department of Civil Engineering, University of Alberta, Edmonton, Alberta for the Alberta Department of Environmental Protection, Natural Services.

ASCE, (1982). **Design of Water Intake Structures for Fish Protection**, Hydraulics Division of the American Society of Civil Engineers, New York, NY., 163 p.

Bates, D.W. and Jewett, S.W. Jr., (1961). "***Louver Efficiency in Deflecting Downstream Migrant Steelhead***", Transactions of the American Fisheries Society, Vol. 90, 336-337.

Bates, D.W. and Vinsonhaler, R., (1957). "***Use of Louvers for Guiding Fish***", Transactions of the American Fisheries Society, Vol. 86, 38-57.

Blaxter, J.H.S., (1969). Swimming Speeds of Fish, Food and Agriculture Organization, Fisheries Report, Vol. 63, No. 2, 69-100.

Brett, J.R., (1963). "***The Energy Required for Swimming by Young Sockeye Salmon with a Comparison of the Drag Force of a Dead Fish***", Transactions of the Royal Society of Canada, Vol.1, 441-457.

Clay, C.H., (1961) **Design of Fishways and Other Fish Facilities**, Queen's Printer, Department of Fisheries, Ottawa, Canada, 301 p.

Ducharme, L.J.A., (1972). "***An Application of Louver Deflectors for Guiding Atlantic Salmon (Salmo salar) Smolts from Power Turbines***", Journal of the Fisheries Research Board of Canada. Vol. 29, No. 20, 1397-1404.

Henderson, F.M., (1966). **Open Channel Flow**, Macmillan Publishing Co., Inc., New York, N.Y., 522 p.

Katopodis, C., (1982). "***A Study of the Hydraulics of Denil Fishways***", M.Sc. Thesis, Department of Civil Engineering, University of Alberta, Edmonton, Alberta, Canada., 158 p.

REFERENCES (continued)

Langford, T.E., Utting, N.J. and Holmes, R.H.A., (1977). ***"Factors Affecting the Impingement of Fishes on Power Station Cooling-Water Intake Screens"***, in D.S. McLusky and A.J. Berry, Physiology and Behaviour of Marine Organisms, 281-288.

Mussalli, Y.G., Taft, E.P. and Micheletti, W., (1988). "***Assessment of Development Needs for Advanced Water Intake Technologies***", Journal of Hydraulic Engineering, Vol. 114, No. 6, 675-688.

Ott, R.F., (1994). "***Fish Screens at Hydroelectric Diversions***", Proceedings of the American Power Conference, Vol. 56, Pt. 1, Illinois Institute of Technology, Chicago, Illinois, 562-567.

Rajaratnam, N., Katopodis, C., and Mainali, A., (1987). "***Pool and Weir Fishways***", Report WRE 87-1, Department of Civil Engineering, University of Alberta, Edmonton, Alberta, Canada.

Rajaratnam, N. and Muralidhar, D., (1967). "***Yaw and Pitch Probes***", Department of Civil Engineering, University of Alberta, Edmonton, Alberta, Canada.

Ruggles, C.P. and Hutt, R., (1984). "***Fish Diversionary Techniques for Hydroelectric Turbine Intakes***" Research Project prepared by Montreal Engineering Company Ltd. for the Canadian Electrical Association [January 1984].

Ruggles, C.P., Robinson, D.A. and Stira, R.J., (1993). "***The Use of Floating Louvers for Guiding Atlantic Salmon Smolts from Hydroelectric Turbine Intakes***", Canadian Technical Report on Fisheries and Aquatic Sciences [February 1993], No. 1905.

Ruggles, C.P. and Ryan, P., (1964). "***An Investigation of Louvers as a Method of Guiding Juvenile Pacific Salmon***", Canadian Fisheries Culturist, Vol. 33, 7-68.

Sikora, G.J., (1997). "***An Experimental Study of Pool and Weir Fishways***", M.Sc. Thesis, Department of Civil Engineering, University of Alberta, Edmonton, Alberta, Canada, 385 p.

Smith, L.W., (1982). ***"Clogging, Cleaning and Corrosion Study of Possible Fish Screens for the Proposed Peripheral Canal"***, for the Interagency Ecological Study Program for the Sacramento-San Joaquin Estuary, Technical Report 1 [September 1982].

REFERENCES (continued)

Stira, R.J. and Robinson, D.A., (1997). "***Effectiveness of a Louver Bypass System for Downstream Passage of Atlantic Salmon Smolts and Juvenile Clupeids in the Holyoke Canal, Connecticut River, Holyoke, Massachusetts***", Northeast Utilities Service Co. (NUSCO), Hartford, Connecticut, presented at the Fish Passage Workshop (May 6-8), Milwaukee, Wisconsin, 9 p.

Turnpenny, A.W.H., (1981). ***"An Analysis of Mesh Sizes Required for Screening Fishes at Water Intakes"***, Estuaries [December 1981], Vol. 4, No. 4, 363-368.

O.T.A., (1995). **Fish Passage Technologies: Protection at Hydropower Facilities** *(Chapter 4: Downstream Fish Passage Technologies: How Well Do They Work?)*, OTA-ENV-641 [September 1995], U.S. Government Printing Office, Washington, D.C., 167 p.

Weitkamp, D.E. and Elder, R.A., (1993). "***Fish Screen Developments: Columbia River Dams"***, Proceedings - National Conference on Hydraulic Engineering, Pt. 2, ASCE, New York, N.Y., 1314-1319.

Winchell, F., Taft, N., Cook, T. and Sullivan, C., (1993). "***Research Update on the Eicher Screen at Elwha Dam"***, Waterpower '93: Proceedings of the International Conference on Hydropower, ASCE, New York, N.Y.

Winchell, F.C. and Sullivan, C.W., (1991). "***Evaluation of an Eicher Fish Diversion Screen at Elwha Dam"***, Waterpower '91: A New View of Hydro Resources, ASCE, New York, N.Y., 93-102.

APPENDIX A

Water Surface Profiles (Phase Two)

- Graphs and Experimental Data -

A-1

Profiles in Transverse Direction

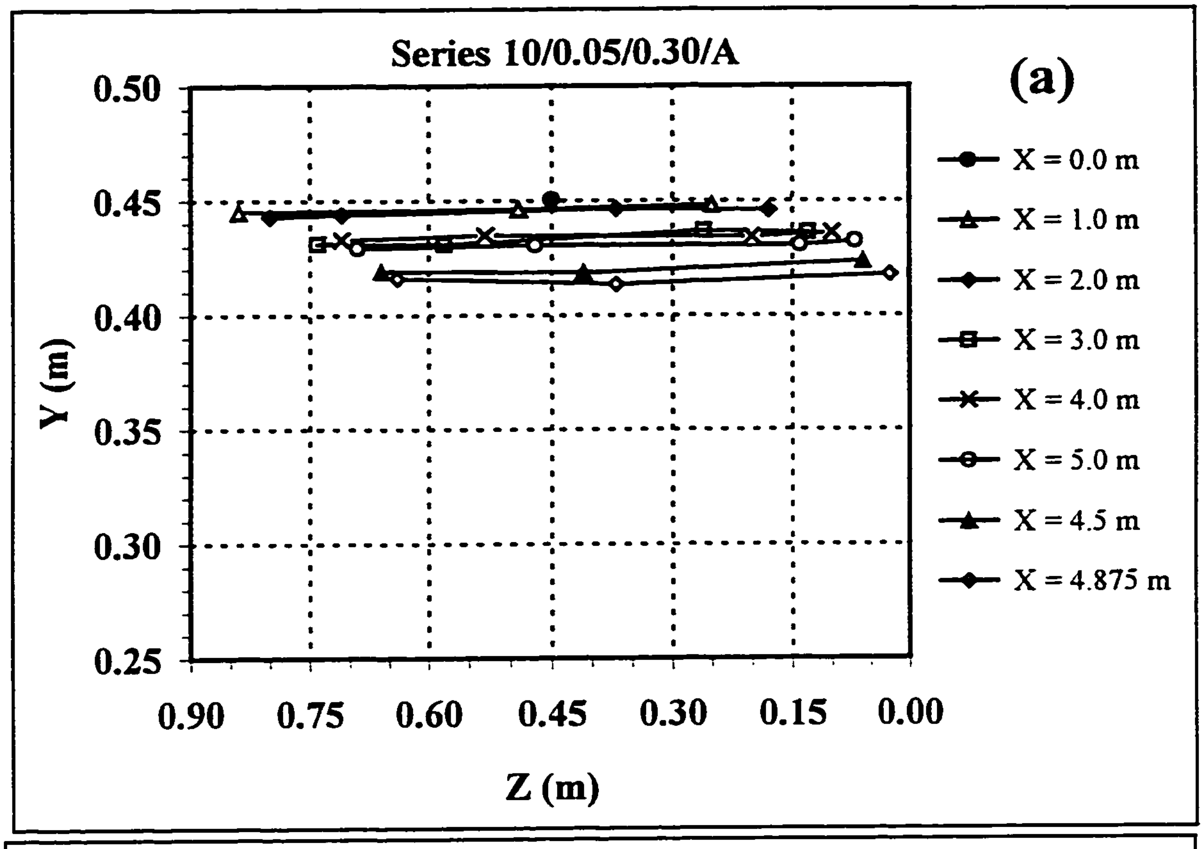

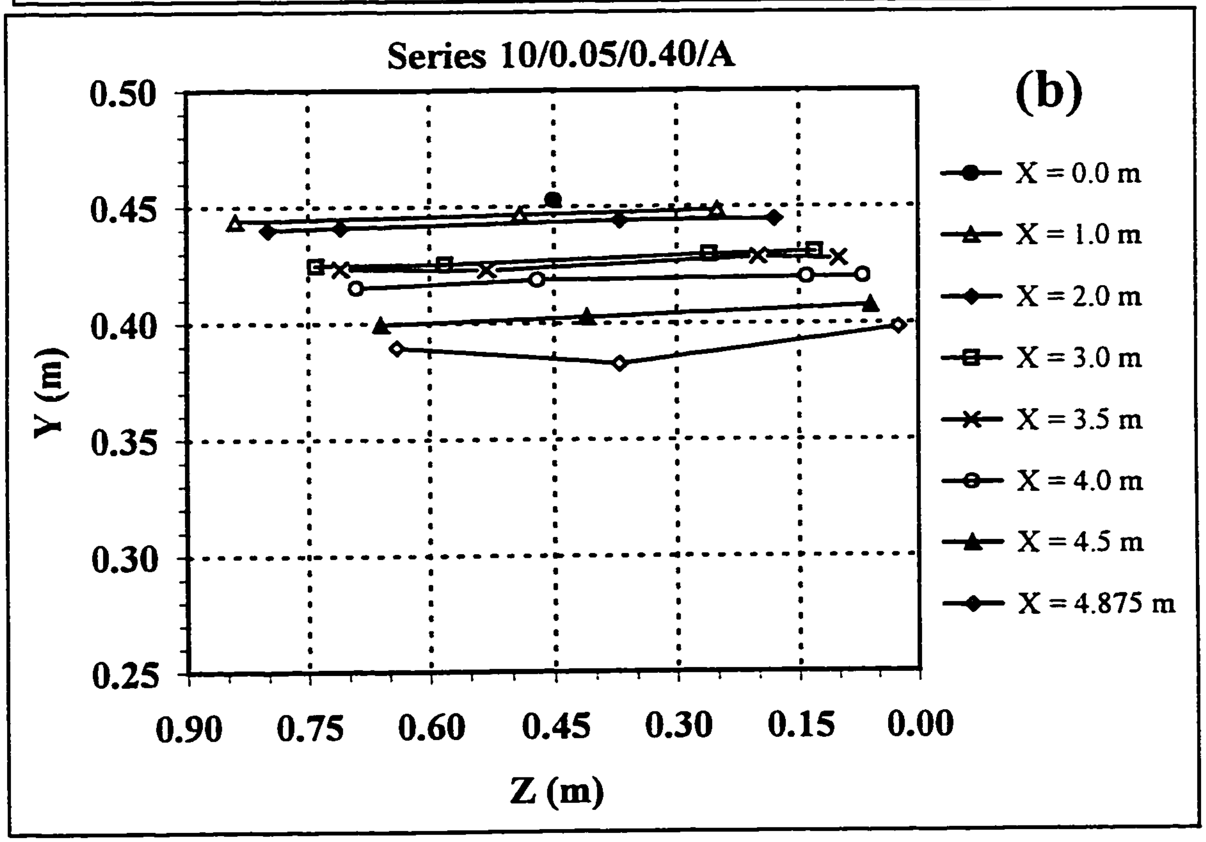

A-1.1(a-b): Depth Profiles of Bypass Section and Canal Section.

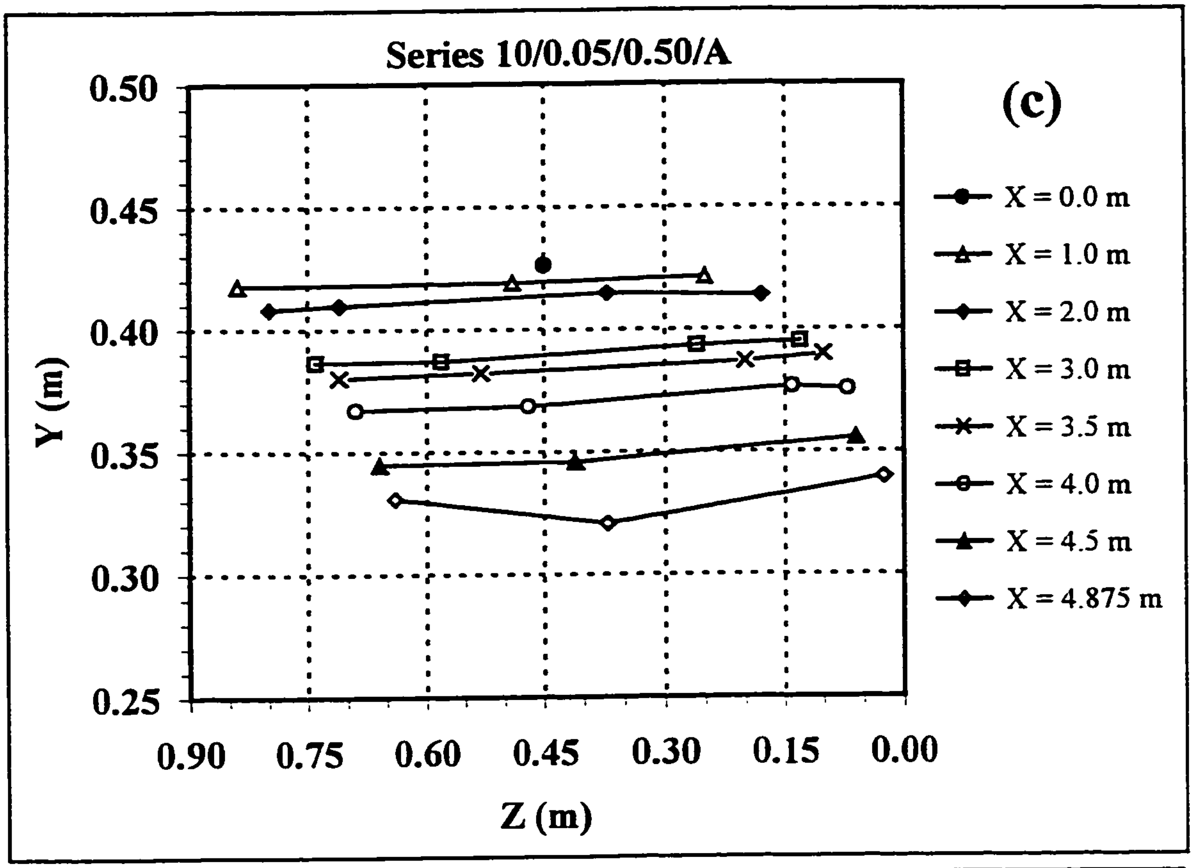

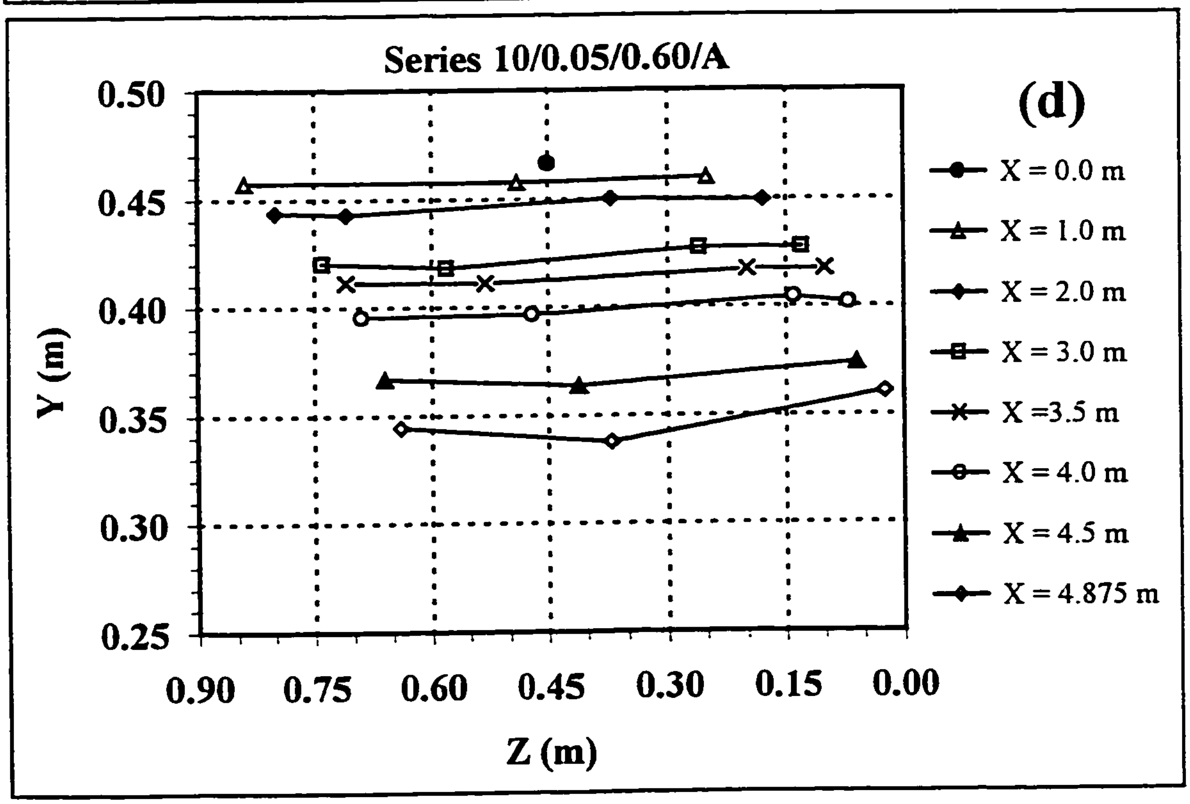

A-1.1(c-d): Depth Profiles of Bypass Section and Canal Section.

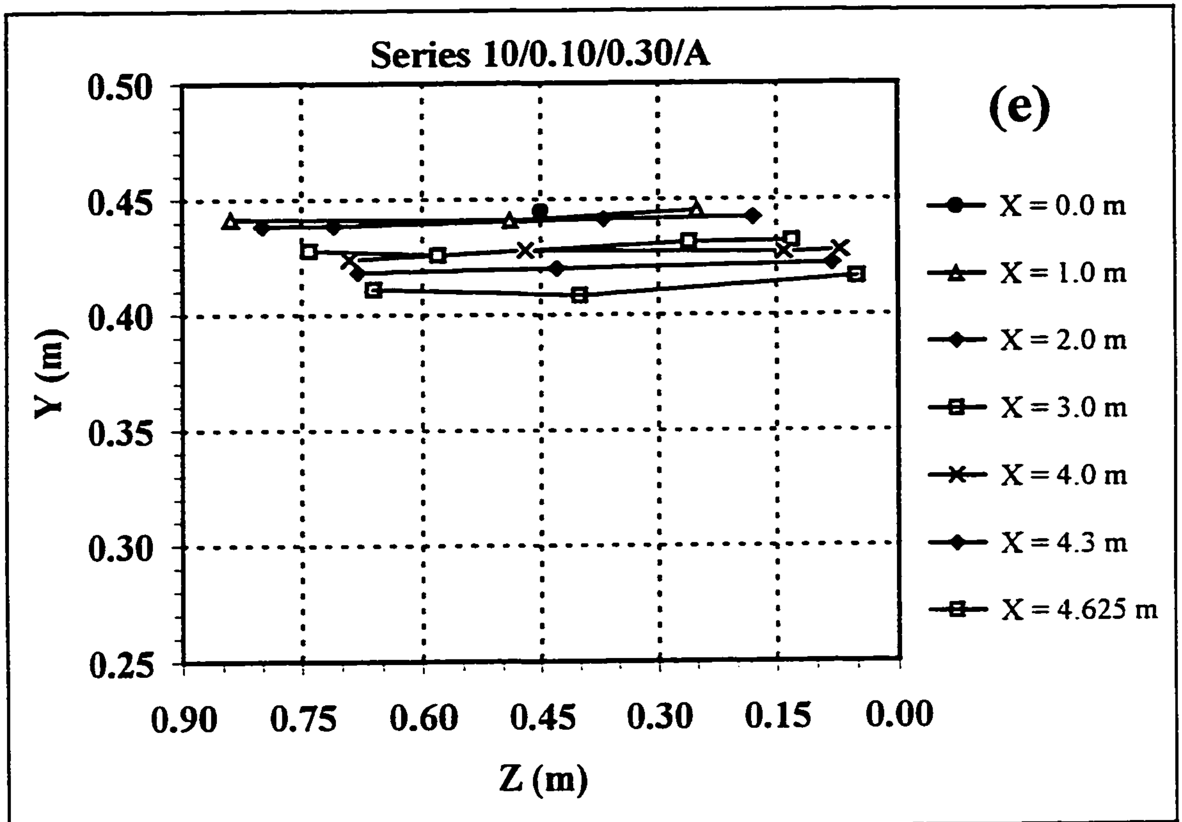

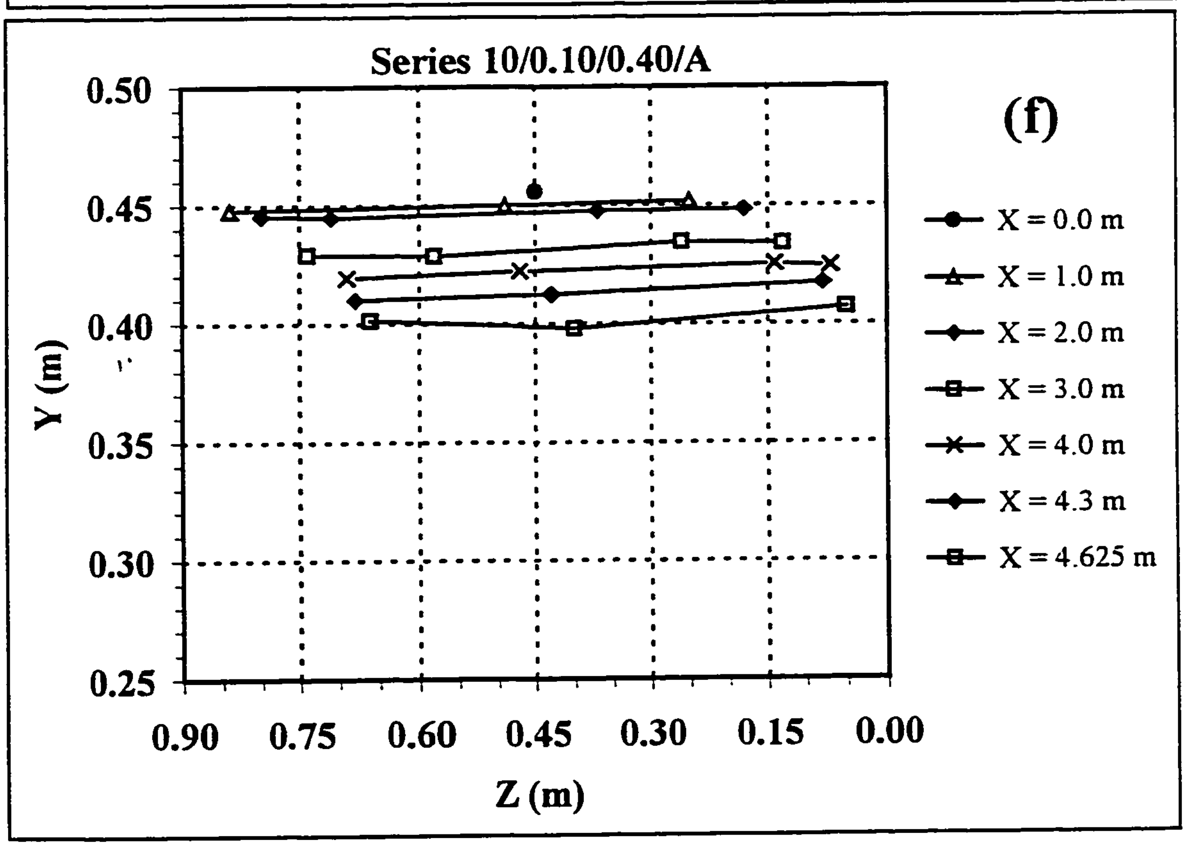

A-1.1(e-f): Depth Profiles of Bypass Section and Canal Section.

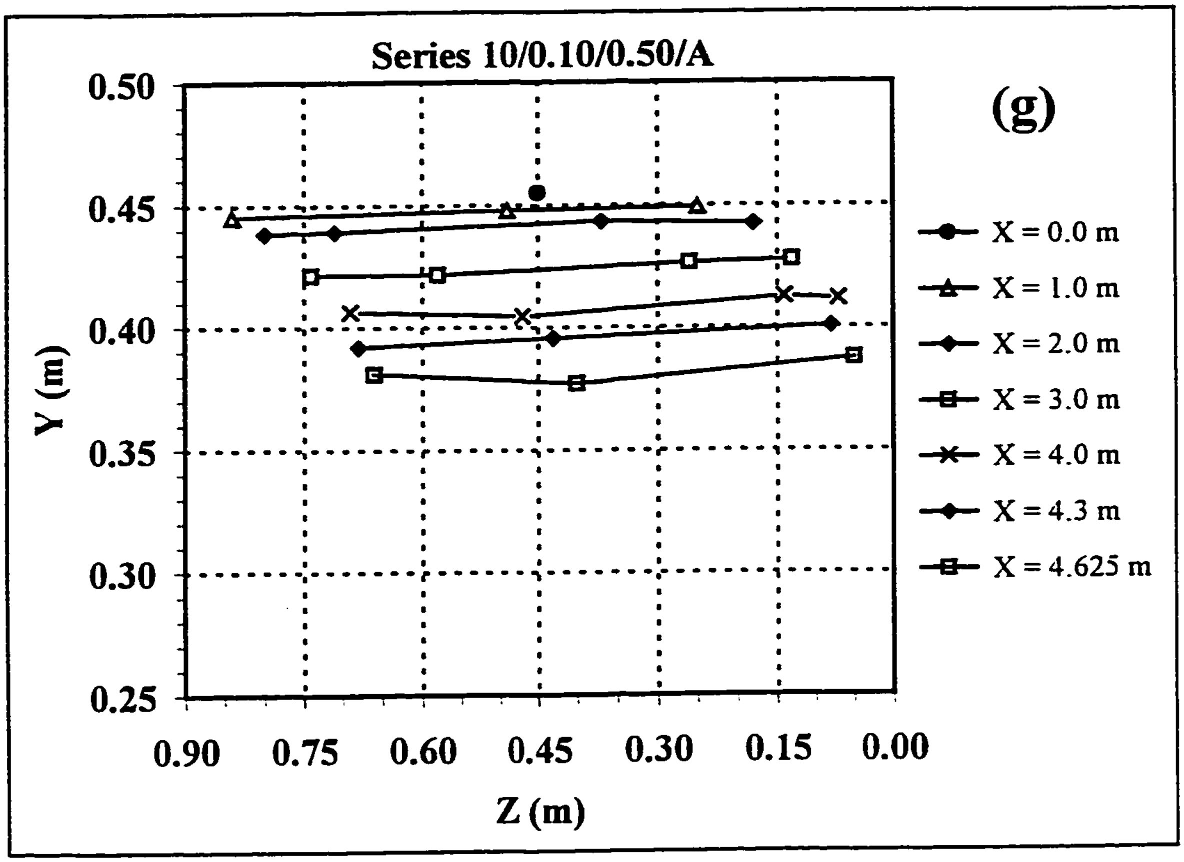

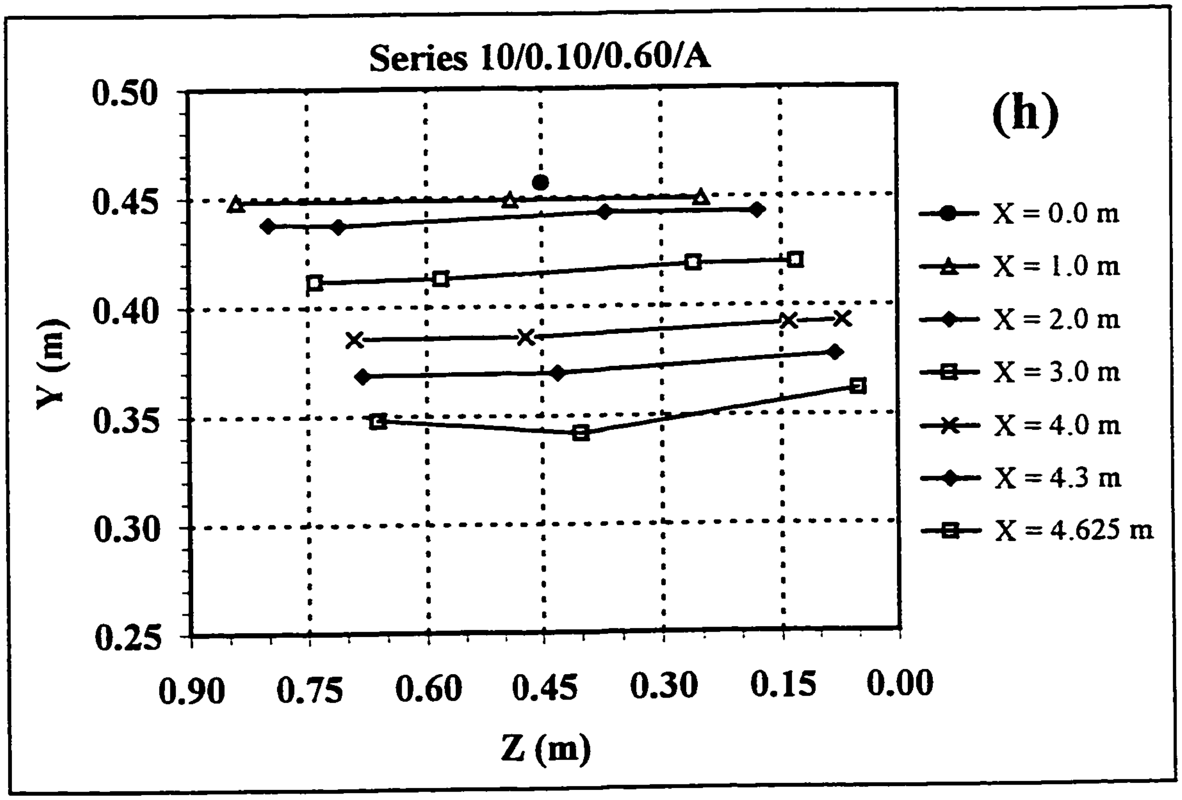

A-1.1(g-h): Depth Profiles of Bypass Section and Canal Section.

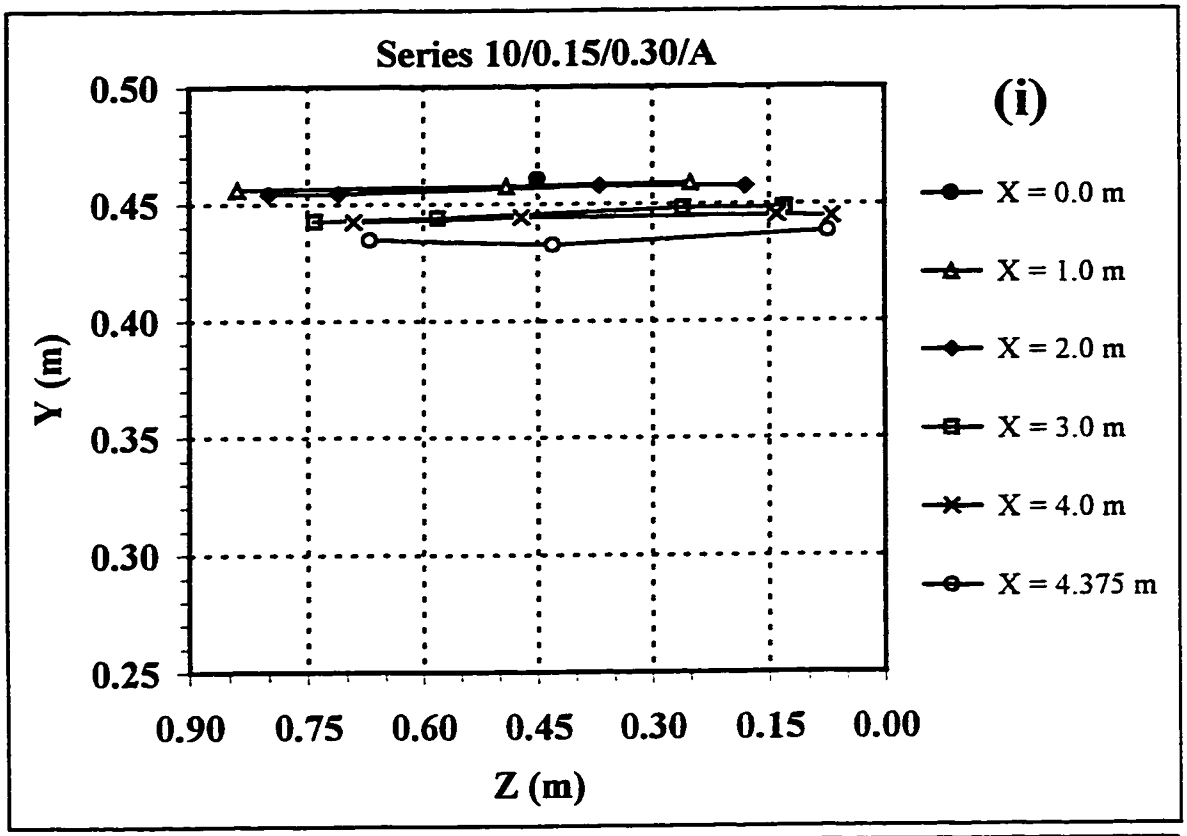

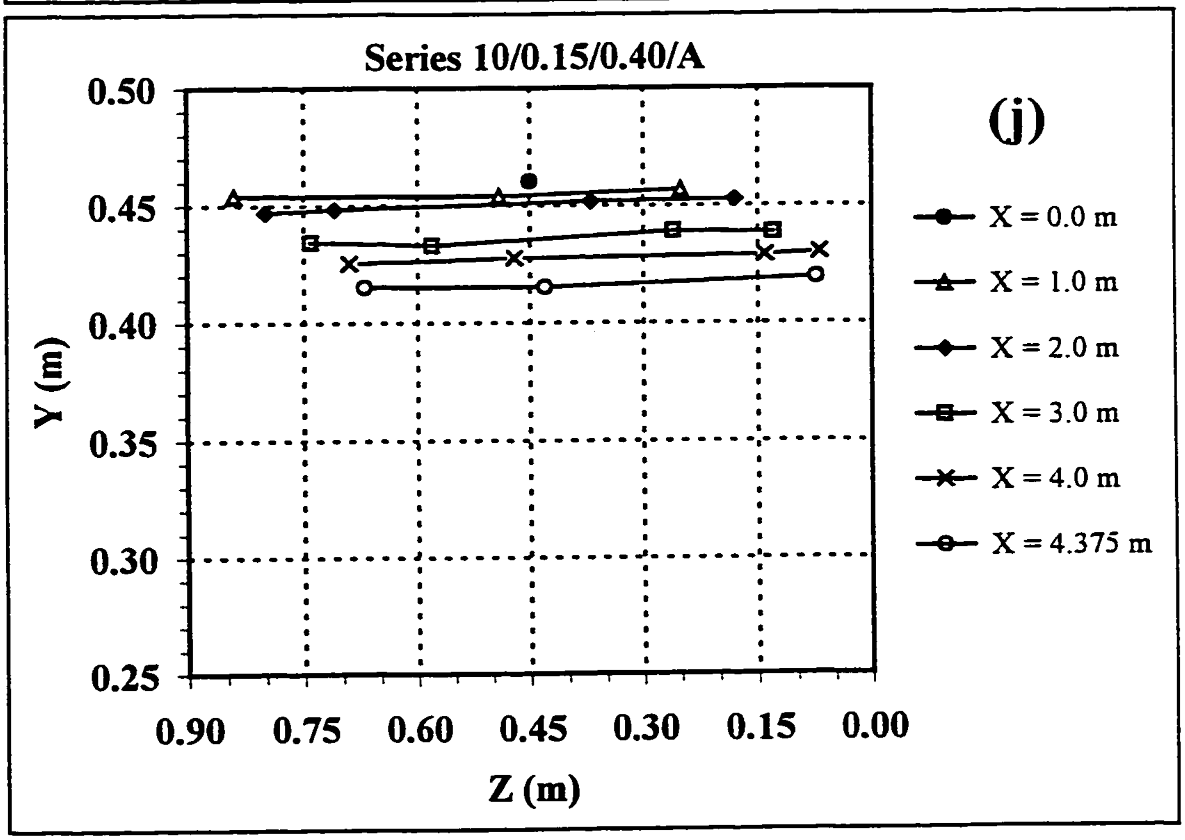

A-1.1(i-j): Depth Profiles of Bypass Section and Canal Section.

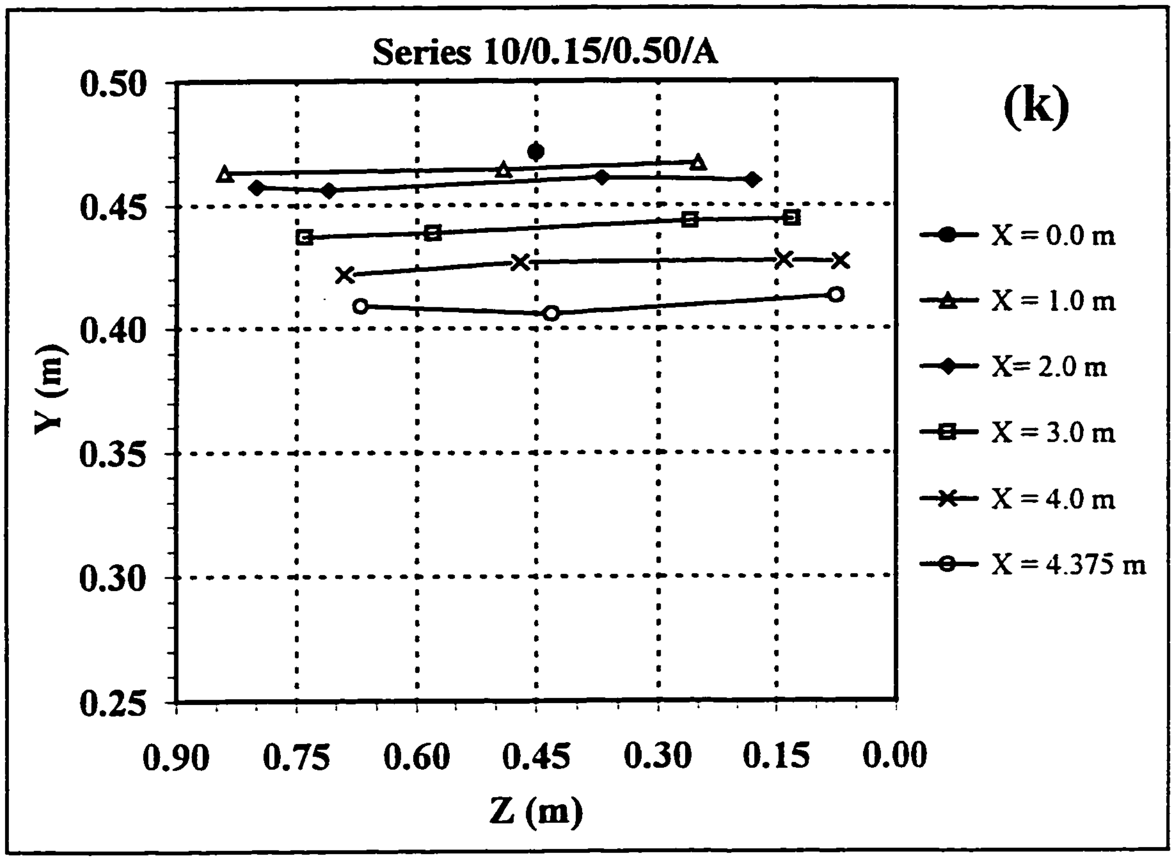

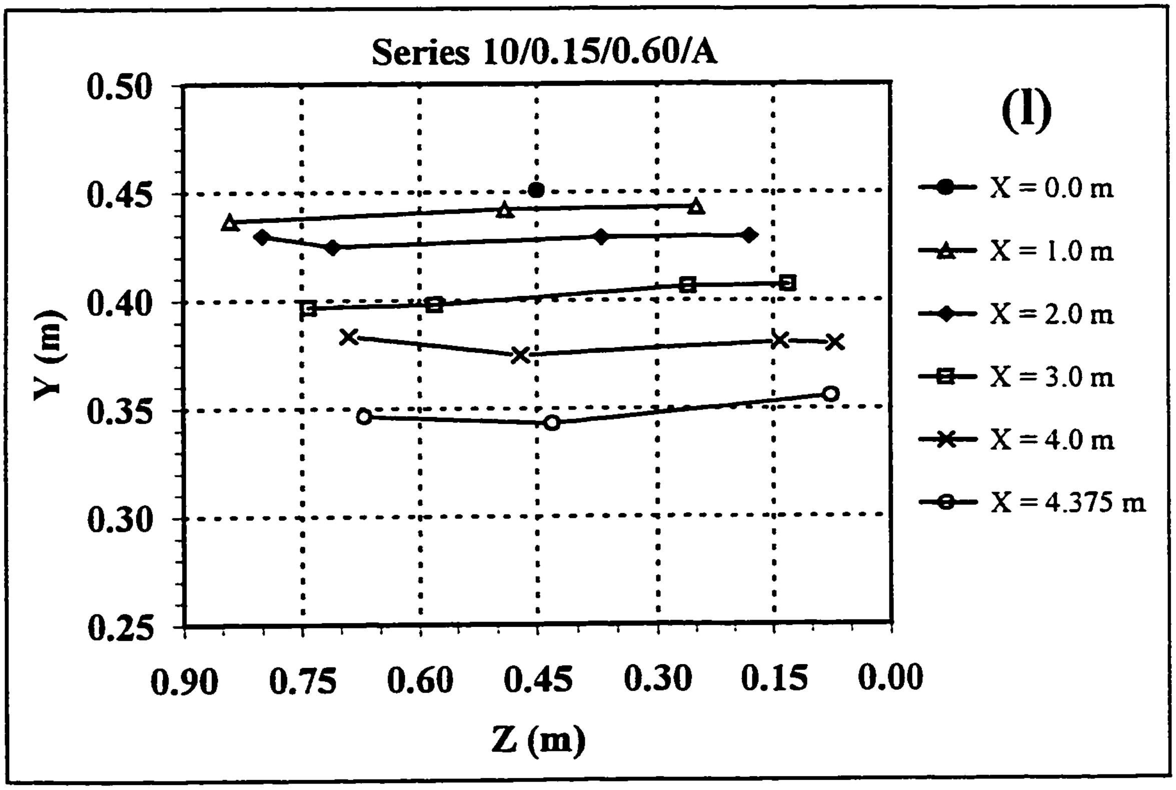

A-1.1(k-l): Depth Profiles of Bypass Section and Canal Section.

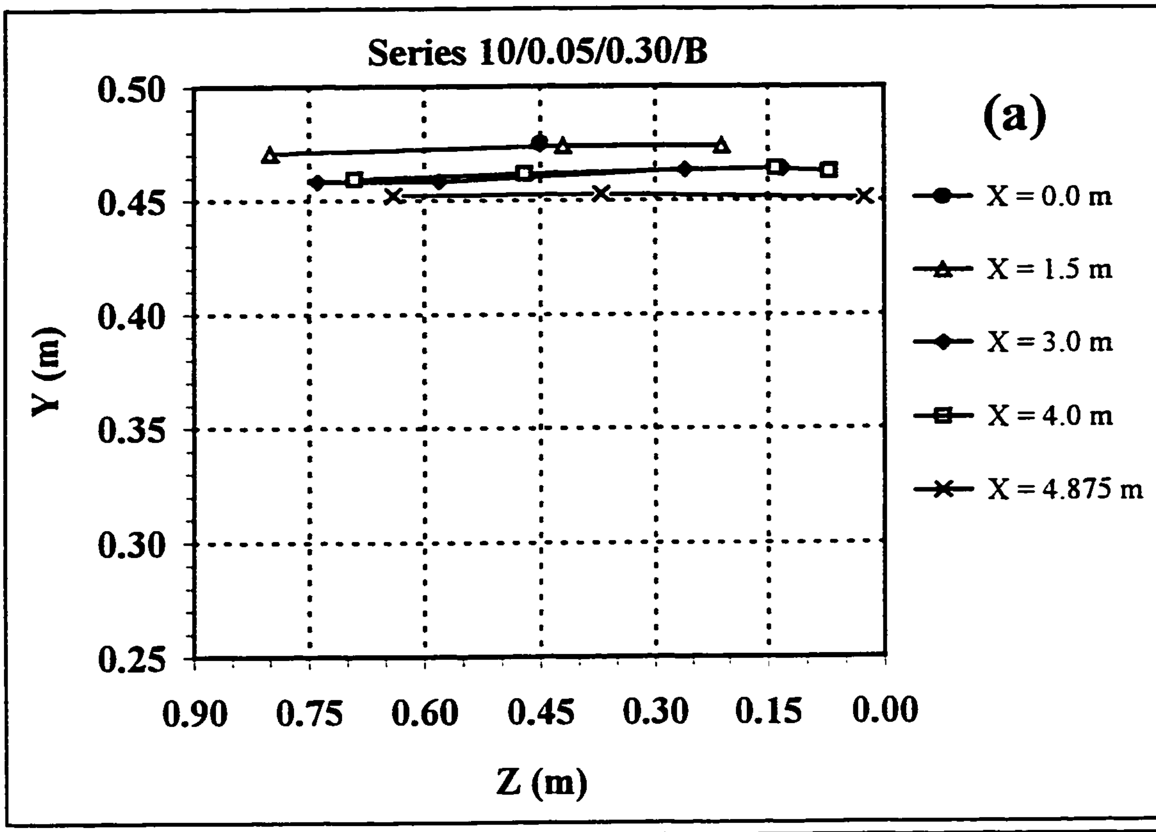

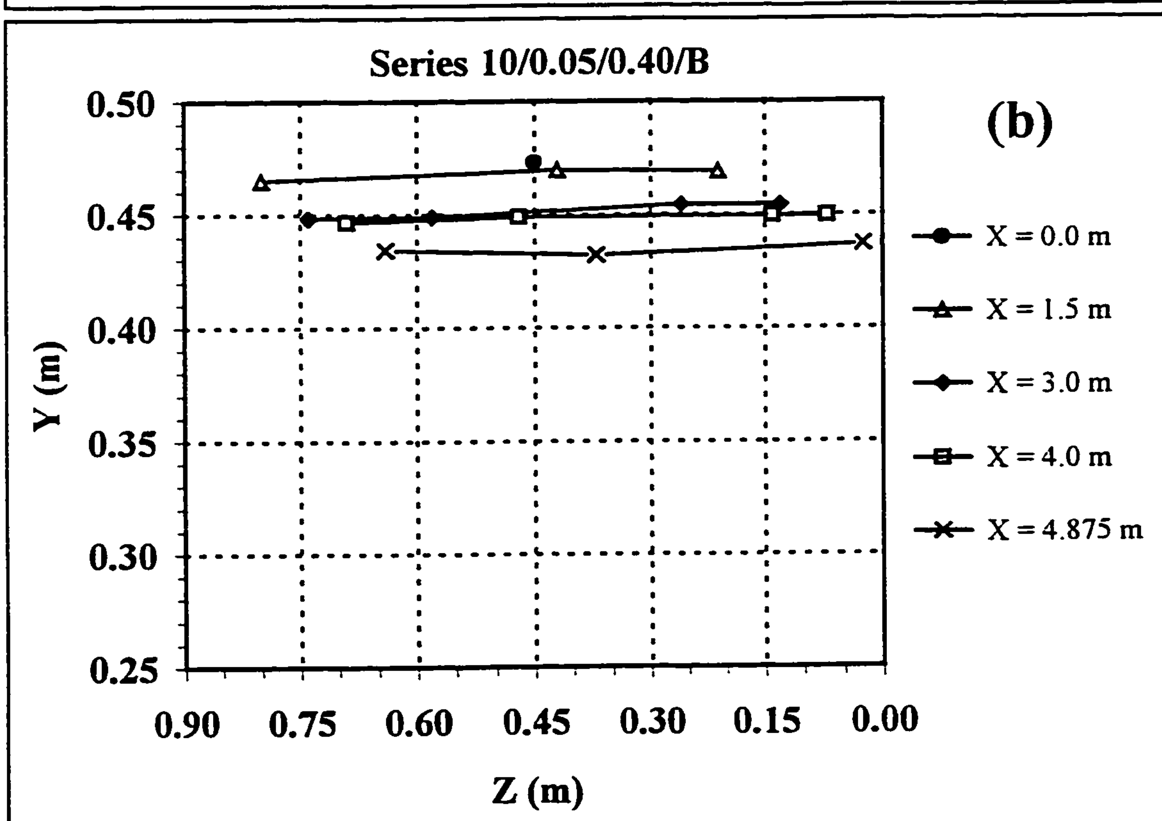

A-1.2(a-b): Depth Profiles of Bypass Section and Canal Section.

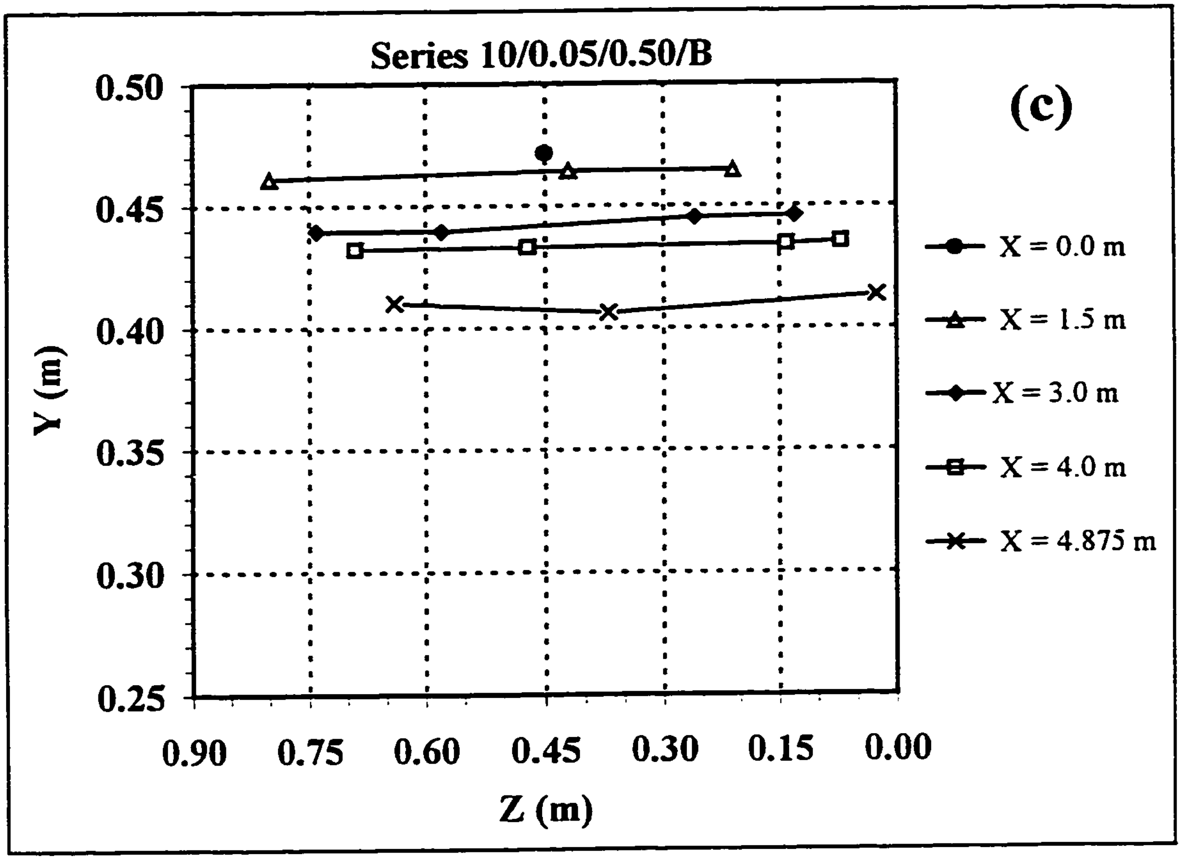

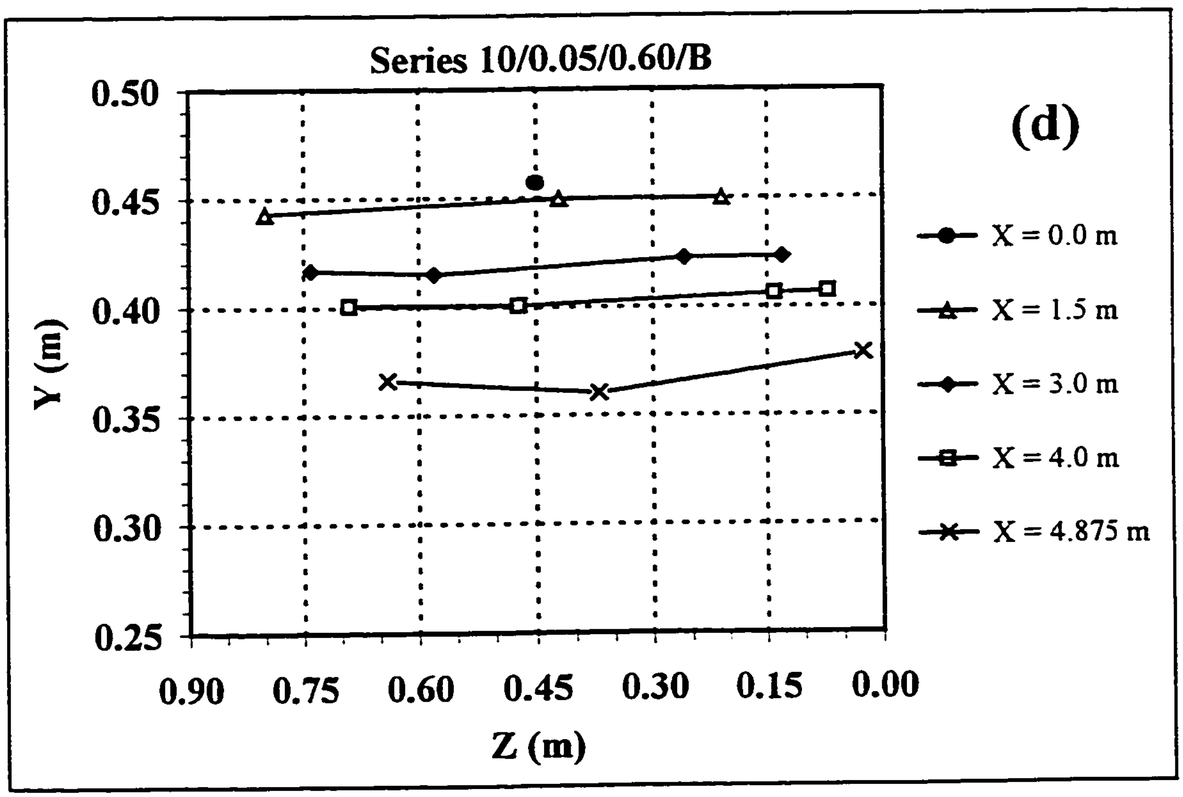

A-1.2(c-d): Depth Profiles of Bypass Section and Canal Section.

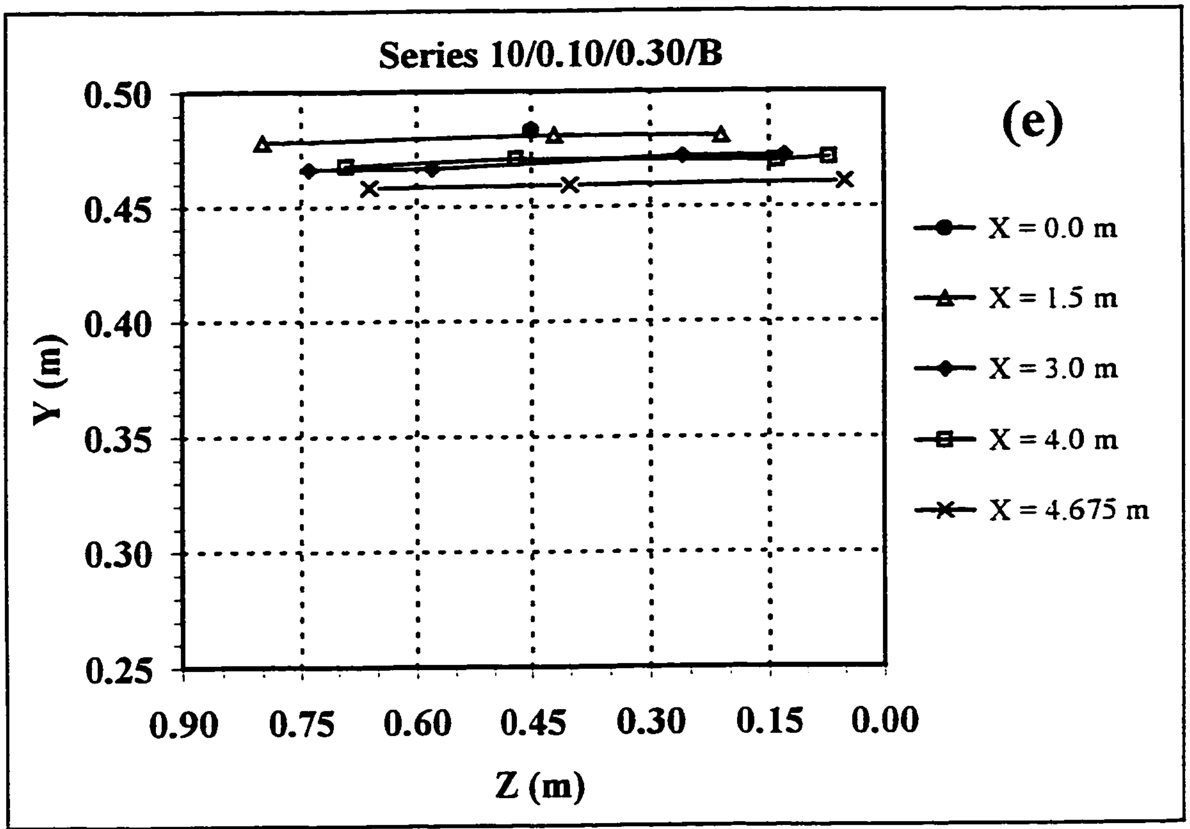

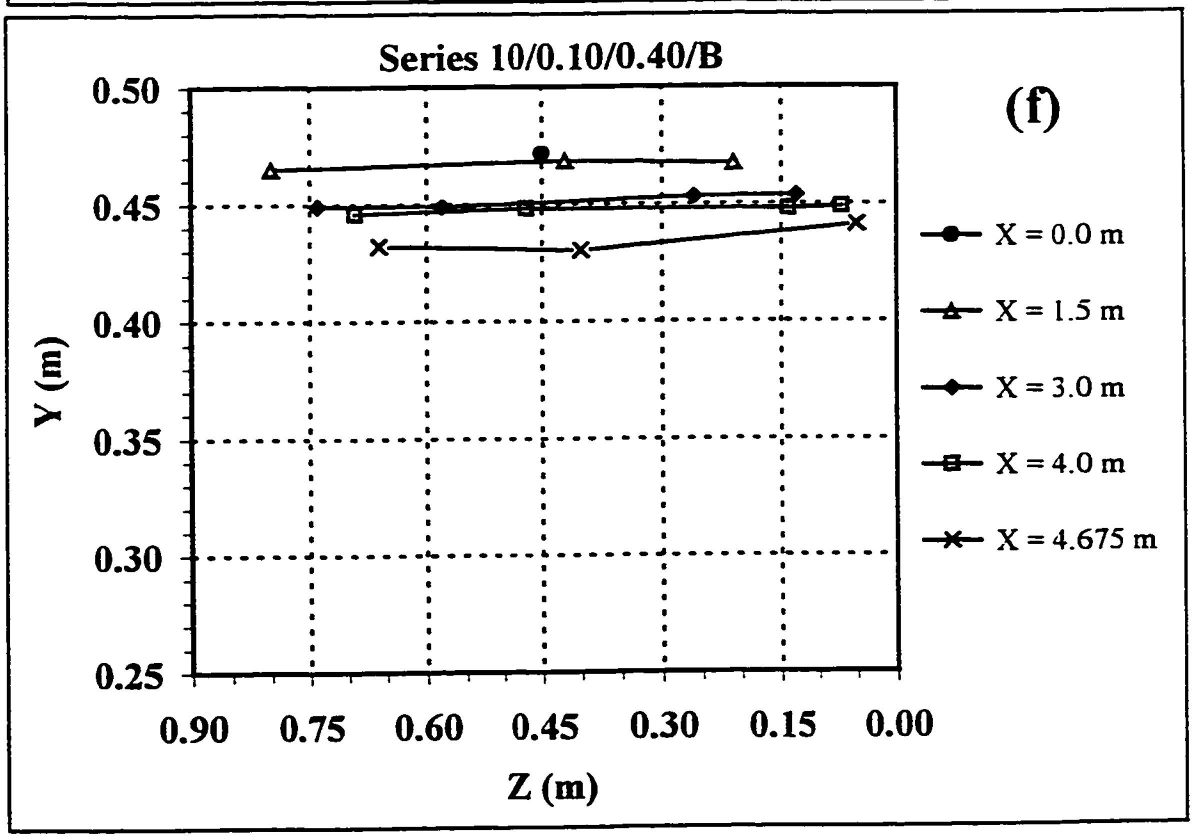

A-1.2(e-f): Depth Profiles of Bypass Section and Canal Section.

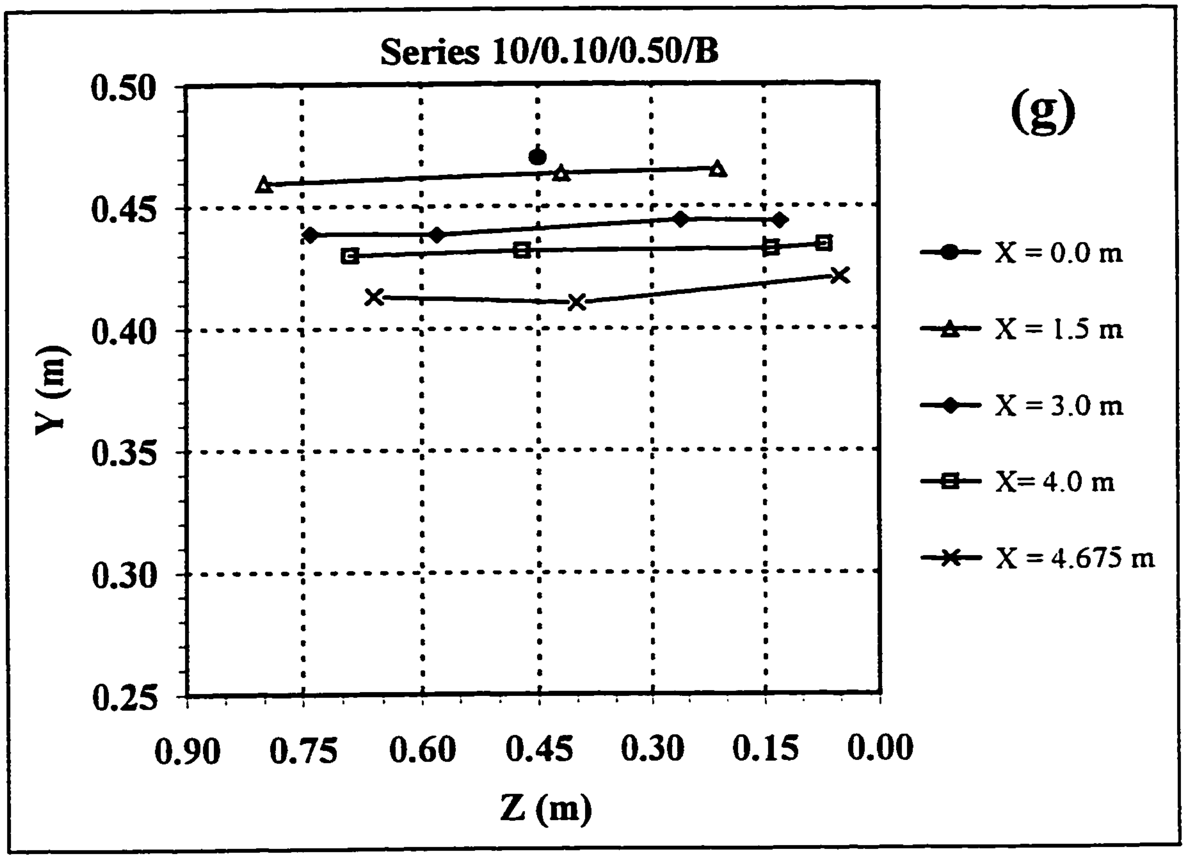

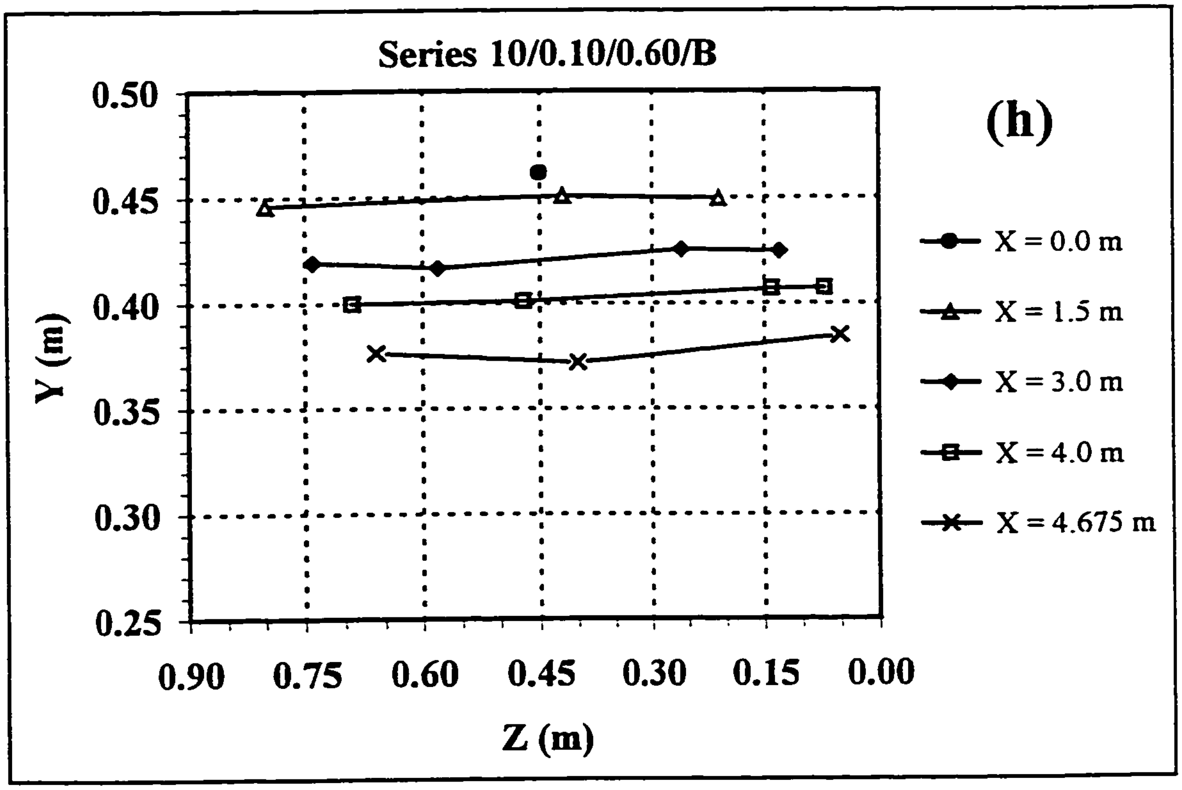

A-1.2(g-h): Depth Profiles of Bypass Section and Canal Section.

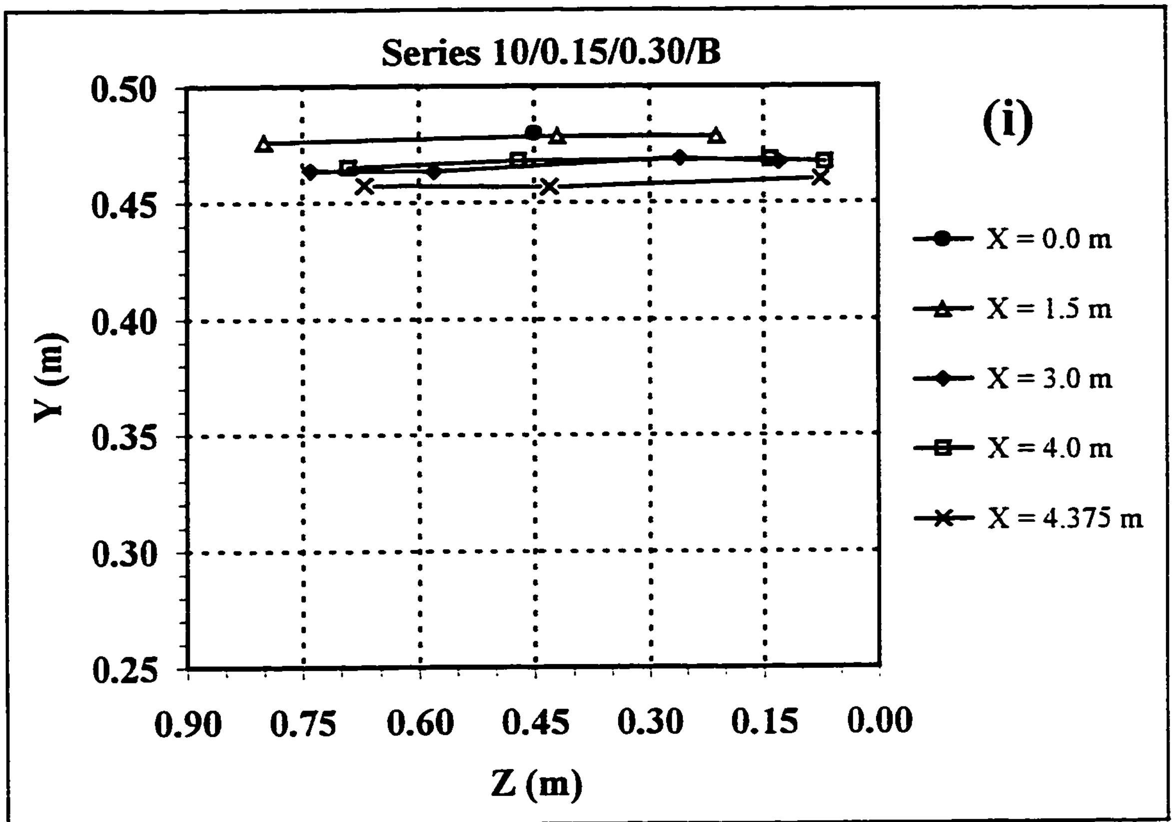

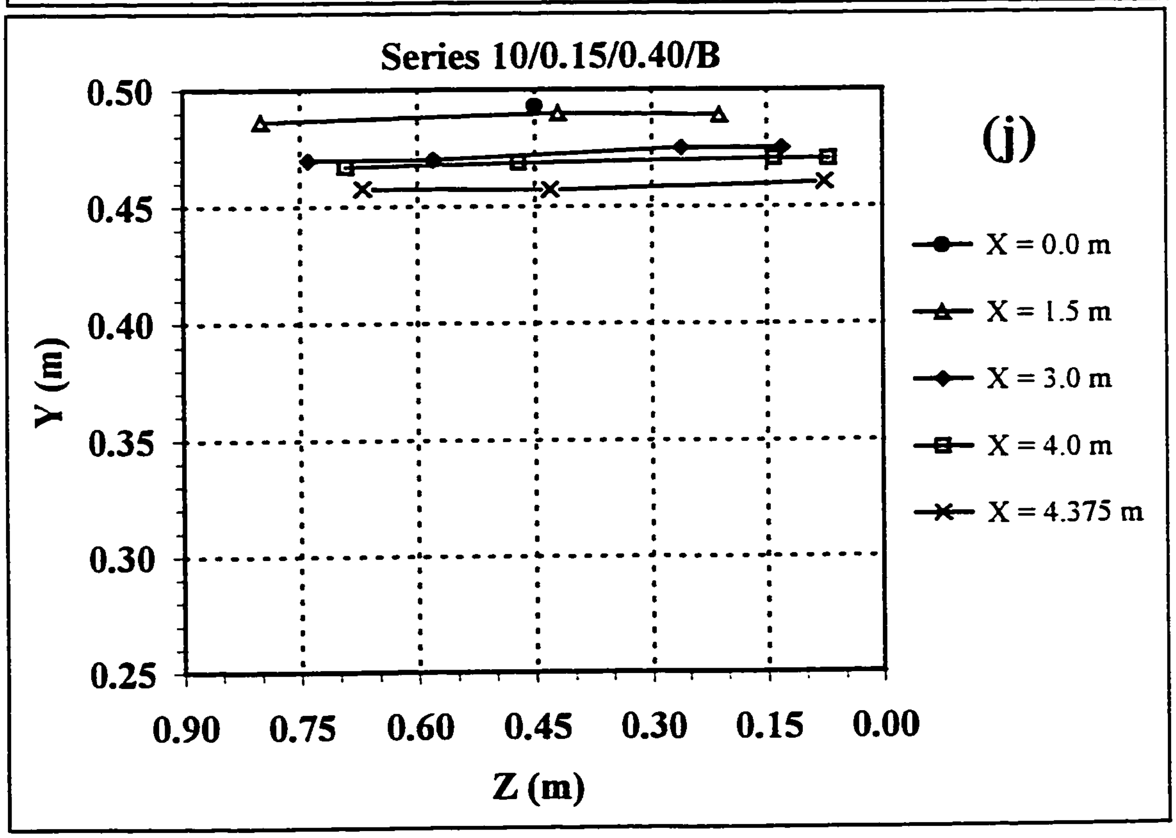

A-1.2(i-j): Depth Profiles of Bypass Section and Canal Section.

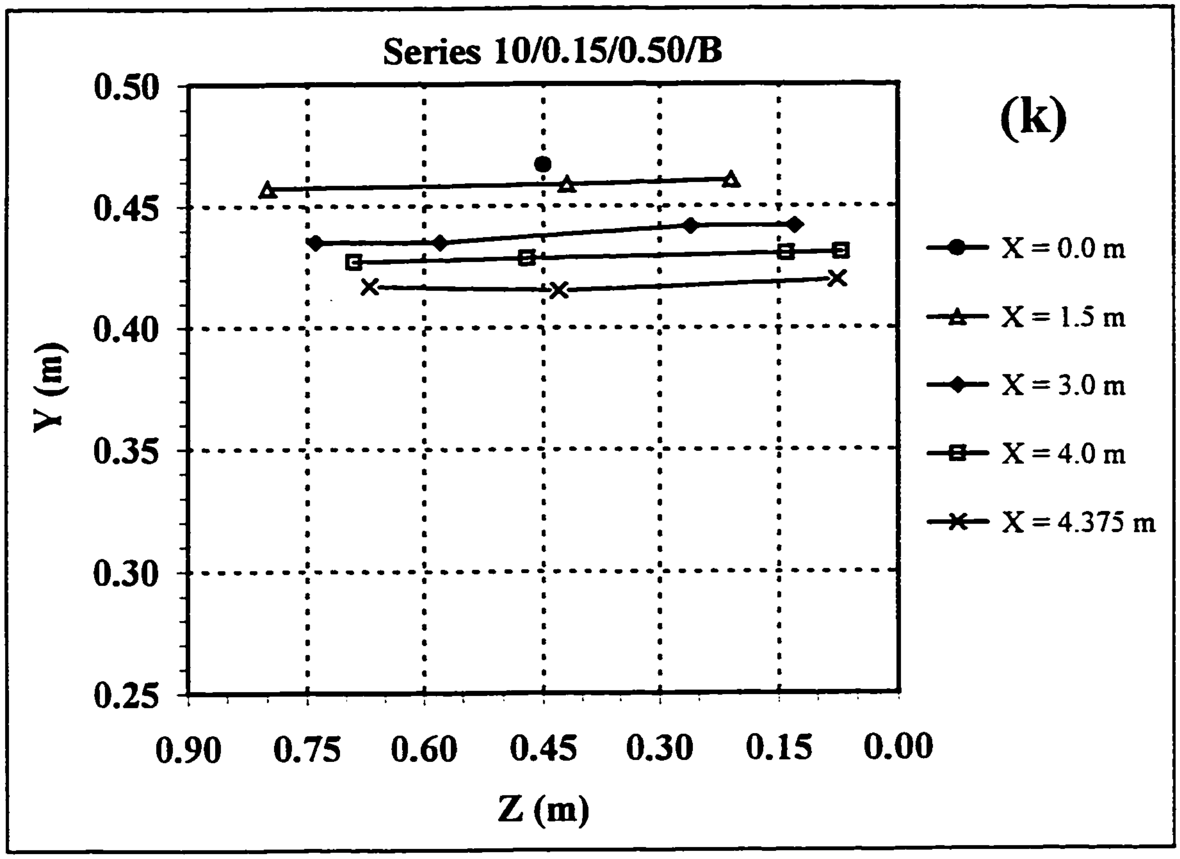

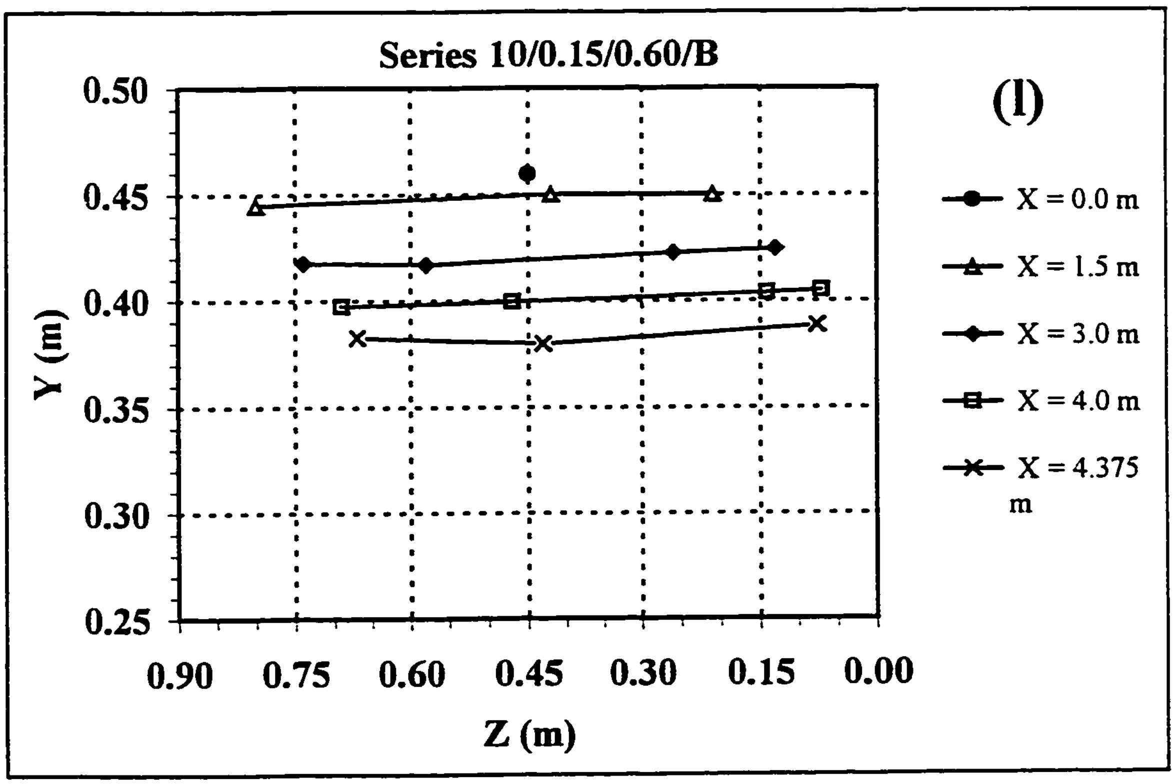

A-1.2(k-l): Depth Profiles of Bypass Section and Canal Section.

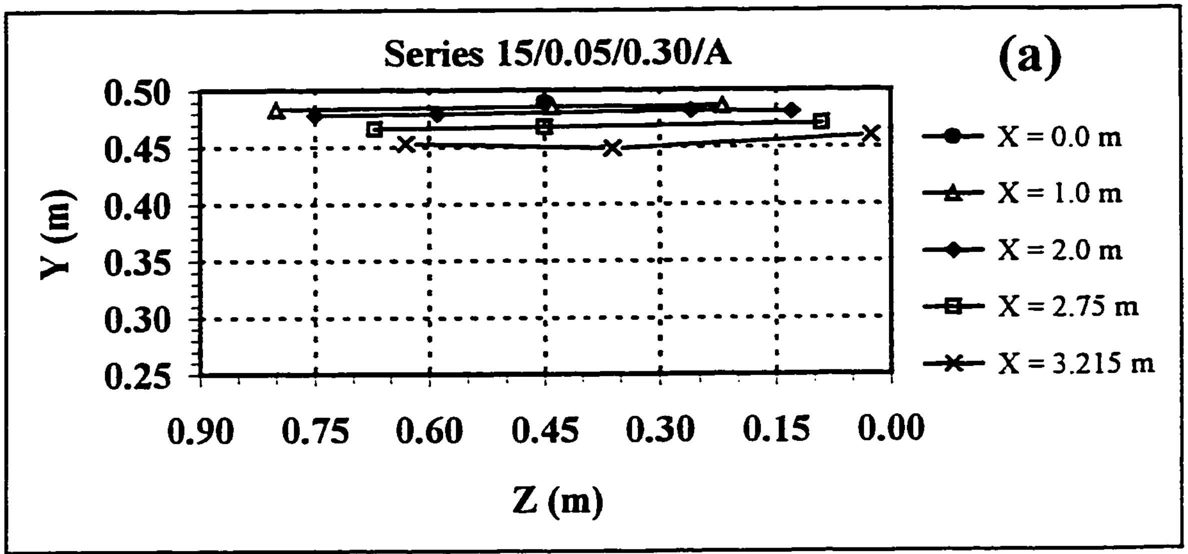

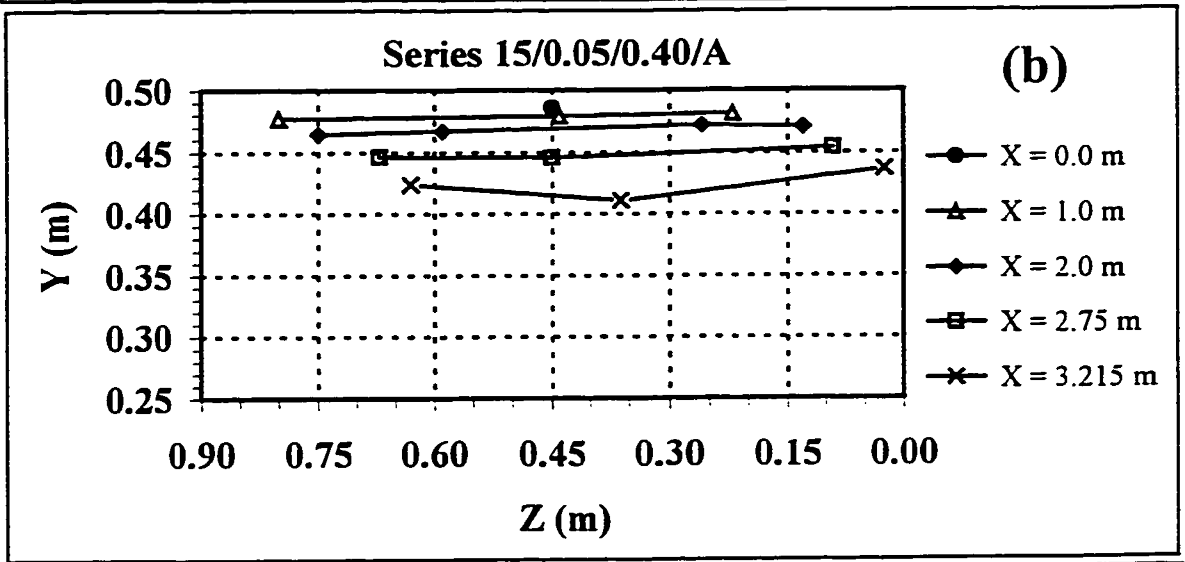

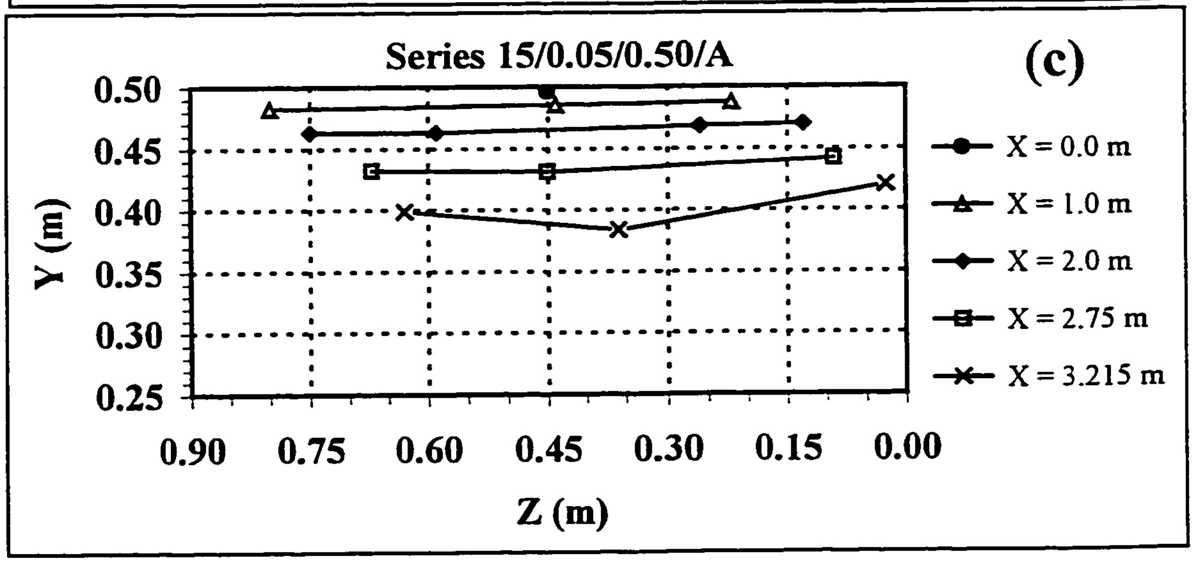

A-1.3(a-c): Depth Profiles of Bypass Section and Canal Section.

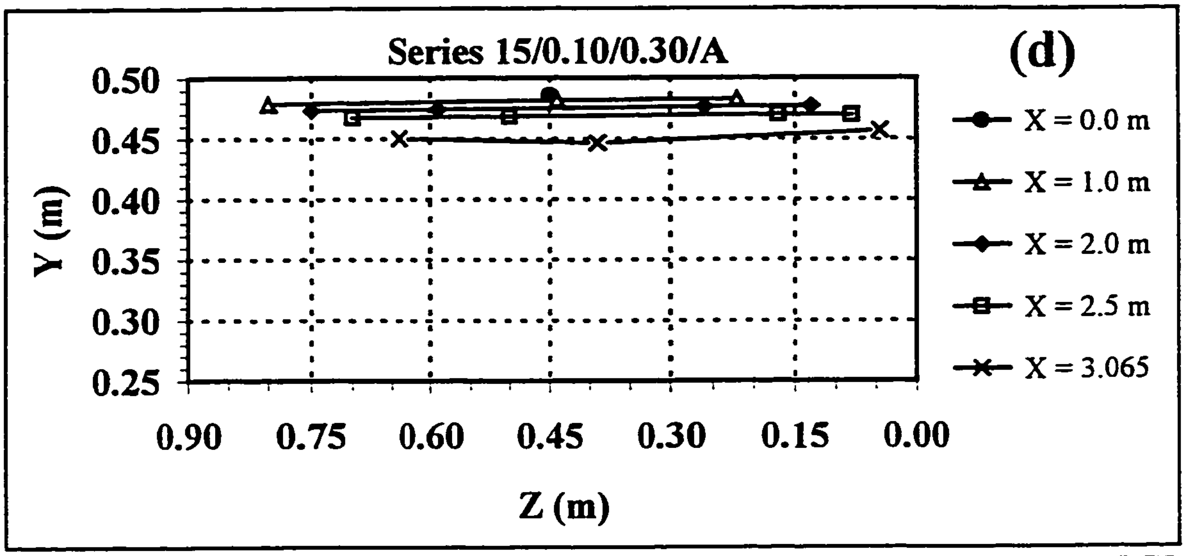

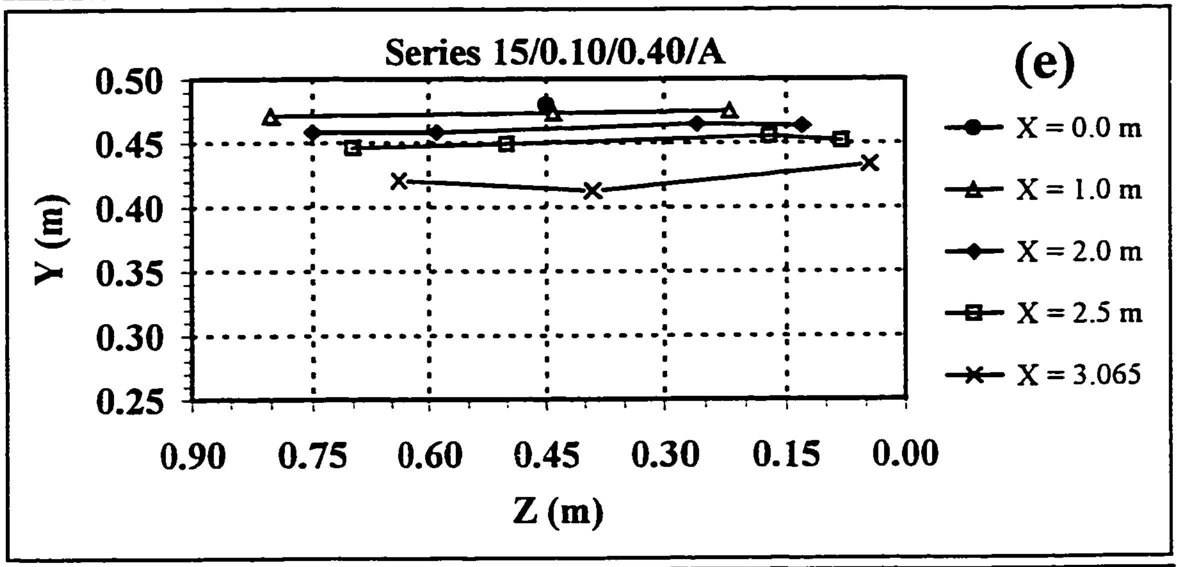

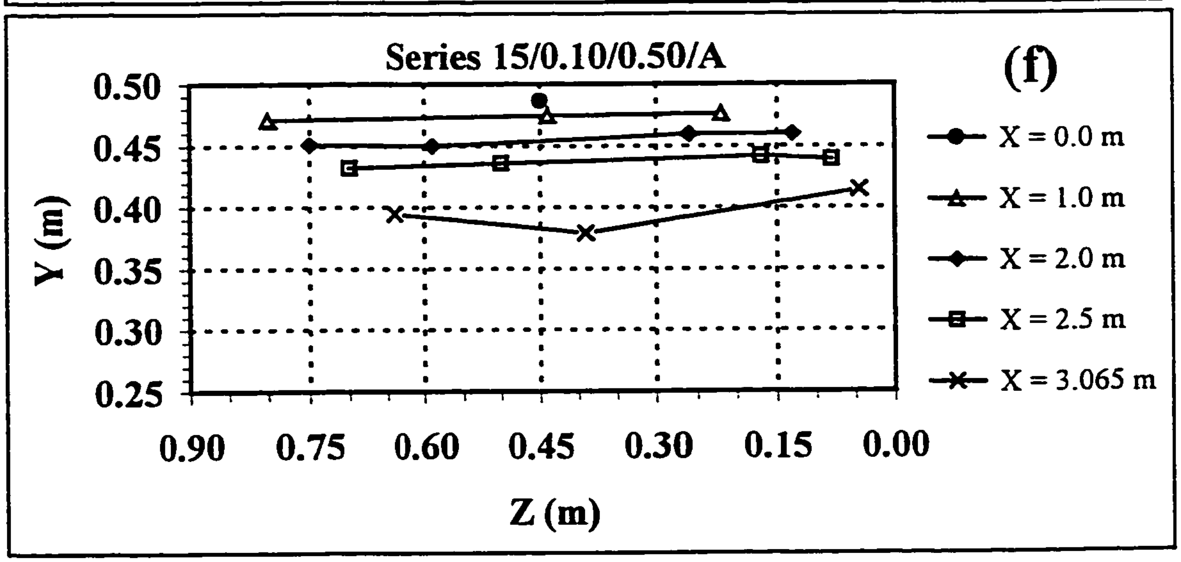

A-1.3(d-f): Depth Profiles of Bypass Section and Canal Section.

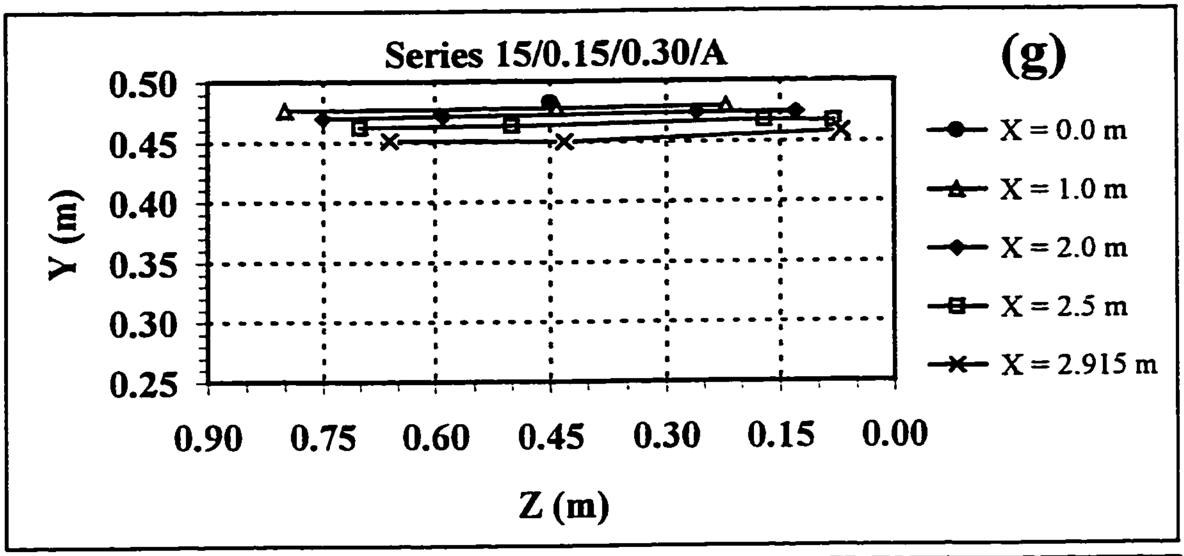

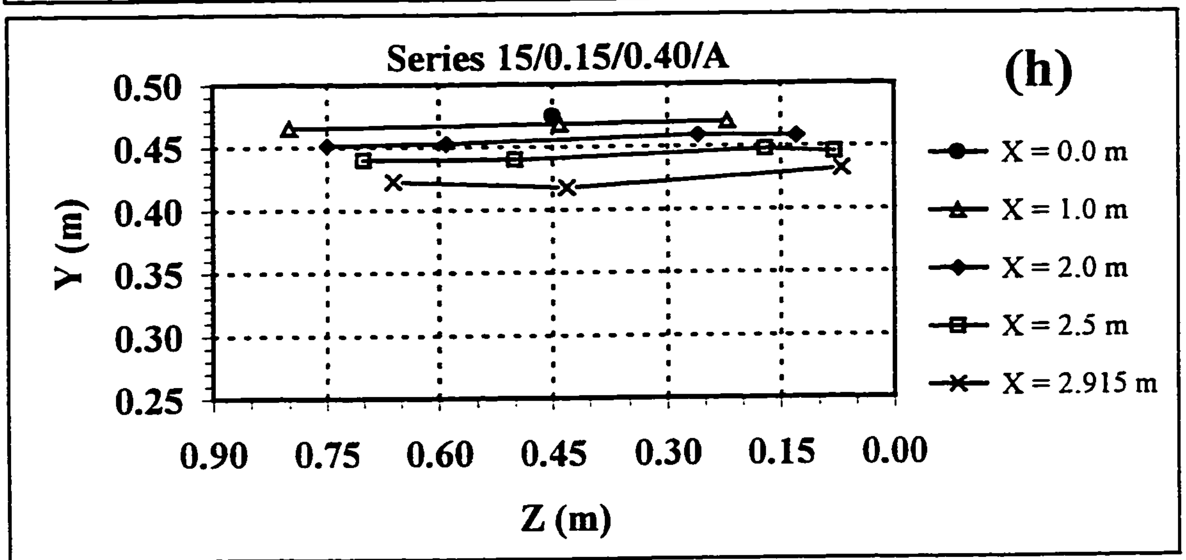

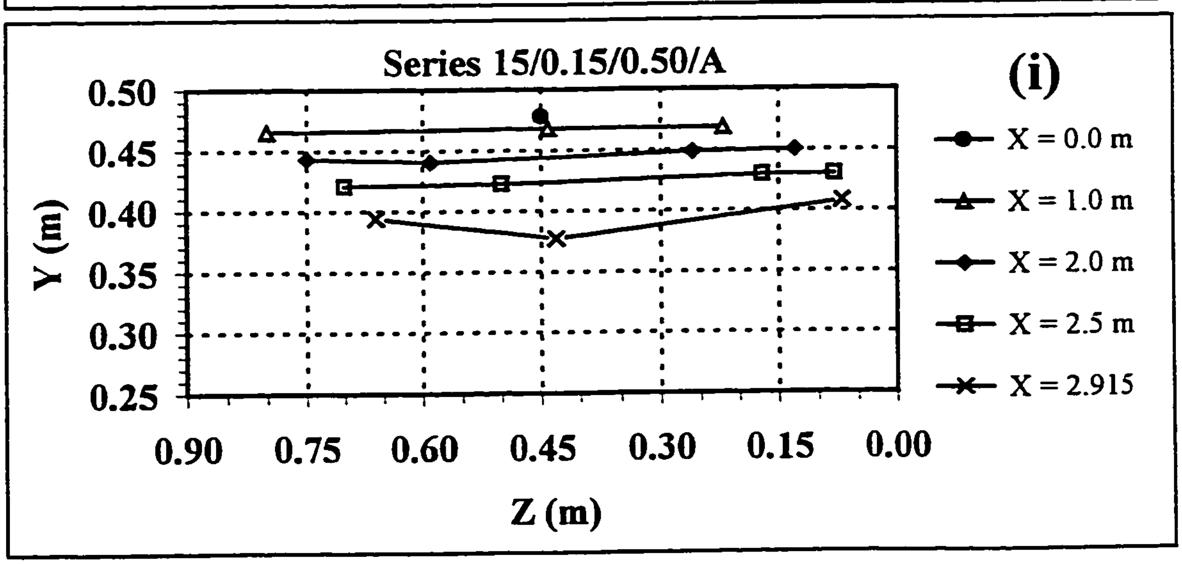

A-1.3(g-i): Depth Profiles of Bypass Section and Canal Section.

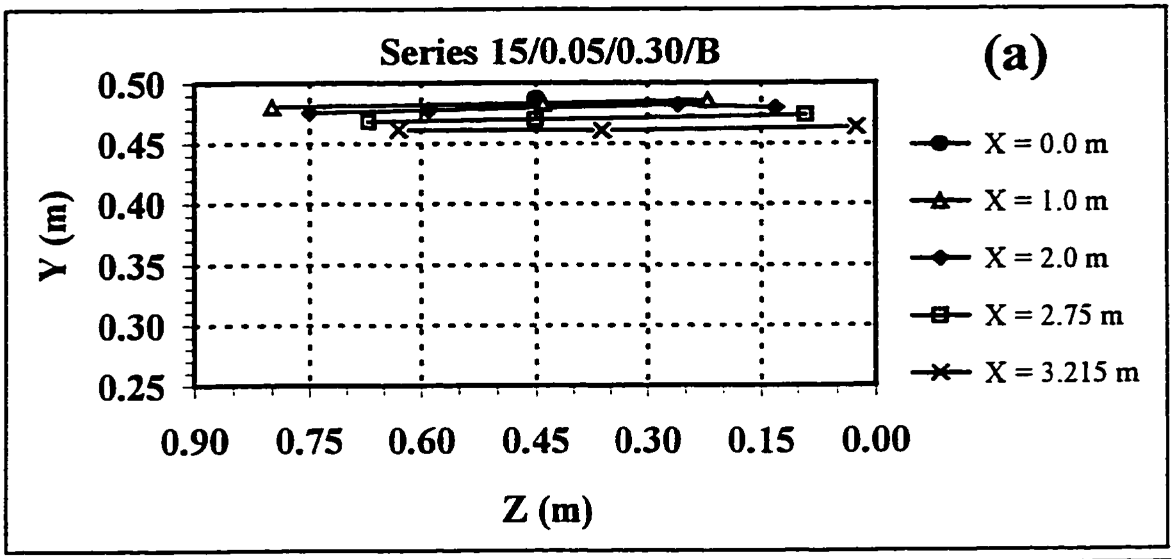

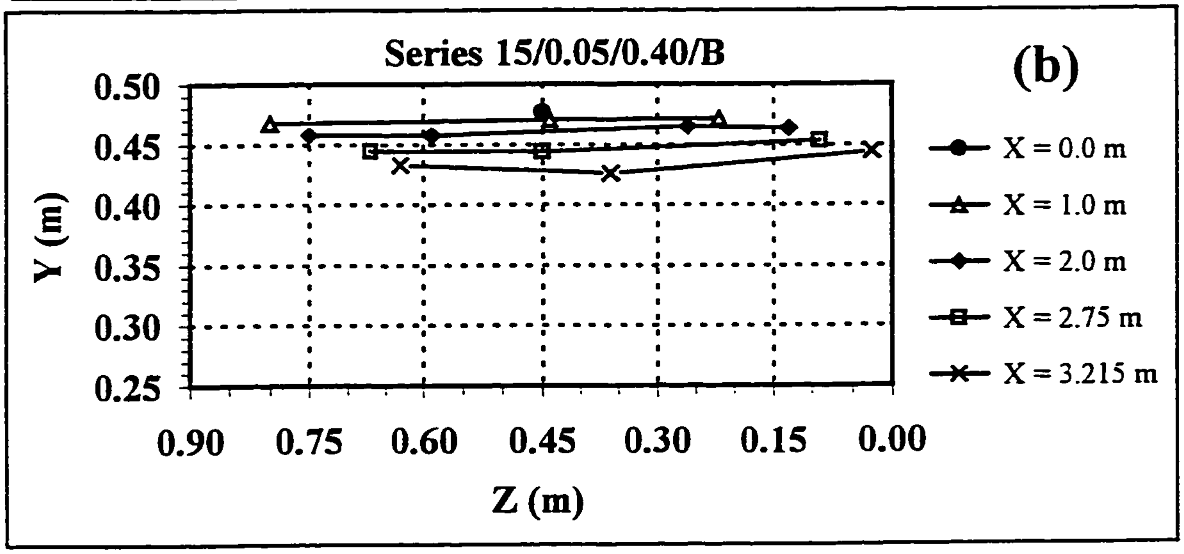

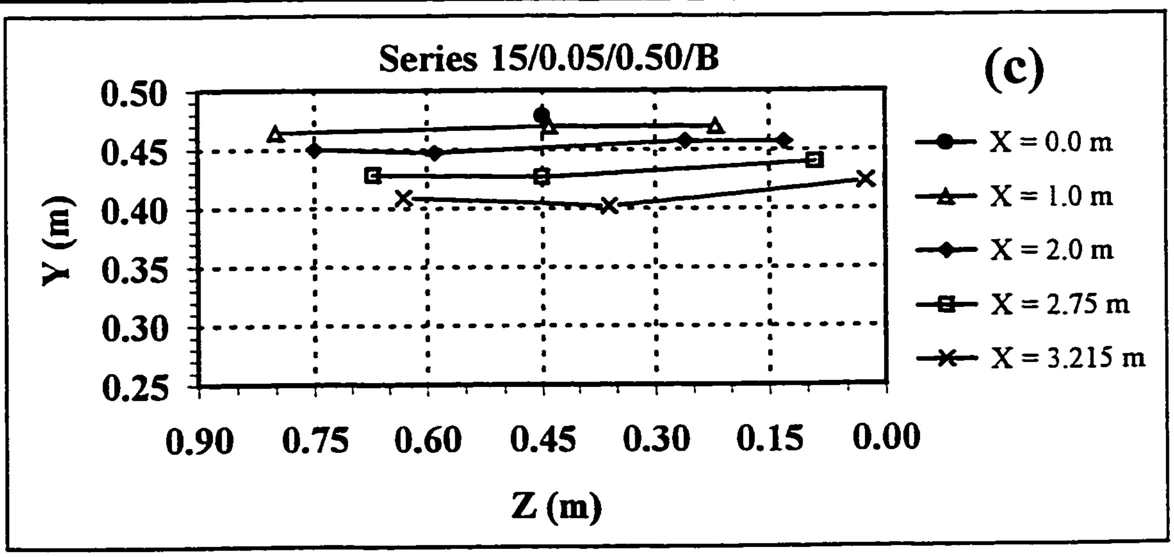

A-1.4(a-c): Depth Profiles of Bypass Section and Canal Section.

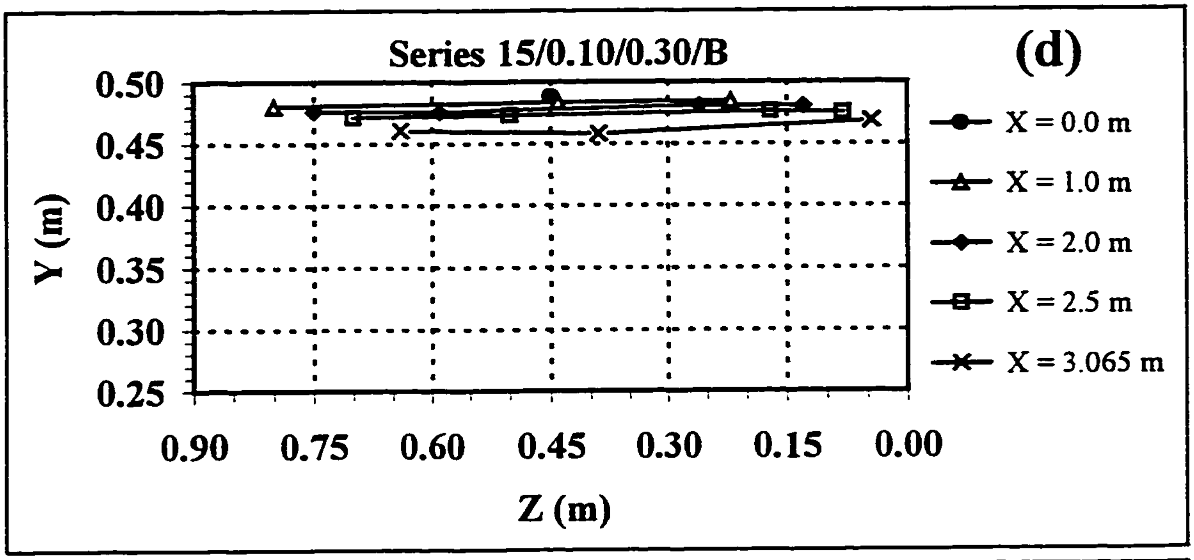

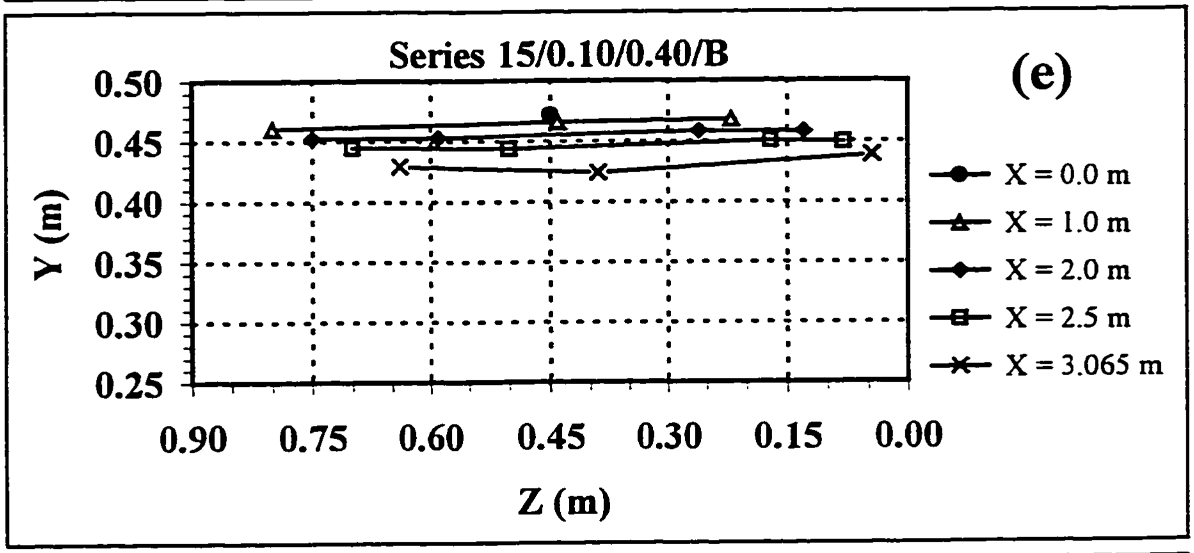

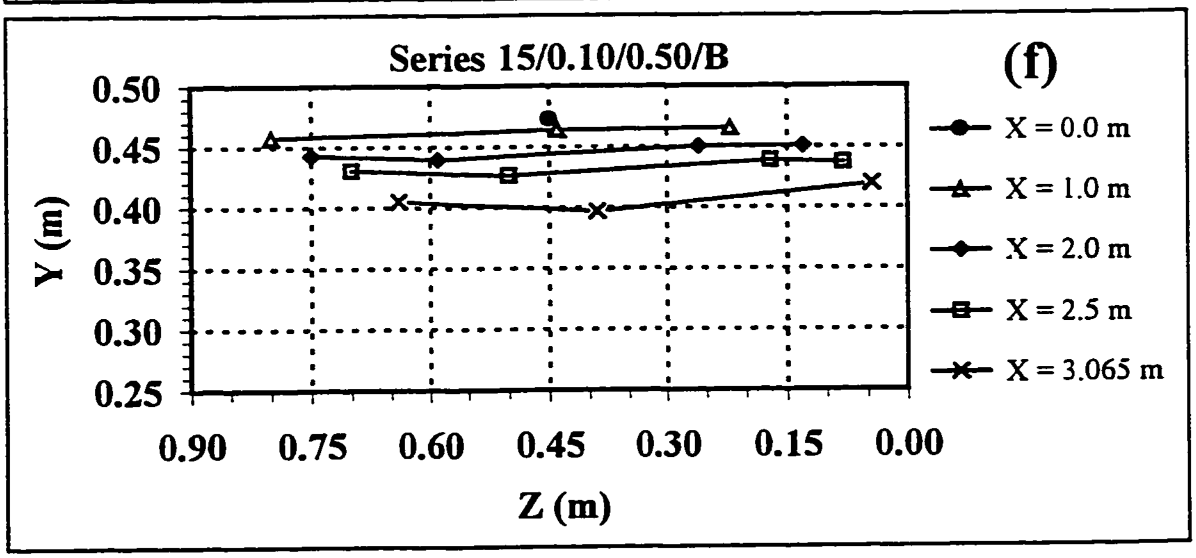

A-1.4(d-f): Depth Profiles of Bypass Section and Canal Section.

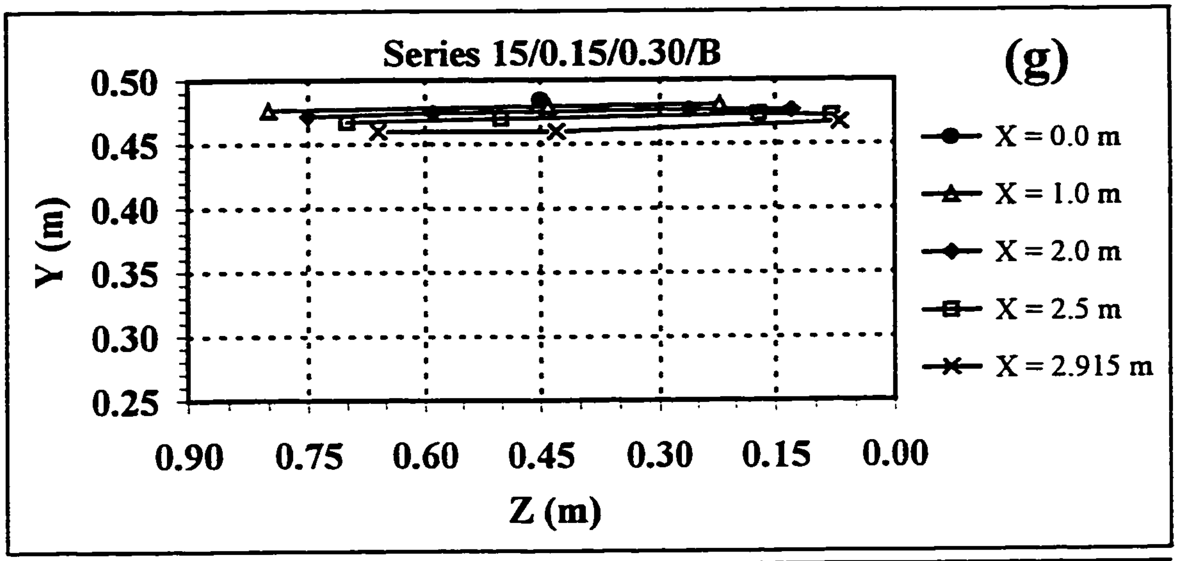

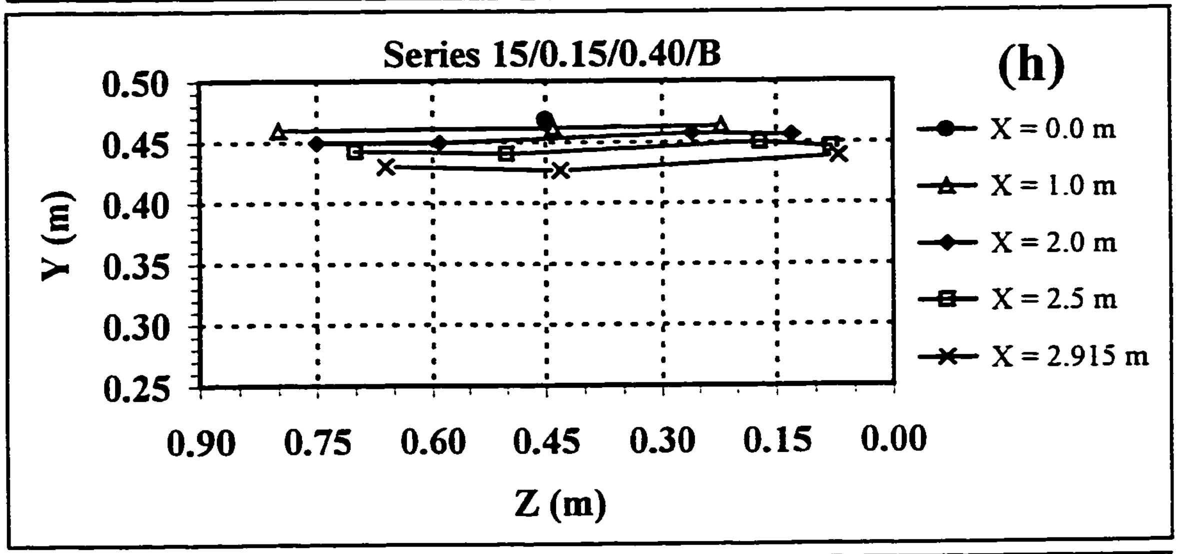

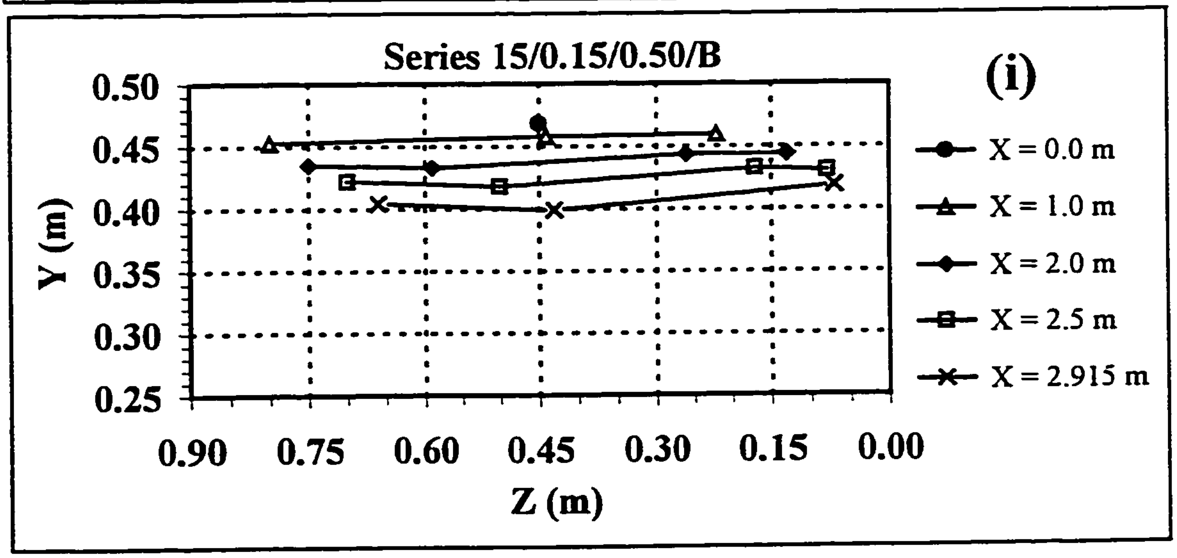

A-1.4(g-i): Depth Profiles of Bypass Section and Canal Section.

A-2

Profiles in Horizontal Direction

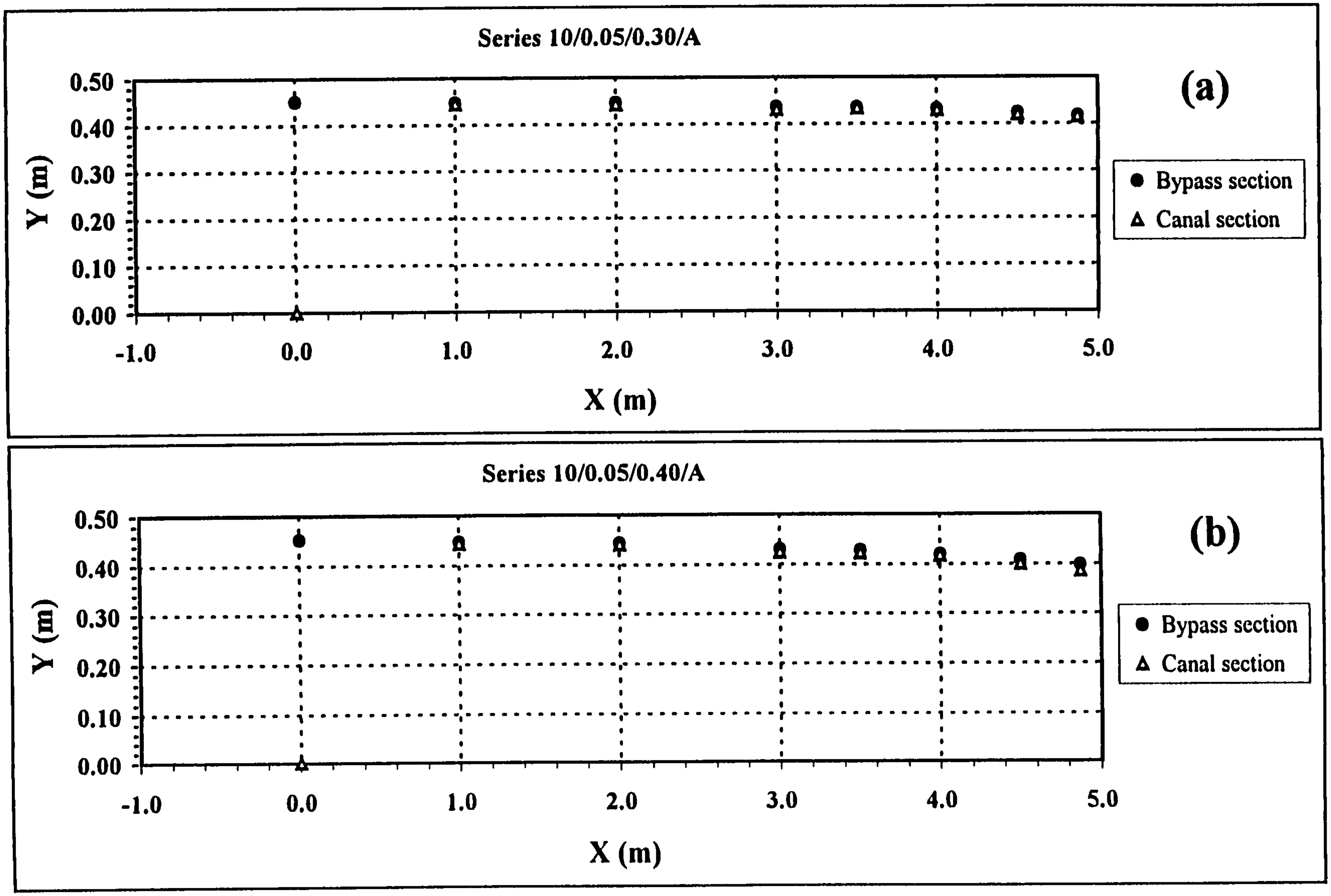

A-2.1(a-b): Depth Profiles of Bypass Section and Canal Section.

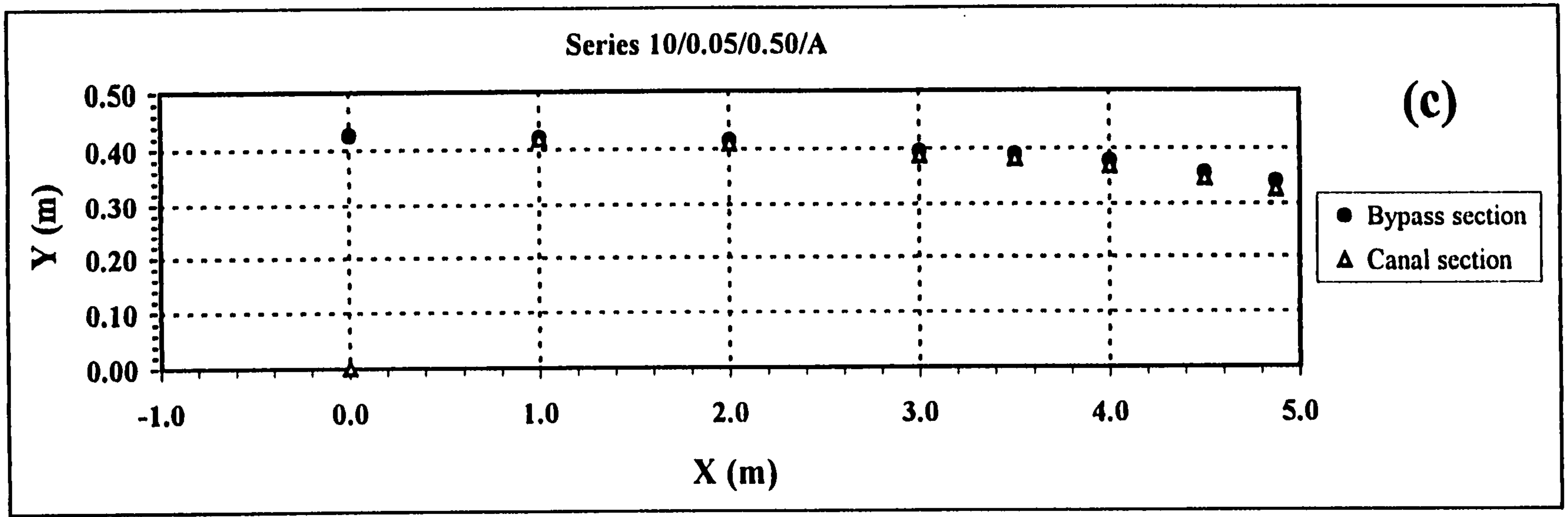

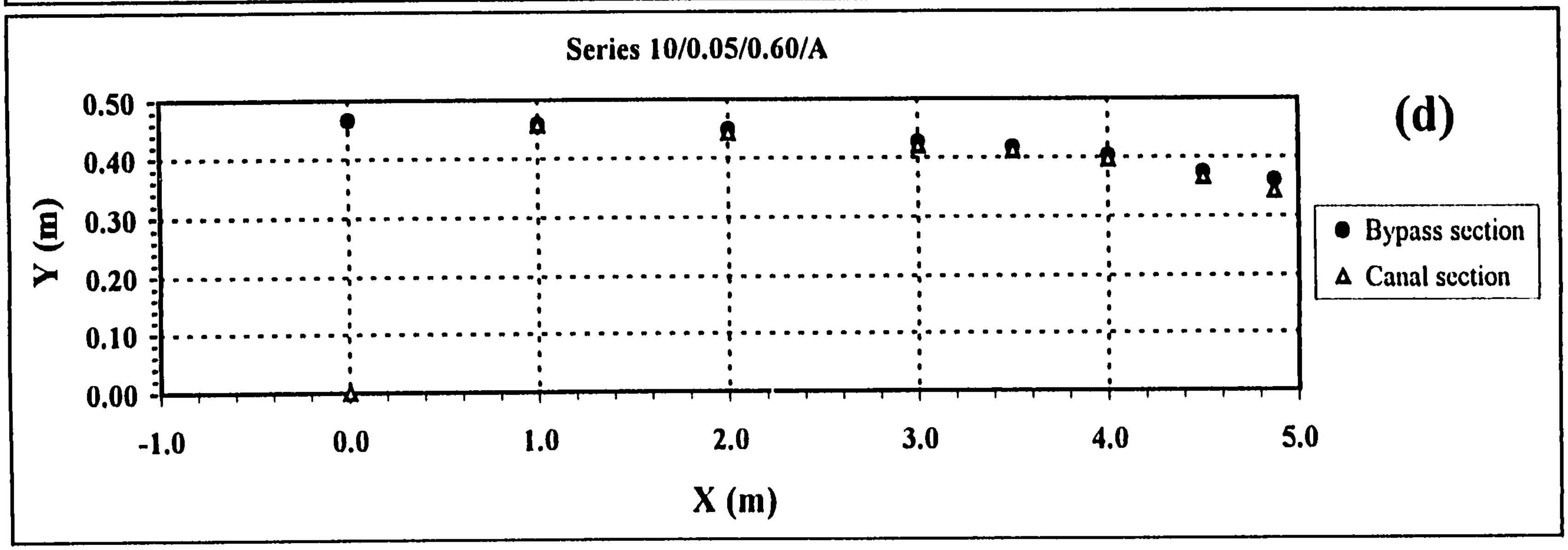

A-2.1(c-d): Depth Profiles of Bypass Section and Canal Section.

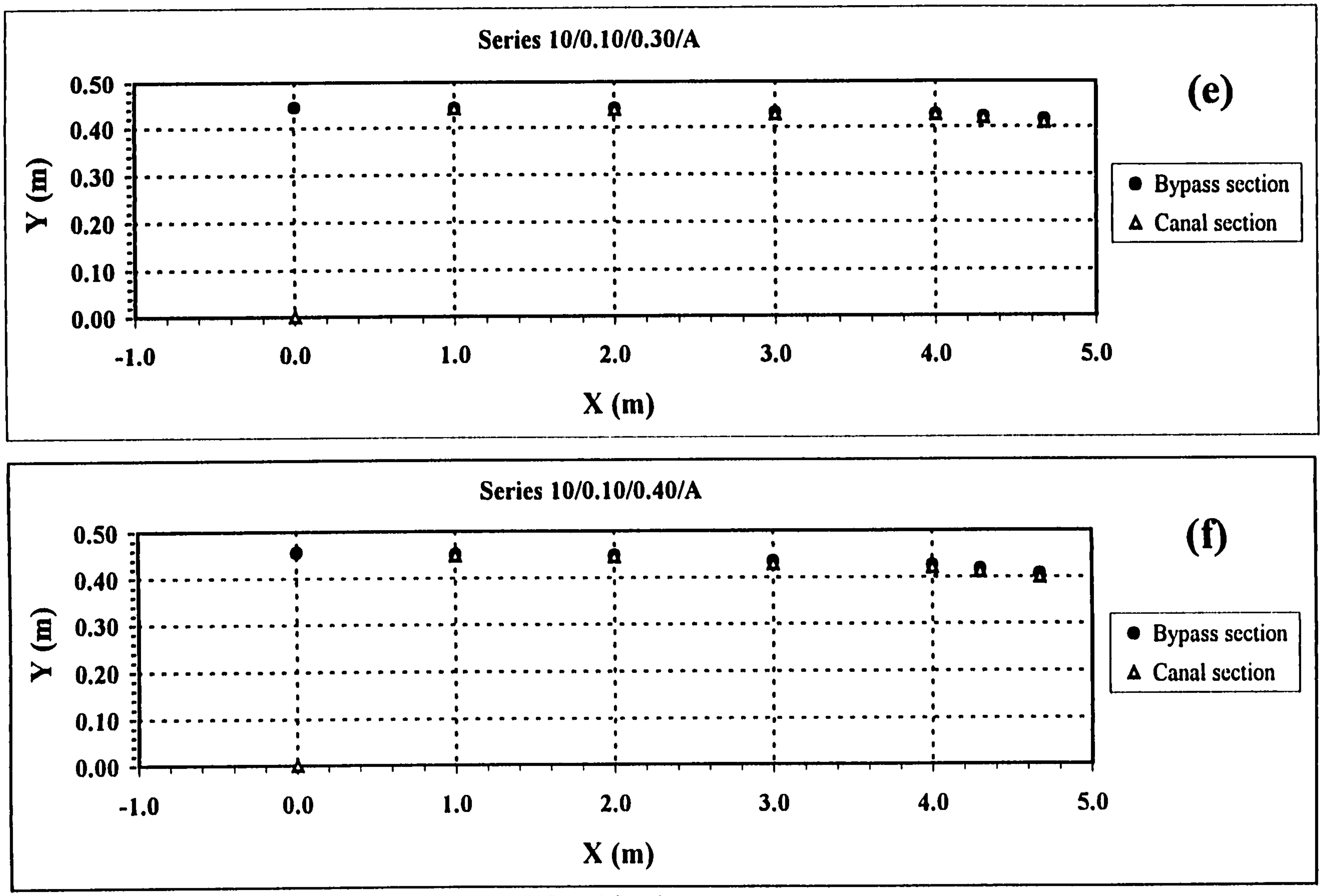

A-2.1(e-f): Depth Profiles of Bypass Section and Canal Section.

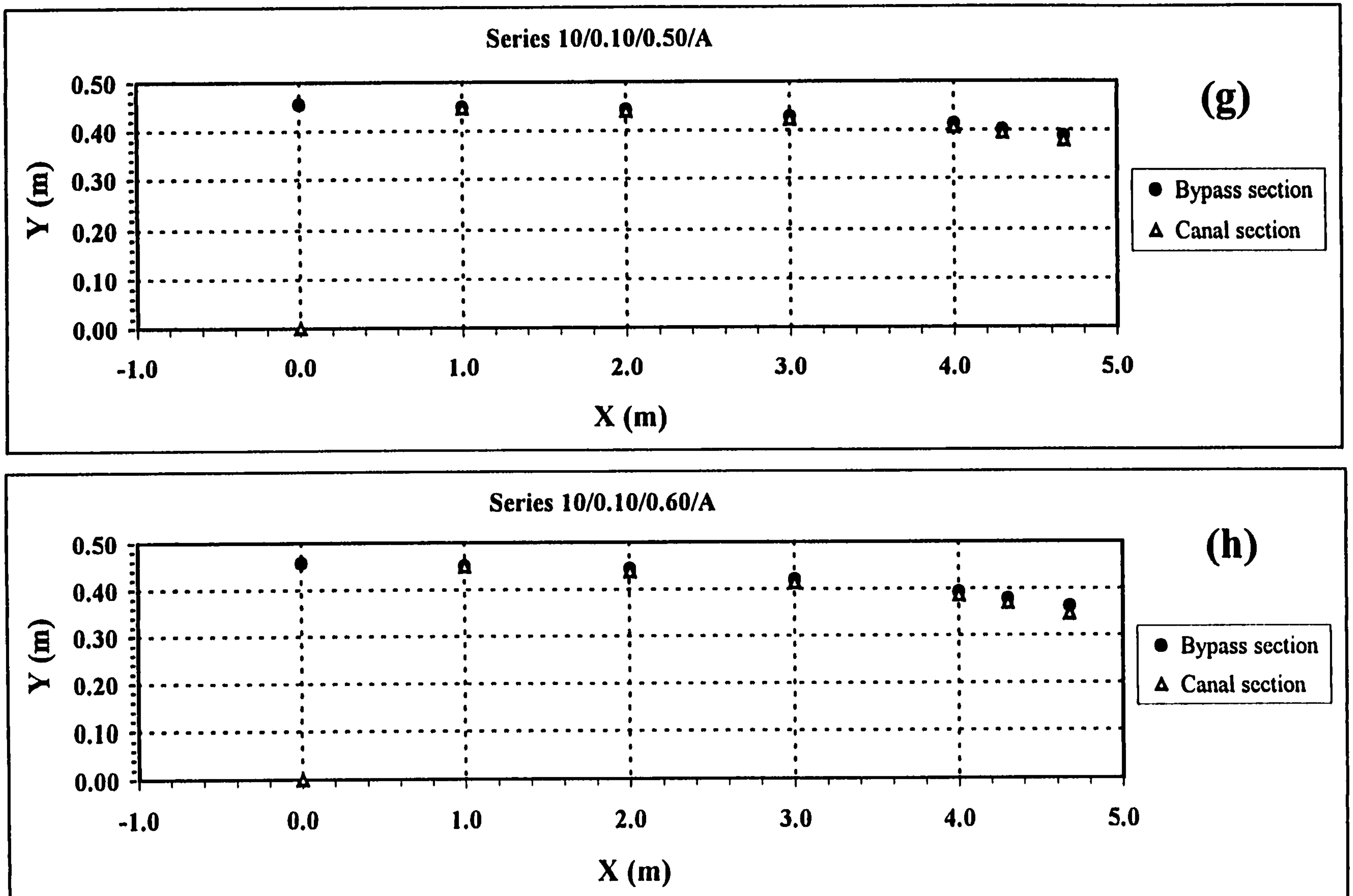

A-2.1(g-h): Depth Profiles of Bypass Section and Canal Section.

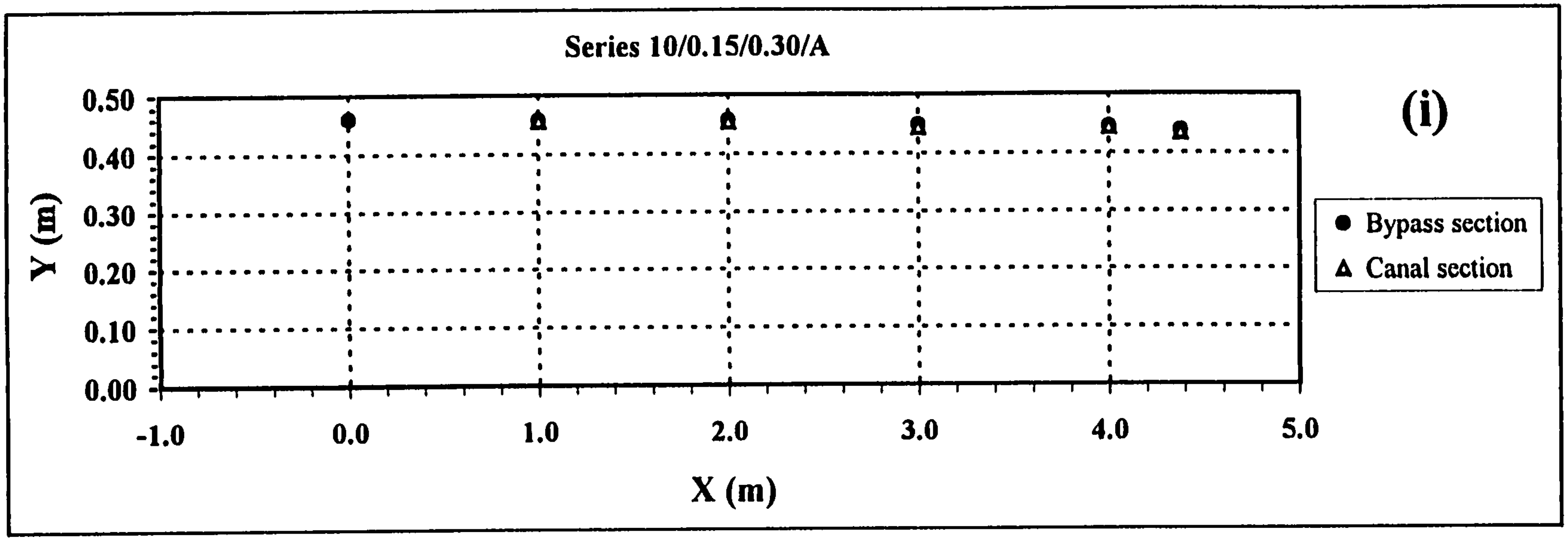

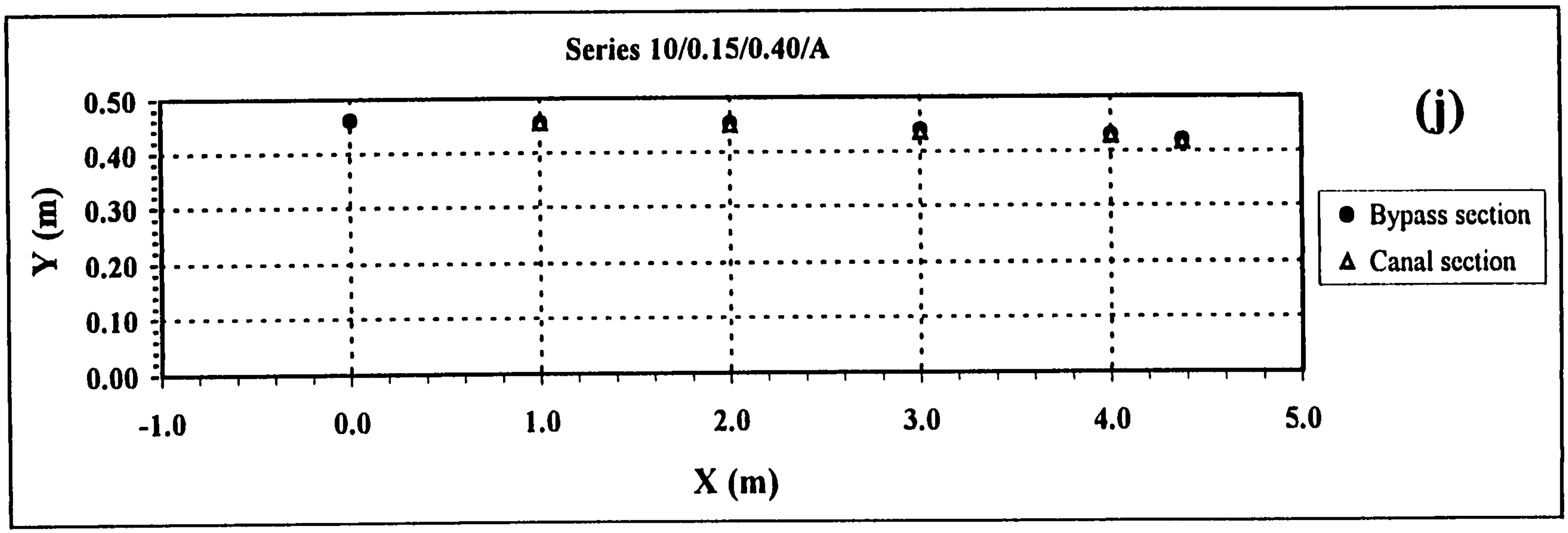

A-2.1(i-j): Depth Profiles of Bypass Section and Canal Section.

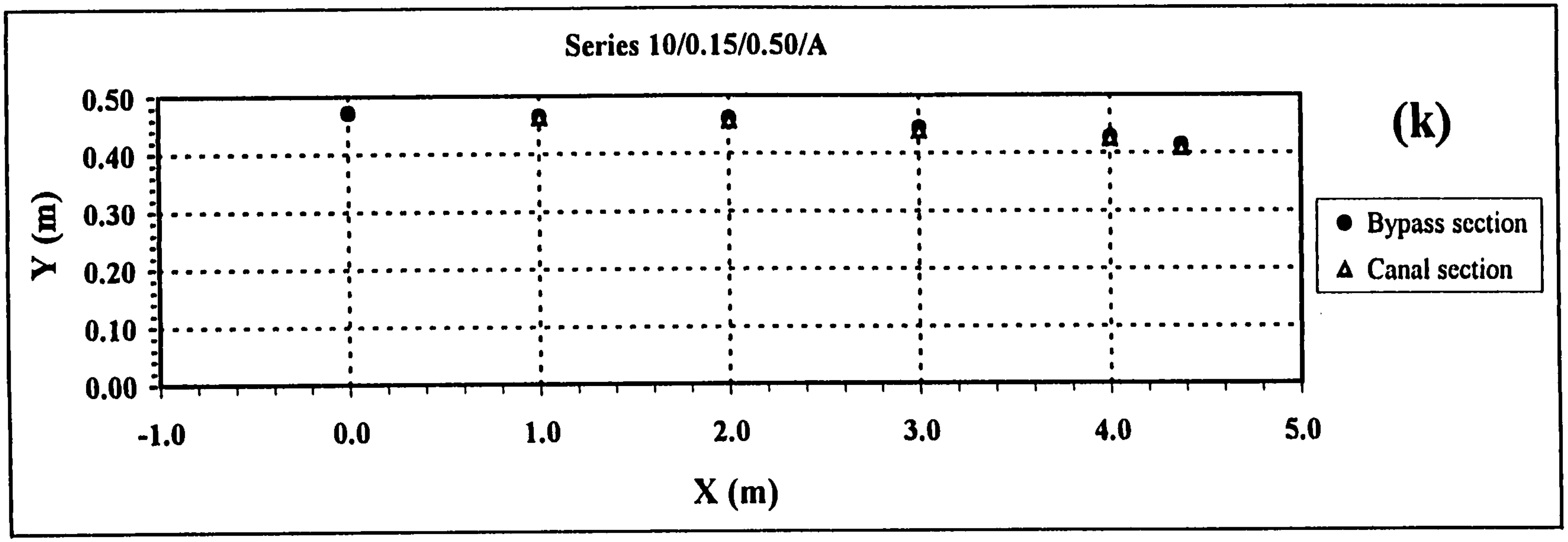

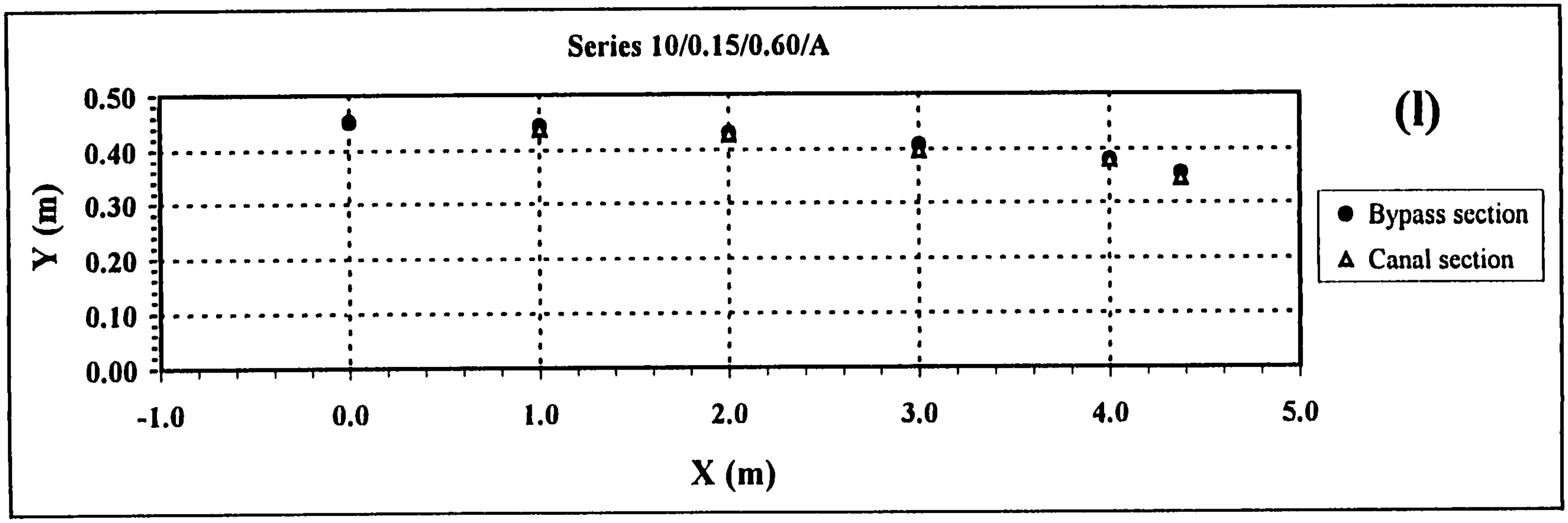

A-2.1(k-l): Depth Profiles of Bypass Section and Canal Section.

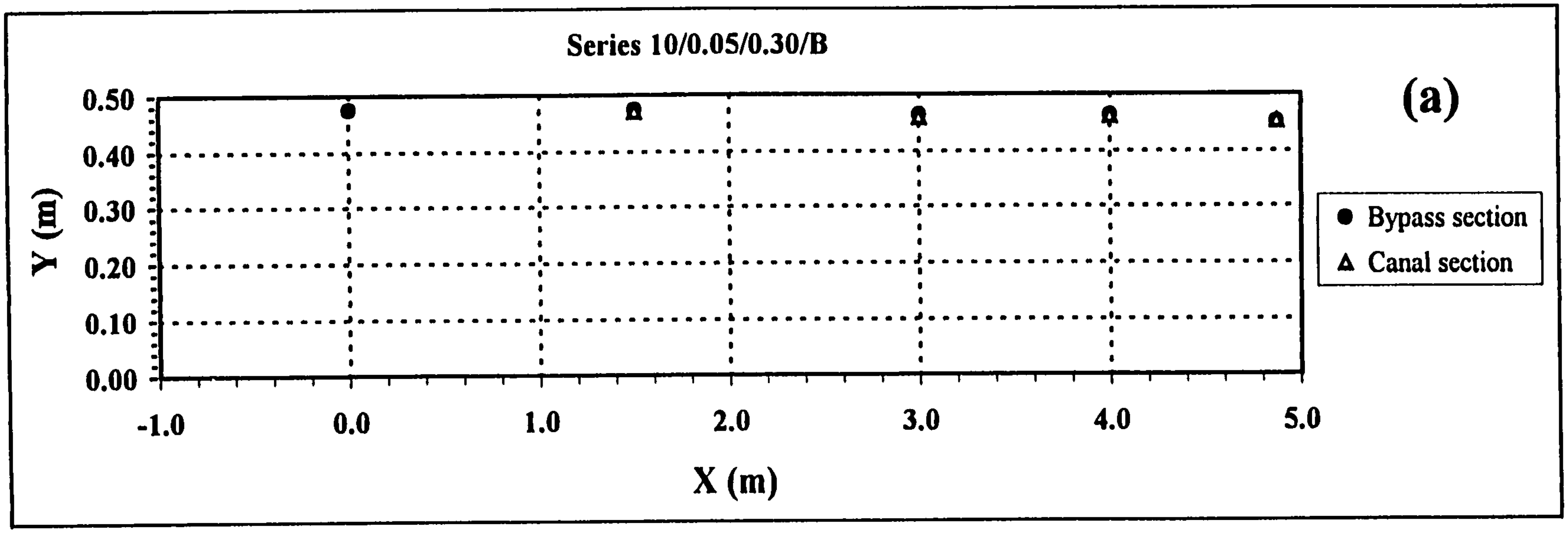

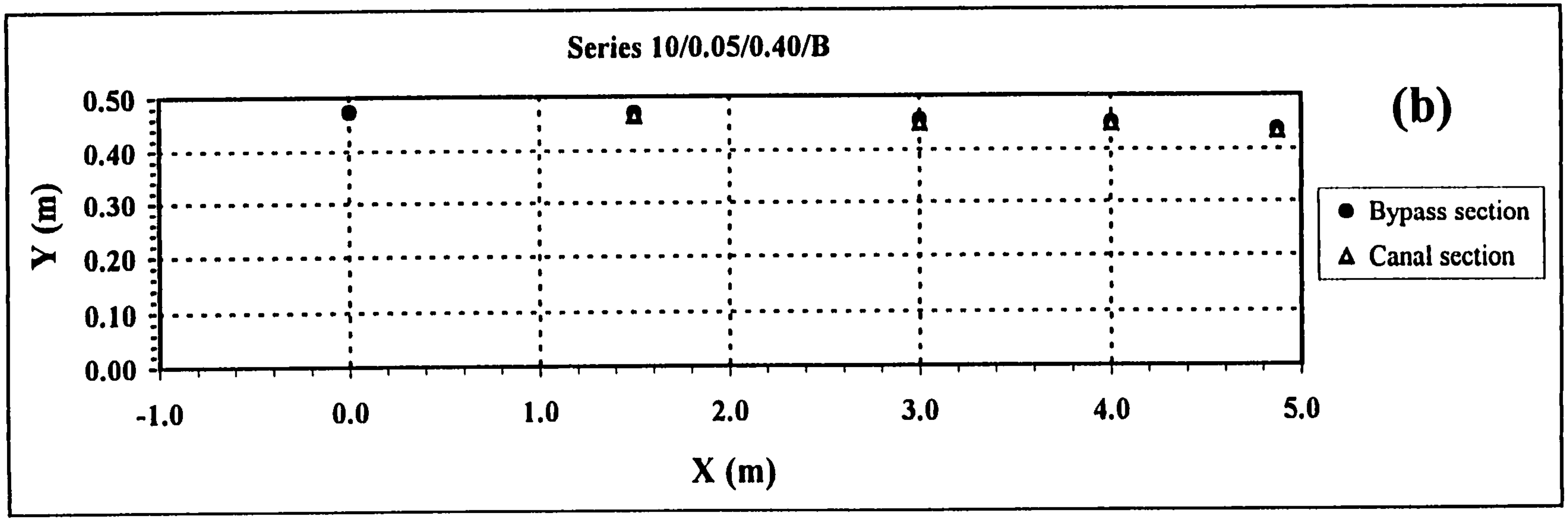

A-2.2(a-b): Depth Profiles of Bypass Section and Canal Section.

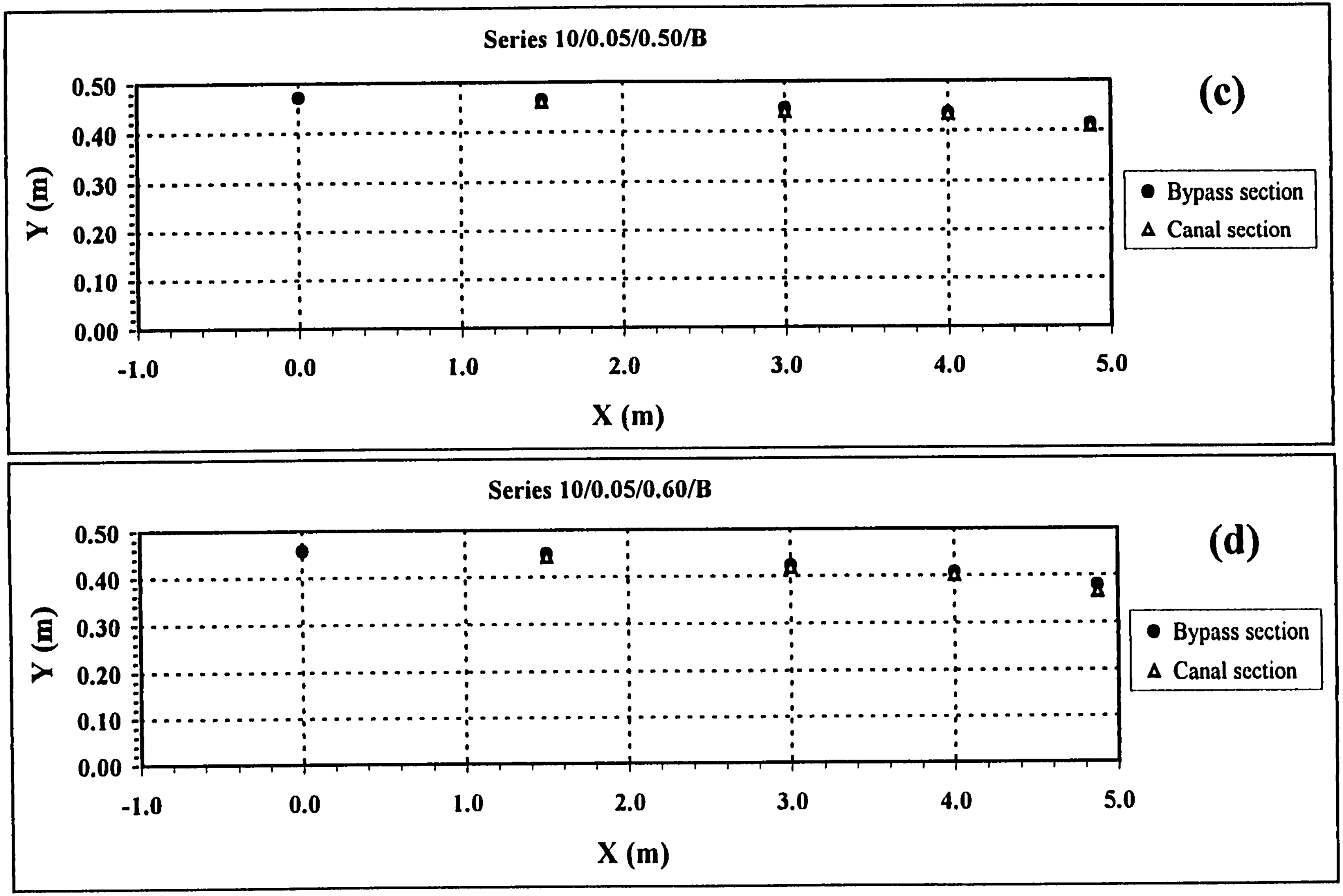

A-2.2(c-d): **Depth Profiles of Bypass Section and Canal Section.**

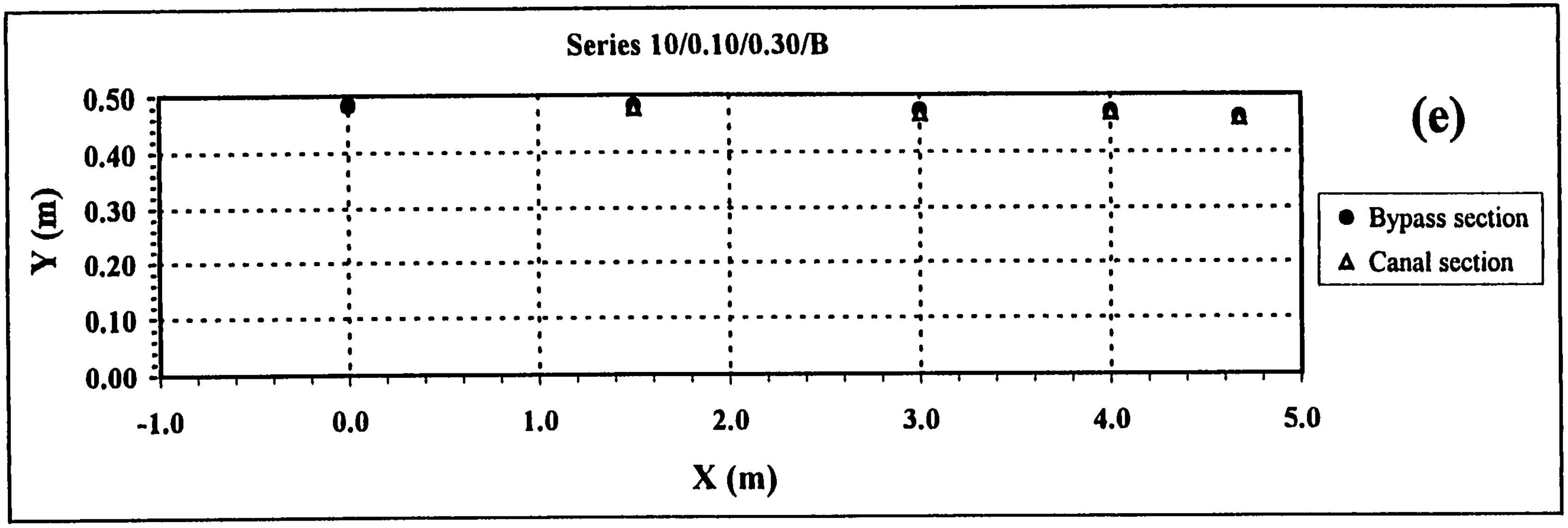

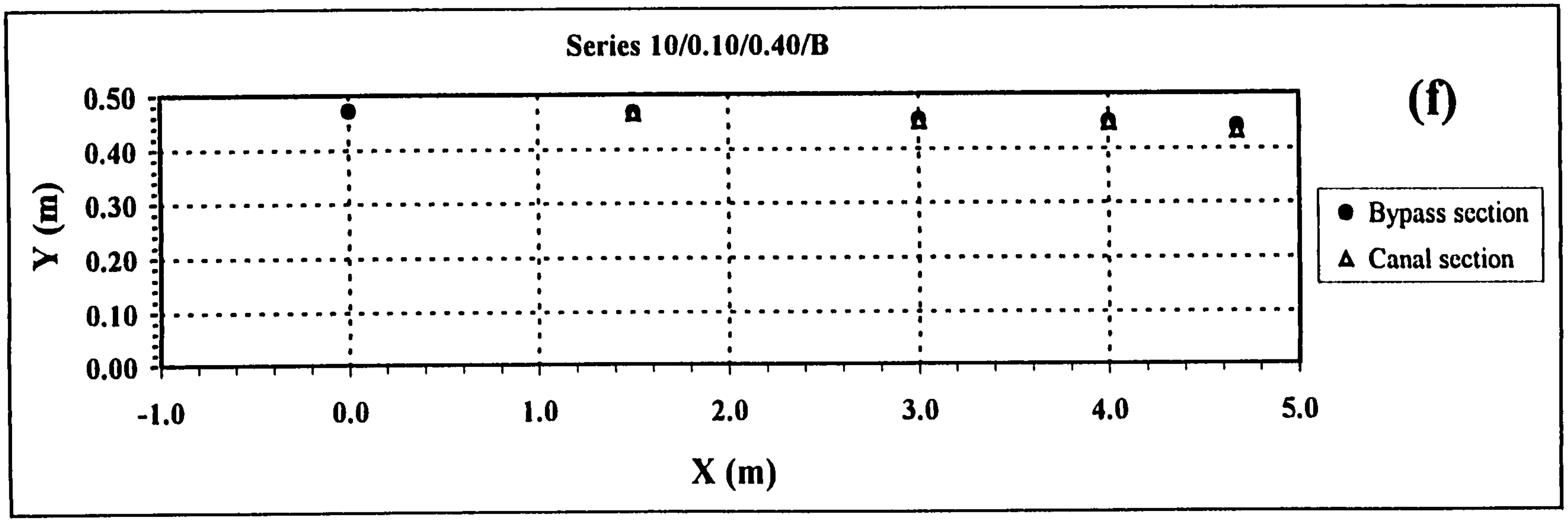

A-2.2(e-f): Depth Profiles of Bypass Section and Canal Section.

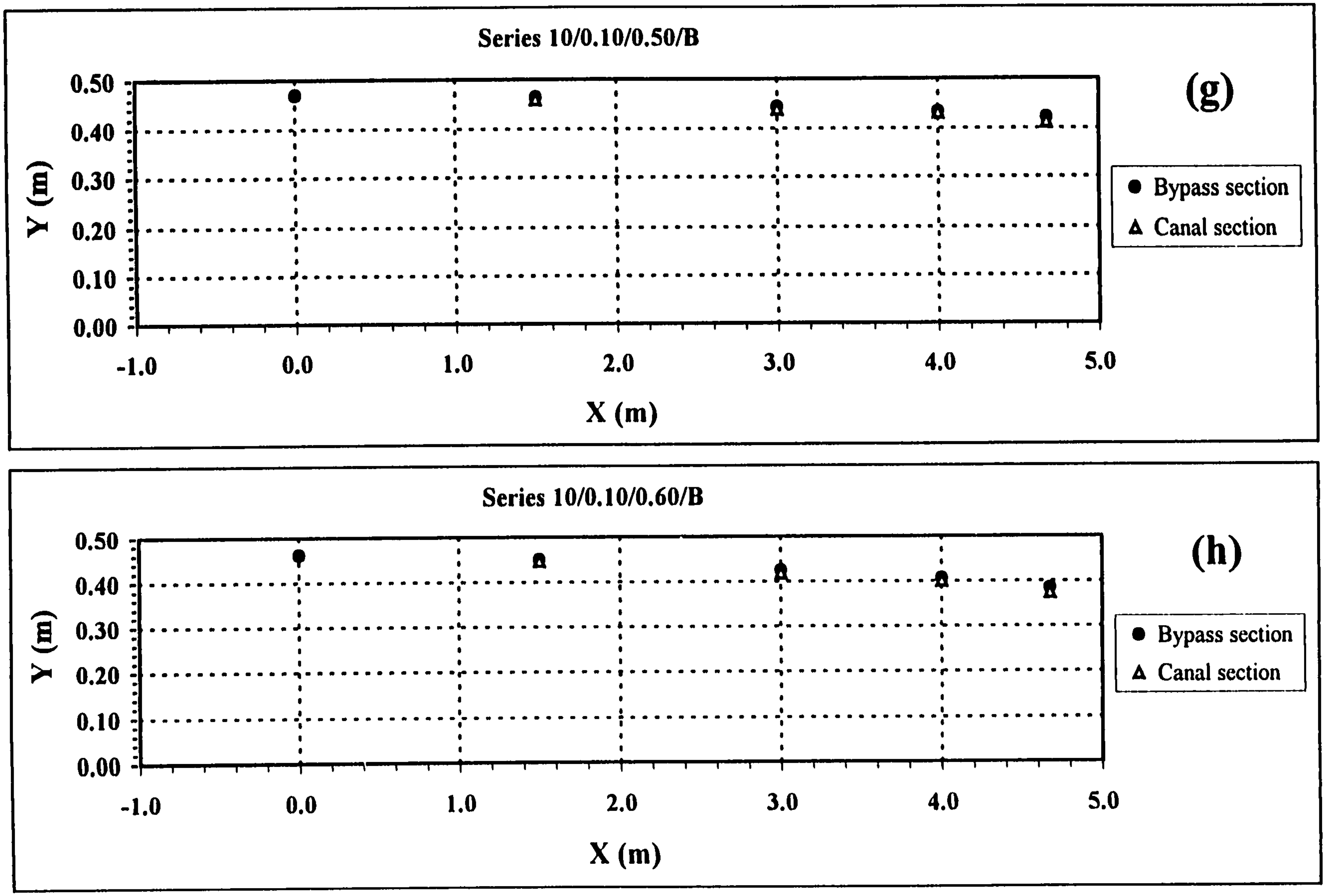

A-2.2(g-h): Depth Profiles of Bypass Section and Canal Section.

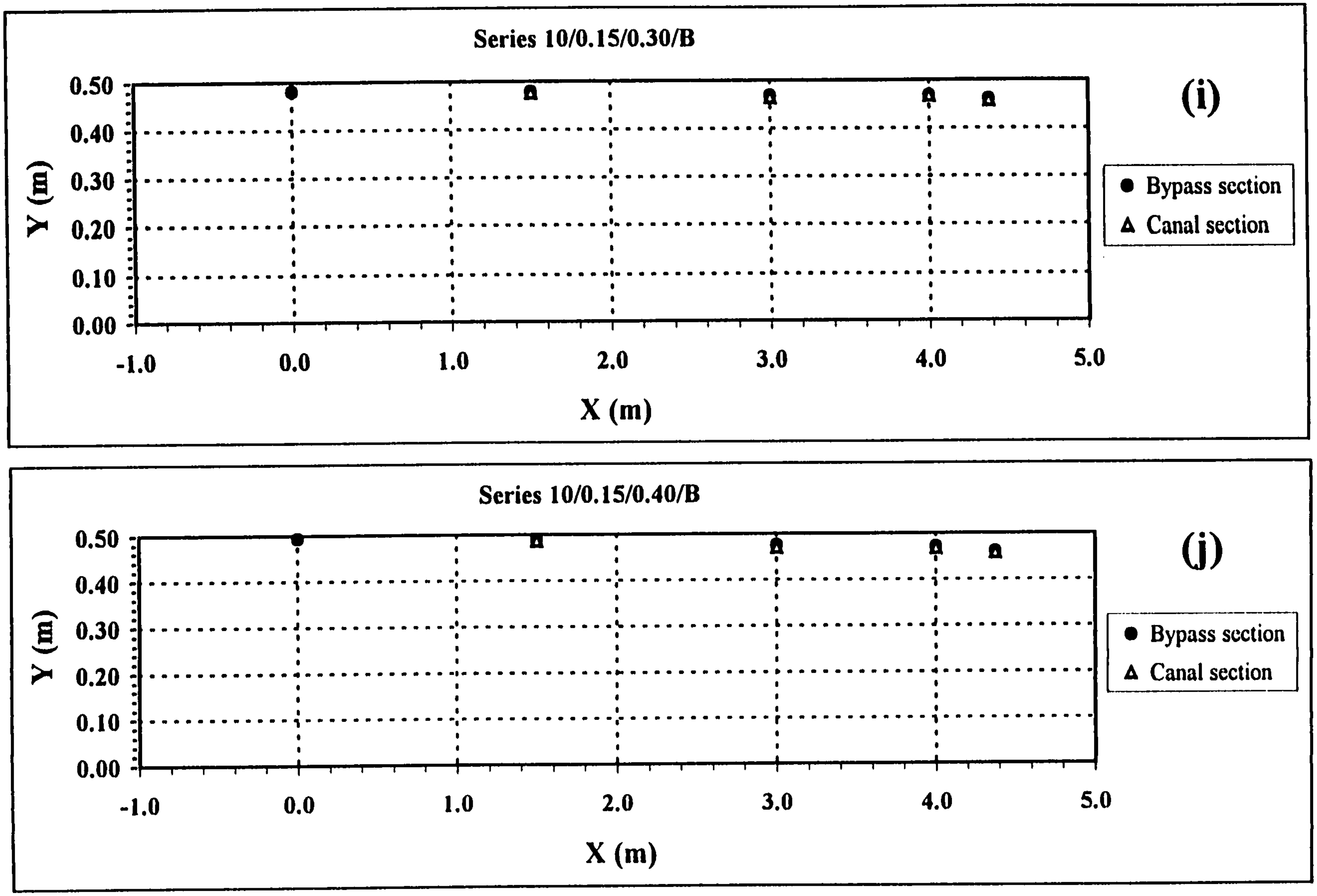

A-2.2(i-j): Depth Profiles of Bypass Section and Canal Section.

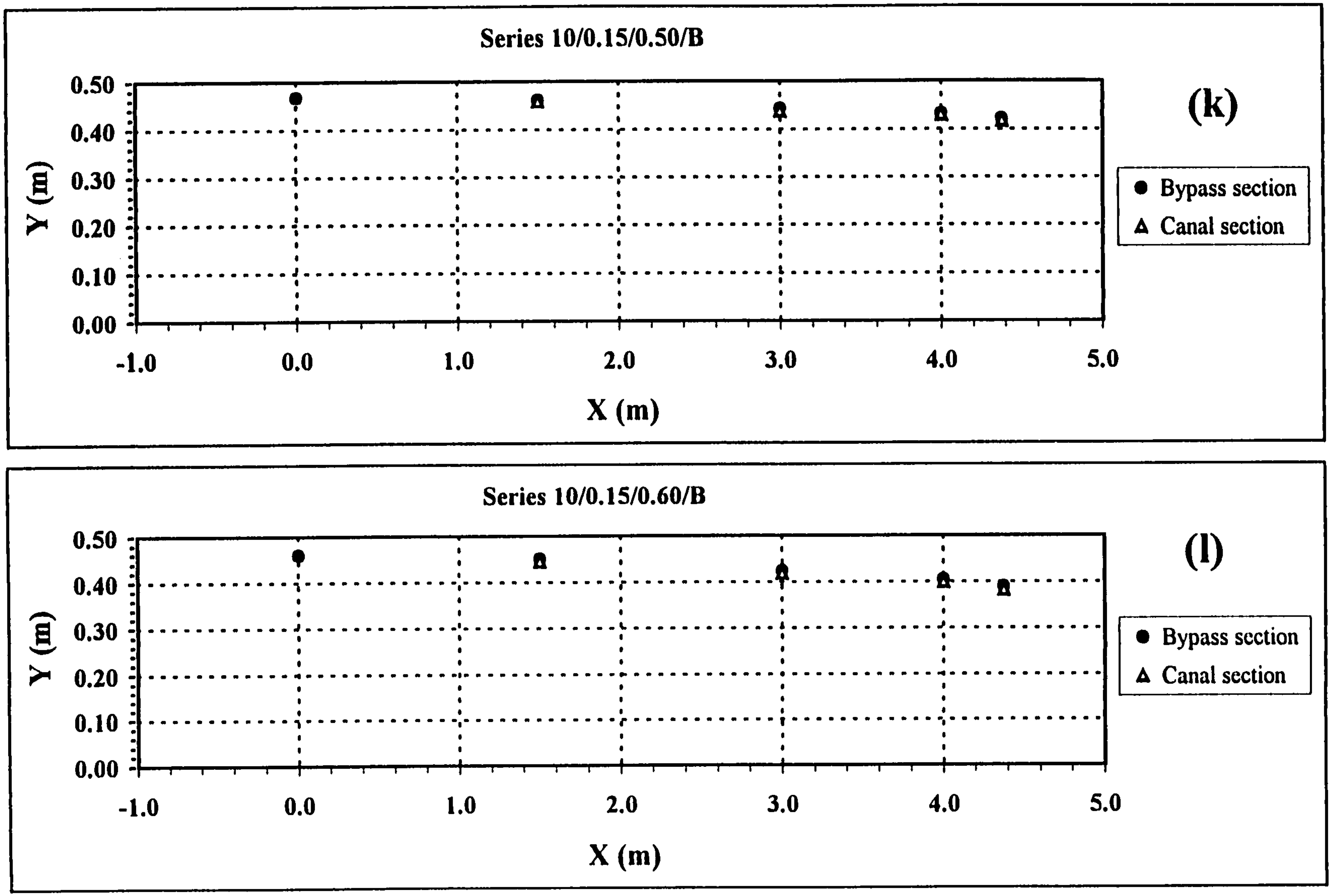

A-2.2(k-l): Depth Profiles of Bypass Section and Canal Section.

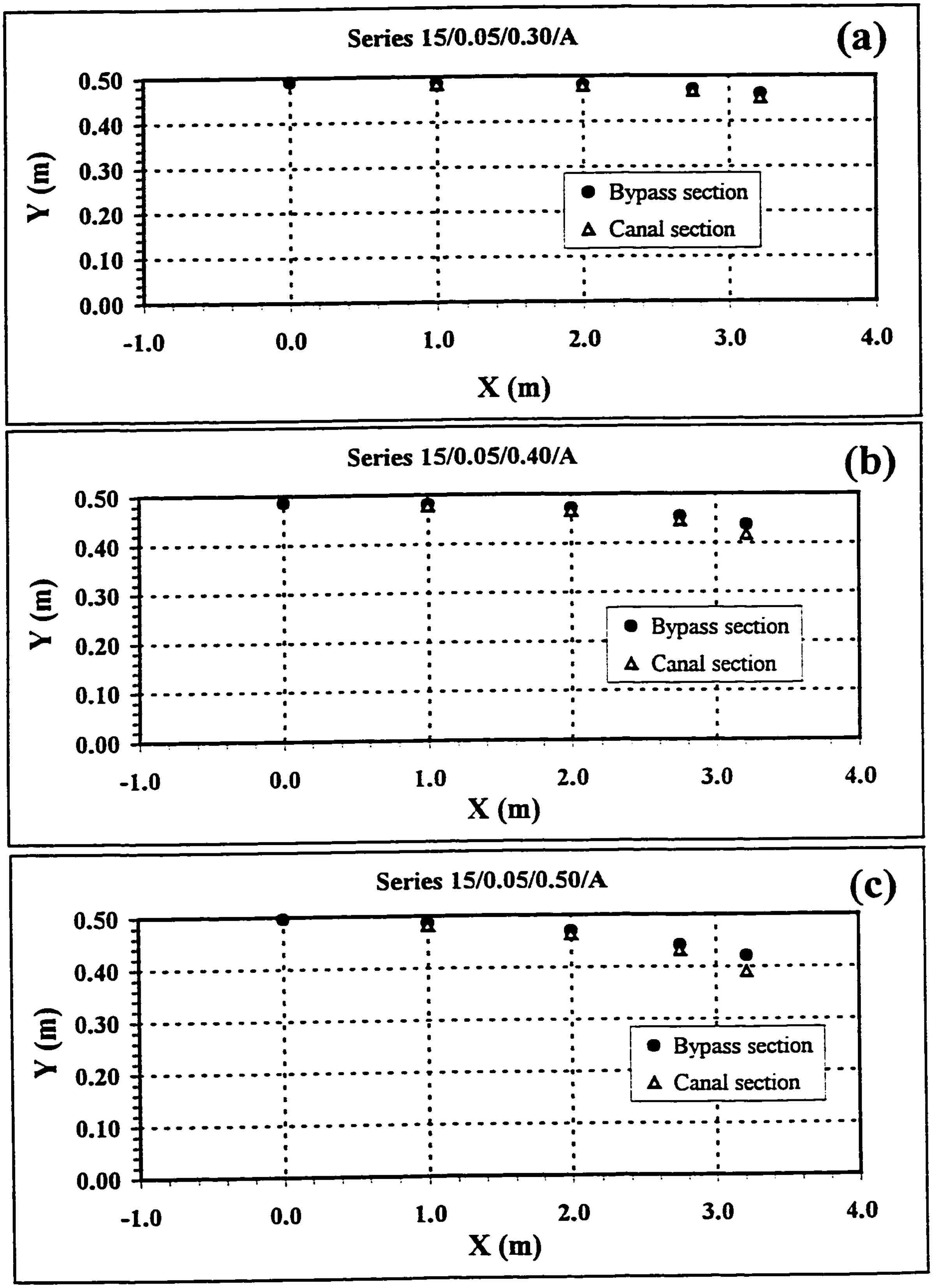

A-2.3(a-c): Depth Profiles of Bypass Section and Canal Section.

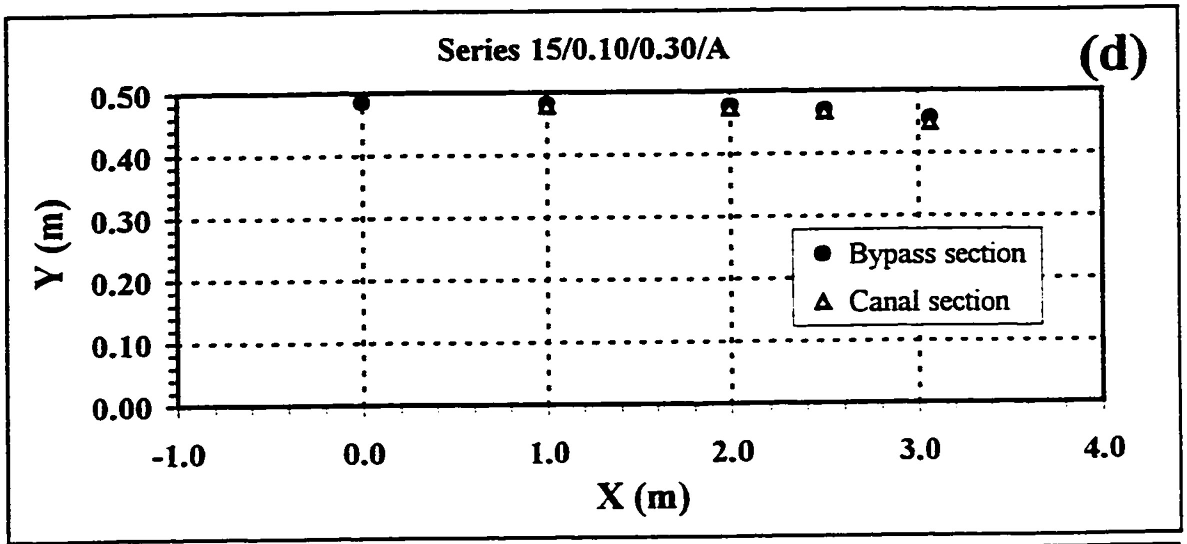

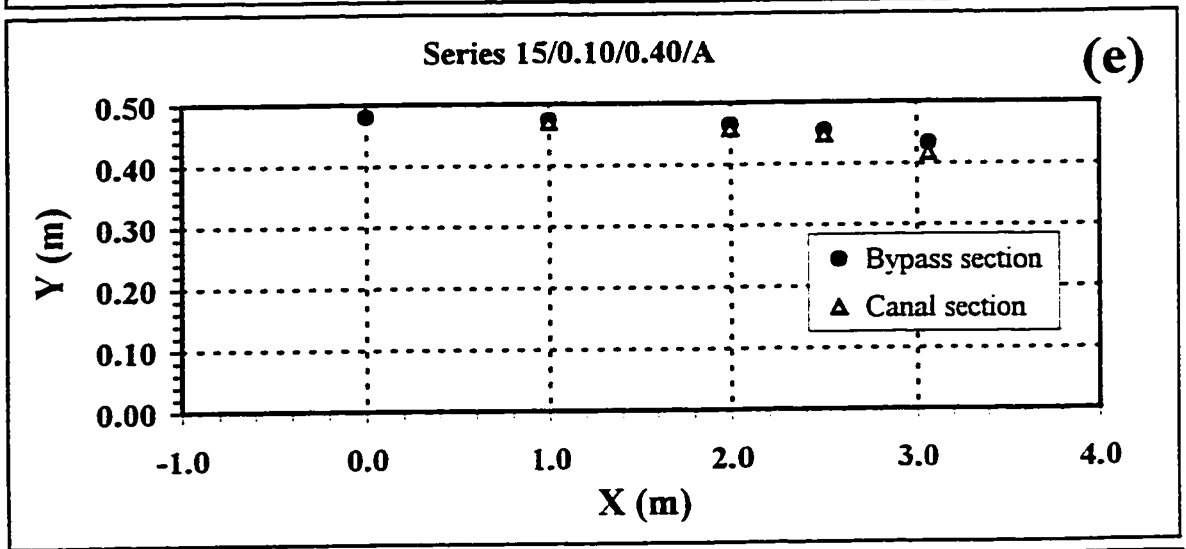

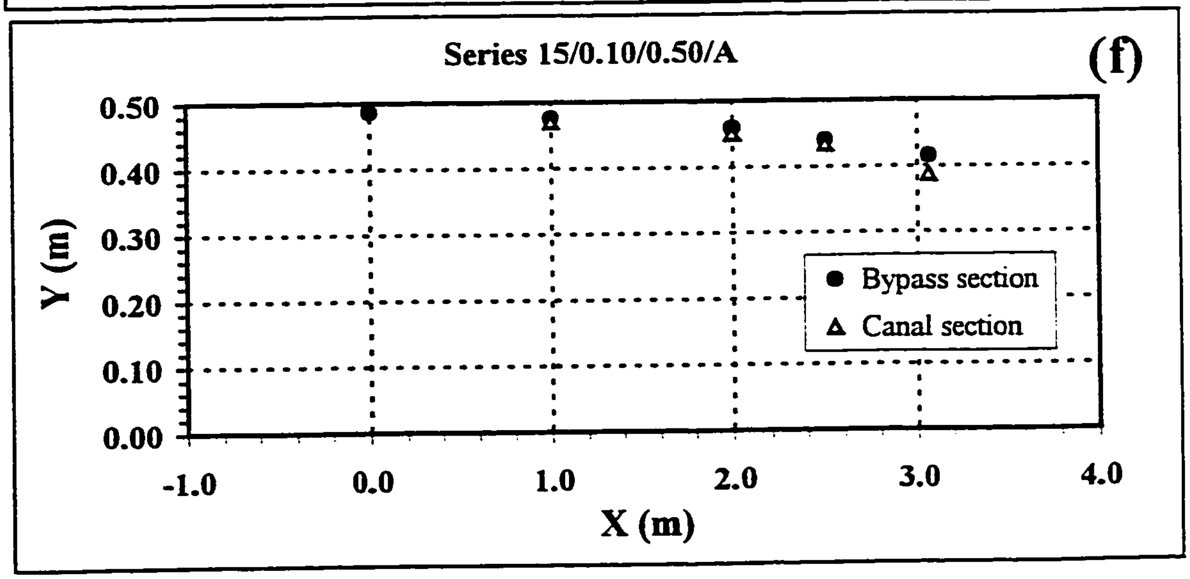

A-2.3(d-f): Depth Profiles of Bypass Section and Canal Section.

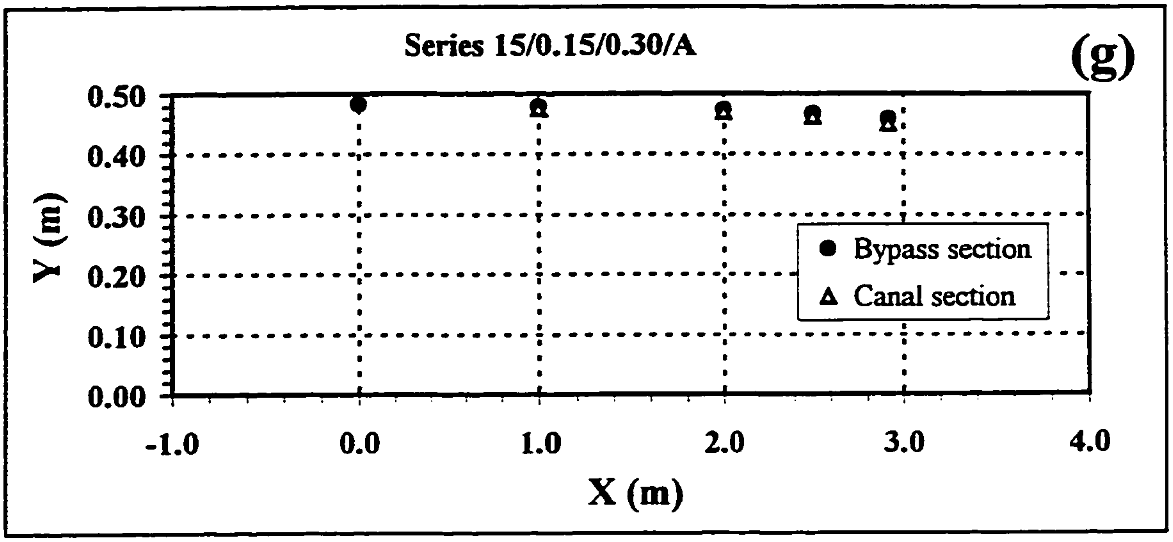

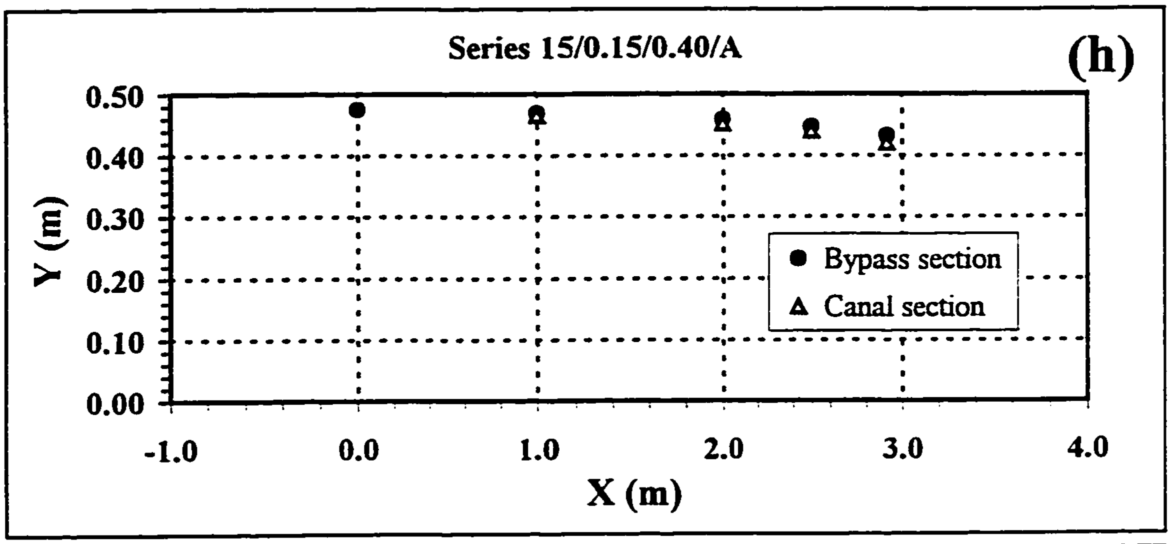

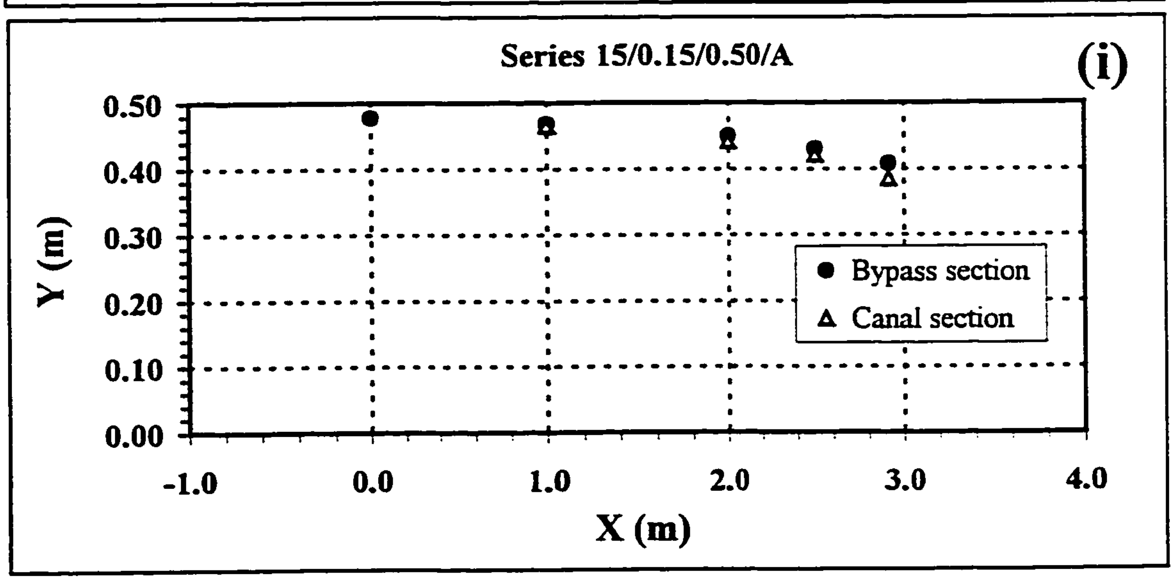

A-2.3(g-i): Depth Profiles of Bypass Section and Canal Section.

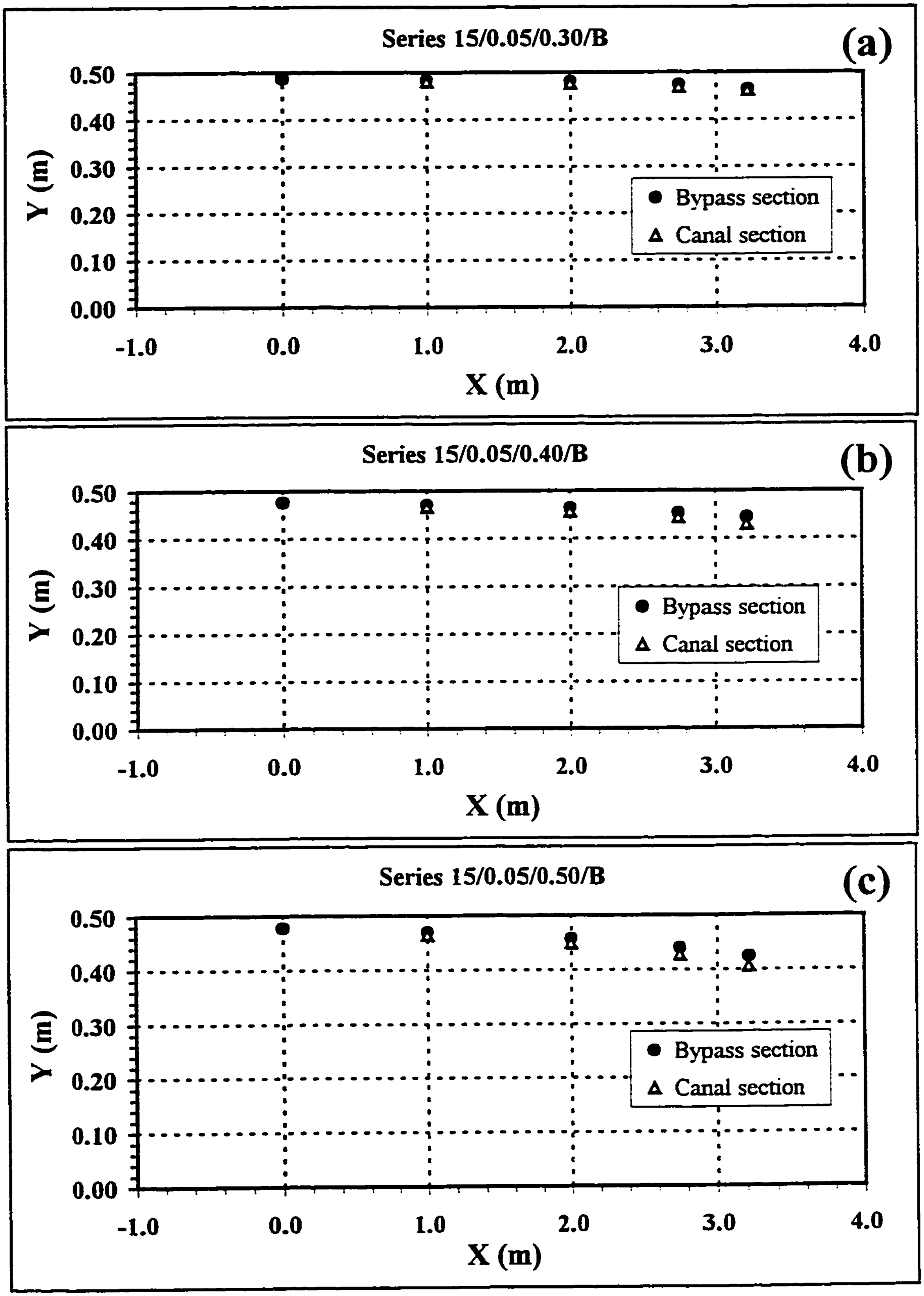

A-2.4(a-c): Depth Profiles of Bypass Section and Canal Section.

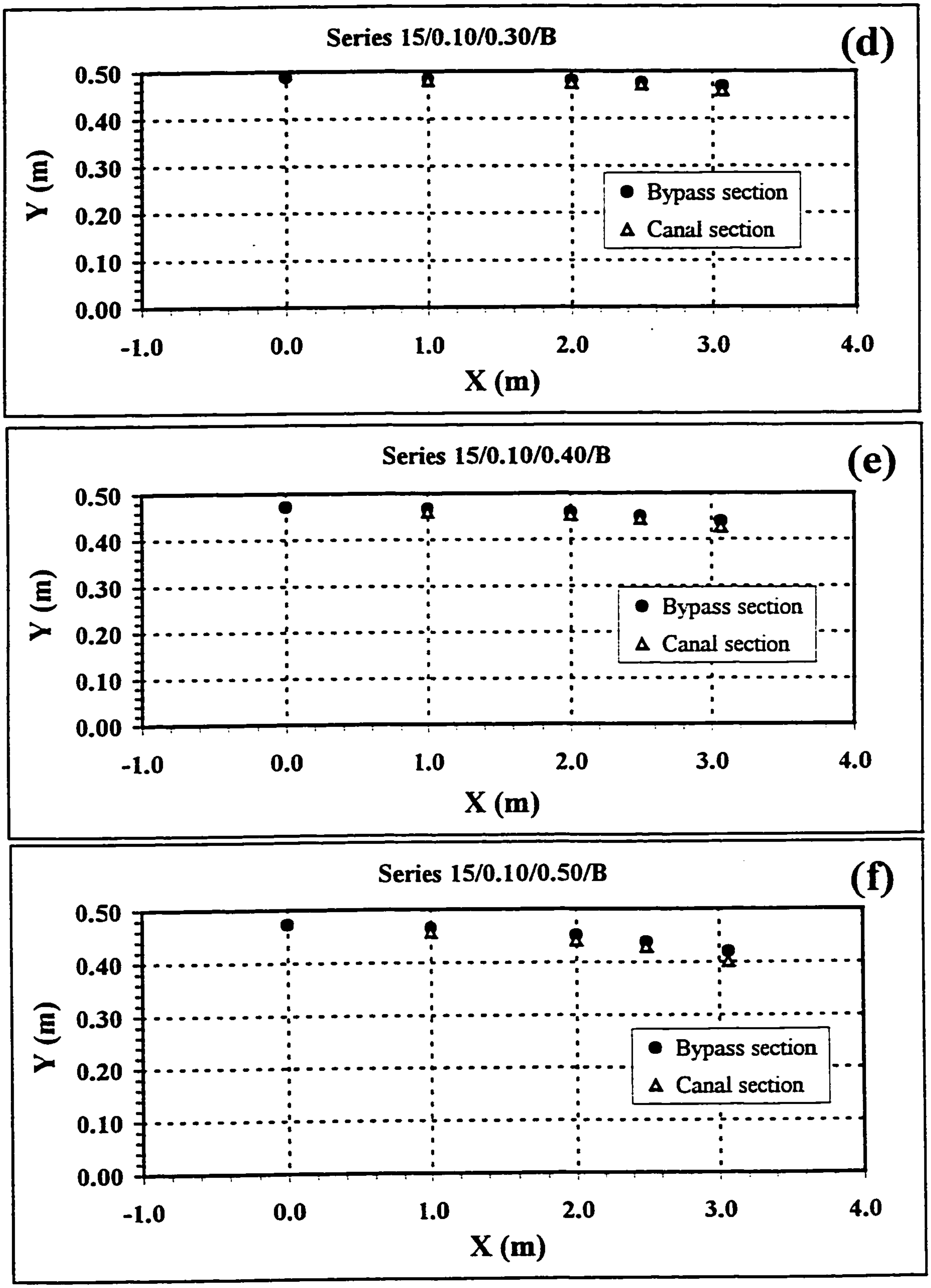

A-2.4(d-f): Depth Profiles of Bypass Section and Canal Section.

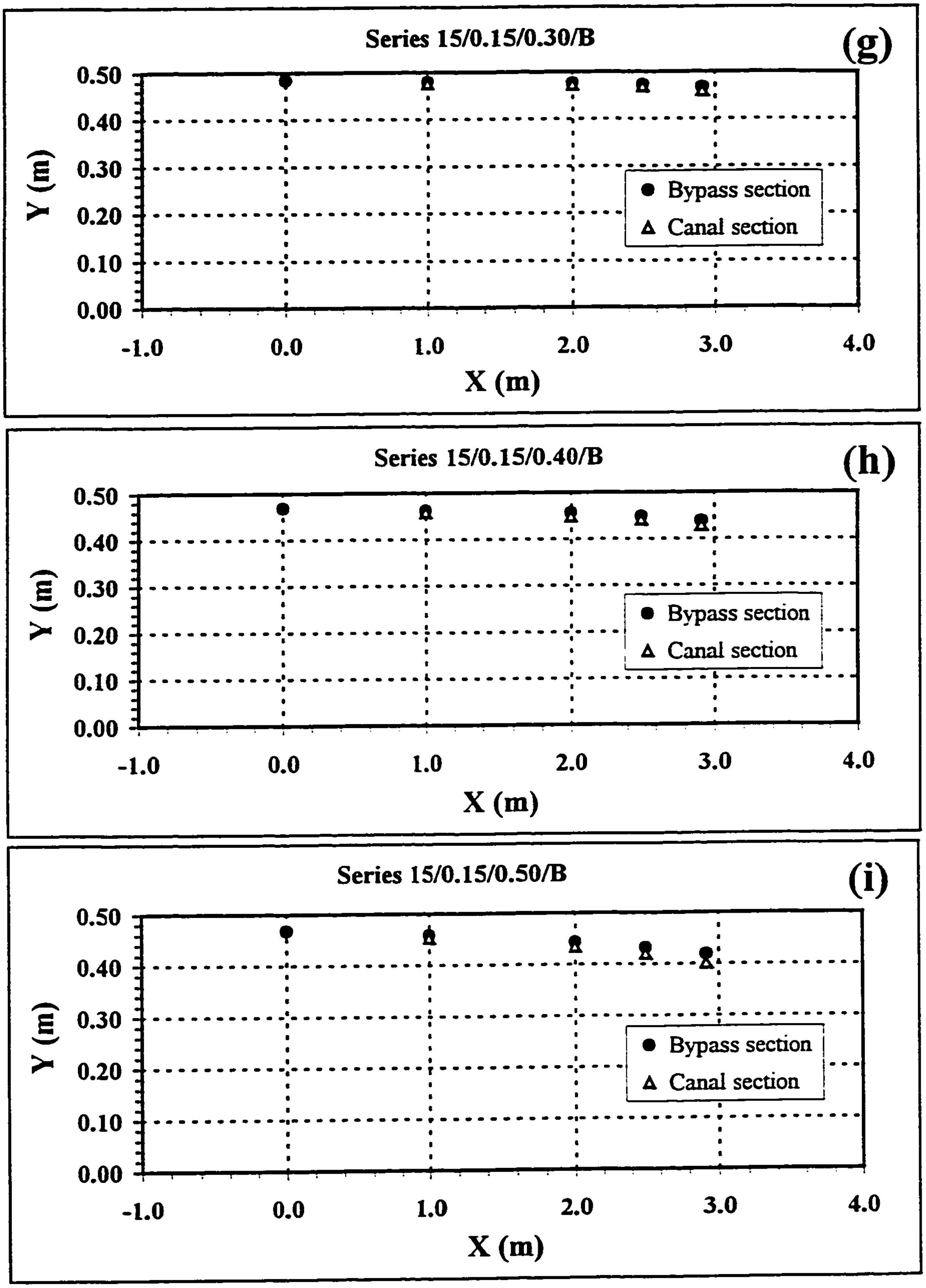

A-2.4(g-i): Depth Profiles of Bypass Section and Canal Section.

A-3

Experimental Data

Table A-3.1: Experimental Flow Depth Data of Louver Array (Series *10/*/*/A*)

LEGEND

- X = horizontal distance (datum = flume entrance)
- Z = transverse location of depth measurement
- bed = point gauge reading at flume bed
- surface = point gauge reading at water surface
- Y/Y_o = normalized flow depth of any measured point
- Y = flow depth of any measured point

NOTE: Canal section flow depths are shown in *ITALICS*.

Test Series	X (m)	Z (m)	bed (cm)	surface (cm)	Y (m)	Y/Y_o
10/0.05/0.30/A	0	0.45	1.33	46.36	0.4503	1.000
	1.0	0.25	1.32	46.11	0.4479	0.995
		0.49	1.47	46.08	0.4461	0.991
		0.84	*1.45*	*45.94*	*0.4449*	*0.988*
	2.0	0.18	1.12	45.69	0.4457	0.990
		0.37	1.10	45.74	0.4464	0.991
		0.71	*1.35*	*45.72*	*0.4437*	*0.985*
		0.80	*1.41*	*45.69*	*0.4428*	*0.983*
	3.0	0.13	1.52	45.11	0.4359	0.968
		0.26	1.56	45.24	0.4368	0.970
		0.58	*1.86*	*44.95*	*0.4309*	*0.957*
		0.74	*1.84*	*44.94*	*0.4310*	*0.957*
	3.5	0.10	1.26	44.85	0.4359	0.968
		0.20	1.23	44.66	0.4343	0.964
		0.53	*1.21*	*44.69*	*0.4348*	*0.966*
		0.71	*1.32*	*44.60*	*0.4328*	*0.961*
	4.0	0.07	1.18	44.40	0.4322	0.960
		0.14	1.15	44.21	0.4306	0.956
		0.47	*0.98*	*44.03*	*0.4305*	*0.956*
		0.69	*1.11*	*44.02*	*0.4291*	*0.953*
	4.5	0.06	1.58	43.94	0.4236	0.941
		0.41	*1.64*	*43.49*	*0.4185*	*0.929*
		0.66	*1.58*	*43.48*	*0.4190*	*0.930*
	4.875	0.025	1.70	43.45	0.4175	0.927
		0.37	*1.28*	*42.62*	*0.4134*	*0.918*
		0.64	*1.33*	*42.92*	*0.4159*	*0.924*
10/0.05/0.40/A	0	0.45	1.48	46.74	0.4526	1.000
	1.0	0.25	1.51	46.36	0.4485	0.991
		0.49	1.64	46.29	0.4465	0.987
		0.84	*1.62*	*46.00*	*0.4438*	*0.981*
	2.0	0.18	1.28	45.73	0.4445	0.982
		0.37	1.25	45.64	0.4439	0.981
		0.71	*1.50*	*45.60*	*0.4410*	*0.974*
		0.80	*1.66*	*45.67*	*0.4401*	*0.972*
	3.0	0.13	1.69	44.73	0.4304	0.951
		0.26	1.74	44.67	0.4293	0.949
		0.58	*2.02*	*44.55*	*0.4253*	*0.940*

Test Series	X (m)	Z (m)	bed (cm)	surface (cm)	Y (m)	Y/Y_o
		0.74	*1.99*	*44.46*	*0.4247*	*0.938*
	3.5	0.10	1.42	44.17	0.4275	0.945
		0.20	1.39	44.21	0.4282	0.946
		0.53	*1.37*	*43.64*	*0.4227*	*0.934*
		0.71	*1.48*	*43.79*	*0.4231*	*0.935*
	4.0	0.07	1.34	43.33	0.4199	0.928
		0.14	1.31	43.28	0.4197	0.927
		0.47	*1.14*	*42.99*	*0.4185*	*0.925*
		0.69	*1.27*	*42.79*	*0.4152*	*0.917*
	4.5	0.06	1.74	42.48	0.4074	0.900
		0.41	*1.80*	*42.05*	*0.4025*	*0.889*
		0.66	*1.74*	*41.68*	*0.3994*	*0.882*
	4.875	0.025	1.86	41.67	0.3981	0.880
		0.37	*1.44*	*39.70*	*0.3826*	*0.845*
		0.64	*1.49*	*40.43*	*0.3894*	*0.860*
10/0.05/0.50/A	0	0.45	1.33	43.92	0.4259	1.000
	1.0	0.25	1.32	43.45	0.4213	0.989
		0.49	*1.47*	*43.36*	*0.4189*	*0.984*
		0.84	*1.45*	*43.22*	*0.4177*	*0.981*
	2.0	0.18	1.12	42.49	0.4137	0.971
		0.37	1.10	42.58	0.4148	0.974
		0.71	*1.35*	*42.32*	*0.4097*	*0.962*
		0.80	*1.41*	*42.22*	*0.4081*	*0.958*
	3.0	0.13	1.52	40.99	0.3947	0.927
		0.26	1.56	40.88	0.3932	0.923
		0.58	*1.86*	*40.55*	*0.3869*	*0.908*
		0.74	*1.84*	*40.47*	*0.3863*	*0.907*
	3.5	0.10	1.26	40.22	0.3896	0.915
		0.20	1.23	39.91	0.3868	0.908
		0.53	*1.21*	*39.44*	*0.3823*	*0.898*
		0.71	*1.32*	*39.32*	*0.3800*	*0.892*
	4.0	0.07	1.18	38.73	0.3755	0.882
		0.14	1.15	38.79	0.3764	0.884
		0.47	*0.98*	*37.83*	*0.3685*	*0.865*
		0.69	*1.11*	*37.82*	*0.3671*	*0.862*
	4.5	0.06	1.58	37.12	0.3554	0.834
		0.41	*1.64*	*36.22*	*0.3458*	*0.812*
		0.66	*1.58*	*36.04*	*0.3446*	*0.809*
	4.875	0.025	1.70	35.64	0.3394	0.797
		0.37	*1.28*	*33.34*	*0.3206*	*0.753*
		0.64	*1.33*	*34.40*	*0.3307*	*0.776*
10/0.05/0.60/A	0	0.45	1.33	47.94	0.4661	1.000
	1.0	0.25	1.32	47.28	0.4596	0.986
		0.49	1.47	47.23	0.4576	0.982
		0.84	*1.45*	*47.18*	*0.4573*	*0.981*
	2.0	0.18	1.12	46.02	0.4490	0.963
		0.37	1.10	46.09	0.4499	0.965
		0.71	*1.35*	*45.63*	*0.4428*	*0.950*
		0.80	*1.41*	*45.79*	*0.4438*	*0.952*
	3.0	0.13	1.52	44.26	0.4274	0.917
		0.26	1.56	44.27	0.4271	0.916
		0.58	*1.86*	*43.68*	*0.4182*	*0.897*

Test Series	X (m)	Z (m)	bed (cm)	surface (cm)	Y (m)	Y/Y$_o$
		0.74	*1.84*	*43.85*	*0.4201*	*0.901*
	3.5	0.10	1.26	42.99	0.4173	0.895
		0.20	1.23	42.92	0.4169	0.894
		0.53	*1.21*	*42.32*	*0.4111*	*0.882*
		0.71	*1.32*	*42.46*	*0.4114*	*0.883*
	4.0	0.07	1.18	41.32	0.4014	0.861
		0.14	1.15	41.58	0.4043	0.867
		0.47	*0.98*	*40.63*	*0.3965*	*0.851*
		0.69	*1.11*	*40.63*	*0.3952*	*0.848*
	4.5	0.06	1.58	38.98	0.3740	0.802
		0.41	*1.64*	*37.99*	*0.3635*	*0.780*
		0.66	*1.58*	*38.25*	*0.3667*	*0.787*
	4.875	0.025	1.70	37.75	0.3605	0.773
		0.37	*1.28*	*35.02*	*0.3374*	*0.724*
		0.64	*1.33*	*35.76*	*0.3443*	*0.739*
10/0.10/0.30/A	0	0.45	1.34	45.79	0.4445	1.000
	1.0	0.25	1.32	45.80	0.4448	1.001
		0.49	1.47	45.54	0.4407	0.991
		0.84	*1.45*	*45.57*	*0.4412*	0.993
	2.0	0.18	1.12	45.32	0.4420	0.994
		0.37	1.10	45.23	0.4413	0.993
		0.71	*1.35*	*45.21*	*0.4386*	0.987
		0.80	*1.41*	*45.23*	*0.4382*	0.986
	3.0	0.13	1.52	44.70	0.4318	0.971
		0.26	1.56	44.67	0.4311	0.970
		0.58	*1.86*	*44.44*	*0.4258*	0.958
		0.74	*1.84*	*44.59*	*0.4275*	0.962
	4.0	0.07	1.18	43.94	0.4276	0.962
		0.14	1.15	43.82	0.4267	0.960
		0.47	*0.98*	*43.73*	*0.4275*	0.962
		0.69	*1.11*	*43.48*	*0.4237*	0.953
	4.3	0.08	1.44	43.64	0.4220	0.949
		0.43	*1.37*	*43.36*	*0.4199*	0.945
		0.68	*1.48*	*43.30*	*0.4182*	0.941
	4.625	0.05	1.66	43.28	0.4162	0.936
		0.40	*1.67*	*42.47*	*0.4080*	0.918
		0.66	*1.65*	*42.74*	*0.4109*	0.924
10/0.10/0.40/A	0	0.45	1.33	46.90	0.4557	1.000
	1.0	0.25	1.32	46.48	0.4516	0.991
		0.49	1.47	46.47	0.4500	0.987
		0.84	*1.45*	*46.24*	*0.4479*	0.983
	2.0	0.18	1.12	45.92	0.4480	0.983
		0.37	1.10	45.85	0.4475	0.982
		0.71	*1.35*	*45.83*	*0.4448*	0.976
		0.80	*1.41*	*45.96*	*0.4455*	0.978
	3.0	0.13	1.52	44.88	0.4336	0.952
		0.26	1.56	44.99	0.4343	0.953
		0.58	*1.86*	*44.70*	*0.4284*	0.940
		0.74	*1.84*	*44.74*	*0.4290*	0.941
	4.0	0.07	1.18	43.61	0.4243	0.931

Test Series	X (m)	Z (m)	bed (cm)	surface (cm)	Y (m)	Y/Y_o
		0.14	1.15	43.64	0.4249	0.932
		0.47	*0.98*	*43.17*	*0.4219*	0.926
		0.69	*1.11*	*43.04*	*0.4193*	0.920
	4.3	0.08	1.44	43.15	0.4171	0.915
		0.43	*1.37*	*42.58*	*0.4121*	0.904
		0.68	*1.48*	*42.48*	*0.4100*	0.900
	4.625	0.05	1.66	42.34	0.4068	0.893
		0.40	*1.67*	*41.45*	*0.3978*	0.873
		0.66	*1.65*	*41.78*	*0.4013*	0.881
10/0.10/0.50/A	0	0.45	1.33	46.82	0.4549	1.000
	1.0	0.25	1.32	46.23	0.4491	0.987
		0.49	1.47	46.25	0.4478	0.984
		0.84	*1.45*	*45.98*	*0.4453*	0.979
	2.0	0.18	1.12	45.35	0.4423	0.972
		0.37	1.10	45.44	0.4434	0.975
		0.71	*1.35*	*45.27*	*0.4392*	0.965
		0.80	*1.41*	*45.24*	*0.4383*	0.964
	3.0	0.13	1.52	44.25	0.4273	0.939
		0.26	1.56	44.20	0.4264	0.937
		0.58	*1.86*	*44.01*	*0.4215*	0.927
		0.74	*1.84*	*43.98*	*0.4214*	0.926
	4.0	0.07	1.18	42.32	0.4114	0.904
		0.14	1.15	42.39	0.4124	0.907
		0.47	*0.98*	*41.42*	*0.4044*	0.889
		0.69	*1.11*	*41.74*	*0.4063*	0.893
	4.3	0.08	1.44	41.46	0.4002	0.880
		0.43	*1.37*	*40.94*	*0.3957*	0.870
		0.68	*1.48*	*40.66*	*0.3918*	0.861
	4.625	0.05	1.66	40.39	0.3873	0.851
		0.40	*1.67*	*39.37*	*0.3770*	0.829
		0.66	*1.65*	*39.73*	*0.3808*	0.837
10/0.10/0.60/A	0	0.45	1.33	47.00	0.4567	1.000
	1.0	0.25	1.32	46.23	0.4491	0.983
		0.49	1.47	46.36	0.4489	0.983
		0.84	*1.45*	*46.29*	*0.4484*	0.982
	2.0	0.18	1.12	45.41	0.4429	0.970
		0.37	1.10	45.41	0.4431	0.970
		0.71	*1.35*	*45.10*	*0.4375*	0.958
		0.80	*1.41*	*45.19*	*0.4378*	0.959
	3.0	0.13	1.52	43.47	0.4195	0.919
		0.26	1.56	43.47	0.4191	0.918
		0.58	*1.86*	*43.13*	*0.4127*	0.904
		0.74	*1.84*	*43.01*	*0.4117*	0.901
	4.0	0.07	1.18	40.44	0.3926	0.860
		0.14	1.15	40.32	0.3917	0.858
		0.47	*0.98*	*39.56*	*0.3858*	0.845
		0.69	*1.11*	*39.64*	*0.3853*	0.844
	4.3	0.08	1.44	39.17	0.3773	0.826
		0.43	*1.37*	*38.30*	*0.3693*	0.809

Test Series	X (m)	Z (m)	bed (cm)	surface (cm)	Y (m)	Y/Y$_o$
		0.68	*1.48*	*38.32*	*0.3684*	0.807
	4.625	0.05	1.66	37.84	0.3618	0.792
		0.40	*1.67*	*35.83*	*0.3416*	0.748
		0.66	*1.65*	*36.44*	*0.3479*	0.762
10/0.15/0.30/A	0	0.45	1.33	47.36	0.4603	1.000
	1.0	0.25	1.32	47.19	0.4587	0.997
		0.49	1.47	47.22	0.4575	0.994
		0.84	*1.45*	*47.04*	*0.4559*	0.990
	2.0	0.18	1.12	46.86	0.4574	0.994
		0.37	1.10	46.86	0.4576	0.994
		0.71	*1.35*	*46.79*	*0.4544*	0.987
		0.80	*1.41*	*46.81*	*0.4540*	0.986
	3.0	0.13	1.52	46.36	0.4484	0.974
		0.26	1.56	46.36	0.4480	0.973
		0.58	*1.86*	*46.24*	*0.4438*	0.964
		0.74	*1.84*	*46.08*	*0.4424*	0.961
	4.0	0.07	1.18	45.62	0.4444	0.965
		0.14	1.15	45.64	0.4449	0.967
		0.47	*0.98*	*45.39*	*0.4441*	0.965
		0.69	*1.11*	*45.34*	*0.4423*	0.961
	4.375	0.075	1.58	45.39	0.4381	0.952
		0.43	*1.58*	*44.82*	*0.4324*	0.939
		0.67	*1.56*	*45.01*	*0.4345*	0.944
10/0.15/0.40/A	0	0.45	1.34	47.36	0.4602	1.000
	1.0	0.25	1.32	46.97	0.4565	0.992
		0.49	1.47	46.86	0.4539	0.986
		0.84	*1.45*	*46.83*	*0.4538*	0.986
	2.0	0.18	1.12	46.37	0.4525	0.983
		0.37	1.10	46.26	0.4516	0.981
		0.71	*1.35*	*46.19*	*0.4484*	0.974
		0.80	*1.41*	*46.11*	*0.4470*	0.971
	3.0	0.13	1.52	45.37	0.4385	0.953
		0.26	1.56	45.45	0.4389	0.954
		0.58	*1.86*	*45.15*	*0.4329*	0.941
		0.74	*1.84*	*45.28*	*0.4344*	0.944
	4.0	0.07	1.18	44.18	0.4300	0.934
		0.14	1.15	44.03	0.4288	0.932
		0.47	*0.98*	*43.73*	*0.4275*	0.929
		0.69	*1.11*	*43.64*	*0.4253*	0.924
	4.375	0.075	1.58	43.51	0.4193	0.911
		0.43	*1.58*	*43.10*	*0.4152*	0.902
		0.67	*1.56*	*43.07*	*0.4151*	0.902
10/0.15/0.50/A	0	0.45	1.34	48.47	0.4713	1.000
	1.0	0.25	1.32	47.99	0.4667	0.990
		0.49	1.47	47.90	0.4643	0.985
		0.84	*1.45*	*47.74*	*0.4629*	0.982
	2.0	0.18	1.12	47.10	0.4598	0.976
		0.37	1.10	47.19	0.4609	0.978
		0.71	*1.35*	*46.94*	*0.4559*	0.967

Test Series	X (m)	Z (m)	bed (cm)	surface (cm)	Y (m)	Y/Y_o
		0.80	*1.41*	*47.12*	*0.4571*	0.970
	3.0	0.13	1.52	45.94	0.4442	0.942
		0.26	1.56	45.91	0.4435	0.941
		0.58	*1.86*	*45.70*	*0.4384*	0.930
		0.74	*1.84*	*45.53*	*0.4369*	0.927
	4.0	0.07	1.18	43.87	0.4269	0.906
		0.14	1.15	43.88	0.4273	0.907
		0.47	*0.98*	*43.63*	*0.4265*	0.905
		0.69	*1.11*	*43.27*	*0.4216*	0.895
	4.375	0.075	1.58	42.88	0.4130	0.876
		0.43	*1.58*	*42.15*	*0.4057*	0.861
		0.67	*1.56*	*42.44*	*0.4088*	0.867
10/0.15/0.60/A	0	0.45	1.34	46.39	0.4505	1.000
	1.0	0.25	1.32	45.60	0.4428	0.983
		0.49	1.47	45.68	0.4421	0.981
		0.84	*1.45*	*45.12*	*0.4367*	0.969
	2.0	0.18	1.12	44.08	0.4296	0.954
		0.37	1.10	44.00	0.4290	0.952
		0.71	*1.35*	*43.81*	*0.4246*	0.943
		0.80	*1.41*	*44.39*	*0.4298*	0.954
	3.0	0.13	1.52	42.23	0.4071	0.904
		0.26	1.56	42.19	0.4063	0.902
		0.58	*1.86*	*41.64*	*0.3978*	0.883
		0.74	*1.84*	*41.52*	*0.3968*	0.881
	4.0	0.07	1.18	39.16	0.3798	0.843
		0.14	1.15	39.23	0.3808	0.845
		0.47	*0.98*	*38.42*	*0.3744*	0.831
		0.69	*1.11*	*39.44*	*0.3833*	0.851
	4.375	0.075	1.58	37.15	0.3557	0.790
		0.43	*1.58*	*35.88*	*0.3430*	0.761
		0.67	*1.56*	*36.18*	*0.3462*	0.768

Table A-3.2: Experimental Flow Depth Data of Louver Array (Series *10/*/*/B*)

LEGEND

X = horizontal distance (datum = flume entrance)

Z = transverse location of depth measurement

bed = point gauge reading at flume bed

surface = point gauge reading at water surface

Y/Y_o = normalized flow depth of any measured point

Y = flow depth of any measured point

NOTE: Canal section flow depths are shown in *ITALICS*.

Test Series	X (m)	Z (m)	bed (cm)	surface (cm)	Y (m)	Y/Y_o
10/0.05/0.30/B	0	0.45	32.93	80.43	0.4750	1.000
	1.5	0.21	32.93	80.30	0.4737	0.997
		0.42	32.89	80.28	0.4739	0.998
		0.80	*33.13*	*80.20*	*0.4707*	0.991
	3.0	0.13	33.41	79.79	0.4638	0.976
		0.26	33.45	79.78	0.4633	0.975
		0.58	*33.75*	*79.58*	*0.4583*	0.965
		0.74	*33.73*	*79.57*	*0.4584*	0.965
	4.0	0.07	33.07	79.31	0.4624	0.973
		0.14	33.04	79.44	0.4640	0.977
		0.47	*32.87*	*79.05*	*0.4618*	0.972
		0.69	*33.00*	*78.95*	*0.4595*	0.967
	4.875	0.025	33.59	78.68	0.4509	0.949
		0.37	*33.17*	*78.43*	*0.4526*	0.953
		0.64	*33.22*	*78.44*	*0.4522*	0.952
10/0.05/0.40/B	0	0.45	32.93	80.22	0.4729	1.000
	1.5	0.21	32.93	79.82	0.4689	0.992
		0.42	32.89	79.86	0.4697	0.993
		0.80	*33.13*	*79.63*	*0.4650*	0.983
	3.0	0.13	33.41	78.85	0.4544	0.961
		0.26	33.45	78.89	0.4544	0.961
		0.58	*33.75*	*78.63*	*0.4488*	0.949
		0.74	*33.73*	*78.57*	*0.4484*	0.948
	4.0	0.07	33.07	78.00	0.4493	0.950
		0.14	33.04	77.98	0.4494	0.950
		0.47	*32.87*	*77.76*	*0.4489*	0.949
		0.69	*33.00*	*77.65*	*0.4465*	0.944
	4.875	0.025	33.59	77.25	0.4366	0.923
		0.37	*33.17*	*76.34*	*0.4317*	0.913
		0.64	*33.22*	*76.63*	*0.4341*	0.918
10/0.05/0.50/B	0	0.45	34.74	81.88	0.4714	1.000
	1.5	0.21	34.74	81.18	0.4644	0.985
		0.42	34.70	81.13	0.4643	0.985
		0.80	*34.94*	*81.03*	*0.4609*	0.978
	3.0	0.13	35.22	79.80	0.4458	0.946
		0.26	35.26	79.76	0.4450	0.944
		0.58	*35.56*	*79.50*	*0.4394*	0.932

Test Series	X (m)	Z (m)	bed (cm)	surface (cm)	Y (m)	Y/Y$_o$
		0.74	*35.54*	*79.49*	*0.4395*	0.932
	4.0	0.07	34.88	78.37	0.4349	0.923
		0.14	34.85	78.27	0.4342	0.921
		0.47	*34.68*	*77.96*	*0.4328*	0.918
		0.69	*34.81*	*78.01*	*0.4320*	0.916
	4.875	0.025	35.40	76.69	0.4129	0.876
		0.37	*34.98*	*75.58*	*0.4060*	0.861
		0.64	*35.03*	*76.02*	*0.4099*	0.870
10/0.05/0.60/B	0	0.45	34.74	80.43	0.4569	1.000
	1.5	0.21	34.74	79.69	0.4495	0.984
		0.42	34.70	79.63	0.4493	0.983
		0.80	*34.94*	*79.23*	*0.4429*	0.969
	3.0	0.13	35.22	77.49	0.4227	0.925
		0.26	35.26	77.47	0.4221	0.924
		0.58	*35.56*	*77.06*	*0.4150*	0.908
		0.74	*35.54*	*77.23*	*0.4169*	0.912
	4.0	0.07	34.88	75.55	0.4067	0.890
		0.14	34.85	75.43	0.4058	0.888
		0.47	*34.68*	*74.74*	*0.4006*	0.877
		0.69	*34.81*	*74.87*	*0.4006*	0.877
	4.875	0.025	35.40	73.23	0.3783	0.828
		0.37	*34.98*	*71.01*	*0.3603*	0.789
		0.64	*35.03*	*71.65*	*0.3662*	0.801
10/0.10/0.30/B	0	0.45	32.93	81.21	0.4828	1.000
	1.5	0.21	32.93	81.01	0.4808	0.996
		0.42	32.89	80.99	0.4810	0.996
		0.80	*33.13*	*80.91*	*0.4778*	0.990
	3.0	0.13	33.41	80.60	0.4719	0.977
		0.26	33.45	80.63	0.4718	0.977
		0.58	*33.75*	*80.38*	*0.4663*	0.966
		0.74	*33.73*	*80.34*	*0.4661*	0.965
	4.0	0.07	33.07	80.19	0.4712	0.976
		0.14	33.04	80.02	0.4698	0.973
		0.47	*32.87*	*79.93*	*0.4706*	0.975
		0.69	*33.00*	*79.74*	*0.4674*	0.968
	4.675	0.05	33.55	79.61	0.4606	0.954
		0.40	*33.56*	*79.48*	*0.4592*	0.951
		0.66	*33.54*	*79.35*	*0.4581*	0.949
10/0.10/0.40/B	0	0.45	32.65	79.80	0.4715	1.000
	1.5	0.21	32.65	79.37	0.4672	0.991
		0.42	32.61	79.44	0.4683	0.993
		0.80	*32.85*	*79.36*	*0.4651*	0.986
	3.0	0.13	33.13	78.47	0.4534	0.962
		0.26	33.17	78.47	0.4530	0.961
		0.58	*33.47*	*78.36*	*0.4489*	0.952
		0.74	*33.45*	*78.36*	*0.4491*	0.952
	4.0	0.07	32.79	77.64	0.4485	0.951
		0.14	32.76	77.54	0.4478	0.950
		0.47	*32.59*	*77.38*	*0.4479*	0.950
		0.69	*32.72*	*77.29*	*0.4457*	0.945
	4.675	0.05	33.27	77.35	0.4408	0.935
		0.40	*33.28*	*76.28*	*0.4300*	0.912

Test Series	X (m)	Z (m)	bed (cm)	surface (cm)	Y (m)	Y/Y_o
		0.66	33.26	76.46	0.4320	0.916
10/0.10/0.50/B	0	0.45	34.74	81.70	0.4696	1.000
	1.5	0.21	34.74	81.22	0.4648	0.990
		0.42	34.70	81.03	0.4633	0.987
		0.80	34.94	80.87	0.4593	0.978
	3.0	0.13	35.22	79.60	0.4438	0.945
		0.26	35.26	79.68	0.4442	0.946
		0.58	35.56	79.37	0.4381	0.933
		0.74	35.54	79.42	0.4388	0.934
	4.0	0.07	34.88	78.28	0.4340	0.924
		0.14	34.85	78.08	0.4323	0.921
		0.47	34.68	77.84	0.4316	0.919
		0.69	34.81	77.79	0.4298	0.915
	4.675	0.05	35.40	77.48	0.4208	0.896
		0.40	34.98	76.00	0.4102	0.874
		0.66	35.03	76.32	0.4129	0.879
10/0.10/0.60/B	0	0.45	34.74	80.85	0.4611	1.000
	1.5	0.21	34.74	79.66	0.4492	0.974
		0.42	34.70	79.76	0.4506	0.977
		0.80	34.94	79.55	0.4461	0.967
	3.0	0.13	35.22	77.66	0.4244	0.920
		0.26	35.26	77.77	0.4251	0.922
		0.58	35.56	77.20	0.4164	0.903
		0.74	35.54	77.45	0.4191	0.909
	4.0	0.07	34.88	75.58	0.4070	0.883
		0.14	34.85	75.50	0.4065	0.882
		0.47	34.68	74.75	0.4007	0.869
		0.69	34.81	74.77	0.3996	0.867
	4.675	0.05	35.40	73.82	0.3842	0.833
		0.40	34.98	72.12	0.3714	0.805
		0.66	35.03	72.64	0.3761	0.816
10/0.15/0.30/B	0	0.45	32.93	80.91	0.4798	1.000
	1.5	0.21	32.93	80.78	0.4785	0.997
		0.42	32.89	80.74	0.4785	0.997
		0.80	33.13	80.73	0.4760	0.992
	3.0	0.13	33.41	80.15	0.4674	0.974
		0.26	33.45	80.34	0.4689	0.977
		0.58	33.75	80.09	0.4634	0.966
		0.74	33.73	80.09	0.4636	0.966
	4.0	0.07	33.07	79.79	0.4672	0.974
		0.14	33.04	79.89	0.4685	0.976
		0.47	32.87	79.66	0.4679	0.975
		0.69	33.00	79.50	0.4650	0.969
	4.375	0.075	33.55	79.55	0.4600	0.959
		0.43	33.56	79.21	0.4565	0.951
		0.67	33.54	79.27	0.4573	0.953
10/0.15/0.40/B	0	0.45	32.65	81.93	0.4928	1.000
	1.5	0.21	32.65	81.54	0.4889	0.992
		0.42	32.61	81.58	0.4897	0.994
		0.80	32.85	81.46	0.4861	0.986
	3.0	0.13	33.13	80.62	0.4749	0.964
		0.26	33.17	80.66	0.4749	0.964

Test Series	X (m)	Z (m)	bed (cm)	surface (cm)	Y (m)	Y/Y_o
		0.58	*33.47*	*80.46*	*0.4699*	0.954
		0.74	*33.45*	*80.42*	*0.4697*	0.953
	4.0	0.07	32.79	79.80	0.4701	0.954
		0.14	32.76	79.80	0.4704	0.955
		0.47	*32.59*	*79.44*	*0.4685*	0.951
		0.69	*32.72*	*79.41*	*0.4669*	0.947
	4.375	0.075	33.27	79.29	0.4602	0.934
		0.43	*33.28*	*78.97*	*0.4569*	0.927
		0.67	*33.26*	*79.00*	*0.4574*	0.928
10/0.15/0.50/B	0	0.45	34.74	81.41	0.4667	1.000
	1.5	0.21	34.74	80.79	0.4605	0.987
		0.42	34.70	80.59	0.4589	0.983
		0.80	*34.94*	*80.66*	*0.4572*	0.980
	3.0	0.13	35.22	79.41	0.4419	0.947
		0.26	35.26	79.42	0.4416	0.946
		0.58	*35.56*	*79.07*	*0.4351*	0.932
		0.74	*35.54*	*79.04*	*0.4350*	0.932
	4.0	0.07	34.88	77.98	0.4310	0.924
		0.14	34.85	77.91	0.4306	0.923
		0.47	*34.68*	*77.53*	*0.4285*	0.918
		0.69	*34.81*	*77.52*	*0.4271*	0.915
	4.375	0.075	35.40	77.37	0.4197	0.899
		0.43	*34.98*	*76.51*	*0.4153*	0.890
		0.67	*35.03*	*76.72*	*0.4169*	0.893
10/0.15/0.60/B	0	0.45	34.74	80.69	0.4595	1.000
	1.5	0.21	34.74	79.74	0.4500	0.979
		0.42	34.70	79.71	0.4501	0.980
		0.80	*34.94*	*79.43*	*0.4449*	0.968
	3.0	0.13	35.22	77.65	0.4243	0.923
		0.26	35.26	77.50	0.4224	0.919
		0.58	*35.56*	*77.27*	*0.4171*	0.908
		0.74	*35.54*	*77.30*	*0.4176*	0.909
	4.0	0.07	34.88	75.39	0.4051	0.882
		0.14	34.85	75.24	0.4039	0.879
		0.47	*34.68*	*74.64*	*0.3996*	0.870
		0.69	*34.81*	*74.56*	*0.3975*	0.865
	4.375	0.075	35.40	74.23	0.3883	0.845
		0.43	*34.98*	*72.92*	*0.3794*	0.826
		0.67	*35.03*	*73.28*	*0.3825*	0.832

Table A-3.3: Experimental Flow Depth Data of Louver Array (Series *15/*/*/A*)

LEGEND

X = horizontal distance (datum = flume entrance)
Z = transverse location of depth measurement
bed = point gauge reading at flume bed
surface = point gauge reading at water surface
Y/Y_o = normalized flow depth of any measured point
Y = flow depth of any measured point

NOTE: Canal section flow depths are shown in *ITALICS*.

Test Series	X (m)	Z (m)	bed (cm)	surface (cm)	Y (m)	Y/Y_o
15/0.05/0.30/A	0	0.45	0.91	49.86	0.4895	1.000
	1.0	0.22	0.94	49.52	0.4858	0.992
		0.44	1.00	49.51	0.4851	0.991
		0.80	*1.03*	*49.33*	*0.4830*	0.987
	2.0	0.13	0.78	48.86	0.4808	0.982
		0.26	0.73	48.94	0.4821	0.985
		0.59	*0.86*	*48.75*	*0.4789*	0.978
		0.75	*0.98*	*48.76*	*0.4778*	0.976
	2.75	0.09	0.84	47.88	0.4704	0.961
		0.45	*0.82*	*47.62*	*0.4680*	0.956
		0.67	*1.03*	*47.61*	*0.4658*	0.952
	3.215	0.025	1.11	47.08	0.4597	0.939
		0.36	*1.14*	*46.02*	*0.4488*	0.917
		0.63	*1.18*	*46.46*	*0.4528*	0.925
15/0.05/0.40/A	0	0.45	0.84	49.42	0.4858	1.000
	1.0	0.22	0.87	49.01	0.4814	0.991
		0.44	0.93	48.86	0.4793	0.987
		0.80	*0.96*	*48.68*	*0.4772*	0.982
	2.0	0.13	0.71	47.75	0.4704	0.968
		0.26	0.66	47.86	0.4720	0.972
		0.59	*0.79*	*47.51*	*0.4672*	0.962
		0.75	*0.91*	*47.37*	*0.4646*	0.956
	2.75	0.09	0.77	46.14	0.4537	0.934
		0.45	*0.75*	*45.32*	*0.4457*	0.917
		0.67	*0.96*	*45.56*	*0.4460*	0.918
	3.215	0.025	1.04	44.64	0.4360	0.897
		0.36	*1.07*	*42.14*	*0.4107*	0.845
		0.63	*1.11*	*43.48*	*0.4237*	0.872
15/0.05/0.50/A	0	0.45	0.84	50.43	0.4959	1.000
	1.0	0.22	0.87	49.62	0.4875	0.983
		0.44	0.93	49.48	0.4855	0.979
		0.80	*0.96*	*49.16*	*0.4820*	0.972
	2.0	0.13	0.71	47.68	0.4697	0.947
		0.26	0.66	47.47	0.4681	0.944

Test Series	X (m)	Z (m)	bed (cm)	surface (cm)	Y (m)	Y/Y_o
		0.59	*0.79*	*47.08*	*0.4629*	0.933
		0.75	*0.91*	*47.22*	*0.4631*	0.934
	2.75	0.09	0.77	44.92	0.4415	0.890
		0.45	*0.75*	*43.87*	*0.4312*	0.870
		0.67	*0.96*	*44.18*	*0.4322*	0.872
	3.215	0.025	1.04	43.06	0.4202	0.847
		0.36	*1.07*	*39.39*	*0.3832*	0.773
		0.63	*1.11*	*40.95*	*0.3984*	0.803
15/0.10/0.30/A	0	0.45	0.91	49.45	0.4854	1.000
	1.0	0.22	0.94	49.17	0.4823	0.994
		0.44	1.00	49.12	0.4812	0.991
		0.80	*1.03*	*48.85*	*0.4782*	0.985
	2.0	0.13	0.78	48.44	0.4766	0.982
		0.26	0.73	48.35	0.4762	0.981
		0.59	*0.86*	*48.24*	*0.4738*	0.976
		0.75	*0.98*	*48.28*	*0.4730*	0.974
	2.5	0.08	0.97	47.90	0.4693	0.967
		0.17	0.82	47.78	0.4696	0.967
		0.50	*0.85*	*47.63*	*0.4678*	0.964
		0.70	*0.92*	*47.63*	*0.4671*	0.962
	3.065	0.045	1.26	46.87	0.4561	0.940
		0.39	*1.32*	*45.91*	*0.4459*	0.919
		0.64	*1.43*	*46.44*	*0.4501*	0.927
15/0.10/0.40/A	0	0.45	0.84	48.82	0.4798	1.000
	1.0	0.22	0.87	48.36	0.4749	0.990
		0.44	0.93	48.28	0.4735	0.987
		0.80	*0.96*	*48.04*	*0.4708*	0.981
	2.0	0.13	0.71	47.05	0.4634	0.966
		0.26	0.66	47.12	0.4646	0.968
		0.59	*0.79*	*46.60*	*0.4581*	0.955
		0.75	*0.91*	*46.72*	*0.4581*	0.955
	2.5	0.08	0.90	46.09	0.4519	0.942
		0.17	0.75	46.28	0.4553	0.949
		0.50	*0.78*	*45.70*	*0.4492*	0.936
		0.70	*0.85*	*45.45*	*0.4460*	0.930
	3.065	0.045	1.19	44.49	0.4330	0.902
		0.39	*1.25*	*42.50*	*0.4125*	0.860
		0.64	*1.36*	*43.39*	*0.4203*	0.876
15/0.10/0.50/A	0	0.45	0.84	49.47	0.4863	1.000
	1.0	0.22	0.87	48.46	0.4759	0.979
		0.44	0.93	48.38	0.4745	0.976
		0.80	*0.96*	*48.01*	*0.4705*	0.968
	2.0	0.13	0.71	46.67	0.4596	0.945
		0.26	0.66	46.57	0.4591	0.944
		0.59	*0.79*	*45.75*	*0.4496*	0.925
		0.75	*0.91*	*45.97*	*0.4506*	0.927
	2.5	0.08	0.90	44.76	0.4386	0.902
		0.17	0.75	44.87	0.4412	0.907
		0.50	*0.78*	*44.34*	*0.4356*	0.896

Test Series	X (m)	Z (m)	bed (cm)	surface (cm)	Y (m)	Y/Y_o
		0.70	*0.85*	*44.04*	*0.4319*	0.888
	3.065	0.045	1.19	42.60	0.4141	0.852
		0.39	*1.25*	*39.14*	*0.3789*	0.779
		0.64	*1.36*	*40.82*	*0.3946*	0.811
15/0.15/0.30/A	0	0.45	0.91	49.15	0.4824	1.000
	1.0	0.22	0.94	48.85	0.4791	0.993
		0.44	1.00	48.74	0.4774	0.990
		0.80	*1.03*	*48.61*	*0.4758*	0.986
	2.0	0.13	0.78	48.15	0.4737	0.982
		0.26	0.73	48.09	0.4736	0.982
		0.59	*0.86*	*47.97*	*0.4711*	0.977
		0.75	*0.98*	*47.94*	*0.4696*	0.973
	2.5	0.08	0.97	47.61	0.4664	0.967
		0.17	0.82	47.54	0.4672	0.968
		0.50	*0.85*	*47.15*	*0.4630*	0.960
		0.70	*0.92*	*47.15*	*0.4623*	0.958
	2.915	0.07	1.11	46.90	0.4579	0.949
		0.43	*1.05*	*46.04*	*0.4499*	0.933
		0.66	*1.23*	*46.32*	*0.4509*	0.935
15/0.15/0.40/A	0	0.45	0.84	48.30	0.4746	1.000
	1.0	0.22	0.87	47.82	0.4695	0.989
		0.44	0.93	47.75	0.4682	0.987
		0.80	*0.96*	*47.48*	*0.4652*	0.980
	2.0	0.13	0.71	46.52	0.4581	0.965
		0.26	0.66	46.53	0.4587	0.966
		0.59	*0.79*	*46.09*	*0.4530*	0.954
		0.75	*0.91*	*46.05*	*0.4514*	0.951
	2.5	0.08	0.90	45.39	0.4449	0.937
		0.17	0.75	45.51	0.4476	0.943
		0.50	*0.78*	*44.76*	*0.4398*	0.927
		0.70	*0.85*	*44.84*	*0.4399*	0.927
	2.915	0.07	1.04	44.22	0.4318	0.910
		0.43	*0.98*	*42.71*	*0.4173*	0.879
		0.66	*1.16*	*43.39*	*0.4223*	0.890
15/0.15/0.50/A	0	0.45	0.84	48.62	0.4778	1.000
	1.0	0.22	0.87	47.71	0.4684	0.980
		0.44	0.93	47.72	0.4679	0.979
		0.80	*0.96*	*47.48*	*0.4652*	0.974
	2.0	0.13	0.71	45.68	0.4497	0.941
		0.26	0.66	45.46	0.4480	0.938
		0.59	*0.79*	*44.83*	*0.4404*	0.922
		0.75	*0.91*	*45.22*	*0.4431*	0.927
	2.5	0.08	0.90	43.89	0.4299	0.900
		0.17	0.75	43.67	0.4292	0.898
		0.50	*0.78*	*43.00*	*0.4222*	0.884
		0.70	*0.85*	*42.90*	*0.4205*	0.880
	2.915	0.07	1.04	41.80	0.4076	0.853
		0.43	*0.98*	*38.69*	*0.3771*	0.789
		0.66	*1.16*	*40.54*	*0.3938*	0.824

Table A-3.4: Experimental Flow Depth Data of Louver Array (Series *15/*/*/B*)

LEGEND

X = horizontal distance (datum = flume entrance)

Z = transverse location of depth measurement

bed = point gauge reading at flume bed

surface = point gauge reading at water surface

Y/Y_o = normalized flow depth of any measured point

Y = flow depth of any measured point

NOTE: Canal section flow depths are shown in *ITALICS*.

Test Series	X (m)	Z (m)	bed (cm)	surface (cm)	Y (m)	Y/Y_o
15/0.05/0.30/B	0	0.45	0.90	49.60	0.4870	1.000
	1.0	0.22	0.93	49.50	0.4857	0.997
		0.44	0.99	49.27	0.4828	0.991
		0.80	*1.02*	*49.03*	*0.4801*	0.986
	2.0	0.13	0.77	48.72	0.4795	0.985
		0.26	0.72	48.91	0.4819	0.990
		0.59	*0.85*	*48.62*	*0.4777*	0.981
		0.75	*0.97*	*48.54*	*0.4757*	0.977
	2.75	0.09	0.83	48.17	0.4734	0.972
		0.45	*0.81*	*47.81*	*0.4700*	0.965
		0.67	*1.02*	*47.85*	*0.4683*	0.962
	3.215	0.025	1.10	47.42	0.4632	0.951
		0.36	*1.13*	*47.19*	*0.4606*	0.946
		0.63	*1.17*	*47.32*	*0.4615*	0.948
15/0.05/0.40/B	0	0.45	0.90	48.55	0.4765	1.000
	1.0	0.22	0.93	48.02	0.4709	0.988
		0.44	0.99	48.00	0.4701	0.987
		0.80	*1.02*	*47.75*	*0.4673*	0.981
	2.0	0.13	0.77	47.06	0.4629	0.971
		0.26	0.72	47.18	0.4646	0.975
		0.59	*0.85*	*46.58*	*0.4573*	0.960
		0.75	*0.97*	*46.74*	*0.4577*	0.961
	2.75	0.09	0.83	46.12	0.4529	0.950
		0.45	*0.81*	*45.21*	*0.4440*	0.932
		0.67	*1.02*	*45.44*	*0.4442*	0.932
	3.215	0.025	1.10	45.49	0.4439	0.932
		0.36	*1.13*	*43.72*	*0.4259*	0.894
		0.63	*1.17*	*44.44*	*0.4327*	0.908
15/0.05/0.50/B	0	0.45	0.90	48.69	0.4779	1.000
	1.0	0.22	0.93	47.89	0.4696	0.983
		0.44	0.99	47.91	0.4692	0.982
		0.80	*1.02*	*47.42*	*0.4640*	0.971
	2.0	0.13	0.77	46.43	0.4566	0.955
		0.26	0.72	46.43	0.4571	0.956
		0.59	*0.85*	*45.54*	*0.4469*	0.935

Test Series	X (m)	Z (m)	bed (cm)	surface (cm)	Y (m)	Y/Y_o
		0.75	*0.97*	*45.93*	*0.4496*	0.941
	2.75	0.09	0.83	44.76	0.4393	0.919
		0.45	*0.81*	*43.45*	*0.4264*	0.892
		0.67	*1.02*	*43.80*	*0.4278*	0.895
	3.215	0.025	1.10	43.40	0.4230	0.885
		0.36	*1.13*	*41.30*	*0.4017*	0.841
		0.63	*1.17*	*42.06*	*0.4089*	0.856
15/0.10/0.30/B	0	0.45	0.90	49.72	0.4882	1.000
	1.0	0.22	0.93	49.37	0.4844	0.992
		0.44	0.99	49.35	0.4836	0.991
		0.80	*1.02*	*49.04*	*0.4802*	0.984
	2.0	0.13	0.77	48.80	0.4803	0.984
		0.26	0.72	48.78	0.4806	0.984
		0.59	*0.85*	*48.43*	*0.4758*	0.975
		0.75	*0.97*	*48.56*	*0.4759*	0.975
	2.5	0.08	0.96	48.47	0.4751	0.973
		0.17	0.81	48.40	0.4759	0.975
		0.50	*0.84*	*48.16*	*0.4732*	0.969
		0.70	*0.91*	*48.07*	*0.4716*	0.966
	3.065	0.045	1.25	48.09	0.4684	0.959
		0.39	*1.31*	*47.12*	*0.4581*	0.938
		0.64	*1.42*	*47.49*	*0.4607*	0.944
15/0.10/0.40/B	0	0.45	0.90	48.04	0.4714	1.000
	1.0	0.22	0.93	47.71	0.4678	0.992
		0.44	0.99	47.54	0.4655	0.987
		0.80	*1.02*	*47.05*	*0.4603*	0.976
	2.0	0.13	0.77	46.56	0.4579	0.971
		0.26	0.72	46.54	0.4582	0.972
		0.59	*0.85*	*46.15*	*0.4530*	0.961
		0.75	*0.97*	*46.20*	*0.4523*	0.959
	2.5	0.08	0.96	45.90	0.4494	0.953
		0.17	0.81	45.82	0.4501	0.955
		0.50	*0.84*	*45.23*	*0.4439*	0.942
		0.70	*0.91*	*45.39*	*0.4448*	0.944
	3.065	0.045	1.25	45.12	0.4387	0.931
		0.39	*1.31*	*43.70*	*0.4239*	0.899
		0.64	*1.42*	*44.34*	*0.4292*	0.910
15/0.10/0.50/B	0	0.45	0.84	48.10	0.4726	1.000
	1.0	0.22	0.87	47.36	0.4649	0.984
		0.44	0.93	47.30	0.4637	0.981
		0.80	*0.96*	*46.68*	*0.4572*	0.967
	2.0	0.13	0.71	45.75	0.4504	0.953
		0.26	0.66	45.66	0.4500	0.952
		0.59	*0.79*	*44.69*	*0.4390*	0.929
		0.75	*0.91*	*45.15*	*0.4424*	0.936
	2.5	0.08	0.90	44.55	0.4365	0.924
		0.17	0.75	44.56	0.4381	0.927
		0.50	*0.78*	*43.38*	*0.4260*	0.901
		0.70	*0.85*	*43.89*	*0.4304*	0.911

Test Series	X (m)	Z (m)	bed (cm)	surface (cm)	Y (m)	Y/Y_o
	3.065	0.045	1.19	43.12	0.4193	0.887
		0.39	*1.25*	*40.88*	*0.3963*	0.839
		0.64	*1.36*	*41.84*	*0.4048*	0.857
15/0.15/0.30/B	0	0.45	0.90	49.34	0.4844	1.000
	1.0	0.22	0.93	49.00	0.4807	0.992
		0.44	0.99	48.92	0.4793	0.989
		0.80	*1.02*	*48.65*	*0.4763*	0.983
	2.0	0.13	0.77	48.39	0.4762	0.983
		0.26	0.72	48.43	0.4771	0.985
		0.59	*0.85*	*48.29*	*0.4744*	0.979
		0.75	*0.97*	*48.15*	*0.4718*	0.974
	2.5	0.08	0.96	48.14	0.4718	0.974
		0.17	0.81	48.12	0.4731	0.977
		0.50	*0.84*	*47.83*	*0.4699*	0.970
		0.70	*0.91*	*47.64*	*0.4673*	0.965
	2.915	0.07	1.10	47.79	0.4669	0.964
		0.43	*1.04*	*47.00*	*0.4596*	0.949
		0.66	*1.22*	*47.22*	*0.4600*	0.950
15/0.15/0.40/B	0	0.45	0.90	47.74	0.4684	1.000
	1.0	0.22	0.93	47.25	0.4632	0.989
		0.44	0.99	47.15	0.4616	0.985
		0.80	*1.02*	*46.95*	*0.4593*	0.981
	2.0	0.13	0.77	46.31	0.4554	0.972
		0.26	0.72	46.42	0.4570	0.976
		0.59	*0.85*	*45.79*	*0.4494*	0.959
		0.75	*0.97*	*45.87*	*0.4490*	0.959
	2.5	0.08	0.96	45.52	0.4456	0.951
		0.17	0.81	45.80	0.4499	0.961
		0.50	*0.84*	*44.89*	*0.4405*	0.940
		0.70	*0.91*	*45.15*	*0.4424*	0.944
	2.915	0.07	1.10	44.91	0.4381	0.935
		0.43	*1.04*	*43.68*	*0.4264*	0.910
		0.66	*1.22*	*44.19*	*0.4297*	0.917
15/0.15/0.50/B	0	0.45	0.90	47.70	0.4680	1.000
	1.0	0.22	0.93	46.84	0.4591	0.981
		0.44	0.99	46.73	0.4574	0.977
		0.80	*1.02*	*46.27*	*0.4525*	0.967
	2.0	0.13	0.77	45.12	0.4435	0.948
		0.26	0.72	45.04	0.4432	0.947
		0.59	*0.85*	*44.11*	*0.4326*	0.924
		0.75	*0.97*	*44.48*	*0.4351*	0.930
	2.5	0.08	0.96	43.99	0.4303	0.919
		0.17	0.81	44.04	0.4323	0.924
		0.50	*0.84*	*42.62*	*0.4178*	0.893
		0.70	*0.91*	*43.13*	*0.4222*	0.902
	2.915	0.07	1.10	42.92	0.4182	0.894
		0.43	*1.04*	*40.90*	*0.3986*	0.852
		0.66	*1.22*	*41.62*	*0.4040*	0.863

APPENDIX B

Velocity Profiles

- *Experimental Data* -

B-1

Experimental Data of Phase One

Table B-1.1: Experimental Velocity Data of Louver Array (Series 7.2/*/*C)

LEGEND	
X = horizontal distance (datum = flume entrance)	u = velocity at depth 'y'
Z = transverse location of velocity measurement	Δu = incremental area of discharge for velocity 'u'
y = vertical location of velocity measurement	U = depth-averaged velocity of the section
y/Y = vertical depth location w.r.t. total flow depth	Q = discharge of the section
f = frequency reading of *StreamFlo* probe	

For Series 7.2/0.23/0.20/C:
$u = (0.00588 \cdot f^2 + 2.756 \cdot f + 5.76) / 185$ for $3.7 < f < 14.7$ Hz
$u = (0.00588 \cdot f^2 + 2.756 \cdot f + 9.931) / 198.3$ for $14.8 < f < 37$ Hz:
$u = 1.727 \cdot f$ for $f > 37$ Hz:

For Series 7.2/0.23/0.35/C and 7.2/0.23/0.50/C:
$u = (f + 5.76) / 185$ for $13 < f < 50$ Hz
$u = (f + 9.931) / 198.3$ for $51 < f < 288$ Hz

Test Series	X (m)	Z (m)	y (m)	y/Y	f (Hz)	u (m/s)	Δu (m/s)	U (m/s)	Q (m^3/s)
7.2/0.23/0.20/C	-0.10	0.50	0.008	0.009	7.75	0.15	0.0007		
			0.018	0.020	9.75	0.18	0.0018		
			0.038	0.042	10.02	0.18	0.0040		
			0.098	0.109	11.08	0.20	0.0128		
			0.158	0.176	11.98	0.21	0.0138		
			0.258	0.287	11.62	0.21	0.0235		
			0.408	0.453	11.10	0.20	0.0341		
			0.608	0.676	11.40	0.21	0.0450		
			0.808	0.898	11.50	0.21	0.0457		
			0.858	0.953	11.20	0.20	0.0113		
			0.90	1.000	11.20	0.20	0.0094	0.20	0.182
	1.01	0.4	0.008	0.009	9.01	0.17	0.0007		
			0.018	0.020	10.82	0.20	0.0020		
			0.038	0.042	12.04	0.22	0.0046		
			0.098	0.109	12.93	0.23	0.0148		
			0.158	0.176	12.97	0.23	0.0153		
			0.258	0.287	12.89	0.23	0.0255		
			0.408	0.453	13.00	0.23	0.0382		
			0.608	0.676	12.14	0.22	0.0496		
			0.808	0.898	11.73	0.21	0.0474		
			0.858	0.953	11.18	0.20	0.0114		
			0.90	1.000	11.18	0.20	0.0094	0.22	0.197
	2.26	0.33	0.008	0.009	10.94	0.20	0.0009		
			0.018	0.020	13.05	0.23	0.0024		
			0.038	0.042	14.07	0.25	0.0053		
			0.098	0.109	15.73	0.28	0.0174		
			0.158	0.176	15.42	0.27	0.0182		
			0.258	0.287	15.57	0.27	0.0303		
			0.408	0.453	15.36	0.27	0.0453		
			0.608	0.676	15.52	0.27	0.0604		
			0.808	0.898	14.49	0.25	0.0585		
			0.858	0.953	14.58	0.26	0.0141		
			0.90	1.000	14.58	0.26	0.0119	0.26	0.157

Test Series	X (m)	Z (m)	y (m)	y/Y	f (Hz)	u (m/s)	Δu (m/s)	U (m/s)	Q (m^3/s)
	3.22	0.27	0.008	0.009	12.34	0.22	0.0010		
			0.018	0.020	14.07	0.25	0.0026		
			0.038	0.042	15.84	0.28	0.0058		
			0.098	0.109	16.70	0.29	0.0189		
			0.158	0.176	16.98	0.29	0.0195		
			0.258	0.287	17.10	0.30	0.0328		
			0.408	0.453	16.95	0.29	0.0492		
			0.608	0.676	17.15	0.30	0.0657		
			0.808	0.898	16.49	0.29	0.0649		
			0.858	0.953	16.27	0.28	0.0159		
			0.90	1.000	16.27	0.28	0.0133	0.29	0.141
	4.31	0.18	0.008	0.009	14.84	0.26	0.0012		
			0.018	0.020	16.34	0.29	0.0030		
			0.038	0.042	17.71	0.31	0.0066		
			0.098	0.109	18.36	0.32	0.0207		
			0.158	0.176	18.50	0.32	0.0211		
			0.258	0.287	18.02	0.31	0.0348		
			0.408	0.453	18.55	0.32	0.0523		
			0.608	0.676	18.35	0.31	0.0703		
			0.808	0.898	18.25	0.31	0.0698		
			0.858	0.953	18.21	0.31	0.0174		
			0.90	1.000	18.21	0.31	0.0146	0.31	0.104
	5.58	0.11	0.008	0.009	15.8	0.28	0.0012		
			0.018	0.020	17.4	0.30	0.0032		
			0.038	0.042	19.0	0.32	0.0070		
			0.098	0.109	19.6	0.33	0.0220		
			0.158	0.176	20.1	0.34	0.0225		
			0.258	0.287	20.0	0.34	0.0378		
			0.408	0.453	20.1	0.34	0.0568		
			0.608	0.676	20.2	0.34	0.0760		
			0.808	0.898	20.0	0.34	0.0759		
			0.858	0.953	19.7	0.34	0.0188		
			0.90	1.000	19.7	0.34	0.0156	0.34	0.070
7.2/0.23/0.35/C	0.50	-0.28	0.008	0.009	45.0	0.27	0.0012		
			0.058	0.064	55.7	0.33	0.0168		
			0.108	0.120	59.8	0.35	0.0190		
			0.208	0.231	60.6	0.36	0.0393		
			0.358	0.398	59.7	0.35	0.0589		
			0.558	0.620	59.7	0.35	0.0780		
			0.808	0.898	55.7	0.33	0.0947		
			0.90	1.000	55.7	0.33	0.0338	0.34	0.308
	0.35	1.73	0.008	0.009	53.1	0.32	0.0014		
			0.058	0.064	65.2	0.38	0.0193		
			0.108	0.120	72.5	0.42	0.0221		
			0.208	0.231	73.3	0.42	0.0464		
			0.358	0.398	74.8	0.43	0.0706		
			0.558	0.620	75.0	0.43	0.0950		
			0.808	0.898	74.0	0.42	0.1182		
			0.90	1.000	74.0	0.42	0.0433	0.42	0.262
	0.23	3.55	0.008	0.009	56.4	0.33	0.0015		
			0.058	0.064	77.2	0.44	0.0215		

Test Series	X (m)	Z (m)	y (m)	y/Y	f (Hz)	u (m/s)	Δu (m/s)	U (m/s)	Q (m^3/s)
			0.108	0.120	82.4	0.47	0.0251		
			0.208	0.231	87.7	0.49	0.0532		
			0.358	0.398	87.4	0.49	0.0819		
			0.558	0.620	89.1	0.50	0.1100		
			0.808	0.898	86.5	0.49	0.1369		
			0.90	1.000	86.5	0.49	0.0497	0.48	0.199
	0.11	5.58	0.008	0.009	68.4	0.40	0.0018		
			0.058	0.064	88.5	0.50	0.0248		
			0.108	0.120	91.2	0.51	0.0280		
			0.208	0.231	94.7	0.53	0.0576		
			0.358	0.398	93.2	0.52	0.0873		
			0.558	0.620	100.0	0.55	0.1194		
			0.808	0.898	97.6	0.54	0.1523		
			0.90	1.000	97.6	0.54	0.0554	0.53	0.109
7.2/0.23/0.50/C	0.50	-0.28	0.008	0.009	69.9	0.40	0.0018		
			0.058	0.064	90.0	0.50	0.0252		
			0.108	0.120	94.8	0.53	0.0287		
			0.208	0.231	92.0	0.51	0.0579		
			0.358	0.398	92.2	0.52	0.0858		
			0.558	0.620	88.7	0.50	0.1125		
			0.808	0.898	86.4	0.49	0.1366		
			0.90	1.000	86.4	0.49	0.0497	0.50	0.448
	0.35	1.73	0.008	0.009	86.5	0.49	0.0022		
			0.058	0.064	107.1	0.59	0.0299		
			0.108	0.120	117.2	0.64	0.0342		
			0.208	0.231	121.1	0.66	0.0723		
			0.358	0.398	119.1	0.65	0.1093		
			0.558	0.620	116.1	0.64	0.1429		
			0.808	0.898	114.1	0.63	0.1751		
			0.90	1.000	114.1	0.63	0.0639	0.63	0.397
	0.23	3.55	0.008	0.009	85.4	0.48	0.0021		
			0.058	0.064	122.3	0.67	0.0319		
			0.108	0.120	128.8	0.70	0.0380		
			0.208	0.231	136.7	0.74	0.0799		
			0.358	0.398	137.3	0.74	0.1235		
			0.558	0.620	137.0	0.74	0.1648		
			0.808	0.898	128.8	0.70	0.2000		
			0.90	1.000	128.8	0.70	0.0715	0.71	0.295
	0.11	5.58	0.008	0.009	109.5	0.60	0.0027		
			0.058	0.064	136.5	0.74	0.0372		
			0.108	0.120	144.9	0.78	0.0422		
			0.208	0.231	148.2	0.80	0.0877		
			0.358	0.398	151.0	0.81	0.1341		
			0.558	0.620	150.2	0.81	0.1799		
			0.808	0.898	147.3	0.79	0.2223		
			0.90	1.000	147.3	0.79	0.0811	0.79	0.163

Table B-1.2: Experimental Velocity Data of Louver Array (Series 17/*/*C)

LEGEND	
X = horizontal distance (datum = flume entrance)	u = velocity at depth 'y'
Z = transverse location of velocity measurement	Δu = incremental area of discharge for velocity 'u'
y = vertical depth of velocity measurement	U = depth-averaged velocity of the profile
y/Y = vertical depth 'y' w.r.t. total flow depth	Q = discharge of the section
f = frequency reading of *StreamFlo* probe	

$$u = (f + 5.76) / 185 \quad \text{for } 13 < f < 50 \text{ Hz}$$
$$u = (f + 9.931) / 198.3 \quad \text{for } 51 < f < 288 \text{ Hz}$$

Test Series	X (m)	Z (m)	y (m)	y/Y	f (Hz)	u (m/s)	Δu (m/s)	U (m/s)	Q (m^3/s)
17/0.23/0.20/C	0.45	-0.29	0.008	0.013	21.7	0.15	0.0010		
			0.028	0.047	25.3	0.17	0.0053		
			0.058	0.097	30.6	0.20	0.0091		
			0.108	0.180	31.8	0.20	0.0166		
			0.208	0.347	32.5	0.21	0.0342		
			0.358	0.597	32.9	0.21	0.0520		
			0.558	0.930	30.9	0.20	0.0678		
			0.60	1.000	30.9	0.20	0.0139	0.20	0.108
	0.28	0.96	0.008	0.013	28.5	0.19	0.0012		
			0.028	0.047	36.1	0.23	0.0069		
			0.058	0.097	38.0	0.24	0.0116		
			0.108	0.180	40.3	0.25	0.0202		
			0.208	0.347	39.7	0.25	0.0412		
			0.358	0.597	38.9	0.24	0.0609		
			0.558	0.930	39.3	0.24	0.0808		
			0.60	1.000	39.3	0.24	0.0170	0.24	0.081
	0.10	2.08	0.008	0.013	36.8	0.23	0.0015		
			0.028	0.047	44.0	0.27	0.0083		
			0.058	0.097	45.5	0.28	0.0136		
			0.108	0.180	48.1	0.29	0.0237		
			0.208	0.347	49.3	0.30	0.0490		
			0.358	0.597	49.3	0.30	0.0744		
			0.558	0.930	49.8	0.30	0.0997		
			0.60	1.000	49.8	0.30	0.0210	0.29	0.037
17/0.23/0.35/C	0.45	-0.29	0.008	0.013	42.1	0.26	0.0017		
			0.028	0.047	50.1	0.30	0.0094		
			0.058	0.097	57.5	0.34	0.0161		
			0.108	0.180	61.3	0.36	0.0291		
			0.208	0.347	63.1	0.37	0.0606		
			0.358	0.597	63.0	0.37	0.0920		
			0.558	0.930	57.4	0.34	0.1179		
			0.60	1.000	57.4	0.34	0.0238	0.35	0.189
	0.28	0.96	0.008	0.013	62.1	0.36	0.0024		
			0.028	0.047	71.6	0.41	0.0129		
			0.058	0.097	71.6	0.41	0.0206		
			0.108	0.180	73.1	0.42	0.0346		
			0.208	0.347	75.4	0.43	0.0708		

Test Series	X (m)	Z (m)	y (m)	y/Y	f (Hz)	u (m/s)	Δu (m/s)	U (m/s)	Q (m^3/s)
			0.358	0.597	75.9	0.43	0.1079		
			0.558	0.930	70.2	0.40	0.1395		
			0.60	1.000	70.2	0.40	0.0283	0.42	0.140
	0.10	2.08	0.008	0.013	77.6	0.44	0.0029		
			0.028	0.047	85.4	0.48	0.0154		
			0.208	0.347	93.9	0.52	0.1506		
			0.358	0.597	94.0	0.52	0.1309		
			0.558	0.930	92.8	0.52	0.1736		
			0.60	1.000	92.8	0.52	0.0363	0.51	0.064
17/0.26/0.50/C	0.50	-0.33	0.008	0.009	71.0	0.41	0.0018		
			0.058	0.064	95.9	0.53	0.0262		
			0.108	0.120	99.1	0.55	0.0301		
			0.208	0.231	101.8	0.56	0.0618		
			0.358	0.398	95.6	0.53	0.0913		
			0.558	0.620	93.4	0.52	0.1170		
			0.808	0.898	91.7	0.51	0.1436		
			0.90	1.000	91.7	0.51	0.0524	0.52	0.472
	0.32	0.98	0.008	0.009	86.8	0.49	0.0022		
			0.058	0.064	107.9	0.59	0.0301		
			0.108	0.120	111.2	0.61	0.0335		
			0.208	0.231	115.4	0.63	0.0690		
			0.358	0.398	114.9	0.63	0.1051		
			0.558	0.620	113.9	0.62	0.1393		
			0.808	0.898	111.0	0.61	0.1714		
			0.90	1.000	111.0	0.61	0.0623	0.61	0.356
	0.13	2.29	0.008	0.009	105.5	0.58	0.0026		
			0.058	0.064	120.3	0.66	0.0344		
			0.108	0.120	125.1	0.68	0.0372		
			0.208	0.231	130.6	0.71	0.0772		
			0.358	0.398	131.9	0.72	0.1187		
			0.558	0.620	132.7	0.72	0.1594		
			0.808	0.898	123.7	0.67	0.1935		
			0.90	1.000	123.7	0.67	0.0689	0.69	0.162

B-2

Experimental Data of Phase Two

Table B-2.1: Experimental Velocity Data of Louver Array (Series *10/0.15/*/A*)

LEGEND

Q* = magmeter reading of the pump discharge
ht = tailgate height
X = horizontal distance (datum = flume entrance)
Z = transverse location of velocity measurement
Z_b = bypass width of a transverse section
F = Froude number

y = vertical depth of velocity measurement
y/Y = vertical depth 'y' w.r.t. total flow depth
u = velocity at depth 'y'
Δu = incremental area of discharge for velocity 'u'
U = depth-averaged velocity of the profile
Q = discharge of the section

Using *LabView* software: Sample number at each velocity 'u' = 200
Sampling rate at each velocity 'u' = 40 per second

NOTE: Velocity measurements re-done if standard deviation of samples > 0.025

Test Series	Q* (m^3/s)	ht (m)	X (m)	Z (m)	Z_b (m)	F	y (m)	y/Y	u (m/s)	Δu (m/s)	U (m/s)	Q (m^3/s)
10/0.15/0.30/A	0.134	0.33	-2.0	0.45	0.90	0.135	0	0	0.1506	0		
							0.02	0.04	0.2642	0.0084		
							0.05	0.10	0.2591	0.0159		
							0.10	0.20	0.3044	0.0286		
							0.15	0.30	0.3278	0.0321		
							0.20	0.41	0.3098	0.0324		
							0.25	0.51	0.3086	0.0314		
							0.35	0.71	0.3048	0.0623		
							0.45	0.91	0.2920	0.0606		
							0.4925	1.00	0.2920	0.0252	0.297	0.132
			1.5	0.16	0.635	0.178	0	0	0.2724	0		
							0.02	0.04	0.3622	0.0131		
							0.05	0.10	0.3893	0.0233		
							0.10	0.21	0.4034	0.0409		
							0.15	0.31	0.3966	0.0413		
							0.20	0.41	0.4079	0.0415		
							0.25	0.52	0.4059	0.0420		
							0.35	0.72	0.4104	0.0842		
							0.45	0.93	0.4056	0.0842		
							0.4848	1.00	0.4056	0.0291	0.399	
				0.32			0	0	0.2432	0		
							0.02	0.04	0.3317	0.0119		
							0.05	0.10	0.3592	0.0214		
							0.10	0.21	0.3925	0.0388		
							0.15	0.31	0.4057	0.0412		
							0.20	0.41	0.4073	0.0419		
							0.25	0.52	0.4132	0.0423		
							0.35	0.72	0.3964	0.0835		
							0.45	0.93	0.3922	0.0813		
							0.4848	1.00	0.3922	0.0224	0.385	
				0.48			0	0	0.2328	0		
							0.02	0.04	0.3201	0.0114		
							0.05	0.10	0.3630	0.0211		

Test Series	Q* (m³/s)	ht (m)	X (m)	Z (m)	Z_b (m)	F	y (m)	y/Y	u (m/s)	Δu (m/s)	U (m/s)	Q (m³/s)
							0.10	0.21	0.3710	0.0379		
							0.15	0.31	0.3963	0.0396		
							0.20	0.41	0.4052	0.0413		
							0.25	0.52	0.3848	0.0407		
							0.35	0.72	0.3903	0.0799		
							0.45	0.93	0.3948	0.0810		
							0.4848	1.00	0.3948	0.0277	0.381	0.120
			3.0	0.09	0.375	0.246	0	0	0.3767	0		
							0.02	0.04	0.4943	0.0184		
							0.05	0.11	0.5272	0.0323		
							0.10	0.21	0.5279	0.0556		
							0.15	0.32	0.5345	0.0560		
							0.20	0.42	0.5493	0.0571		
							0.25	0.53	0.5390	0.0573		
							0.35	0.74	0.5371	0.1134		
							0.45	0.95	0.5497	0.1145		
							0.4746	1.00	0.5497	0.0285	0.533	
				0.19			0	0	0.3652	0		
							0.02	0.04	0.5101	0.0184		
							0.05	0.11	0.5204	0.0326		
							0.10	0.21	0.5299	0.0553		
							0.15	0.32	0.5445	0.0566		
							0.20	0.42	0.5408	0.0572		
							0.25	0.53	0.5399	0.0569		
							0.35	0.74	0.5397	0.1137		
							0.45	0.95	0.5378	0.1135		
							0.4746	1.00	0.5378	0.0279	0.532	
				0.29			0	0	0.3530	0		
							0.02	0.04	0.4647	0.0172		
							0.05	0.11	0.5223	0.0312		
							0.10	0.21	0.5392	0.0559		
							0.15	0.32	0.5364	0.0567		
							0.20	0.42	0.5377	0.0566		
							0.25	0.53	0.5353	0.0565		
							0.35	0.74	0.5369	0.1130		
							0.45	0.95	0.5233	0.1117		
							0.4746	1.00	0.5233	0.0271	0.526	0.094
			3.7	0.09	0.26	0.281	0	0	0.3848	0		
							0.02	0.04	0.5540	0.0199		
							0.05	0.11	0.6103	0.0370		
							0.10	0.21	0.6055	0.0644		
							0.15	0.32	0.6119	0.0645		
							0.20	0.42	0.6089	0.0647		
							0.25	0.53	0.6085	0.0645		
							0.35	0.74	0.6136	0.1295		
							0.45	0.95	0.6121	0.1298		
							0.472	1.00	0.6121	0.0285	0.603	
				0.17			0	0	0.3803	0		
							0.02	0.04	0.5629	0.0200		

Test Series	Q* (m^3/s)	ht (m)	X (m)	Z (m)	Z_b (m)	F	y (m)	y/Y	u (m/s)	Δu (m/s)	U (m/s)	Q (m^3/s)
							0.05	0.11	0.6058	0.0371		
							0.10	0.21	0.6147	0.0646		
							0.15	0.32	0.6082	0.0648		
							0.20	0.42	0.6200	0.0651		
							0.25	0.53	0.6171	0.0655		
							0.35	0.74	0.6091	0.1299		
							0.45	0.95	0.6196	0.1302		
							0.472	1.00	0.6196	0.0289	0.606	0.074
			4.375	0.07	0.14	0.329	0	0	0.4673	0		
							0.02	0.04	0.6680	0.0245		
							0.05	0.11	0.6995	0.0442		
							0.10	0.22	0.7067	0.0758		
							0.15	0.32	0.7314	0.0775		
							0.20	0.43	0.7173	0.0781		
							0.25	0.54	0.7063	0.0767		
							0.35	0.75	0.7082	0.1525		
							0.45	0.97	0.7016	0.1520		
							0.4639	1.00	0.7016	0.0210	0.702	0.046
10/0.15/0.40/A	0.178	0.29	-2.0	0.45	0.90	0.185	0	0	0.2035	0		
							0.02	0.04	0.3365	0.0110		
							0.05	0.10	0.4271	0.0234		
							0.10	0.20	0.3966	0.0420		
							0.15	0.31	0.4414	0.0428		
							0.20	0.41	0.4279	0.0444		
							0.25	0.51	0.4016	0.0423		
							0.35	0.71	0.4225	0.0841		
							0.45	0.92	0.3953	0.0835		
							0.4899	1.00	0.3953	0.0322	0.406	0.179
			1.5	0.16	0.635	0.249	0	0	0.3645	0		
							0.02	0.04	0.4905	0.0179		
							0.05	0.10	0.5365	0.0322		
							0.10	0.21	0.5668	0.0576		
							0.15	0.31	0.5570	0.0587		
							0.20	0.42	0.5733	0.0591		
							0.25	0.52	0.5647	0.0595		
							0.35	0.73	0.5642	0.1180		
							0.45	0.94	0.5631	0.1178		
							0.4785	1.00	0.5631	0.0335	0.554	
				0.32			0	0	0.3551	0		
							0.02	0.04	0.4707	0.0173		
							0.05	0.10	0.5197	0.0310		
							0.10	0.21	0.5577	0.0563		
							0.15	0.31	0.5713	0.0590		
							0.20	0.42	0.5643	0.0593		
							0.25	0.52	0.5693	0.0592		
							0.35	0.73	0.5540	0.1174		
							0.45	0.94	0.5599	0.1164		
							0.4785	1.00	0.5599	0.0264	0.542	
				0.48			0	0	0.3278	0		

Test Series	Q* (m³/s)	ht (m)	X (m)	Z (m)	Z_* (m)	F	y (m)	y/Y	u (m/s)	Δu (m/s)	U (m/s)	Q (m³/s)
							0.02	0.04	0.4684	0.0166		
							0.05	0.10	0.5040	0.0305		
							0.10	0.21	0.5344	0.0543		
							0.15	0.31	0.5228	0.0552		
							0.20	0.42	0.5175	0.0544		
							0.25	0.52	0.5449	0.0555		
							0.35	0.73	0.5419	0.1136		
							0.45	0.94	0.5287	0.1119		
							0.4785	1.00	0.5287	0.0313	0.523	0.164
			3.0	0.09	0.375	0.348	0	0	0.5223	0		
							0.02	0.04	0.7151	0.0267		
							0.05	0.11	0.7432	0.0473		
							0.10	0.22	0.7470	0.0805		
							0.15	0.32	0.7582	0.0813		
							0.20	0.43	0.7542	0.0817		
							0.25	0.54	0.7473	0.0811		
							0.35	0.76	0.7585	0.1627		
							0.44	0.95	0.7547	0.1471		
							0.463	1.00	0.7547	0.0372	0.746	
				0.19			0	0	0.5002	0		
							0.02	0.04	0.6864	0.0256		
							0.05	0.11	0.7483	0.0465		
							0.10	0.22	0.7623	0.0816		
							0.15	0.32	0.7564	0.0820		
							0.20	0.43	0.7607	0.0820		
							0.25	0.54	0.7714	0.0828		
							0.35	0.76	0.7603	0.1655		
							0.44	0.95	0.7510	0.1470		
							0.463	1.00	0.7510	0.0370	0.750	
				0.29			0	0	0.4865	0		
							0.02	0.04	0.6564	0.0247		
							0.05	0.11	0.7223	0.0447		
							0.10	0.22	0.7428	0.0791		
							0.15	0.32	0.7442	0.0803		
							0.20	0.43	0.7580	0.0811		
							0.25	0.54	0.7632	0.0822		
							0.35	0.76	0.7217	0.1604		
							0.44	0.95	0.7398	0.1421		
							0.463	1.00	0.7398	0.0364	0.731	0.129
			3.7	0.09	0.26	0.403	0	0	0.5622	0		
							0.02	0.04	0.8136	0.0302		
							0.05	0.11	0.8379	0.0543		
							0.10	0.22	0.8548	0.0928		
							0.15	0.33	0.8689	0.0945		
							0.20	0.44	0.8719	0.0955		
							0.25	0.55	0.8692	0.0955		
							0.35	0.77	0.8756	0.1914		
							0.43	0.94	0.8607	0.1523		
							0.4559	1.00	0.8607	0.0489	0.855	

Test Series	Q* (m^3/s)	ht (m)	X (m)	Z (m)	Z_b (m)	F	y (m)	y/Y	u (m/s)	Δu (m/s)	U (m/s)	Q (m^3/s)
				0.17			0	0	0.5530	0		
							0.02	0.04	0.7878	0.0294		
							0.05	0.11	0.8408	0.0536		
							0.10	0.22	0.8571	0.0931		
							0.15	0.33	0.8655	0.0945		
							0.20	0.44	0.8556	0.0944		
							0.25	0.55	0.8670	0.0945		
							0.35	0.77	0.8546	0.1888		
							0.43	0.94	0.8568	0.1502		
							0.4559	1.00	0.8568	0.0487	0.847	0.101
			4.375	0.07	0.14	0.480	0	0	0.6595	0		
							0.02	0.05	0.9232	0.0358		
							0.05	0.11	1.0081	0.0655		
							0.10	0.23	1.0027	0.1137		
							0.15	0.34	1.0271	0.1147		
							0.20	0.45	1.0368	0.1167		
							0.25	0.57	1.0133	0.1159		
							0.35	0.79	1.0132	0.2291		
							0.42	0.95	0.9948	0.1589		
							0.4423	1.00	0.9948	0.0502	1.000	0.062
10/0.15/0.50/A	0.216	0.26	-2.0	0.45	0.90	0.223	0	0	0.2958	0		
							0.02	0.04	0.4180	0.0143		
							0.05	0.10	0.4649	0.0264		
							0.10	0.20	0.4935	0.0478		
							0.15	0.30	0.5367	0.0514		
							0.20	0.40	0.5108	0.0523		
							0.25	0.50	0.5266	0.0518		
							0.35	0.70	0.4774	0.1002		
							0.45	0.90	0.5045	0.0980		
							0.501	1.00	0.5045	0.0513	0.493	0.222
			1.5	0.16	0.635	0.304	0	0	0.4462	0		
							0.02	0.04	0.6329	0.0223		
							0.05	0.10	0.6876	0.0409		
							0.10	0.21	0.6888	0.0710		
							0.15	0.31	0.6932	0.0713		
							0.20	0.41	0.6978	0.0717		
							0.25	0.52	0.6953	0.0719		
							0.35	0.72	0.6785	0.1417		
							0.45	0.93	0.6809	0.1402		
							0.4847	1.00	0.6809	0.0487	0.680	
				0.32			0	0	0.4224	0		
							0.02	0.04	0.6142	0.0214		
							0.05	0.10	0.6649	0.0396		
							0.10	0.21	0.6689	0.0688		
							0.15	0.31	0.6736	0.0692		
							0.20	0.41	0.6897	0.0703		
							0.25	0.52	0.7016	0.0718		
							0.35	0.72	0.6732	0.1418		
							0.45	0.93	0.6622	0.1378		

Test Series	Q* (m^3/s)	ht (m)	X (m)	Z (m)	Z_b (m)	F	y (m)	y/Y	u (m/s)	Δu (m/s)	U (m/s)	Q (m^3/s)
							0.4847	1.00	0.6622	0.0394	0.660	
				0.48			0	0	0.4380	0		
							0.02	0.04	0.5859	0.0211		
							0.05	0.10	0.5840	0.0362		
							0.10	0.21	0.6338	0.0628		
							0.15	0.31	0.6687	0.0672		
							0.20	0.41	0.6352	0.0673		
							0.25	0.52	0.6811	0.0679		
							0.35	0.72	0.6803	0.1404		
							0.45	0.93	0.6584	0.1381		
							0.4847	1.00	0.6584	0.0462	0.647	0.204
			3.0	0.09	0.375	0.426	0	0	0.6333	0		
							0.02	0.04	0.8771	0.0325		
							0.05	0.11	0.9149	0.0578		
							0.10	0.22	0.9183	0.0986		
							0.15	0.32	0.9243	0.0991		
							0.20	0.43	0.9341	0.1000		
							0.25	0.54	0.9444	0.1011		
							0.35	0.75	0.9136	0.1999		
							0.44	0.95	0.9242	0.1780		
							0.465	1.00	0.9242	0.0491	0.916	
				0.19			0	0	0.6445	0		
							0.02	0.04	0.8654	0.0325		
							0.05	0.11	0.9260	0.0578		
							0.10	0.22	0.9231	0.0995		
							0.15	0.32	0.9291	0.0996		
							0.20	0.43	0.9251	0.0998		
							0.25	0.54	0.9269	0.0996		
							0.35	0.75	0.9280	0.1996		
							0.44	0.95	0.9002	0.1770		
							0.465	1.00	0.9002	0.0478	0.913	
				0.29			0	0	0.6421	0		
							0.02	0.04	0.8323	0.0317		
							0.05	0.11	0.8599	0.0546		
							0.10	0.22	0.9094	0.0952		
							0.15	0.32	0.9246	0.0987		
							0.20	0.43	0.9103	0.0987		
							0.25	0.54	0.9275	0.0989		
							0.35	0.75	0.9211	0.1989		
							0.44	0.95	0.8830	0.1747		
							0.465	1.00	0.8830	0.0469	0.898	0.158
			3.7	0.09	0.26	0.497	0	0	0.6882	0		
							0.02	0.04	0.9963	0.0372		
							0.05	0.11	1.0391	0.0675		
							0.10	0.22	1.0651	0.1163		
							0.15	0.33	1.0693	0.1179		
							0.20	0.44	1.0651	0.1179		
							0.25	0.55	1.0676	0.1178		
							0.35	0.77	1.0666	0.2358		

Test Series	Q* (m³/s)	ht (m)	X (m)	Z (m)	Z_b (m)	F	y (m)	y/Y	u (m/s)	Δu (m/s)	U (m/s)	Q (m³/s)
							0.44	0.97	1.0619	0.2117		
							0.4525	1.00	1.0619	0.0293	1.051	
				0.17			0	0	0.6766	0		
							0.02	0.04	0.9569	0.0361		
							0.05	0.11	1.0387	0.0662		
							0.10	0.22	1.0534	0.1156		
							0.15	0.33	1.0737	0.1175		
							0.20	0.44	1.0575	0.1177		
							0.25	0.55	1.0706	0.1176		
							0.35	0.77	1.0491	0.2342		
							0.43	0.95	1.0477	0.1854		
							0.4525	1.00	1.0477	0.0521	1.042	0.123
			4.375	0.07	0.14	0.604	0	0	0.8827	0		
							0.02	0.05	1.1865	0.0479		
							0.05	0.12	1.2437	0.0843		
							0.10	0.23	1.2609	0.1448		
							0.15	0.35	1.2552	0.1455		
							0.20	0.46	1.2426	0.1444		
							0.25	0.58	1.2647	0.1450		
							0.35	0.81	1.2667	0.2927		
							0.40	0.93	1.2450	0.1452		
							0.4324	1.00	1.2450	0.0933	1.243	0.075
10/0.15/0.60/A	0.220	0.18	-2.0	0.45	0.90	0.275	0	0	0.3139	0		
							0.02	0.04	0.4893	0.0179		
							0.05	0.11	0.4922	0.0329		
							0.10	0.22	0.6023	0.0611		
							0.15	0.33	0.6034	0.0673		
							0.20	0.45	0.5988	0.0671		
							0.25	0.56	0.6019	0.0670		
							0.35	0.78	0.6023	0.1344		
							0.40	0.89	0.5837	0.0662		
							0.4479	1.00	0.5837	0.0624	0.576	0.232
			1.5	0.16	0.635	0.378	0	0	0.5542	0		
							0.02	0.05	0.7433	0.0303		
							0.05	0.12	0.7329	0.0517		
							0.10	0.23	0.8154	0.0903		
							0.15	0.35	0.8062	0.0946		
							0.20	0.47	0.8263	0.0952		
							0.25	0.58	0.8265	0.0964		
							0.35	0.82	0.8050	0.1903		
							0.40	0.93	0.7985	0.0935		
							0.4287	1.00	0.7985	0.0535	0.796	
				0.32			0	0	0.5189	0		
							0.02	0.05	0.6565	0.0274		
							0.05	0.12	0.7682	0.0498		
							0.10	0.23	0.7774	0.0901		
							0.15	0.35	0.7840	0.0911		
							0.20	0.47	0.8138	0.0932		
							0.25	0.58	0.8169	0.0951		

Test Series	Q* (m³/s)	ht (m)	X (m)	Z (m)	Z_b (m)	F	y (m)	y/Y	u (m/s)	Δu (m/s)	U (m/s)	Q (m³/s)
							0.35	0.82	0.8068	0.1894		
							0.40	0.93	0.7871	0.0929		
							0.4287	1.00	0.7871	0.0427	0.772	
				0.48			0	0	0.4872	0		
							0.02	0.05	0.6433	0.0264		
							0.05	0.12	0.6799	0.0463		
							0.10	0.23	0.7635	0.0842		
							0.15	0.35	0.7638	0.0891		
							0.20	0.47	0.7741	0.0897		
							0.25	0.58	0.7992	0.0917		
							0.35	0.82	0.8057	0.1872		
							0.40	0.93	0.7255	0.0893		
							0.4287	1.00	0.7255	0.0503	0.754	0.211
			3.0	0.09	0.375	0.546	0	0	0.7762	0		
							0.02	0.05	1.0391	0.0454		
							0.05	0.13	1.0581	0.0786		
							0.10	0.25	1.1039	0.1351		
							0.15	0.38	1.0896	0.1371		
							0.20	0.50	1.1071	0.1373		
							0.25	0.63	1.1025	0.1381		
							0.35	0.88	1.0995	0.2753		
							0.40	1.00	1.0995	0.1374	1.084	
				0.19			0	0	0.7741	0		
							0.02	0.05	1.0151	0.0447		
							0.05	0.13	1.0836	0.0787		
							0.10	0.25	1.0911	0.1359		
							0.15	0.38	1.1056	0.1373		
							0.20	0.50	1.1127	0.1386		
							0.25	0.63	1.1013	0.1384		
							0.35	0.88	1.0946	0.2745		
							0.4	1.00	1.0946	0.1368	1.085	
				0.29			0	0	0.7518	0		
							0.02	0.05	0.9832	0.0434		
							0.05	0.13	1.0593	0.0766		
							0.10	0.25	1.0940	0.1346		
							0.15	0.38	1.1089	0.1377		
							0.20	0.50	1.0888	0.1374		
							0.25	0.63	1.0964	0.1366		
							0.35	0.88	1.0864	0.2729		
							0.4	1.00	1.0864	0.1358	1.075	0.162
			3.7	0.09	0.26	0.647	0	0	0.8449	0		
							0.02	0.05	1.2088	0.0538		
							0.05	0.13	1.2282	0.0957		
							0.10	0.26	1.2601	0.1629		
							0.15	0.39	1.2825	0.1665		
							0.20	0.52	1.2742	0.1674		
							0.25	0.65	1.2834	0.1675		
							0.35	0.92	1.2646	0.3337		
							0.3818	1.00	1.2646	0.1053	1.253	

Test Series	Q* (m³/s)	ht (m)	X (m)	Z (m)	Z_b (m)	F	y (m)	y/Y	u (m/s)	Δu (m/s)	U (m/s)	Q (m³/s)
				0.17			0	0	0.8327	0		
							0.02	0.05	1.1564	0.0521		
							0.05	0.13	1.2381	0.0941		
							0.10	0.26	1.2802	0.1649		
							0.15	0.39	1.2717	0.1671		
							0.20	0.52	1.2733	0.1666		
							0.25	0.65	1.2847	0.1675		
							0.35	0.92	1.2537	0.3324		
							0.3818	1.00	1.2537	0.1044	1.249	0.124
			4.375	0.07	0.14	0.821	0	0	1.0590	0		
							0.02	0.06	1.4585	0.0719		
							0.05	0.14	1.5360	0.1284		
							0.10	0.29	1.5525	0.2207		
							0.15	0.43	1.5557	0.2221		
							0.20	0.57	1.5491	0.2218		
							0.25	0.71	1.5485	0.2213		
							0.32	0.91	1.5110	0.3060		
							0.3499	1.00	1.5110	0.1291	1.521	0.075

Table B-2.2: Experimental Velocity Data of Louver Array (Series *10/*/*/B*)

LEGEND

Q* = magmeter reading of the pump discharge	y = vertical depth of velocity measurement
ht = tailgate height	y/Y = vertical depth 'y' w.r.t. total flow depth
X = horizontal distance (datum = flume entrance)	u = velocity at depth 'y'
Z = transverse location of velocity measurement	Δu = incremental area of discharge for velocity 'u'
Z_b = bypass width of a transverse section	U = depth-averaged velocity of the profile
F = Froude number	Q = discharge of the section

Using *LabView* software: Sample number at each velocity 'u' = 200
Sampling rate at each velocity 'u' = 40 per second

NOTE: Velocity measurements re-done if standard deviation of samples > 0.025

Test Series	Q* (m^3/s)	ht (m)	X (m)	Z (m)	Z_b (m)	F	y (m)	y/Y	u (m/s)	Δu (m/s)	U (m/s)	Q (m^3/s)
10/0.05/0.30/B	0.129	0.325	-2.0	0.45	0.90	0.129	0	0	0.0902	0		
							0.02	0.04	0.2065	0.0060		
							0.05	0.10	0.2909	0.0151		
							0.10	0.20	0.2920	0.0296		
							0.15	0.30	0.2998	0.0300		
							0.20	0.41	0.3047	0.0307		
							0.25	0.51	0.2833	0.0298		
							0.35	0.71	0.2969	0.0589		
							0.45	0.91	0.2803	0.0586		
							0.4925	1.00	0.2803	0.0242	0.283	0.125
			1.5	0.16	0.635	0.178	0	0	0.2178	0		
							0.02	0.04	0.3395	0.0114		
							0.05	0.10	0.3930	0.0225		
							0.10	0.20	0.4227	0.0417		
							0.15	0.31	0.4079	0.0425		
							0.20	0.41	0.4093	0.0418		
							0.25	0.51	0.4162	0.0422		
							0.35	0.72	0.4174	0.0853		
							0.45	0.92	0.4105	0.0847		
							0.4887	1.00	0.4105	0.0325	0.405	
				0.32			0	0	0.2312	0		
							0.02	0.04	0.3526	0.0119		
							0.05	0.10	0.3835	0.0226		
							0.10	0.20	0.4091	0.0405		
							0.15	0.31	0.4081	0.0418		
							0.20	0.41	0.3956	0.0411		
							0.25	0.51	0.4087	0.0411		
							0.35	0.72	0.4065	0.0834		
							0.45	0.92	0.3903	0.0815		
							0.4887	1.00	0.3903	0.0239	0.388	
				0.48			0	0	0.2121	0		
							0.02	0.04	0.3022	0.0105		
							0.05	0.10	0.3772	0.0209		

Test Series	Q* (m^3/s)	ht (m)	X (m)	Z (m)	Z_b (m)	F	y (m)	y/Y	u (m/s)	Δu (m/s)	U (m/s)	Q (m^3/s)
							0.10	0.20	0.3482	0.0371		
							0.15	0.31	0.4015	0.0384		
							0.20	0.41	0.3944	0.0407		
							0.25	0.51	0.3922	0.0402		
							0.35	0.72	0.3880	0.0798		
							0.45	0.92	0.3806	0.0786		
							0.4887	1.00	0.3806	0.0289	0.375	0.121
			3.0	0.09	0.375	0.243	0	0	0.3504	0		
							0.02	0.04	0.4873	0.0175		
							0.05	0.10	0.5269	0.0318		
							0.10	0.21	0.5315	0.0553		
							0.15	0.31	0.5352	0.0558		
							0.20	0.42	0.5406	0.0563		
							0.25	0.52	0.5380	0.0564		
							0.35	0.73	0.5343	0.1121		
							0.45	0.94	0.5362	0.1120		
							0.4781	1.00	0.5362	0.0315	0.529	
				0.19			0	0	0.3292	0		
							0.02	0.04	0.4759	0.0168		
							0.05	0.10	0.5215	0.0313		
							0.10	0.21	0.5394	0.0555		
							0.15	0.31	0.5375	0.0563		
							0.20	0.42	0.5387	0.0563		
							0.25	0.52	0.5419	0.0565		
							0.35	0.73	0.5339	0.1125		
							0.45	0.94	0.5324	0.1115		
							0.4781	1.00	0.5324	0.0313	0.528	
				0.29			0	0	0.3274	0		
							0.02	0.04	0.4532	0.0163		
							0.05	0.10	0.4944	0.0297		
							0.10	0.21	0.5255	0.0533		
							0.15	0.31	0.5409	0.0558		
							0.20	0.42	0.5369	0.0564		
							0.25	0.52	0.5299	0.0558		
							0.35	0.73	0.5342	0.1113		
							0.45	0.94	0.5199	0.1102		
							0.4781	1.00	0.5199	0.0306	0.519	0.094
			4.0	0.07	0.205	0.289	0	0	0.4117	0		
							0.02	0.04	0.5866	0.0209		
							0.05	0.10	0.6016	0.0373		
							0.10	0.21	0.6112	0.0635		
							0.15	0.31	0.6396	0.0654		
							0.20	0.42	0.6339	0.0666		
							0.25	0.52	0.6442	0.0669		
							0.35	0.73	0.6387	0.1343		
							0.45	0.94	0.6404	0.1339		
							0.4778	1.00	0.6404	0.0373	0.626	
				0.14			0	0	0.3808	0		
							0.02	0.04	0.5606	0.0197		

Test Series	Q* (m^3/s)	ht (m)	X (m)	Z (m)	Z_b (m)	F	y (m)	y/Y	u (m/s)	Δu (m/s)	U (m/s)	Q (m^3/s)
							0.05	0.10	0.6147	0.0369		
							0.10	0.21	0.6234	0.0648		
							0.15	0.31	0.6331	0.0657		
							0.20	0.42	0.6343	0.0663		
							0.25	0.52	0.6398	0.0667		
							0.35	0.73	0.6429	0.1342		
							0.45	0.94	0.6346	0.1337		
							0.4778	1.00	0.6346	0.0369	0.625	0.061
			4.875	0.025	0.05	0.341	0	0	0.5158	0		
							0.02	0.04	0.7066	0.0263		
							0.05	0.11	0.7325	0.0464		
							0.10	0.22	0.7181	0.0780		
							0.15	0.32	0.7333	0.0780		
							0.20	0.43	0.7650	0.0805		
							0.25	0.54	0.7614	0.0820		
							0.35	0.75	0.7627	0.1638		
							0.45	0.97	0.6583	0.1528		
							0.4651	1.00	0.6583	0.0214	0.729	0.017
10/0.05/0.40/B	0.176	0.29	-2.0	0.45	0.90	0.094	0	0	0.1730	0		
							0.02	0.02	0.3065	0.0053		
							0.05	0.06	0.3871	0.0116		
							0.10	0.11	0.4027	0.0219		
							0.15	0.17	0.3924	0.0221		
							0.20	0.22	0.4111	0.0223		
							0.25	0.28	0.3822	0.0220		
							0.35	0.39	0.3958	0.0432		
							0.45	0.50	0.3750	0.0428		
							0.4849	0.54	0.3750	0.0145	0.206	0.090
			1.5	0.16	0.635	0.234	0	0	0.2822	0		
							0.02	0.04	0.4475	0.0152		
							0.05	0.10	0.5039	0.0298		
							0.10	0.21	0.5222	0.0535		
							0.15	0.31	0.5399	0.0554		
							0.20	0.42	0.5345	0.0560		
							0.25	0.52	0.5236	0.0552		
							0.35	0.73	0.5204	0.1088		
							0.45	0.94	0.5190	0.1084		
							0.4796	1.00	0.5190	0.0320	0.514	
				0.32			0	0	0.3286	0		
							0.02	0.04	0.4540	0.0163		
							0.05	0.10	0.5088	0.0301		
							0.10	0.21	0.5258	0.0539		
							0.15	0.31	0.5424	0.0557		
							0.20	0.42	0.5378	0.0563		
							0.25	0.52	0.5374	0.0560		
							0.35	0.73	0.5302	0.1113		
							0.45	0.94	0.4981	0.1072		
							0.4796	1.00	0.4981	0.0233	0.510	
				0.48			0	0	0.2559	0		

Test Series	Q* (m^3/s)	ht (m)	X (m)	Z (m)	Z_b (m)	F	y (m)	y/Y	u (m/s)	Δu (m/s)	U (m/s)	Q (m^3/s)
							0.02	0.04	0.4295	0.0143		
							0.05	0.10	0.4603	0.0278		
							0.10	0.21	0.4910	0.0496		
							0.15	0.31	0.5296	0.0532		
							0.20	0.42	0.5169	0.0546		
							0.25	0.52	0.5241	0.0543		
							0.35	0.73	0.5179	0.1086		
							0.45	0.94	0.5067	0.1068		
							0.4796	1.00	0.5067	0.0300	0.499	0.155
			3.0	0.09	0.375	0.317	0	0	0.4661	0		
							0.02	0.04	0.6376	0.0238		
							0.05	0.11	0.6587	0.0419		
							0.10	0.22	0.6817	0.0722		
							0.15	0.32	0.6803	0.0733		
							0.20	0.43	0.6864	0.0736		
							0.25	0.54	0.7017	0.0747		
							0.35	0.75	0.6916	0.1500		
							0.45	0.97	0.6806	0.1478		
							0.4643	1.00	0.6806	0.0210	0.678	
				0.19			0	0	0.4521	0		
							0.02	0.04	0.6473	0.0237		
							0.05	0.11	0.6786	0.0428		
							0.10	0.22	0.6896	0.0737		
							0.15	0.32	0.6881	0.0742		
							0.20	0.43	0.6930	0.0744		
							0.25	0.54	0.6924	0.0746		
							0.35	0.75	0.6871	0.1486		
							0.45	0.97	0.6797	0.1472		
							0.4643	1.00	0.6797	0.0209	0.680	
				0.29			0	0	0.4374	0		
							0.02	0.04	0.6168	0.0227		
							0.05	0.11	0.6584	0.0412		
							0.10	0.22	0.6868	0.0724		
							0.15	0.32	0.6713	0.0731		
							0.20	0.43	0.6928	0.0734		
							0.25	0.54	0.6785	0.0738		
							0.35	0.75	0.6872	0.1471		
							0.45	0.97	0.6722	0.1464		
							0.4643	1.00	0.6722	0.0207	0.671	0.118
			4.0	0.07	0.205	0.378	0	0	0.5434	0		
							0.02	0.04	0.7457	0.0281		
							0.05	0.11	0.7975	0.0504		
							0.10	0.22	0.7943	0.0867		
							0.15	0.33	0.8171	0.0877		
							0.20	0.44	0.8148	0.0888		
							0.25	0.54	0.8209	0.0891		
							0.35	0.76	0.8165	0.1783		
							0.45	0.98	0.8154	0.1777		
							0.4592	1.00	0.8154	0.0163	0.803	

Test Series	Q* (m^3/s)	ht (m)	X (m)	Z (m)	Z_o (m)	F	y (m)	y/Y	u (m/s)	Δu (m/s)	U (m/s)	Q (m^3/s)
				0.14			0	0	0.5151	0		
							0.02	0.04	0.7211	0.0269		
							0.05	0.11	0.7900	0.0494		
							0.10	0.22	0.8034	0.0867		
							0.15	0.33	0.8129	0.0880		
							0.20	0.44	0.8154	0.0886		
							0.25	0.54	0.8180	0.0889		
							0.35	0.76	0.8150	0.1778		
							0.45	0.98	0.8245	0.1785		
							0.4592	1.00	0.8245	0.0165	0.801	0.076
			4.875	0.025	0.05	0.461	0	0	0.7090	0		
							0.02	0.04	0.9328	0.0368		
							0.05	0.11	0.9449	0.0631		
							0.10	0.22	0.9770	0.1077		
							0.15	0.34	0.9784	0.1096		
							0.20	0.45	0.9835	0.1099		
							0.25	0.56	1.0107	0.1117		
							0.35	0.78	0.9932	0.2246		
							0.44	0.99	0.8803	0.1889		
							0.4462	1.00	0.8803	0.0122	0.965	0.022
10/0.05/0.50/B	0.214	0.25	-2.0	0.45	0.90	0.218	0	0	0.2729	0		
							0.02	0.04	0.4028	0.0135		
							0.05	0.10	0.4717	0.0261		
							0.10	0.20	0.4980	0.0483		
							0.15	0.30	0.4913	0.0493		
							0.20	0.40	0.5152	0.0501		
							0.25	0.50	0.5052	0.0508		
							0.35	0.70	0.4826	0.0984		
							0.45	0.90	0.4871	0.0966		
							0.5019	1.00	0.4871	0.0504	0.484	0.218
			1.5	0.16	0.635	0.291	0	0	0.4256	0		
							0.02	0.04	0.5817	0.0205		
							0.05	0.10	0.6446	0.0374		
							0.10	0.20	0.6590	0.0663		
							0.15	0.31	0.6722	0.0678		
							0.20	0.41	0.6778	0.0687		
							0.25	0.51	0.6644	0.0683		
							0.35	0.71	0.6726	0.1361		
							0.45	0.92	0.6578	0.1354		
							0.4912	1.00	0.6578	0.0552	0.656	
				0.32			0	0	0.3881	0		
							0.02	0.04	0.5641	0.0194		
							0.05	0.10	0.6340	0.0366		
							0.10	0.20	0.6656	0.0661		
							0.15	0.31	0.6702	0.0680		
							0.20	0.41	0.6680	0.0681		
							0.25	0.51	0.6434	0.0667		
							0.35	0.71	0.6734	0.1340		
							0.45	0.92	0.6563	0.1354		

Test Series	Q* (m^3/s)	ht (m)	X (m)	Z (m)	Z_b (m)	F	y (m)	y/Y	u (m/s)	Δu (m/s)	U (m/s)	Q (m^3/s)
							0.4912	1.00	0.6563	0.0444	0.639	
				0.48			0	0	0.4028	0		
							0.02	0.04	0.5664	0.0197		
							0.05	0.10	0.5902	0.0353		
							0.10	0.20	0.5926	0.0602		
							0.15	0.31	0.6616	0.0638		
							0.20	0.41	0.6318	0.0658		
							0.25	0.51	0.6522	0.0654		
							0.35	0.71	0.6317	0.1307		
							0.45	0.92	0.6140	0.1268		
							0.4912	1.00	0.6140	0.0508	0.619	0.199
			3.0	0.09	0.375	0.396	0	0	0.5964	0		
							0.02	0.04	0.7946	0.0295		
							0.05	0.11	0.8358	0.0519		
							0.10	0.21	0.8679	0.0904		
							0.15	0.32	0.8651	0.0920		
							0.20	0.42	0.8765	0.0924		
							0.25	0.53	0.8727	0.0928		
							0.35	0.74	0.8666	0.1846		
							0.45	0.96	0.8458	0.1817		
							0.4711	1.00	0.8458	0.0379	0.853	
				0.19			0	0	0.5596	0		
							0.02	0.04	0.8189	0.0293		
							0.05	0.11	0.8530	0.0532		
							0.10	0.21	0.8618	0.0910		
							0.15	0.32	0.8786	0.0924		
							0.20	0.42	0.8716	0.0929		
							0.25	0.53	0.8683	0.0923		
							0.35	0.74	0.8566	0.1831		
							0.45	0.96	0.8543	0.1816		
							0.4711	1.00	0.8543	0.0383	0.854	
				0.29			0	0	0.5817	0		
							0.02	0.04	0.7847	0.0290		
							0.05	0.11	0.8054	0.0506		
							0.10	0.21	0.8596	0.0884		
							0.15	0.32	0.8740	0.0920		
							0.20	0.42	0.8760	0.0929		
							0.25	0.53	0.8621	0.0922		
							0.35	0.74	0.8558	0.1823		
							0.45	0.96	0.8402	0.1800		
							0.4711	1.00	0.8402	0.0376	0.845	0.150
			4.0	0.07	0.205	0.475	0	0	0.6761	0		
							0.02	0.04	0.9563	0.0355		
							0.05	0.11	1.0011	0.0639		
							0.10	0.22	0.9994	0.1088		
							0.15	0.33	1.0182	0.1097		
							0.20	0.44	1.0275	0.1113		
							0.25	0.54	1.0338	0.1121		
							0.35	0.76	1.0167	0.2231		

Test Series	Q* (m³/s)	ht (m)	X (m)	Z (m)	Z_b (m)	F	y (m)	y/Y	u (m/s)	Δu (m/s)	U (m/s)	Q (m³/s)
							0.44	0.96	1.0236	0.1998		
							0.4596	1.00	1.0236	0.0437	1.008	
				0.14			0	0	0.6571	0		
							0.02	0.04	0.9397	0.0347		
							0.05	0.11	0.9964	0.0632		
							0.10	0.22	1.0150	0.1094		
							0.15	0.33	1.0125	0.1103		
							0.20	0.44	1.0292	0.1111		
							0.25	0.54	1.0236	0.1117		
							0.35	0.76	1.0195	0.2223		
							0.44	0.96	1.0278	0.2005		
							0.4596	1.00	1.0278	0.0438	1.007	0.095
			4.875	0.025	0.05	0.589	0	0	0.9435	0		
							0.02	0.05	1.1939	0.0489		
							0.05	0.11	1.2124	0.0826		
							0.10	0.23	1.2310	0.1398		
							0.15	0.34	1.2308	0.1409		
							0.20	0.46	1.2394	0.1414		
							0.25	0.57	1.2565	0.1429		
							0.35	0.80	1.2395	0.2857		
							0.42	0.96	1.1535	0.1917		
							0.4368	1.00	1.1535	0.0444	1.218	0.027
10/0.05/0.60/B	0.224	0.165	-2.0	0.45	0.90	0.278	0	0	0.3308	0		
							0.02	0.04	0.4610	0.0177		
							0.05	0.11	0.5365	0.0335		
							0.10	0.22	0.5986	0.0636		
							0.15	0.34	0.6013	0.0672		
							0.20	0.45	0.6017	0.0674		
							0.25	0.56	0.6176	0.0683		
							0.35	0.78	0.6000	0.1364		
							0.40	0.90	0.5869	0.0665		
							0.4462	1.00	0.5869	0.0608	0.582	0.234
			1.5	0.16	0.635	0.368	0	0	0.5172	0		
							0.02	0.05	0.7265	0.0286		
							0.05	0.12	0.7735	0.0518		
							0.10	0.23	0.7946	0.0902		
							0.15	0.35	0.8059	0.0921		
							0.20	0.46	0.7996	0.0924		
							0.25	0.58	0.8051	0.0924		
							0.35	0.81	0.7937	0.1840		
							0.40	0.92	0.7736	0.0902		
							0.4344	1.00	0.7736	0.0613	0.783	
				0.32			0	0	0.5117	0		
							0.02	0.05	0.6722	0.0273		
							0.05	0.12	0.7563	0.0493		
							0.10	0.23	0.7799	0.0884		
							0.15	0.35	0.7926	0.0905		
							0.20	0.46	0.8031	0.0918		
							0.25	0.58	0.8043	0.0925		

Test Series	Q* (m³/s)	ht (m)	X (m)	Z (m)	Z_o (m)	F	y (m)	y/Y	u (m/s)	Δu (m/s)	U (m/s)	Q (m³/s)
							0.35	0.81	0.7727	0.1815		
							0.40	0.92	0.7717	0.0889		
							0.4344	1.00	0.7717	0.0486	0.759	
				0.48			0	0	0.4547	0		
							0.02	0.05	0.6728	0.0260		
							0.05	0.12	0.7055	0.0476		
							0.10	0.23	0.7295	0.0826		
							0.15	0.35	0.7645	0.0860		
							0.20	0.46	0.7387	0.0865		
							0.25	0.58	0.7729	0.0870		
							0.35	0.81	0.7495	0.1752		
							0.40	0.92	0.7678	0.0873		
							0.4344	1.00	0.7678	0.0588	0.737	0.210
			3.0	0.09	0.375	0.511	0	0	0.7182	0		
							0.02	0.05	0.9675	0.0413		
							0.05	0.12	1.0264	0.0733		
							0.10	0.24	1.0328	0.1261		
							0.15	0.37	1.0417	0.1270		
							0.20	0.49	1.0524	0.1282		
							0.25	0.61	1.0502	0.1287		
							0.35	0.86	1.0415	0.2561		
							0.38	0.93	1.0244	0.0759		
							0.4083	1.00	1.0244	0.0710	1.028	
				0.19			0	0	0.7178	0		
							0.02	0.05	0.9744	0.0414		
							0.05	0.12	1.0076	0.0728		
							0.10	0.24	1.0466	0.1258		
							0.15	0.37	1.0507	0.1284		
							0.20	0.49	1.0473	0.1285		
							0.25	0.61	1.0505	0.1284		
							0.35	0.86	1.0239	0.2540		
							0.38	0.93	1.0313	0.0755		
							0.4083	1.00	1.0313	0.0715	1.026	
				0.29			0	0	0.7117	0		
							0.02	0.05	0.9516	0.0407		
							0.05	0.12	1.0039	0.0718		
							0.10	0.24	1.0284	0.1244		
							0.15	0.37	1.0412	0.1267		
							0.20	0.49	1.0421	0.1276		
							0.25	0.61	1.0397	0.1275		
							0.35	0.86	1.0189	0.2521		
							0.38	0.93	1.0083	0.0745		
							0.4083	1.00	1.0083	0.0699	1.015	0.157
			4.0	0.07	0.205	0.627	0	0	0.8601	0		
							0.02	0.05	1.1610	0.0515		
							0.05	0.13	1.2143	0.0907		
							0.10	0.25	1.2424	0.1564		
							0.15	0.38	1.2506	0.1587		
							0.20	0.51	1.2613	0.1599		

Test Series	Q* (m^3/s)	ht (m)	X (m)	Z (m)	Z_b (m)	F	y (m)	y/Y	u (m/s)	Δu (m/s)	U (m/s)	Q (m^3/s)
							0.25	0.64	1.2548	0.1602		
							0.35	0.89	1.2379	0.3174		
							0.3927	1.00	1.2379	0.1346	1.229	
				0.14			0	0	0.8222	0		
							0.02	0.05	1.1547	0.0503		
							0.05	0.13	1.2099	0.0903		
							0.10	0.25	1.2471	0.1564		
							0.15	0.38	1.2555	0.1593		
							0.20	0.51	1.2557	0.1599		
							0.25	0.64	1.2512	0.1596		
							0.35	0.89	1.2582	0.3195		
							0.3927	1.00	1.2582	0.1368	1.232	0.099
			4.875	0.025	0.05	0.791	0	0	1.1378	0		
							0.02	0.05	1.4289	0.0702		
							0.05	0.14	1.4825	0.1194		
							0.10	0.27	1.5124	0.2047		
							0.15	0.41	1.5222	0.2075		
							0.20	0.55	1.5262	0.2084		
							0.25	0.68	1.5217	0.2084		
							0.35	0.96	1.5115	0.4147		
							0.3657	1.00	1.5115	0.0649	1.498	0.027
10/0.10/0.30/B	0.132	0.305	-2.0	0.45	0.90	0.131	0	0.00	0.0919	0		
							0.02	0.04	0.1978	0.0062		
							0.05	0.11	0.2630	0.0149		
							0.10	0.22	0.2943	0.0300		
							0.15	0.32	0.2863	0.0312		
							0.20	0.43	0.2876	0.0309		
							0.25	0.54	0.3128	0.0323		
							0.35	0.75	0.2948	0.0654		
							0.40	0.86	0.2764	0.0307		
							0.4645	1.00	0.2764	0.0384	0.280	0.117
			1.5	0.16	0.635	0.180	0	0.00	0.2192	0		
							0.02	0.04	0.3614	0.0126		
							0.05	0.11	0.4026	0.0249		
							0.10	0.22	0.3975	0.0434		
							0.15	0.33	0.4155	0.0441		
							0.20	0.43	0.4200	0.0453		
							0.25	0.54	0.4086	0.0449		
							0.35	0.76	0.4108	0.0889		
							0.40	0.87	0.3978	0.0439		
							0.461	1.00	0.3978	0.0526	0.401	
				0.32			0	0.00	0.1969	0		
							0.02	0.04	0.3477	0.0118		
							0.05	0.11	0.3865	0.0239		
							0.10	0.22	0.3959	0.0424		
							0.15	0.33	0.3996	0.0431		
							0.20	0.43	0.4018	0.0435		
							0.25	0.54	0.4062	0.0438		
							0.35	0.76	0.3891	0.0863		

Test Series	Q* (m³/s)	ht (m)	X (m)	Z (m)	Z_b (m)	F	y (m)	y/Y	u (m/s)	Δu (m/s)	U (m/s)	Q (m³/s)
							0.40	0.87	0.4073	0.0432		
							0.461	1.00	0.4073	0.0397	0.378	
				0.48			0	0.00	0.1923	0		
							0.02	0.04	0.3415	0.0116		
							0.05	0.11	0.3505	0.0225		
							0.10	0.22	0.3663	0.0389		
							0.15	0.33	0.3807	0.0405		
							0.20	0.43	0.3705	0.0407		
							0.25	0.54	0.3783	0.0406		
							0.35	0.76	0.3864	0.0829		
							0.40	0.87	0.3878	0.0420		
							0.461	1.00	0.3878	0.0481	0.368	0.112
			3.0	0.09	0.375	0.246	0	0.00	0.339	0		
							0.02	0.04	0.4827	0.0182		
							0.05	0.11	0.5174	0.0332		
							0.10	0.22	0.5118	0.0569		
							0.15	0.33	0.5245	0.0573		
							0.20	0.44	0.5400	0.0588		
							0.25	0.55	0.5402	0.0597		
							0.35	0.77	0.5300	0.1183		
							0.40	0.88	0.5233	0.0582		
							0.4523	1.00	0.5233	0.0605	0.521	
				0.19			0	0.00	0.3578	0		
							0.02	0.04	0.4863	0.0187		
							0.05	0.11	0.5130	0.0331		
							0.10	0.22	0.5335	0.0578		
							0.15	0.33	0.5428	0.0595		
							0.20	0.44	0.5374	0.0597		
							0.25	0.55	0.5344	0.0592		
							0.35	0.77	0.5285	0.1175		
							0.40	0.88	0.5240	0.0582		
							0.4523	1.00	0.5240	0.0606	0.524	
				0.29			0	0.00	0.3306	0		
							0.02	0.04	0.4436	0.0171		
							0.05	0.11	0.5015	0.0313		
							0.10	0.22	0.5153	0.0562		
							0.15	0.33	0.5208	0.0573		
							0.20	0.44	0.5288	0.0580		
							0.25	0.55	0.5288	0.0585		
							0.35	0.77	0.5189	0.1158		
							0.40	0.88	0.5271	0.0578		
							0.4523	1.00	0.5271	0.0609	0.513	0.088
			3.8	0.08	0.245	0.285	0	0.00	0.3625	0		
							0.02	0.04	0.5543	0.0203		
							0.05	0.11	0.5937	0.0382		
							0.10	0.22	0.5938	0.0658		
							0.15	0.33	0.6055	0.0664		
							0.20	0.44	0.6119	0.0674		
							0.25	0.55	0.6078	0.0676		

Test Series	Q* (m^3/s)	ht (m)	X (m)	Z (m)	Z_o (m)	F	y (m)	y/Y	u (m/s)	Δu (m/s)	U (m/s)	Q (m^3/s)
							0.35	0.78	0.6148	0.1355		
							0.40	0.89	0.6097	0.0678		
							0.4513	1.00	0.6097	0.0693	0.598	
				0.16			0	0.00	0.3590	0		
							0.02	0.04	0.5437	0.0200		
							0.05	0.11	0.6025	0.0381		
							0.10	0.22	0.6109	0.0672		
							0.15	0.33	0.6122	0.0678		
							0.20	0.44	0.6125	0.0678		
							0.25	0.55	0.6096	0.0677		
							0.35	0.78	0.6058	0.1347		
							0.40	0.89	0.6029	0.0670		
							0.4513	1.00	0.6029	0.0685	0.599	0.066
			4.62	0.045	0.09	0.324	0	0.00	0.4212	0		
							0.02	0.05	0.6212	0.0236		
							0.05	0.11	0.6655	0.0437		
							0.10	0.23	0.6762	0.0760		
							0.15	0.34	0.6896	0.0773		
							0.20	0.45	0.6994	0.0787		
							0.25	0.57	0.6968	0.0791		
							0.35	0.79	0.6865	0.1567		
							0.40	0.91	0.6718	0.0769		
							0.4415	1.00	0.6718	0.0631	0.675	0.027
10/0.10/0.40/B	0.173	0.30	-2.0	0.45	0.90	0.171	0	0	0.1638	0		
							0.02	0.04	0.2800	0.0089		
							0.05	0.10	0.3349	0.0185		
							0.10	0.20	0.3846	0.0361		
							0.15	0.30	0.3838	0.0385		
							0.20	0.40	0.3965	0.0391		
							0.25	0.50	0.3970	0.0398		
							0.35	0.70	0.3960	0.0795		
							0.45	0.90	0.3924	0.0790		
							0.4987	1.00	0.3924	0.0383	0.378	0.170
			1.5	0.16	0.635	0.227	0	0	0.3143	0		
							0.02	0.04	0.4675	0.0159		
							0.05	0.10	0.4898	0.0292		
							0.10	0.20	0.4953	0.0501		
							0.15	0.31	0.5237	0.0518		
							0.20	0.41	0.5351	0.0538		
							0.25	0.51	0.5221	0.0537		
							0.35	0.71	0.5243	0.1064		
							0.45	0.92	0.5134	0.1055		
							0.4918	1.00	0.5134	0.0436	0.510	
				0.32			0	0	0.2952	0		
							0.02	0.04	0.4647	0.0155		
							0.05	0.10	0.4831	0.0289		
							0.10	0.20	0.5097	0.0505		
							0.15	0.31	0.5160	0.0521		
							0.20	0.41	0.5183	0.0526		

Test Series	Q* (m^3/s)	ht (m)	X (m)	Z (m)	Z_o (m)	F	y (m)	y/Y	u (m/s)	Δu (m/s)	U (m/s)	Q (m^3/s)
							0.25	0.51	0.5208	0.0528		
							0.35	0.71	0.5201	0.1058		
							0.45	0.92	0.5128	0.1050		
							0.4918	1.00	0.5128	0.0336	0.497	
				0.48			0	0	0.2781	0		
							0.02	0.04	0.4175	0.0141		
							0.05	0.10	0.4758	0.0272		
							0.10	0.20	0.5149	0.0504		
							0.15	0.31	0.4955	0.0514		
							0.20	0.41	0.5076	0.0510		
							0.25	0.51	0.5172	0.0521		
							0.35	0.71	0.5069	0.1041		
							0.45	0.92	0.4749	0.0998		
							0.4918	1.00	0.4749	0.0391	0.489	0.156
			3.0	0.09	0.375	0.309	0	0	0.4442	0		
							0.02	0.04	0.6174	0.0223		
							0.05	0.10	0.6713	0.0406		
							0.10	0.21	0.6779	0.0708		
							0.15	0.31	0.6886	0.0717		
							0.20	0.42	0.6813	0.0719		
							0.25	0.52	0.6738	0.0711		
							0.35	0.73	0.6824	0.1423		
							0.45	0.94	0.6649	0.1414		
							0.4765	1.00	0.6649	0.0370	0.669	
				0.19			0	0	0.4447	0		
							0.02	0.04	0.6336	0.0226		
							0.05	0.10	0.6748	0.0412		
							0.10	0.21	0.6826	0.0712		
							0.15	0.31	0.6898	0.0720		
							0.20	0.42	0.6839	0.0721		
							0.25	0.52	0.6892	0.0720		
							0.35	0.73	0.6834	0.1440		
							0.45	0.94	0.6750	0.1425		
							0.4765	1.00	0.6750	0.0375	0.675	
				0.29			0	0	0.4553	0		
							0.02	0.04	0.6157	0.0225		
							0.05	0.10	0.6740	0.0406		
							0.10	0.21	0.6737	0.0707		
							0.15	0.31	0.6742	0.0707		
							0.20	0.42	0.6749	0.0708		
							0.25	0.52	0.6739	0.0708		
							0.35	0.73	0.6696	0.1410		
							0.45	0.94	0.6551	0.1390		
							0.4765	1.00	0.6551	0.0364	0.662	0.119
			3.8	0.08	0.245	0.355	0	0	0.4966	0		
							0.02	0.04	0.6943	0.0252		
							0.05	0.11	0.7505	0.0459		
							0.10	0.21	0.7621	0.0801		
							0.15	0.32	0.7699	0.0811		

Test Series	Q* (m³/s)	ht (m)	X (m)	Z (m)	Z_b (m)	F	y (m)	y/Y	u (m/s)	Δu (m/s)	U (m/s)	Q (m³/s)
							0.20	0.42	0.7773	0.0819		
							0.25	0.53	0.7751	0.0822		
							0.35	0.74	0.7761	0.1642		
							0.45	0.95	0.7778	0.1645		
							0.4723	1.00	0.7778	0.0367	0.762	
				0.16			0	0	0.4835	0		
							0.02	0.04	0.7073	0.0252		
							0.05	0.11	0.7458	0.0461		
							0.10	0.21	0.7787	0.0807		
							0.15	0.32	0.7808	0.0825		
							0.20	0.42	0.7784	0.0825		
							0.25	0.53	0.7834	0.0827		
							0.35	0.74	0.7702	0.1645		
							0.45	0.95	0.7754	0.1636		
							0.4723	1.00	0.7754	0.0366	0.765	0.088
			4.62	0.045	0.09	0.407	0	0	0.5685	0		
							0.02	0.04	0.8008	0.0295		
							0.05	0.11	0.8494	0.0534		
							0.10	0.22	0.8660	0.0925		
							0.15	0.32	0.9073	0.0956		
							0.20	0.43	0.8988	0.0974		
							0.25	0.54	0.8847	0.0962		
							0.35	0.76	0.8770	0.1900		
							0.43	0.93	0.8588	0.1498		
							0.4635	1.00	0.8588	0.0621	0.867	0.036
10/0.10/0.50/B	0.213	0.25	-2.0	0.45	0.90	0.234	0	0	0.2251	0		
							0.02	0.04	0.4200	0.0132		
							0.05	0.10	0.4535	0.0268		
							0.10	0.20	0.5261	0.0500		
							0.15	0.31	0.5258	0.0537		
							0.20	0.41	0.5272	0.0538		
							0.25	0.51	0.5517	0.0551		
							0.35	0.72	0.5327	0.1108		
							0.45	0.92	0.5219	0.1077		
							0.4895	1.00	0.5219	0.0421	0.513	0.226
			1.5	0.16	0.635	0.306	0	0	0.4253	0		
							0.02	0.04	0.6464	0.0223		
							0.05	0.10	0.6562	0.0407		
							0.10	0.21	0.6690	0.0690		
							0.15	0.31	0.6952	0.0711		
							0.20	0.42	0.6895	0.0721		
							0.25	0.52	0.7026	0.0725		
							0.35	0.73	0.7024	0.1464		
							0.45	0.94	0.6826	0.1443		
							0.4799	1.00	0.6826	0.0425	0.681	
				0.32			0	0	0.3843	0		
							0.02	0.04	0.6011	0.0205		
							0.05	0.10	0.6540	0.0392		
							0.10	0.21	0.6980	0.0704		

Test Series	Q* (m^3/s)	ht (m)	X (m)	Z (m)	Z_o (m)	F	y (m)	y/Y	u (m/s)	Δu (m/s)	U (m/s)	Q (m^3/s)
							0.15	0.31	0.6776	0.0717		
							0.20	0.42	0.6952	0.0715		
							0.25	0.52	0.6787	0.0716		
							0.35	0.73	0.6682	0.1403		
							0.45	0.94	0.6739	0.1398		
							0.4799	1.00	0.6739	0.0420	0.667	
				0.48			0	0	0.4065	0		
							0.02	0.04	0.5715	0.0204		
							0.05	0.10	0.6250	0.0374		
							0.10	0.21	0.6481	0.0663		
							0.15	0.31	0.6499	0.0676		
							0.20	0.42	0.6464	0.0675		
							0.25	0.52	0.6498	0.0675		
							0.35	0.73	0.6769	0.1382		
							0.45	0.94	0.6388	0.1371		
							0.4799	1.00	0.6388	0.0398	0.642	0.202
			3.0	0.09	0.375	0.415	0	0	0.6315	0		
							0.02	0.04	0.8330	0.0319		
							0.05	0.11	0.8757	0.0558		
							0.10	0.22	0.8926	0.0963		
							0.15	0.33	0.8896	0.0970		
							0.20	0.44	0.9048	0.0977		
							0.25	0.54	0.8989	0.0982		
							0.35	0.76	0.8970	0.1956		
							0.43	0.94	0.8893	0.1556		
							0.4591	1.00	0.8893	0.0564	0.885	
				0.19			0	0	0.6145	0		
							0.02	0.04	0.8587	0.0321		
							0.05	0.11	0.8921	0.0572		
							0.10	0.22	0.8941	0.0973		
							0.15	0.33	0.9091	0.0982		
							0.20	0.44	0.9080	0.0989		
							0.25	0.54	0.8949	0.0982		
							0.35	0.76	0.8938	0.1948		
							0.43	0.94	0.8791	0.1545		
							0.4591	1.00	0.8791	0.0557	0.887	
				0.29			0	0	0.5593	0		
							0.02	0.04	0.7991	0.0296		
							0.05	0.11	0.8460	0.0537		
							0.10	0.22	0.8989	0.0950		
							0.15	0.33	0.9021	0.0981		
							0.20	0.44	0.8934	0.0978		
							0.25	0.54	0.8964	0.0975		
							0.35	0.76	0.8865	0.1942		
							0.43	0.94	0.8573	0.1519		
							0.4591	1.00	0.8573	0.0543	0.872	0.152
			3.8	0.08	0.245	0.480	0	0	0.6620	0		
							0.02	0.04	0.9217	0.0352		
							0.05	0.11	0.9899	0.0637		

Test Series	Q* (m³/s)	ht (m)	X (m)	Z (m)	Z_b (m)	F	y (m)	y/Y	u (m/s)	Δu (m/s)	U (m/s)	Q (m³/s)
							0.10	0.22	1.0132	0.1113		
							0.15	0.33	1.0281	0.1134		
							0.20	0.44	1.0349	0.1146		
							0.25	0.56	1.0319	0.1148		
							0.35	0.78	1.0219	0.2281		
							0.43	0.96	1.0180	0.1813		
							0.4501	1.00	1.0180	0.0455	1.008	
				0.16			0	0	0.6621	0		
							0.02	0.04	0.9314	0.0354		
							0.05	0.11	0.9988	0.0643		
							0.10	0.22	1.0148	0.1118		
							0.15	0.33	1.0216	0.1131		
							0.20	0.44	1.0392	0.1145		
							0.25	0.56	1.0296	0.1149		
							0.35	0.78	1.0273	0.2285		
							0.43	0.96	1.0134	0.1814		
							0.4501	1.00	1.0134	0.0453	1.009	0.111
			4.62	0.045	0.09	0.566	0	0	0.7610	0		
							0.02	0.05	1.0901	0.0425		
							0.05	0.11	1.1600	0.0776		
							0.10	0.23	1.1891	0.1350		
							0.15	0.34	1.1746	0.1358		
							0.20	0.46	1.1967	0.1363		
							0.25	0.57	1.2052	0.1380		
							0.35	0.80	1.1812	0.2742		
							0.40	0.92	1.1654	0.1348		
							0.4351	1.00	1.1654	0.0940	1.168	0.046
10/0.10/0.60/B	0.223	0.17	-2.0	0.45	0.90	0.279	0	0	0.3112	0		
							0.02	0.05	0.4927	0.0182		
							0.05	0.11	0.5299	0.0347		
							0.10	0.23	0.5726	0.0624		
							0.15	0.34	0.5794	0.0652		
							0.20	0.45	0.6194	0.0679		
							0.25	0.57	0.6330	0.0709		
							0.35	0.79	0.5937	0.1389		
							0.40	0.91	0.5922	0.0671		
							0.4417	1.00	0.5922	0.0559	0.581	0.231
			1.5	0.16	0.635	0.372	0	0	0.5279	0		
							0.02	0.05	0.7100	0.0289		
							0.05	0.12	0.7492	0.0510		
							0.10	0.23	0.7972	0.0901		
							0.15	0.35	0.8039	0.0933		
							0.20	0.47	0.8055	0.0938		
							0.25	0.58	0.8074	0.0940		
							0.35	0.82	0.7928	0.1865		
							0.40	0.93	0.7961	0.0926		
							0.429	1.00	0.7961	0.0538	0.784	
				0.32			0	0	0.4979	0		
							0.02	0.05	0.7443	0.0290		

Test Series	Q* (m³/s)	ht (m)	X (m)	Z (m)	Z_* (m)	F	y (m)	y/Y	u (m/s)	Δu (m/s)	U (m/s)	Q (m³/s)
							0.05	0.12	0.7379	0.0518		
							0.10	0.23	0.7584	0.0872		
							0.15	0.35	0.7562	0.0883		
							0.20	0.47	0.8135	0.0915		
							0.25	0.58	0.7787	0.0928		
							0.35	0.82	0.7909	0.1829		
							0.40	0.93	0.7698	0.0909		
							0.429	1.00	0.7698	0.0426	0.757	
				0.48			0	0	0.4894	0		
							0.02	0.05	0.6514	0.0266		
							0.05	0.12	0.7285	0.0482		
							0.10	0.23	0.7289	0.0849		
							0.15	0.35	0.758	0.0866		
							0.20	0.47	0.7816	0.0897		
							0.25	0.58	0.7705	0.0904		
							0.35	0.82	0.7709	0.1797		
							0.40	0.93	0.7838	0.0906		
							0.429	1.00	0.7838	0.0500	0.747	0.208
			3.0	0.09	0.375	0.518	0	0	0.6968	0		
							0.02	0.05	0.9767	0.0413		
							0.05	0.12	1.0281	0.0743		
							0.10	0.25	1.0423	0.1278		
							0.15	0.37	1.0369	0.1283		
							0.20	0.49	1.0686	0.1300		
							0.25	0.62	1.0608	0.1314		
							0.35	0.86	1.0327	0.2585		
							0.405	1.00	1.0327	0.1402	1.032	
				0.19			0	0	0.7306	0		
							0.02	0.05	0.9561	0.0416		
							0.05	0.12	1.0515	0.0744		
							0.10	0.25	1.0741	0.1312		
							0.15	0.37	1.0623	0.1319		
							0.20	0.49	1.0720	0.1317		
							0.25	0.62	1.0636	0.1318		
							0.35	0.86	1.0363	0.2592		
							0.405	1.00	1.0363	0.1407	1.043	
				0.29			0	0	0.7123	0		
							0.02	0.05	0.9508	0.0411		
							0.05	0.12	0.9829	0.0716		
							0.10	0.25	1.0267	0.1240		
							0.15	0.37	1.0470	0.1280		
							0.20	0.49	1.0544	0.1297		
							0.25	0.62	1.0561	0.1303		
							0.35	0.86	1.0370	0.2584		
							0.405	1.00	1.0370	0.1408	1.024	0.157
			3.8	0.08	0.245	0.610	0	0	0.7997	0		
							0.02	0.05	1.1450	0.0497		
							0.05	0.13	1.1825	0.0892		
							0.10	0.26	1.2125	0.1530		

Test Series	Q* (m³/s)	ht (m)	X (m)	Z (m)	Z_b (m)	F	y (m)	y/Y	u (m/s)	Δu (m/s)	U (m/s)	Q (m³/s)
							0.15	0.38	1.2150	0.1551		
							0.20	0.51	1.2216	0.1557		
							0.25	0.64	1.2198	0.1560		
							0.35	0.89	1.1897	0.3079		
							0.391	1.00	1.1897	0.1256	1.192	
				0.16			0	0	0.7926	0		
							0.02	0.05	1.1036	0.0485		
							0.05	0.13	1.1925	0.0880		
							0.10	0.26	1.2259	0.1545		
							0.15	0.38	1.2232	0.1565		
							0.20	0.51	1.2280	0.1566		
							0.25	0.64	1.2189	0.1563		
							0.35	0.89	1.2084	0.3102		
							0.391	1.00	1.2084	0.1275	1.198	0.115
			4.62	0.045	0.09	0.741	0	0	0.9718	0		
							0.02	0.05	1.3505	0.0634		
							0.05	0.14	1.4011	0.1127		
							0.10	0.27	1.4053	0.1915		
							0.15	0.41	1.4381	0.1941		
							0.20	0.55	1.4644	0.1981		
							0.25	0.68	1.4426	0.1984		
							0.33	0.90	1.3846	0.3087		
							0.3663	1.00	1.3846	0.1372	1.404	0.046
10/0.15/0.30/B	0.140	0.33	-2.0	0.45	0.90	0.138	0	0	0.1352	0		
							0.02	0.04	0.2706	0.0082		
							0.05	0.10	0.2722	0.0165		
							0.10	0.20	0.3106	0.0296		
							0.15	0.30	0.3100	0.0315		
							0.20	0.41	0.3352	0.0327		
							0.25	0.51	0.3176	0.0331		
							0.35	0.71	0.3167	0.0644		
							0.45	0.91	0.2939	0.0620		
							0.4927	1.00	0.2939	0.0255	0.303	0.135
			1.5	0.16	0.635	0.184	0	0	0.2373	0		
							0.02	0.04	0.3727	0.0125		
							0.05	0.10	0.3962	0.0236		
							0.10	0.20	0.4281	0.0421		
							0.15	0.31	0.4193	0.0433		
							0.20	0.41	0.4366	0.0437		
							0.25	0.51	0.416	0.0436		
							0.35	0.72	0.4253	0.0860		
							0.45	0.92	0.4146	0.0858		
							0.4892	1.00	0.4146	0.0332	0.414	
				0.32			0	0	0.2492	0		
							0.02	0.04	0.3736	0.0127		
							0.05	0.10	0.4236	0.0244		
							0.10	0.20	0.4145	0.0428		
							0.15	0.31	0.4232	0.0428		
							0.20	0.41	0.4254	0.0434		

Test Series	Q* (m^3/s)	ht (m)	X (m)	Z (m)	Z_b (m)	F	y (m)	y/Y	u (m/s)	Δu (m/s)	U (m/s)	Q (m^3/s)
							0.25	0.51	0.4223	0.0433		
							0.35	0.72	0.4197	0.0861		
							0.45	0.92	0.4171	0.0855		
							0.4892	1.00	0.4171	0.0253	0.406	
				0.48			0	0	0.2152	0		
							0.02	0.04	0.3274	0.0111		
							0.05	0.10	0.3836	0.0218		
							0.10	0.20	0.3954	0.0398		
							0.15	0.31	0.3722	0.0392		
							0.20	0.41	0.3945	0.0392		
							0.25	0.51	0.4078	0.0410		
							0.35	0.72	0.4016	0.0827		
							0.45	0.92	0.4030	0.0822		
							0.4892	1.00	0.4030	0.0303	0.387	0.125
			3.0	0.09	0.375	0.248	0	0	0.3530	0		
							0.02	0.04	0.5132	0.0181		
							0.05	0.10	0.5326	0.0328		
							0.10	0.21	0.5356	0.0558		
							0.15	0.31	0.5488	0.0566		
							0.20	0.42	0.5499	0.0574		
							0.25	0.52	0.5482	0.0573		
							0.35	0.73	0.5536	0.1151		
							0.45	0.94	0.5356	0.1138		
							0.4787	1.00	0.5356	0.0321	0.539	
				0.19			0	0	0.3517	0		
							0.02	0.04	0.4839	0.0175		
							0.05	0.10	0.5476	0.0323		
							0.10	0.21	0.5449	0.0571		
							0.15	0.31	0.5450	0.0569		
							0.20	0.42	0.5499	0.0572		
							0.25	0.52	0.5483	0.0574		
							0.35	0.73	0.5488	0.1146		
							0.45	0.94	0.5419	0.1139		
							0.4787	1.00	0.5419	0.0325	0.539	
				0.29			0	0	0.3242	0		
							0.02	0.04	0.4951	0.0171		
							0.05	0.10	0.5213	0.0318		
							0.10	0.21	0.5494	0.0559		
							0.15	0.31	0.5429	0.0570		
							0.20	0.42	0.5516	0.0572		
							0.25	0.52	0.5399	0.0570		
							0.35	0.73	0.5398	0.1128		
							0.45	0.94	0.5368	0.1125		
							0.4787	1.00	0.5368	0.0322	0.533	0.096
			3.7	0.09	0.26	0.277	0	0	0.3955	0		
							0.02	0.04	0.5590	0.0199		
							0.05	0.10	0.6000	0.0363		
							0.10	0.21	0.5938	0.0624		
							0.15	0.31	0.6021	0.0625		

Test Series	Q* (m³/s)	ht (m)	X (m)	Z (m)	Z_b (m)	F	y (m)	y/Y	u (m/s)	Δu (m/s)	U (m/s)	Q (m³/s)
							0.20	0.42	0.6152	0.0636		
							0.25	0.52	0.6166	0.0644		
							0.35	0.73	0.6085	0.1280		
							0.45	0.94	0.6039	0.1267		
							0.4785	1.00	0.6039	0.0360	0.600	
				0.17			0	0	0.3781	0		
							0.02	0.04	0.5516	0.0194		
							0.05	0.10	0.5928	0.0359		
							0.10	0.21	0.6153	0.0631		
							0.15	0.31	0.6224	0.0647		
							0.20	0.42	0.6134	0.0646		
							0.25	0.52	0.6124	0.0640		
							0.35	0.73	0.6146	0.1282		
							0.45	0.94	0.5953	0.1264		
							0.4785	1.00	0.5953	0.0355	0.602	0.075
			4.375	0.07	0.14	0.324	0	0	0.4635	0		
							0.02	0.04	0.6318	0.0233		
							0.05	0.11	0.6948	0.0423		
							0.10	0.21	0.7055	0.0744		
							0.15	0.32	0.7079	0.0751		
							0.20	0.43	0.7123	0.0755		
							0.25	0.53	0.7105	0.0756		
							0.35	0.74	0.7050	0.1505		
							0.45	0.96	0.6901	0.1483		
							0.4703	1.00	0.6901	0.0298	0.695	0.046
10/0.15/0.40/B	0.186	0.31	-2.0	0.45	0.90	0.179	0	0	0.2193	0		
							0.02	0.04	0.3379	0.0109		
							0.05	0.10	0.3567	0.0204		
							0.10	0.20	0.3994	0.0371		
							0.15	0.29	0.4045	0.0394		
							0.20	0.39	0.4201	0.0404		
							0.25	0.49	0.4129	0.0408		
							0.35	0.69	0.4146	0.0811		
							0.45	0.88	0.4134	0.0812		
							0.5101	1.00	0.4134	0.0487	0.400	0.184
			1.5	0.16	0.635	0.237	0	0	0.3546	0		
							0.02	0.04	0.5052	0.0171		
							0.05	0.10	0.5350	0.0310		
							0.10	0.20	0.5479	0.0537		
							0.15	0.30	0.555	0.0547		
							0.20	0.40	0.5488	0.0548		
							0.25	0.50	0.5606	0.0551		
							0.35	0.69	0.5527	0.1105		
							0.45	0.89	0.5392	0.1084		
							0.5038	1.00	0.5392	0.0576	0.543	
				0.32			0	0	0.3541	0		
							0.02	0.04	0.4877	0.0167		
							0.05	0.10	0.5344	0.0304		
							0.10	0.20	0.5643	0.0545		

Test Series	Q* (m^3/s)	ht (m)	X (m)	Z (m)	Z_o (m)	F	y (m)	y/Y	u (m/s)	Δu (m/s)	U (m/s)	Q (m^3/s)
							0.15	0.30	0.5559	0.0556		
							0.20	0.40	0.5591	0.0553		
							0.25	0.50	0.5632	0.0557		
							0.35	0.69	0.5405	0.1095		
							0.45	0.89	0.5405	0.1073		
							0.5038	1.00	0.5405	0.0451	0.530	
				0.48			0	0	0.3035	0		
							0.02	0.04	0.4426	0.0148		
							0.05	0.10	0.4627	0.0270		
							0.10	0.20	0.4905	0.0473		
							0.15	0.30	0.5236	0.0503		
							0.20	0.40	0.5263	0.0521		
							0.25	0.50	0.5135	0.0516		
							0.35	0.69	0.5318	0.1037		
							0.45	0.89	0.5320	0.1056		
							0.5038	1.00	0.5320	0.0543	0.507	0.168
			3.0	0.09	0.375	0.318	0	0	0.4842	0		
							0.02	0.04	0.6561	0.0233		
							0.05	0.10	0.6708	0.0407		
							0.10	0.20	0.705	0.0703		
							0.15	0.31	0.709	0.0723		
							0.20	0.41	0.7118	0.0726		
							0.25	0.51	0.7143	0.0729		
							0.35	0.72	0.7101	0.1456		
							0.45	0.92	0.6935	0.1435		
							0.489	1.00	0.6935	0.0553	0.697	
				0.19			0	0	0.4832	0		
							0.02	0.04	0.6707	0.0236		
							0.05	0.10	0.7124	0.0424		
							0.10	0.20	0.7226	0.0734		
							0.15	0.31	0.7147	0.0735		
							0.20	0.41	0.7183	0.0733		
							0.25	0.51	0.7114	0.0731		
							0.35	0.72	0.7112	0.1455		
							0.45	0.92	0.7004	0.1443		
							0.489	1.00	0.7004	0.0559	0.705	
				0.29			0	0	0.4684	0		
							0.02	0.04	0.6397	0.0227		
							0.05	0.10	0.6590	0.0398		
							0.10	0.20	0.7053	0.0697		
							0.15	0.31	0.714	0.0726		
							0.20	0.41	0.7145	0.0730		
							0.25	0.51	0.7022	0.0724		
							0.35	0.72	0.7002	0.1434		
							0.45	0.92	0.6986	0.1430		
							0.489	1.00	0.6986	0.0557	0.692	0.128
			3.7	0.09	0.26	0.359	0	0	0.5221	0		
							0.02	0.04	0.7358	0.0259		
							0.05	0.10	0.7710	0.0465		

Test Series	Q* (m³/s)	ht (m)	X (m)	Z (m)	Z_b (m)	F	y (m)	y/Y	u (m/s)	Δu (m/s)	U (m/s)	Q (m³/s)
							0.10	0.21	0.7858	0.0801		
							0.15	0.31	0.7944	0.0814		
							0.20	0.41	0.7918	0.0817		
							0.25	0.51	0.7957	0.0817		
							0.35	0.72	0.8016	0.1645		
							0.45	0.93	0.7893	0.1638		
							0.4856	1.00	0.7893	0.0579	0.783	
				0.17			0	0	0.5211	0		
							0.02	0.04	0.7446	0.0261		
							0.05	0.10	0.7741	0.0469		
							0.10	0.21	0.7939	0.0807		
							0.15	0.31	0.7979	0.0820		
							0.20	0.41	0.798	0.0822		
							0.25	0.51	0.7955	0.0820		
							0.35	0.72	0.7984	0.1641		
							0.45	0.93	0.7842	0.1630		
							0.4856	1.00	0.7842	0.0575	0.784	0.099
			4.375	0.07	0.14	0.423	0	0	0.6179	0		
							0.02	0.04	0.864	0.0313		
							0.05	0.11	0.8985	0.0558		
							0.10	0.21	0.9370	0.0968		
							0.15	0.32	0.9485	0.0995		
							0.20	0.42	0.9273	0.0990		
							0.25	0.53	0.9231	0.0976		
							0.35	0.74	0.9139	0.1939		
							0.45	0.95	0.9077	0.1922		
							0.4738	1.00	0.9077	0.0456	0.912	0.060
10/0.15/0.50/B	0.212	0.26	-2.0	0.45	0.90	0.228	0	0	0.2873	0		
							0.02	0.04	0.4037	0.0140		
							0.05	0.10	0.5119	0.0279		
							0.10	0.20	0.5252	0.0526		
							0.15	0.30	0.5356	0.0538		
							0.20	0.41	0.5211	0.0536		
							0.25	0.51	0.5123	0.0524		
							0.35	0.71	0.5142	0.1041		
							0.45	0.91	0.4846	0.1013		
							0.493	1.00	0.4846	0.0423	0.502	0.223
			1.5	0.16	0.635	0.297	0	0	0.4521	0		
							0.02	0.04	0.6248	0.0223		
							0.05	0.10	0.6675	0.0402		
							0.10	0.21	0.6709	0.0693		
							0.15	0.31	0.6843	0.0702		
							0.20	0.41	0.6861	0.0710		
							0.25	0.52	0.6719	0.0703		
							0.35	0.72	0.6710	0.1391		
							0.45	0.93	0.6615	0.1380		
							0.4828	1.00	0.6615	0.0449	0.665	
				0.32			0	0	0.4277	0		
							0.02	0.04	0.6222	0.0217		

Test Series	Q* (m^3/s)	ht (m)	X (m)	Z (m)	Z_b (m)	F	y (m)	y/Y	u (m/s)	Δu (m/s)	U (m/s)	Q (m^3/s)
							0.05	0.10	0.6373	0.0391		
							0.10	0.21	0.6826	0.0683		
							0.15	0.31	0.6797	0.0705		
							0.20	0.41	0.6779	0.0703		
							0.25	0.52	0.6802	0.0703		
							0.35	0.72	0.6567	0.1385		
							0.45	0.93	0.6560	0.1359		
							0.4828	1.00	0.6560	0.0357	0.650	
				0.48			0	0	0.3952	0		
							0.02	0.04	0.5848	0.0203		
							0.05	0.10	0.5924	0.0366		
							0.10	0.21	0.6077	0.0621		
							0.15	0.31	0.6258	0.0639		
							0.20	0.41	0.6481	0.0660		
							0.25	0.52	0.6386	0.0666		
							0.35	0.72	0.6557	0.1340		
							0.45	0.93	0.6273	0.1329		
							0.4828	1.00	0.6273	0.0418	0.624	0.198
			3.0	0.09	0.375	0.399	0	0	0.6044	0		
							0.02	0.04	0.8073	0.0304		
							0.05	0.11	0.8369	0.0532		
							0.10	0.22	0.8507	0.0909		
							0.15	0.32	0.8736	0.0929		
							0.20	0.43	0.8705	0.0940		
							0.25	0.54	0.8692	0.0937		
							0.35	0.75	0.8693	0.1873		
							0.44	0.95	0.8594	0.1677		
							0.464	1.00	0.8594	0.0445	0.855	
				0.19			0	0	0.5963	0		
							0.02	0.04	0.8328	0.0308		
							0.05	0.11	0.8609	0.0548		
							0.10	0.22	0.8635	0.0929		
							0.15	0.32	0.8750	0.0937		
							0.20	0.43	0.8677	0.0939		
							0.25	0.54	0.8653	0.0934		
							0.35	0.75	0.8604	0.1860		
							0.45	0.97	0.8466	0.1839		
							0.464	1.00	0.8466	0.0255	0.855	
				0.29			0	0	0.5723	0		
							0.02	0.04	0.7903	0.0294		
							0.05	0.11	0.8547	0.0532		
							0.10	0.22	0.8510	0.0919		
							0.15	0.32	0.8411	0.0912		
							0.20	0.43	0.8788	0.0927		
							0.25	0.54	0.8627	0.0938		
							0.35	0.75	0.8505	0.1846		
							0.45	0.97	0.8266	0.1807		
							0.464	1.00	0.8266	0.0249	0.842	0.148
			3.7	0.09	0.26	0.450	0	0	0.6119	0		

Test Series	Q* (m^3/s)	ht (m)	X (m)	Z (m)	Z_b (m)	F	y (m)	y/Y	u (m/s)	Δu (m/s)	U (m/s)	Q (m^3/s)
							0.02	0.04	0.9091	0.0334		
							0.05	0.11	0.9341	0.0606		
							0.10	0.22	0.9580	0.1038		
							0.15	0.33	0.9589	0.1051		
							0.20	0.44	0.9824	0.1065		
							0.25	0.55	0.9778	0.1075		
							0.35	0.77	0.9670	0.2133		
							0.44	0.97	0.9492	0.1891		
							0.4559	1.00	0.9492	0.0331	0.952	
				0.17			0	0	0.6022	0		
							0.02	0.04	0.8606	0.0321		
							0.05	0.11	0.9550	0.0597		
							0.10	0.22	0.9690	0.1055		
							0.15	0.33	0.9729	0.1065		
							0.20	0.44	0.9742	0.1068		
							0.25	0.55	0.9744	0.1069		
							0.35	0.77	0.9660	0.2128		
							0.44	0.97	0.9501	0.1891		
							0.4559	1.00	0.9501	0.0331	0.953	0.113
			4.375	0.07	0.14	0.539	0	0	0.7855	0		
							0.02	0.05	1.0700	0.0421		
							0.05	0.11	1.1209	0.0746		
							0.10	0.23	1.1476	0.1287		
							0.15	0.34	1.1584	0.1308		
							0.20	0.45	1.1584	0.1314		
							0.25	0.57	1.1399	0.1303		
							0.35	0.79	1.1090	0.2551		
							0.42	0.95	1.0964	0.1751		
							0.4408	1.00	1.0964	0.0517	1.120	0.069
10/0.15/0.60/B	0.224	0.20	-2.0	0.45	0.90	0.273	0	0	0.3555	0		
							0.02	0.04	0.4899	0.0186		
							0.05	0.11	0.5477	0.0343		
							0.10	0.22	0.5930	0.0628		
							0.15	0.33	0.6047	0.0659		
							0.20	0.44	0.5975	0.0662		
							0.25	0.55	0.6033	0.0661		
							0.35	0.77	0.5748	0.1297		
							0.40	0.88	0.5842	0.0638		
							0.4542	1.00	0.5842	0.0697	0.577	0.236
			1.5	0.16	0.635	0.357	0	0	0.5100	0		
							0.02	0.05	0.6736	0.0268		
							0.05	0.11	0.7454	0.0481		
							0.10	0.23	0.7686	0.0856		
							0.15	0.34	0.7789	0.0874		
							0.20	0.45	0.8011	0.0893		
							0.25	0.57	0.7926	0.0901		
							0.35	0.79	0.7769	0.1774		
							0.40	0.90	0.7600	0.0869		
							0.4424	1.00	0.7600	0.0728	0.764	

Test Series	Q* (m^3/s)	ht (m)	X (m)	Z (m)	Z_b (m)	F	y (m)	y/Y	u (m/s)	Δu (m/s)	U (m/s)	Q (m^3/s)
				0.32			0	0	0.5226	0		
							0.02	0.05	0.6904	0.0274		
							0.05	0.11	0.7271	0.0481		
							0.10	0.23	0.7802	0.0852		
							0.15	0.34	0.7813	0.0882		
							0.20	0.45	0.7944	0.0890		
							0.25	0.57	0.7826	0.0891		
							0.35	0.79	0.7830	0.1769		
							0.40	0.90	0.7667	0.0876		
							0.4424	1.00	0.7667	0.0590	0.751	
				0.48			0	0	0.4639	0		
							0.02	0.05	0.6559	0.0253		
							0.05	0.11	0.6606	0.0446		
							0.10	0.23	0.7027	0.0770		
							0.15	0.34	0.7431	0.0817		
							0.20	0.45	0.7420	0.0839		
							0.25	0.57	0.7538	0.0845		
							0.35	0.79	0.7410	0.1689		
							0.40	0.90	0.7362	0.0835		
							0.4424	1.00	0.7362	0.0682	0.718	0.209
			3.0	0.09	0.375	0.495	0	0	0.6871	0		
							0.02	0.05	0.9738	0.0399		
							0.05	0.12	0.9900	0.0708		
							0.10	0.24	1.0008	0.1196		
							0.15	0.36	1.0293	0.1219		
							0.20	0.48	1.0223	0.1232		
							0.25	0.60	1.0299	0.1233		
							0.35	0.84	1.0080	0.2448		
							0.40	0.96	0.9933	0.1202		
							0.4162	1.00	0.9933	0.0387	1.002	
				0.19			0	0	0.6819	0		
							0.02	0.05	0.9724	0.0397		
							0.05	0.12	0.9882	0.0707		
							0.10	0.24	1.0317	0.1213		
							0.15	0.36	1.0240	0.1235		
							0.20	0.48	1.0293	0.1233		
							0.25	0.60	1.0313	0.1238		
							0.35	0.84	1.0071	0.2449		
							0.40	0.96	1.0155	0.1215		
							0.4162	1.00	1.0155	0.0395	1.008	
				0.29			0	0	0.6818	0		
							0.02	0.05	0.9122	0.0383		
							0.05	0.12	0.9652	0.0677		
							0.10	0.24	1.0069	0.1185		
							0.15	0.36	0.9989	0.1205		
							0.20	0.48	1.0179	0.1211		
							0.25	0.60	1.0093	0.1218		
							0.35	0.84	1.0042	0.2419		
							0.40	0.96	1.0010	0.1204		

Test Series	Q* (m^3/s)	ht (m)	X (m)	Z (m)	Z_b (m)	F	y (m)	y/Y	u (m/s)	Δu (m/s)	U (m/s)	Q (m^3/s)
							0.4162	1.00	1.0010	0.0390	0.989	0.156
			3.7	0.09	0.26	0.570	0	0	0.7642	0		
							0.02	0.05	1.0853	0.0459		
							0.05	0.12	1.1279	0.0823		
							0.10	0.25	1.1438	0.1409		
							0.15	0.37	1.1503	0.1422		
							0.20	0.50	1.1611	0.1433		
							0.25	0.62	1.1471	0.1431		
							0.35	0.87	1.1426	0.2839		
							0.4032	1.00	1.1426	0.1508	1.132	
				0.17			0	0	0.7484	0		
							0.02	0.05	1.0510	0.0446		
							0.05	0.12	1.1279	0.0811		
							0.10	0.25	1.1581	0.1417		
							0.15	0.37	1.1645	0.1440		
							0.20	0.50	1.1453	0.1432		
							0.25	0.62	1.1557	0.1427		
							0.35	0.87	1.1405	0.2847		
							0.4032	1.00	1.1405	0.1505	1.133	0.119
			4.375	0.07	0.14	0.699	0	0	0.9559	0		
							0.02	0.05	1.2630	0.0581		
							0.05	0.13	1.3657	0.1033		
							0.10	0.26	1.3847	0.1801		
							0.15	0.39	1.3790	0.1810		
							0.20	0.52	1.3898	0.1813		
							0.25	0.65	1.3803	0.1814		
							0.35	0.92	1.3341	0.3555		
							0.3818	1.00	1.3341	0.1111	1.352	0.072

Table B-2.3: Experimental Velocity Data of Louver Array (Series *15/0.05/*/A*)

LEGEND	
Q* = magmeter reading of the pump discharge	y = vertical depth of velocity measurement
ht = tailgate height	y/Y = vertical depth 'y' w.r.t. total flow depth
X = horizontal distance (datum = flume entrance)	u = velocity at depth 'y'
Z = transverse location of velocity measurement	Δu = incremental area of discharge for velocity 'u'
Z_b = bypass width of a transverse section	U = depth-averaged velocity of the profile
F = Froude number	Q = discharge of the section
Using *LabView* software:	Sample number at each velocity 'u' = 200 Sampling rate at each velocity 'u' = 40 per second
NOTE: Velocity measurements re-done if standard deviation of samples > 0.025	

Test Series	Q* (m^3/s)	ht (m)	X (m)	Z (m)	Z_b (m)	F	y (m)	y/Y	u (m/s)	Δu (m/s)	U (m/s)	Q (m^3/s)
15/0.05/0.30/A	0.136	0.33	0	0.45	0.90	0.135	0	0	0.1515	0		
							0.02	0.04	0.2338	0.0078		
							0.05	0.10	0.2889	0.0159		
							0.10	0.20	0.3136	0.0305		
							0.15	0.30	0.3051	0.0313		
							0.20	0.40	0.3177	0.0315		
							0.25	0.51	0.3100	0.0317		
							0.35	0.71	0.3059	0.0623		
							0.45	0.91	0.2848	0.0598		
							0.4943	1.00	0.2848	0.0255	0.2962	0.1318
			1.0	0.22	0.67	0.171	0	0	0.2237	0		
							0.02	0.04	0.3417	0.0115		
							0.05	0.10	0.3661	0.0217		
							0.10	0.20	0.3898	0.0386		
							0.15	0.31	0.3917	0.0399		
							0.20	0.41	0.3939	0.0401		
							0.25	0.51	0.3835	0.0396		
							0.35	0.71	0.3829	0.0782		
							0.45	0.92	0.3809	0.0779		
							0.4902	1.00	0.3809	0.0312	0.3786	
				0.45			0	0	0.2358	0		
							0.02	0.04	0.3385	0.0117		
							0.05	0.10	0.3545	0.0212		
							0.10	0.20	0.3884	0.0379		
							0.15	0.31	0.3722	0.0388		
							0.20	0.41	0.3917	0.0390		
							0.25	0.51	0.3658	0.0386		
							0.35	0.71	0.3763	0.0757		
							0.45	0.92	0.3788	0.0770		
							0.4902	1.00	0.3788	0.0304	0.3703	0.1230
			2.0	0.13	0.37	0.243	0	0	0.3630	0		
							0.02	0.04	0.4933	0.0176		
							0.05	0.10	0.5104	0.0310		

Test Series	Q* (m^3/s)	ht (m)	X (m)	Z (m)	Z_b (m)	F	y (m)	y/Y	u (m/s)	Δu (m/s)	U (m/s)	Q (m^3/s)
							0.10	0.21	0.5210	0.0530		
							0.15	0.31	0.5339	0.0542		
							0.20	0.41	0.5363	0.0550		
							0.25	0.51	0.5324	0.0550		
							0.35	0.72	0.5252	0.1088		
							0.45	0.93	0.5254	0.1080		
							0.4862	1.00	0.5254	0.0391	0.5218	
				0.25			0	0	0.3315	0		
							0.02	0.04	0.4718	0.0165		
							0.05	0.10	0.5104	0.0303		
							0.10	0.21	0.5246	0.0532		
							0.15	0.31	0.5219	0.0538		
							0.20	0.41	0.5239	0.0538		
							0.25	0.51	0.5263	0.0540		
							0.35	0.72	0.5195	0.1075		
							0.45	0.93	0.5062	0.1055		
							0.4862	1.00	0.5062	0.0377	0.5123	0.0955
			2.75	0.06	0.18	0.303	0	0	0.4398	0		
							0.02	0.04	0.5901	0.0217		
							0.05	0.11	0.6412	0.0389		
							0.10	0.21	0.6544	0.0682		
							0.15	0.32	0.6622	0.0693		
							0.20	0.42	0.6687	0.0700		
							0.25	0.53	0.6714	0.0705		
							0.35	0.74	0.663	0.1405		
							0.45	0.95	0.6597	0.1392		
							0.475	1.00	0.6597	0.0347	0.6530	
				0.12			0	0	0.4163	0		
							0.02	0.04	0.6107	0.0216		
							0.05	0.11	0.6462	0.0397		
							0.10	0.21	0.6584	0.0687		
							0.15	0.32	0.6687	0.0698		
							0.20	0.42	0.6723	0.0706		
							0.25	0.53	0.6717	0.0707		
							0.35	0.74	0.6605	0.1402		
							0.45	0.95	0.6551	0.1385		
							0.475	1.00	0.6551	0.0345	0.6543	0.0559
			3.215	0.025	0.05	0.390	0	0	0.6353	0		
							0.02	0.04	0.7707	0.0303		
							0.05	0.11	0.8505	0.0524		
							0.10	0.22	0.8432	0.0912		
							0.15	0.32	0.8375	0.0905		
							0.20	0.43	0.8497	0.0909		
							0.25	0.54	0.8575	0.0919		
							0.35	0.75	0.8504	0.1840		
							0.45	0.97	0.7943	0.1772		
							0.4642	1.00	0.7943	0.0243	0.8326	0.0193
15/0.05/0.40/A	0.176	0.28	0	0.45	0.90	0.183	0	0	0.2346	0		
							0.02	0.04	0.3476	0.0119		

Test Series	Q* (m^3/s)	ht (m)	X (m)	Z (m)	Z_s (m)	F	y (m)	y/Y	u (m/s)	Δu (m/s)	U (m/s)	Q (m^3/s)
							0.05	0.10	0.383	0.0224		
							0.10	0.20	0.3873	0.0393		
							0.15	0.31	0.4315	0.0418		
							0.20	0.41	0.4205	0.0435		
							0.25	0.51	0.4157	0.0427		
							0.35	0.71	0.4035	0.0836		
							0.45	0.92	0.4089	0.0829		
							0.4899	1.00	0.4089	0.0333	0.4013	0.1769
			1.0	0.22	0.67	0.236	0	0	0.3407	0		
							0.02	0.04	0.4757	0.0169		
							0.05	0.10	0.5050	0.0304		
							0.10	0.21	0.5199	0.0529		
							0.15	0.31	0.5332	0.0544		
							0.20	0.41	0.5427	0.0555		
							0.25	0.52	0.5407	0.0559		
							0.35	0.72	0.5269	0.1102		
							0.45	0.93	0.5277	0.1089		
							0.4844	1.00	0.5277	0.0375	0.5224	
				0.45			0	0	0.3245	0		
							0.02	0.04	0.4351	0.0157		
							0.05	0.10	0.4982	0.0289		
							0.10	0.21	0.5138	0.0522		
							0.15	0.31	0.5313	0.0539		
							0.20	0.41	0.5228	0.0544		
							0.25	0.52	0.5267	0.0542		
							0.35	0.72	0.5080	0.1068		
							0.45	0.93	0.4927	0.1033		
							0.4844	1.00	0.4927	0.0348	0.5042	0.1666
			2.0	0.13	0.37	0.330	0	0	0.4880	0		
							0.02	0.04	0.6585	0.0241		
							0.05	0.11	0.6864	0.0425		
							0.10	0.21	0.7014	0.0730		
							0.15	0.32	0.7024	0.0739		
							0.20	0.42	0.6964	0.0736		
							0.25	0.53	0.7115	0.0741		
							0.35	0.74	0.7047	0.1490		
							0.45	0.95	0.7007	0.1479		
							0.4752	1.00	0.7007	0.0372	0.6951	
				0.25			0	0	0.4688	0		
							0.02	0.04	0.6434	0.0234		
							0.05	0.11	0.6804	0.0418		
							0.10	0.21	0.6987	0.0726		
							0.15	0.32	0.6943	0.0733		
							0.20	0.42	0.7047	0.0736		
							0.25	0.53	0.7049	0.0742		
							0.35	0.74	0.7022	0.1481		
							0.45	0.95	0.7009	0.1476		
							0.4752	1.00	0.7009	0.0372	0.6916	0.1252
			2.75	0.06	0.18	0.414	0	0	0.6154	0		

Test Series	Q* (m^3/s)	ht (m)	X (m)	Z (m)	Z_b (m)	F	y (m)	y/Y	u (m/s)	Δu (m/s)	U (m/s)	Q (m^3/s)
							0.02	0.04	0.8206	0.0314		
							0.05	0.11	0.8624	0.0552		
							0.10	0.22	0.8842	0.0954		
							0.15	0.33	0.8877	0.0968		
							0.20	0.44	0.8927	0.0973		
							0.25	0.55	0.8944	0.0977		
							0.35	0.77	0.8797	0.1939		
							0.44	0.96	0.8669	0.1718		
							0.458	1.00	0.8669	0.0332	0.8726	
				0.12			0	0	0.5977	0		
							0.02	0.04	0.8297	0.0312		
							0.05	0.11	0.8736	0.0558		
							0.10	0.22	0.888	0.0963		
							0.15	0.33	0.8984	0.0976		
							0.20	0.44	0.8901	0.0977		
							0.25	0.55	0.8991	0.0978		
							0.35	0.77	0.8964	0.1962		
							0.44	0.96	0.8827	0.1750		
							0.458	1.00	0.8827	0.0338	0.8814	0.0722
			3.215	0.025	0.05	0.536	0	0	0.8735	0		
							0.02	0.05	1.0891	0.0446		
							0.05	0.11	1.1288	0.0757		
							0.10	0.23	1.1421	0.1291		
							0.15	0.34	1.1505	0.1304		
							0.20	0.45	1.1228	0.1293		
							0.25	0.57	1.1418	0.1288		
							0.35	0.80	1.1113	0.2562		
							0.42	0.96	1.0447	0.1716		
							0.44	1.00	1.0447	0.0468	1.1124	0.0245
15/0.05/0.50/A	0.224	0.23	0	0.45	0.90	0.219	0	0	0.2971	0		
							0.02	0.04	0.4055	0.0140		
							0.05	0.10	0.4695	0.0262		
							0.10	0.20	0.5024	0.0486		
							0.15	0.30	0.5075	0.0505		
							0.20	0.40	0.5072	0.0507		
							0.25	0.50	0.4869	0.0497		
							0.35	0.70	0.5060	0.0992		
							0.45	0.90	0.4748	0.0980		
							0.50	1.00	0.4748	0.0477	0.4847	0.2182
			1.0	0.22	0.67	0.288	0	0	0.4287	0		
							0.02	0.04	0.5907	0.0208		
							0.05	0.10	0.6539	0.0380		
							0.10	0.20	0.6451	0.0662		
							0.15	0.31	0.6402	0.0655		
							0.20	0.41	0.6545	0.0659		
							0.25	0.51	0.6551	0.0667		
							0.35	0.71	0.6497	0.1329		
							0.45	0.92	0.6354	0.1309		
							0.4908	1.00	0.6354	0.0528	0.6398	

Test Series	Q* (m³/s)	ht (m)	X (m)	Z (m)	Z_b (m)	F	y (m)	y/Y	u (m/s)	Δu (m/s)	U (m/s)	Q (m³/s)
				0.45			0	0	0.4095	0		
							0.02	0.04	0.5847	0.0203		
							0.05	0.10	0.6035	0.0363		
							0.10	0.20	0.6434	0.0635		
							0.15	0.31	0.6457	0.0657		
							0.20	0.41	0.6432	0.0657		
							0.25	0.51	0.6378	0.0653		
							0.35	0.71	0.6361	0.1298		
							0.45	0.92	0.6069	0.1266		
							0.4908	1.00	0.6069	0.0504	0.6235	0.2077
			2.0	0.13	0.37	0.412	0	0	0.6057	0		
							0.02	0.04	0.8386	0.0305		
							0.05	0.11	0.8526	0.0536		
							0.10	0.21	0.8578	0.0904		
							0.15	0.32	0.8870	0.0922		
							0.20	0.42	0.8851	0.0936		
							0.25	0.53	0.8831	0.0934		
							0.35	0.74	0.8835	0.1867		
							0.45	0.95	0.8627	0.1845		
							0.4731	1.00	0.8627	0.0421	0.8672	
				0.25			0	0	0.6099	0		
							0.02	0.04	0.7914	0.0296		
							0.05	0.11	0.8586	0.0523		
							0.10	0.21	0.8792	0.0918		
							0.15	0.32	0.8711	0.0925		
							0.20	0.42	0.8838	0.0927		
							0.25	0.53	0.8781	0.0931		
							0.35	0.74	0.8608	0.1838		
							0.45	0.95	0.8568	0.1815		
							0.4731	1.00	0.8568	0.0418	0.8592	0.1552
			2.75	0.06	0.18	0.534	0	0	0.7552	0		
							0.02	0.04	1.0785	0.0412		
							0.05	0.11	1.1149	0.0739		
							0.10	0.22	1.1135	0.1251		
							0.15	0.34	1.1403	0.1265		
							0.20	0.45	1.1436	0.1282		
							0.25	0.56	1.1333	0.1278		
							0.35	0.79	1.1361	0.2548		
							0.43	0.97	1.1205	0.2027		
							0.445	1.00	1.1205	0.0387	1.1188	
				0.12			0	0	0.7455	0		
							0.02	0.04	1.0511	0.0403		
							0.05	0.11	1.1035	0.0726		
							0.10	0.22	1.1321	0.1255		
							0.15	0.34	1.1333	0.1272		
							0.20	0.45	1.1340	0.1273		
							0.25	0.56	1.1303	0.1271		
							0.35	0.79	1.1313	0.2539		
							0.43	0.97	1.1200	0.2022		

Test Series	Q* (m^3/s)	ht (m)	X (m)	Z (m)	Z_b (m)	F	y (m)	y/Y	u (m/s)	Δu (m/s)	U (m/s)	Q (m^3/s)
							0.445	1.00	1.1200	0.0387	1.1147	0.0895
			3.215	0.025	0.05	0.720	0	0	1.2459	0		
							0.02	0.05	1.4403	0.0634		
							0.05	0.12	1.5019	0.1041		
							0.10	0.24	1.5002	0.1771		
							0.15	0.35	1.5077	0.1774		
							0.20	0.47	1.4965	0.1772		
							0.25	0.59	1.5043	0.1770		
							0.35	0.83	1.4673	0.3505		
							0.42	0.99	1.3041	0.2288		
							0.4239	1.00	1.3041	0.0120	1.4674	0.0311

Table B-2.4: Experimental Velocity Data of Louver Array (Series *15/0.05/*/B*)

LEGEND

Q* = magmeter reading of the pump discharge	y = vertical depth of velocity measurement
ht = tailgate height	y/Y = vertical depth 'y' w.r.t. total flow depth
X = horizontal distance (datum = flume entrance)	u = velocity at depth 'y'
Z = transverse location of velocity measurement	Δu = incremental area of discharge for velocity 'u'
Z_b = bypass width of a transverse section	U = depth-averaged velocity of the profile
F = Froude number	Q = discharge of the section

Using *LabView* software: Sample number at each velocity 'u' = 200
Sampling rate at each velocity 'u' = 40 per second

NOTE: Velocity measurements re-done if standard deviation of samples > 0.025

Test Series	Q* (m^3/s)	ht (m)	X (m)	Z (m)	Z_b (m)	F	y (m)	y/Y	u (m/s)	Δu (m/s)	U (m/s)	Q (m^3/s)
15/0.05/0.30/B	0.136	0.33	0	0.45	0.90	0.135	0	0	0.1552	0		
							0.02	0.04	0.2335	0.0079		
							0.05	0.10	0.2835	0.0159		
							0.10	0.20	0.2856	0.0291		
							0.15	0.31	0.2952	0.0297		
							0.20	0.41	0.3079	0.0308		
							0.25	0.51	0.3211	0.0321		
							0.35	0.72	0.2957	0.0630		
							0.45	0.92	0.3065	0.0615		
							0.4892	1.00	0.3065	0.0246	0.2947	0.1297
			1.0	0.22	0.67	0.170	0	0	0.2257	0		
							0.02	0.04	0.3622	0.0121		
							0.05	0.10	0.3608	0.0223		
							0.10	0.21	0.3942	0.0388		
							0.15	0.31	0.3853	0.0401		
							0.20	0.41	0.3972	0.0402		
							0.25	0.51	0.3941	0.0407		
							0.35	0.72	0.3953	0.0811		
							0.45	0.92	0.3771	0.0794		
							0.4865	1.00	0.3771	0.0283	0.3829	
				0.45			0	0	0.1885	0		
							0.02	0.04	0.3186	0.0104		
							0.05	0.10	0.3393	0.0203		
							0.10	0.21	0.3663	0.0363		
							0.15	0.31	0.3561	0.0371		
							0.20	0.41	0.3755	0.0376		
							0.25	0.51	0.3823	0.0389		
							0.35	0.72	0.3740	0.0777		
							0.45	0.92	0.3745	0.0769		
							0.4865	1.00	0.3745	0.0259	0.3612	0.1213
			2.0	0.13	0.38	0.221	0	0	0.3171	0		
							0.02	0.04	0.4428	0.0157		
							0.05	0.10	0.4771	0.0286		

Test Series	Q* (m^3/s)	ht (m)	X (m)	Z (m)	Z_o (m)	F	y (m)	y/Y	u (m/s)	Δu (m/s)	U (m/s)	Q (m^3/s)
							0.10	0.21	0.4894	0.0500		
							0.15	0.31	0.4809	0.0502		
							0.20	0.41	0.4921	0.0504		
							0.25	0.52	0.4923	0.0510		
							0.35	0.72	0.4857	0.1013		
							0.45	0.93	0.4929	0.1013		
							0.4829	1.00	0.4929	0.0336	0.4821	
				0.25			0	0	0.3038	0		
							0.02	0.04	0.424	0.0151		
							0.05	0.10	0.4716	0.0278		
							0.10	0.21	0.4915	0.0499		
							0.15	0.31	0.494	0.0510		
							0.20	0.41	0.5002	0.0515		
							0.25	0.52	0.4945	0.0515		
							0.35	0.72	0.4827	0.1012		
							0.45	0.93	0.4849	0.1002		
							0.4829	1.00	0.4849	0.0330	0.4811	0.0884
			2.75	0.06	0.18	0.263	0	0	0.3708	0		
							0.02	0.04	0.5257	0.0188		
							0.05	0.11	0.5518	0.0340		
							0.10	0.21	0.5621	0.0586		
							0.15	0.32	0.5764	0.0598		
							0.20	0.42	0.5754	0.0605		
							0.25	0.53	0.5872	0.0611		
							0.35	0.74	0.5855	0.1233		
							0.45	0.95	0.5759	0.1221		
							0.4756	1.00	0.5759	0.0310	0.5693	
				0.12			0	0	0.3409	0		
							0.02	0.04	0.5058	0.0178		
							0.05	0.11	0.5571	0.0335		
							0.10	0.21	0.571	0.0593		
							0.15	0.32	0.5818	0.0606		
							0.20	0.42	0.5768	0.0609		
							0.25	0.53	0.5809	0.0609		
							0.35	0.74	0.5775	0.1218		
							0.45	0.95	0.5803	0.1217		
							0.4756	1.00	0.5803	0.0312	0.5677	0.0487
			3.215	0.025	0.05	0.329	0	0	0.5377	0		
							0.02	0.04	0.6674	0.0259		
							0.05	0.11	0.7149	0.0446		
							0.10	0.21	0.6852	0.0752		
							0.15	0.32	0.7205	0.0755		
							0.20	0.43	0.7152	0.0771		
							0.25	0.54	0.7323	0.0778		
							0.35	0.75	0.7224	0.1563		
							0.45	0.97	0.6613	0.1487		
							0.4653	1.00	0.6613	0.0217	0.7029	0.0164
15/0.05/0.40/B	0.176	0.28	0	0.45	0.90	0.187	0	0	0.2377	0		
							0.02	0.04	0.3491	0.0123		

Test Series	Q* (m^3/s)	ht (m)	X (m)	Z (m)	Z_o (m)	F	y (m)	y/Y	u (m/s)	Δu (m/s)	U (m/s)	Q (m^3/s)
							0.05	0.10	0.3868	0.0231		
							0.10	0.21	0.4088	0.0417		
							0.15	0.31	0.4269	0.0438		
							0.20	0.42	0.4243	0.0446		
							0.25	0.52	0.4245	0.0445		
							0.35	0.73	0.4057	0.0870		
							0.45	0.94	0.3967	0.0841		
							0.4773	1.00	0.3967	0.0227	0.4036	0.1734
			1.0	0.22	0.67	0.234	0	0	0.3292	0		
							0.02	0.04	0.4665	0.0169		
							0.05	0.11	0.4895	0.0304		
							0.10	0.21	0.5207	0.0536		
							0.15	0.32	0.5202	0.0552		
							0.20	0.42	0.5350	0.0560		
							0.25	0.53	0.5376	0.0569		
							0.35	0.74	0.5059	0.1107		
							0.45	0.95	0.5119	0.1080		
							0.4713	1.00	0.5119	0.0231	0.5108	
				0.45			0	0	0.3164	0		
							0.02	0.04	0.4351	0.0159		
							0.05	0.11	0.4802	0.0291		
							0.10	0.21	0.5126	0.0527		
							0.15	0.32	0.5271	0.0552		
							0.20	0.42	0.5107	0.0550		
							0.25	0.53	0.5218	0.0548		
							0.35	0.74	0.4955	0.1079		
							0.45	0.95	0.4779	0.1033		
							0.4713	1.00	0.4779	0.0205	0.4944	0.1587
			2.0	0.13	0.38	0.303	0	0	0.4275	0		
							0.02	0.04	0.5807	0.0217		
							0.05	0.11	0.6526	0.0398		
							0.10	0.22	0.6537	0.0703		
							0.15	0.32	0.6604	0.0707		
							0.20	0.43	0.6627	0.0712		
							0.25	0.54	0.6648	0.0714		
							0.35	0.75	0.6592	0.1425		
							0.45	0.97	0.6612	0.1421		
							0.4645	1.00	0.6612	0.0206	0.6505	
				0.25			0	0	0.4235	0		
							0.02	0.04	0.5980	0.0220		
							0.05	0.11	0.6227	0.0394		
							0.10	0.22	0.6423	0.0681		
							0.15	0.32	0.6570	0.0699		
							0.20	0.43	0.6575	0.0707		
							0.25	0.54	0.6581	0.0708		
							0.35	0.75	0.6574	0.1416		
							0.45	0.97	0.6420	0.1399		
							0.4645	1.00	0.6420	0.0200	0.6425	0.1141
			2.75	0.06	0.18	0.363	0	0	0.5110	0		

Test Series	Q* (m³/s)	ht (m)	X (m)	Z (m)	Z_o (m)	F	y (m)	y/Y	u (m/s)	Δu (m/s)	U (m/s)	Q (m³/s)
							0.02	0.04	0.7238	0.0272		
							0.05	0.11	0.7542	0.0489		
							0.10	0.22	0.7589	0.0834		
							0.15	0.33	0.7752	0.0845		
							0.20	0.44	0.7855	0.0860		
							0.25	0.55	0.7832	0.0864		
							0.35	0.77	0.7848	0.1728		
							0.44	0.97	0.7587	0.1531		
							0.4537	1.00	0.7587	0.0229	0.7652	
				0.12			0	0	0.4998	0		
							0.02	0.04	0.6898	0.0262		
							0.05	0.11	0.7435	0.0474		
							0.10	0.22	0.7647	0.0831		
							0.15	0.33	0.7752	0.0849		
							0.20	0.44	0.7731	0.0853		
							0.25	0.55	0.7828	0.0857		
							0.35	0.77	0.7770	0.1719		
							0.44	0.97	0.7954	0.1560		
							0.4537	1.00	0.7954	0.0240	0.7645	0.0625
			3.215	0.025	0.05	0.453	0	0	0.7590	0		
							0.02	0.04	0.9163	0.0377		
							0.05	0.11	0.9859	0.0642		
							0.10	0.22	0.9571	0.1092		
							0.15	0.34	0.9793	0.1089		
							0.20	0.45	0.9600	0.1090		
							0.25	0.56	0.9777	0.1089		
							0.35	0.79	0.9559	0.2174		
							0.43	0.97	0.8575	0.1631		
							0.4447	1.00	0.8575	0.0283	0.9467	0.0211
15/0.05/0.50/B	0.224	0.23	0	0.45	0.90	0.238	0	0	0.3100	0		
							0.02	0.04	0.4240	0.0152		
							0.05	0.10	0.4779	0.0280		
							0.10	0.21	0.5257	0.0520		
							0.15	0.31	0.5476	0.0556		
							0.20	0.41	0.5582	0.0573		
							0.25	0.52	0.5423	0.0570		
							0.35	0.72	0.5389	0.1120		
							0.45	0.93	0.5016	0.1078		
							0.4828	1.00	0.5016	0.0341	0.5188	0.2254
			1.0	0.22	0.67	0.300	0	0	0.4151	0		
							0.02	0.04	0.5979	0.0214		
							0.05	0.11	0.6338	0.0390		
							0.10	0.21	0.6657	0.0685		
							0.15	0.32	0.6843	0.0712		
							0.20	0.42	0.6698	0.0714		
							0.25	0.53	0.6674	0.0705		
							0.35	0.74	0.6647	0.1405		
							0.45	0.95	0.6579	0.1395		
							0.4742	1.00	0.6579	0.0336	0.6554	

Test Series	Q* (m³/s)	ht (m)	X (m)	Z (m)	Z_o (m)	F	y (m)	y/Y	u (m/s)	Δu (m/s)	U (m/s)	Q (m³/s)
				0.45			0	0	0.4033	0		
							0.02	0.04	0.5495	0.0201		
							0.05	0.11	0.6107	0.0367		
							0.10	0.21	0.6476	0.0663		
							0.15	0.32	0.6674	0.0693		
							0.20	0.42	0.6520	0.0696		
							0.25	0.53	0.6592	0.0691		
							0.35	0.74	0.6579	0.1389		
							0.45	0.95	0.6313	0.1359		
							0.4742	1.00	0.6313	0.0306	0.6366	0.2052
			2.0	0.13	0.38	0.392	0	0	0.5684	0		
							0.02	0.04	0.7867	0.0294		
							0.05	0.11	0.8225	0.0523		
							0.10	0.22	0.8453	0.0903		
							0.15	0.32	0.8499	0.0918		
							0.20	0.43	0.8586	0.0925		
							0.25	0.54	0.8549	0.0928		
							0.35	0.76	0.8347	0.1830		
							0.44	0.95	0.8377	0.1630		
							0.4616	1.00	0.8377	0.0392	0.8344	
				0.25			0	0	0.5737	0		
							0.02	0.04	0.7756	0.0292		
							0.05	0.11	0.8152	0.0517		
							0.10	0.22	0.8383	0.0896		
							0.15	0.32	0.8575	0.0918		
							0.20	0.43	0.8520	0.0926		
							0.25	0.54	0.8504	0.0922		
							0.35	0.76	0.8436	0.1835		
							0.44	0.95	0.8397	0.1641		
							0.4616	1.00	0.8397	0.0393	0.8340	0.1463
			2.75	0.06	0.18	0.473	0	0	0.6719	0		
							0.02	0.05	0.9251	0.0360		
							0.05	0.11	0.9753	0.0642		
							0.10	0.23	0.9799	0.1101		
							0.15	0.34	1.0084	0.1120		
							0.20	0.45	1.0152	0.1140		
							0.25	0.56	1.0132	0.1143		
							0.35	0.79	1.0074	0.2276		
							0.42	0.95	0.9997	0.1583		
							0.4438	1.00	0.9997	0.0536	0.9902	
				0.12			0	0	0.6194	0		
							0.02	0.05	0.9111	0.0345		
							0.05	0.11	0.9643	0.0634		
							0.10	0.23	0.9789	0.1095		
							0.15	0.34	0.9995	0.1114		
							0.20	0.45	1.0110	0.1133		
							0.25	0.56	1.0052	0.1136		
							0.35	0.79	0.9977	0.2257		
							0.42	0.95	1.0080	0.1582		

Test Series	Q* (m³/s)	ht (m)	X (m)	Z (m)	Z_o (m)	F	y (m)	y/Y	u (m/s)	Δu (m/s)	U (m/s)	Q (m³/s)
							0.4438	1.00	1.0080	0.0541	0.9835	0.0788
			3.215	0.025	0.05	0.623	0	0	1.0886	0		
							0.02	0.05	1.2731	0.0553		
							0.05	0.12	1.3182	0.0910		
							0.10	0.23	1.3197	0.1543		
							0.15	0.35	1.3260	0.1548		
							0.20	0.47	1.2744	0.1521		
							0.25	0.59	1.3075	0.1511		
							0.35	0.82	1.2511	0.2994		
							0.40	0.94	1.1771	0.1421		
							0.4273	1.00	1.1771	0.0752	1.2752	0.0272

IMAGE EVALUATION TEST TARGET (QA-3)

150mm

6"

APPLIED IMAGE . Inc
1653 East Main Street
Rochester, NY 14609 USA
Phone: 716/482-0300
Fax: 716/288-5989